Source identification of Pu and ^{236}U deposited on Norwegian territories

Identifisering av kilder til radioaktiv forurensing på norsk territorium

Philosophiae Doctor (PhD) Thesis

Cato Christian Wendel

Department of Plant and Environmental Sciences
Norwegian University of Life Sciences

Ås 2013

Thesis number 2013:56
ISSN 1503-1667
ISBN 978-82-575-1156-2

Preface

This thesis has been an interdisciplinary collaboration between the University of Life Sciences (UMB), the Norwegian defence research establishment (FFI), the Norwegian meteorological institution (MET), the Norwegian polar institution (NPI). The project has been financed by the Norwegian Research council, and this is gratefully acknowledged.

I would like to express my gratitude to my main supervisors Brit Salbu, Ole Christian Lind and Lindis Skipperud. Your scientific support, guidance, understanding and inspiration through these years have been absolutely crucial for the fulfilment of the work. I am also very thankful to my co-supervisors, Jerzy Bartnicki (Norwegian meteorological institute), Elisabeth Isaksson (Norwegian Polar Institute) and Steinar Høibråten (Norwegian Defence Research Establishment) for valuable discussions, scientific advice and support. I also wish to thank Deborah Oughton and Keith Fifield for very valuable advice and discussions during the work. Thank you Signe Dahl for all your kind assistance with the layout of the papers and the thesis.

For your valuable expertise and time, Karl Andreas Jensen, Solfrid Lohne; Syverin Lierhagen; Eiliv Steinnes; Stephen Tims; Marit Nandrup Pettersen; Tove Loftaas; Elin Ørmen and Hilde Raanaas Kolstad.

I also wish to thank all my colleagues at “miljøkjemi” for the friendly and humoristic atmosphere and for being such good friends and colleagues.

Finally, I would like to thank my friends and Family, and my dear Torunn.

Abstract

Plutonium (Pu) is a predominately anthropogenic element produced during neutron irradiation of U in reactors and nuclear weapon detonations. Pu has been released to the environment during nuclear weapon detonations, nuclear reactor accidents, and in association with reprocessing of spent nuclear fuel. The most important source of Pu in the environment were the 543 atmospheric nuclear detonations conducted worldwide in the period 1945 – 1980 by the former Soviet Union (FSU), USA, United Kingdom (UK), China and France. The most intensive period of atmospheric nuclear testing was 1945 – 1962, interrupted by a moratorium during November 1958 to September 1961. This period was dominated by US testing during the pre-moratorium period and FSU testing during the post-moratorium period. Debris from the atmospheric nuclear detonations was deposited on a local, regional and global scale depending on detonation height, yield and meteorological conditions.

The isotopic composition of Pu is source dependent. Pu is produced by neutron capture in ^{238}U, generating ^{239}U which rapidly ($t_{1/2}$=23.5 min) decay to ^{239}Pu. Heavier isotopes are produced due to neutron capture in this ^{239}Pu. Heavier isotopes of Pu are successively produced during continued neutron irradiation. Reactor derived Pu would have ^{240}Pu/^{239}Pu atom ratios reflecting the irradiation history of the fuel (burn up). For technical reasons, the ^{240}Pu/^{239}Pu atom ratios in weapon purpose Pu has to be below 0.07. The burn up in weapon production reactors kept low by frequent exchange of the fuel in order to ensure this. For power production reactors on the other hand, frequent exchange of the fuel is impracticable and uneconomical. The fuel is exchanged after a prolonged irradiation and high burn up. As the proportion of heavier Pu isotopes increase in relation to ^{239}Pu, all Pu atom ratios, and in particular the ^{240}Pu/^{239}Pu atom ratios increase; ^{240}Pu/^{239}Pu atom ratios up to 0.67 have been reported. Debris from undetonated weapons and low yield detonations would also have low ^{240}Pu/^{239}Pu atom ratios, similar to the original weapon material. Post detonation Pu atom ratios depend on the yield and design of the device with high yield detonations generally producing Pu with higher ^{240}Pu/^{239}Pu atom ratios than low yield detonations. Global fallout was the mixed debris injected into the stratosphere by high yield detonations. After a considerable retention time in the stratosphere, this debris was deposited to form a general Pu background with an easily recognisable ^{240}Pu/^{239}Pu signature of ~0.18. Pu isotopic signatures substantially different from global fallout indicates significant influence from local or regionally deposited Pu from nuclear weapon test sites, reactor accidents or releases from reprocessing.

In the present thesis U and Pu isotopic signatures has been utilised for source identification and quantification purposes. The samples employed have been humic surface soils from 45 geographically well distributed sites in Norway (*Paper I*); an ice core from Austfonna (Svalbard) covering the period 1949 – 1999 (*Paper II*); and air filter samples from Norway during 1957 - 1963(Paper III). Radioactive particles have been identified in the air filter samples the ice core samples (*Paper II*) and (Paper III), while atmospheric dispersion modelling (NOAA HYSPLIT_4) has been used to corroborate the source identification in (Paper III).

Debris from the Chernobyl accident in 1986 was distributed over vast areas of Europe, including Fenno-Scandinavia. Whereas the deposition of caesium from the Chernobyl accident is known to have been strong in Norway, knowledge of the Pu deposition is scarce. In order to assess the relative importance of sources to Pu deposition in mainland Norway, Pu concentrations and atom ratios in humic surface soil samples collected from 45 geographically well distributed sites were determined by SF-ICP-MS (sector field inductively coupled plasma – mass spectrometry) and AMS (Accelerator mass spectrometry). Pu concentrations in samples collected from the same sites in 1990 and 2005 were compared in order to assess the relative migration of Pu from the surface layers. Pu concentrations (0.7 – 149 Bq m^{-2}) were found to be higher at coastal sites with high annual precipitation than at inland sites with lower annual precipitation, this is in accordance with the global fallout theory. The $^{240}Pu/^{239}$ Pu atom ratios were found to vary within 0.161 – 0.211, mainly in accordance with the global fallout signature. However, at some inland sites Pu atom ratios were found to exceed global fallout Pu signatures, indicating a slight Chernobyl influence.

Time resolved samples permit the investigation of variations of deposition and isotopic signatures in deposited debris. Pu and ^{236}U concentrations and atom ratios were determined by AMS in an Arctic ice core from Austfonna (Svalbard) covering the period 1951 – 1999, and in air filter samples collected during 1957 – 1963.

The Austfonna represents an interesting sampling location in its proximity to FSU test site Novaya Zemlya (NZ). In addition tropospheric transport from Eurasia, and possibly the FSU test site in Semipalatinsk (STS) is facilitated by a semi-permanent high pressure area above Siberia during winter. Digital autoradiography indicated the presence of radioactive particles at depths corresponding to atmospheric nuclear testing (1949 – 1962) and the Chernobyl accident or a vented NZ underground detonation (1985 – 1989). Concentrations of Pu and ^{236}U in the Austfonna ice core (0.008 to 0.254 mBq cm^{-2} and 0.0039 to 0.053 μBq cm^{-2} respectively) were found to be higher at depths corresponding to the pre-moratorium period (1956 – 1959) than at

depths corresponding to the post- moratorium period (1959 – 1962). This observation contrasts with observations at other sites where the deposition of anthropogenic radionuclides was found to be higher in the post-moratorium period. The discordance either indicates post depositional redistribution or a different depositional regime at the Austfonna glacier than at other sites.

The $^{240}Pu/^{239}Pu$ atom ratio measured in air filters (0.0517 – 0.237) showed a strong dependence on northern hemisphere atmospheric test activities, tending towards a value reflecting stratospheric fallout during periods without atmospheric nuclear testing, and substantially lower ratios in periods associated with atmospheric nuclear testing activities. The lower Pu atom ratios observed during periods of atmospheric nuclear testing indicates significant influence of tropospherically transported Pu from FSU atmospheric nuclear testing. A further indication is provided by the presence of radioactive particles in filters from the autumn and winter seasons of 1961 and 1962, i.e. periods associated with atmospheric testing at FSU test sites NZ and STS. Direct tropospheric transport from FSU test site STS was indicated by high Pu and ^{236}U concentrations and low $^{240}Pu/^{239}Pu$, $^{241}Pu/^{239}Pu$ and $^{236}U/^{239}Pu$ atom ratios during November 1962. Atmospheric dispersion modelling (HYSPLIT) using real time meteorological data confirmed the plausibility of this transport, and limited the potential source to three low yield STS test detonations during 30 October – 1 November 1962.

Sammendrag

Plutonium (Pu) er et hovedsakelig menneskeskapt grunnstoff, dannet ved nøytronbestråling av uran (U) i reaktorer og atomvåpendetonasjoner. Plutonium har blitt sluppet ut i naturmiljøet som en følge av atomprøvesprengninger, reaktorulykker, og i forbindelse med gjenvinning av brukt reaktorbrensel. Den viktigste kilden til Pu i miljøet var 543 atmosfæriske atomvåpensprengninger, foretatt på begge halvkuler i perioden 1945 - 1990. Atmosfæriske atomprøvesprengninger ble foretatt av den tidligere Sovjetunionen (FSU), USA, Storbritannia (UK), Kina og Frankrike. Den mest intense prøvesprengningsperioden var 1945 – 1962, avbrutt av et moratorium fra november 1958 til september 1961. Denne perioden var dominert av detonasjoner foretatt av USA før moratoriet og FSU i perioden etter moratoriet. Nedfall fra de atmosfæriske prøvesprengningene ble deponert på et lokalt, regionalt og globalt plan hovedsakelig avhengig av prøvesprengningens sprengkraft, detonasjonshøyde samt meteorologiske forhold.

Isotopsammensetningen av Pu er kildeavhengig. I reaktorer blir Pu produsert ved nøytroninnfangning hovedsakelig i ^{238}U, som gir dannelse av ^{239}U som raskt ($t_{1/2}$=23,5 min) henfaller til ^{239}Pu. Tyngre Pu isotoper dannes ved fortsatt nøytronbestråling av brenselet. Pu i reaktorer vil ha et $^{240}Pu/^{239}Pu$ atomforhold som avhenger av brenselets bestrålingshistorie (burn up). Våpenteknisk Pu vil ha en høy andel ^{239}Pu og et lavt $^{240}Pu/^{239}Pu$ atomforhold. Typiske $^{240}Pu/^{239}Pu$ atomforhold i våpenmateriale er under 0,07, $^{240}Pu/^{239}Pu$ atomforholdet i reaktorer tiltenkt våpenproduksjon er tilsvarende lavt. Pu med lavt $^{240}Pu/^{239}Pu$ atomforhold produseres ved å la reaktoren være i drift i en kort periode før brenselet byttes (lav burn up). Dette er imidlertid en lite økonomisk måte å drive energiproduserende atomreaktorer på, her tilstrebes god utnyttelse av brenselet og få avbrudd i driften. Ved forlenget drift øker dannelse av tyngre Pu-isotoper på bekostning av ^{239}Pu; derfor øker alle Pu atomforhold i reaktoren, og spesielt $^{240}Pu/^{239}Pu$. Det har i litteraturen vært referert til atomforhold opp til 0,67 for energiproduserende reaktorer. Pu atomforhold i materiale fra udetonerte atomvåpen og fra detonasjoner med lav sprengkraft vil også være lavt, ofte tilsvarende det opprinnelige våpenmaterialet. Pu atomforhold i nedfall fra et detonert atomvåpen avhenger av bombens sprengkraft og design, hvor detonasjoner med høy sprengkraft som oftest produserer nedfall med høyere $^{240}Pu/^{239}Pu$ atomforhold enn detonasjoner med lav sprengkraft. Globalt nedfall (GFO) ble dannet av de detonasjonene som hadde tilstrekkelig kraft til å injisere store deler materiale i stratosfæren. Dette nedfallet hadde en betydelig oppholdstid i stratosfæren for det ble

deponert på bakken. Globalt nedfall er relativt jevnt fordelt, og har dannet et gjenkjennelig Pu bakgrunnssignal med et $^{240}Pu/^{239}Pu$ atomforhold på omtrent 0,18 på begge halvkuler. Pu med atomforhold vesentlig forskjellig fra GFO antyder signifikant lokalt eller regionalt nedfall fra atomprøvesprengninger, materiale fra reaktorulykker eller utslipp forbundet med gjenvinning av brukt reaktorbrensel.

Dette arbeidet har omfattet kildeidentifisering og kildekvantifisering basert på Pu og U atom og aktivitetsforhold. Prøver av overflatejord fra 45 steder i Norge (artikkel I); en iskjerne fra Austfonna, Svalbard som dekker perioden 1949 – 1999 (artikkel II); samt luftfiltre samlet inn i Norge i perioden 1957 – 1963 (artikkel III). Radioaktive partikler har blitt gjenfunnet i iskjerneprøvene og luftfilterprøvene (artikkel II og III), og en atmosfærisk spredningsmodell (NOAA HYSPLIT_4) har vært brukt for å forsterke kildeidentifisering i artikkel III.

Tsjernobyl-ulykken i 1986 forårsaket spredning av radioaktivt materiale over store deler av Europa, inkludert Fennoskandia. Det er kjent at deponeringen av cesium fra Tsjernobyl-ulykken var kraftig i Norge, imidlertid er deponeringen av Pu dårlig beskrevet. For å anslå påvirkningen av Pu fra Tsjernobyl-ulykken ble konsentrasjoner og atomforhold av Pu bestemt ved bruk av SF-ICP-MS (sector field-inductively coupled plasma-mass spectrometry) og AMS (accelerator mass spectrometry) i prøver av overflatejord samlet inn fra til sammen 45 steder i 1990 og 2005. Prøvestedene var geografisk jevnt fordelt i hele Norge, og det ble tilstrebet å samle inn prøver fra de samme stedene i 1990 og 2005. Videre ble Pu konsentrasjonene påvist i prøvene fra 199 og 2005 sammenliknet for å anslå den relative retensjonen i overflatejorden. Pu- konsentrasjonene i begge datasettene ble funnet å variere mellom 0,7 og 149 mBq m^{-2}. Konsentrasjonene av Pu i jordprøvene ble funnet å være høyere ved kysten, i samsvar med høyere årlig nedbør, tilsvarende ble lavere konsentrasjoner funnet ved innlandslokasjoner. Dette er i samsvar med generelle teorier om at globalt nedfall i stor grad følger nedbørsmønsteret. Pu-240/Pu-239 atomforholdene ble funnet å ligge mellom 0,161 og 0,211, hovedsakelig i samsvar med globalt nedfall. Noen av prøvestedene i innlandet ble funnet å inneholde Pu med atomforhold vesentlig høyere enn globalt nedfall, noe som indikerte en viss påvirkning av Pu fra Tsjernobyl-ulykken.

Variasjoner og trender i deponeringen kan undersøkes ved hjelp av prøvetyper med tidsoppløsning. Pu og U atomforhold ble bestemt ved hjelp av AMS i en iskjerne fra Austfonna (Svalbard) og i luftfilterprøver fra årene før og etter moratoriet.

Austfonna er et spesielt interessant prøvetakingssted grunnet nærheten til de tidligere Sovjetiske prøvesprengningsfeltene ved Novaja Semlja (NZ). I tillegg fører et semi-

permanent høytrykksområde over sentrale Sibir vinterstid til økt transport av troposfærisk luft fra Eurasia mot Arktis. Dette vil potensielt kunne øke transport av materiale fra atomprøvesprengninger over prøvesprengningsfeltet Semipalatinsk (STS) til Arktis. Digital autoradiografi indikerte radioaktive partikler på dybder som svarer til periodene med atomprøvesprengninger ved STS og NZ (1949 – 1962) samt på dybder som svarer til 1985 – 1989 (Tsjernobyl-ulykken og en underjordisk prøvesprengning med lekkasje av radioaktive gasser til atmosfæren ved NZ). Pu og ^{236}U konsentrasjonene (henholdsvis 0,008 til 0,254 mBq cm^{-2} og 0,0039 til 0,053 µBq cm^{-2}) ble funnet å være høyere i perioden før moratoriet (1956 - 1959) enn i dybder svarende til perioden etter moratoriet (1959 – 1962). Dette er i motsetning til observasjoner fra andre prøvetakingssteder, hvor deponeringen av radionuklider har vært høyere i perioden etter moratoriet. Forskjellen mellom resultatene oppnådd for iskjernen fra Austfonna og andre arbeider antyder enten at prosesser i isbreen etter deponering har forstyrret kronologien, eller at deponeringen av radioaktivt nedfall har vært annerledes ved Austfonna.

I luftfiltrene fra perioden 1957 – 1963 ble det funnet en sterk sammenheng mellom ^{240}Pu/^{239}Pu atomforhold (0,0517 – 0,237) og perioder med atomprøvesprengninger på den nordlige halvkule. I de perioder uten atomprøvesprengninger på den nordlige halvkule antok ^{240}Pu/^{239}Pu atomforholdet målt i filtrene en verdi som gjenspeilte globalt nedfall, mens i perioder hvor det ble foretatt atomprøvesprengninger ved FSU prøvesprengningssteder NZ og STS lå dette atomforholdet betydelig lavere. Dette antyder at materiale fra FSU prøvesprengninger har blitt transportert i betydelig grad til Norge via troposfæren. Denne indikasjonen ble forsterket av resultatene fra autoradiografi. Her ble det funnet betydelig flere radioaktive partikler i perioder med atomprøvesprengninger på den nordlige halvkule enn i perioder uten. En episode med direkte troposfærisk transport av materiale fra atomvåpensprengninger ved STS prøvesprengningsområde til Norge ble indikert av høye Pu og ^{236}U konsentrasjoner, og svært lave ^{240}Pu/^{239}Pu, ^{241}Pu/^{239}Pu and ^{236}U/^{239}Pu atomforhold i november 1962. Beregninger foretatt på basis av historiske sanntids meteorologiske data med en atmosfærisk spredningsmodell (HYSPLIT) forsterket plausibiliteten for at det radioaktive materialet påvist i disse filtrene stammet fra prøvesprengninger over ved Semipalatinsk. Modellen, og værforholdene i Eurasia på dette tidspunktet avgrenset den sannsynlige kilden til tre mindre atomprøvesprengninger ved STS i perioden 30. oktober til 1. november 1962.

List of papers

Paper I

C.C. Wendel, L. Skipperud, O.C. Lind, E. Steinnes, S. Lierhagen, B. Salbu. Levels and trends of Pu deposited on humic surface soils. Submitted, Journal of environmental radioactivity.

Paper II

C.C. Wendel, D.H. Oughton, O.C. Lind, L. Skipperud, L.K. Fifield, E. Isaksson, S.G. Tims, B. Salbu. Chronology of Pu isotopes and 236U in an arctic ice core. *Science of the total environment.* **461 – 462,** 734 - 741

Paper III

Cato Christian Wendel, Deborah H. Oughton, Ole Christian Lind, Lindis Skipperud, L. Keith Fifield, Jerzy Bartnicki, Stephen G. Tims, Steinar Høibråten, Brit Salbu. Long-range tropospheric transport of uranium and plutonium weapons fallout from Semipalatinsk nuclear test site to Norway. *Environment international.* **59,** 92 - 102

Abbreviations and definitions

AMS	Accelerator Mass Spectrometry
SF-ICP-MS	Sector field Inductively Coupled Plasma –Mass Spectrometry
SEM	Scanning electron microscope
ESEM-XRMA	Environmental Scanning Electron Microscope with X-ray Microanalysis
HYSPLIT	Hybrid single particle Lagrangian integrated trajectory
CCN	Cloud Condensation Nuclei
GFO	Global fallout
NAO	North Atlantic Oscillation
FSU	Former Soviet Union
NZ	Novaya Zemlya test sites
STS	Semipalatinsk test site
PPG	Pacific proving grounds
NTS	Nevada test site (continental USA)
LN	Lop Nor test site (China)
GCR	Magnox reactor
PHWR	Pressurised heavy water reactor
AGR	Advanced gas cooled reactor
RMBK	Pressure tube boiling water reactor
PWR	Pressurised water reactor
LWR	Light water reactor
RTG	Radioisotope thermoelectric generator
HEU	Highly enriched uranium, >90% ^{235}U
DU	Depleted uranium, < 0.72% ^{235}U
Fission detonations	The energy released during the detonation originates from fission of (usually) ^{235}U and / or ^{239}Pu. Yield <~ 50 kt

Boosted fission detonations	Fission weapons wherein a fusion reaction during detonation contributes with neutrons boosting the fission. Yield range 50 – 500 kt.
Thermonuclear detonations	Fission device providing sufficient energy and compression to yield fusion in one or more fusion devices arranged close to the fission device. Additional secondary fission devices triggered by escape neutrons from the fusion processes possible. Historical yield range 0.5 Mt – 58 Mt
kt	10^6 kg TNT equivalents, corresponds to ~1×10^{12} MJ
Mt	10^9 kg TNT equivalents, corresponds to ~1×10^{15} MJ
ng	Nanograms (10^{-9} g)
pg	Picograms (10^{-12} g)
fg	Femtograms (10^{-15} g)
H_{det}	Detonation height

Table of contents

1 Introduction

Anthropogenic (man-made) radionuclides have been introduced to the environment in significant quantities since the start of the nuclear era. The most important sources were nuclear detonations, carried out by eight nations (USA, FSU, UK, China, France, India, Pakistan and North Korea). Altogether more than 2422 atmospheric, underground and underwater tests were conducted in the period 1945 – 2013, with a total yield equivalent to 530 Mt TNT (UNSCEAR, 2000a; Björklund and Goliath, 2009). A number of safety tests without fission yield have been included in the total number of atmospheric tests.

The largest proportion of the yield (440 Mt) is attributed to atmospheric tests carried out in the period 1945 – 1980, with the most intensive period 1951 – 1962 (409 Mt) (UNSCEAR, 2000a; Björklund and Goliath, 2009). Debris from these tests was distributed between the local (~15 %), tropospheric (~8.5 %) and stratospheric (~76%) compartments (UNSCEAR, 2000a). These releases were not only the largest releases, but due to their nature, also caused the most widespread contamination.

Releases of radionuclides from the nuclear fuel cycle (mining, milling, fuel fabrication, reactor operation and reprocessing) have also been a major source of radioactive contamination (Jones *et al.,* 1996; Beasley *et al.,* 1998a; Cooper *et al.,* 2000; Lind, 2006). A series of nuclear reactor accidents have occurred, however, most of them have only had a local impact. The consequences of the Chernobyl accident in 1986 and the Fukushima accident in 2011 have been more severe; these have caused widespread contamination (UNSCEAR, 2000b; Stohl *et al.,* 2012). Finally, discharges to the aquatic environment from reprocessing installations have been distributed regionally.

Releases of radionuclides have also occurred in connection with satellite accidents and during transport of nuclear weapons. Three satellite accidents with global and regional importance have taken place; the disintegration of a transit navigational satellite containing a SNAP-9A radioisotope thermoelectric generator (RTG) in the high stratosphere of the southern hemisphere; the Cosmos–954 satellite disintegrating above Canada in 1978; and the Cosmos-1402 satellite disintegrating over the south Atlantic ocean in 1983 (Krey, 1967; Bakhtiar *et al.,* 1985; Leifer *et al.,* 1987; UNSCEAR, 1993; Jia *et al.,* 1999).

Local contamination has been caused by aircraft accidents involving nuclear weapons in Palomares, Spain and at Thule, Greenland in 1966 and 1968,

respectively, (e.g. Mitchell *et al.* (1997), Pöllänen *et al.* (2006), Lind *et al.* (2007)). Likewise, dumping of radioactive waste at sea has had local environmental influence due to a poor state of the containers and leakage (Salbu *et al.,* 1997).

All major nuclear sources of release such as nuclear weapon tests and nuclear reactor accidents have contributed to the presence of Pu and anthropogenic U in the environment. These radionuclides are of particular interest, as the isotopic signature can be used for source identification. U is a natural radionuclide with the isotopes ^{234}U, ^{235}U and ^{238}U occurring with isotopic abundances of 0.005 %, 0.72 % and 99.27 %, respectively. Pu isotopes and ^{236}U are, however, almost exclusively anthropogenic, and formed during reactor operation and nuclear weapon detonations.

Nuclear weapon material is composed of Pu (more than 93 % ^{239}Pu), enriched U (more than 90 % ^{235}U) or a combination of the two. Enriched U is normally produced from natural U trough ultracentrifugation, while ^{239}Pu is produced through neutron irradiation of ^{238}U in reactors. The production of Pu with a high concentration of ^{239}Pu is accomplished through short irradiation times within the reactor. In power production reactors, irradiation times are longer, and heavier Pu isotopes (^{240}Pu and heavier) are produced throughout fuel utilisation. Thus, the ^{240}Pu/^{239}Pu atom ratio in particular, becomes successively higher the longer the fuel is irradiated.

Reactor irradiation of fuel is associated with low neutron fluxes and long irradiation times. In this process the short lived heavier U isotopes (^{239}U, $t_{1/2}$=23.5 min) transmute to Pu isotopes prior to further neutron capture. Therefore, in reactors ^{239}Pu is formed, and heavier Pu isotopes originates from neutron activation in this ^{239}Pu. Heavier isotopes up to ^{243}Pu are formed as shown in Figure 1, however, due to the short half live of ^{243}Pu (4.96 h), this isotope decays to ^{243}Am prior to further neutron capture, and the production of ^{244}Pu is insignificant in reactors in comparison with thermonuclear devices (Winkler, 2007).

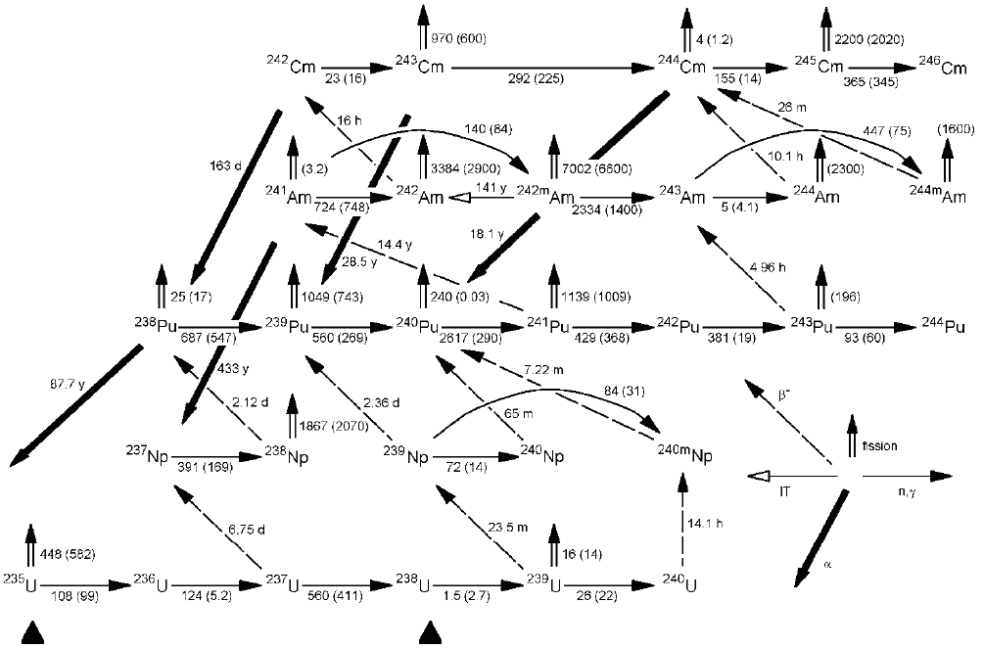

Figure 1. Neutron irradiation and decay during reactor operation of a typical power production LW reactor. Numbers along axis refer to half-lives or effective cross sections. From (Choppin *et al.*, 2002).

In the high neutron fluxes and short irradiation times associated with thermonuclear detonations (fission – fusion and fission-fusion-fission detonations), heavier Pu isotopes (^{240}Pu and heavier) are produced according to the reactions shown in Figure 2. Low yield detonations release Pu with an isotopic composition close to that of the original weapon material, the ^{240}Pu/^{239}Pu atom ratio is usually within the range 0.01 – 0.07. In general, higher yield detonations, in particular boosted detonations and thermonuclear detonations, produce Pu isotopes heavier than ^{240}Pu during the detonation, increasing the ^{240}Pu/^{239}Pu, ^{241}Pu/^{239}Pu, ^{242}Pu/^{239}Pu and ^{244}Pu/^{239}Pu atom ratios. However, this is device dependent, as Pu is mainly produced from ^{238}U present as a tamper or secondary fission material (fission – fusion – fission devices).

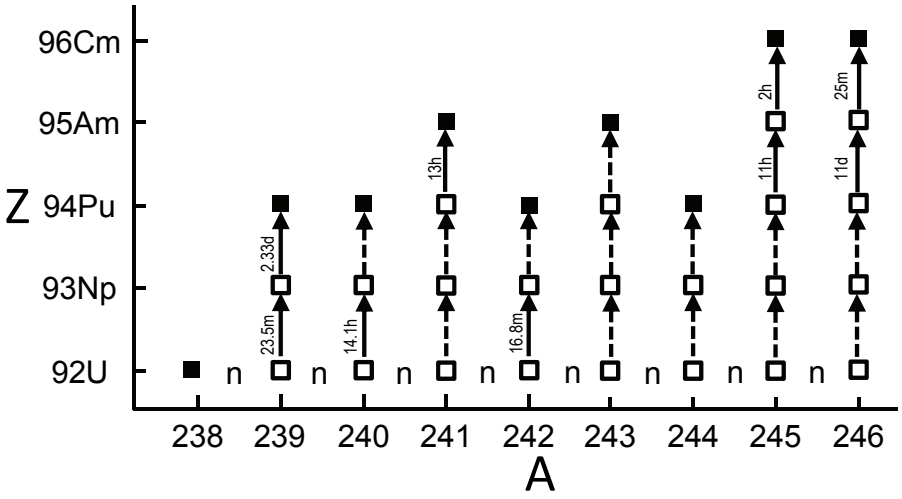

Figure 2. Neutron activation and decay to beta stable nuclides in thermonuclear detonations. □ - Beta emitting nuclide, ■ - alpha emitting nuclide. Half-lives indicated along the arrows. Modified from Diamond *et al.* (1960).

Key sources of Pu isotopes and ^{236}U are summarised in chapter 2. Typical $^{240}Pu/^{239}Pu$, $^{241}Pu/^{239}Pu$, $^{242}Pu/^{239}Pu$ and $^{236}U/^{239}Pu$ atom ratios for a range of different sources are presented in Table 1.

Table 1. Atom ratios characteristic for debris from nuclear detonations and various reactor types, ref. date (01.12.2011)

Source	$^{240}Pu/^{239}Pu$	$^{241}Pu/^{239}Pu$	$^{242}Pu/^{239}Pu$	$^{236}U/^{239}Pu$	Ref.
Undetonated weapons plutonium	0.01 – 0.07	-	-	-	a
Low yield detonations, U-based	0.00015 – 0.053	$(0.2 – 2.3) \times 10^{-4}$	-	-	b
Low yield detonations, Pu based	0.01 – 0.08	$(0.2 – 6.7) \times 10^{-4}$	-	-	b
Low yield detonations, GZ Semipalatinsk	0.0438 ± 0.0001	$(2.21 \pm 0.035) \times 10^{-4}$	$(7.89 \pm 0.26)\times10^{-5}$	0.0244 ± 0.001	c
Global fallout, N. hemisphere	0.182 ± 0.005	$(1.12 \pm 0.85) \times 10^{-3}$	$(3.71 \pm 0.3)\times10^{-3}$	0.235 ± 0.014	d, e
Bikini atoll, Ivy Mike	0.46 ± 0.01	-	0.019 ± 0.003	-	f
Reactor debris, Chernobyl	0.13 – 0.53	0.12 – 0.13	0.034 – 0.048	5.43 - 8.14	g
GCR-reactor, fuel burn up 3.6 GWd t^{-1}	0.23	0.045	0.006		h
PHWR-reactor, fuel burn up 7.5 GWd t^{-1}	0.41	0.077	0.023		h
AGR-reactor, fuel burn up 18 GWd t^{-1}	0.57	0.184	0.093		h
RMBK-reactor, fuel burn up 27.5 GWd t^{-1}	0.67	0.203	0.108		h
PWR-reactor, fuel burn up 33 GWd t^{-1}	0.43	0.229	0.096		h

a Warneke *et al.* (2002), Rokop *et al.* (1995), Eriksson *et al.* (2008)
b Hicks and Barr (1984), Hansen (1995), Oughton *et al.* (2000), Smith *et al.* (2000)
c Beasley *et al.* (1998b)
d Kelley *et al.* (1999)
e Sakaguchi *et al.* (2009)
f Lindahl *et al.* (2012), Diamond *et al.* (1960)
g Oughton *et al.* (2001), Entwistle *et al.* (2003), Salminen-Paatero *et al.* (2012)
h Carlson *et al.* (1988)

Particles containing Pu and U

Refractory (high melting point) radionuclides (e.g. Pu, U) tend to be in a particulate form when released to the environment (Salbu, 2000a). Radioactive particles released during nuclear events, are formed due to mechanical destruction of the original material, evaporation and later condensation of radioactive material, or formed during transport or residence in the environment (Salbu, 2001; Lind *et al.,* 2008; IAEA, 2011).

In a report from 2011 (IAEA, 2011), the international Atomic Energy Agency (IAEA) defines radioactive particles as:

> *"Localized aggregation of radioactive atoms that give rise to an inhomogeneous distribution of radionuclides significantly different from that of the matrix background. In water, particles are defined as entities having diameters larger than 0.45 μm, i.e. that will settle due to gravity. Radionuclide species within the molecular mass range 0.001 μm - 0.45 μm are referred to as radioactive colloids or pseudo-colloids. Using the grain size categories for sand, silt and clays, particles larger than 2 mm should be referred to as fragments. In air, radioactive particles ranging from submicron in aerosols to fragments are classified according to the aerodynamic diameters, where particles less than 10 μm are considered respiratory."*

Whereas the elemental and isotopic composition of the particles are source dependent, the shape, size, density and aerodynamic properties affecting both transport conditions and biological significance depend heavily on the release conditions such as temperature, pressure and redox-conditions (Salbu, 2000a). Any source may generate several different classes of particles during the different phases of a release. Using the Chernobyl accident as an example, large particles and fragments deposited close to the destroyed reactor were found to have different chemical and physical properties depending on the scenario under which they were released. Particles released during the initial explosion were found to be less soluble than particles released during the following graphite fire (Oughton *et al.,* 1993; Salbu *et al.,* 1994; Salbu *et al.,* 2001). Similarly, particles released during surface and low altitude atmospheric nuclear detonations exhibit different physical and chemical properties than particles from high altitude detonations due to the incorporation of environmental materials (e.g. Kemmochi (1966), Crocker *et al.* (1966), Yamamoto *et al.* (1996)).

Particle transport

The extents to which radioactive particles released to the atmosphere are subjected to transport prior to deposition depend heavily on particle size, density, release height and meteorological conditions. Particles larger than 20 μm tend to separate from the main aerosol stream relatively rapidly due to gravitational settling, and may be subjected to a different transport regime than smaller particles (Pöllänen, 2002; Bartnicki *et al.,* 2003). Smaller particles may be subjected to considerable atmospheric transport and deposit far away from the release site. Consequently large particles, smaller particles and gas phase radionuclides may deposit onto vastly different areas.

The upwards transport of debris depends on release and meteorological conditions. Materials released during fires, explosions and nuclear detonations experience significant upward transport due to convection. The extent of this transport depends on the energy released during the event, and may vary from a few hundred meters from fires to several tens of kilometres for the largest detonations (e.g. Peterson (1970), Bartnicki *et al.* (2001), Garland and Wakeford (2007)). The settling height of the debris has a large impact on transport and deposition. Debris injected into the troposphere (0 – 9 km above ground) is deposited locally and regionally, while debris injected into the lower and upper stratosphere (~9 – 17 and ~17 – 50 km above ground respectively) is deposited globally (e.g. Peterson (1970), UNSCEAR (1993)). This is further discussed in chapter 3.

Impact of particles containing U and Pu

Radioactive particles may be highly radioactive due to the presence of fuel and device remnants as well as fission and activation products. These entities represent point sources of radioactivity in the environment. If taken up by living organisms, they can deliver doses to tissues. Particles smaller than 10 μm may enter the lungs, and particles smaller than 2.5 μm may deposit in the alveoli of the lungs, representing a point source of radioactivity in the lung tissue (Yassi, 2001; IAEA, 2011). The deposited particle may cause a zone of dead tissue extending several mm, at further distance the irradiation may be sub-lethal but with an increased carcinogenic risk (Entwistle *et al.,* 2003).

Depending on the particle characteristics, weathering and remobilisation of particles can take place over time, as illustrated in Figure 3, allowing the entrance into the food chain (Salbu, 2001). Radioactive particles also represent analytical challenges due to inhomogeneous distribution in the environment and incomplete dissolution of

samples (partial leaching), possibly resulting in an underestimation of the inventory (IAEA, 2011).

The retrieval and analysis of radioactive particles originating from nuclear accidents or atmospheric nuclear detonations could release considerable information regarding source and release conditions, atmospheric behaviour and transport as well as post depositional processes influencing mobility and bioavailability.

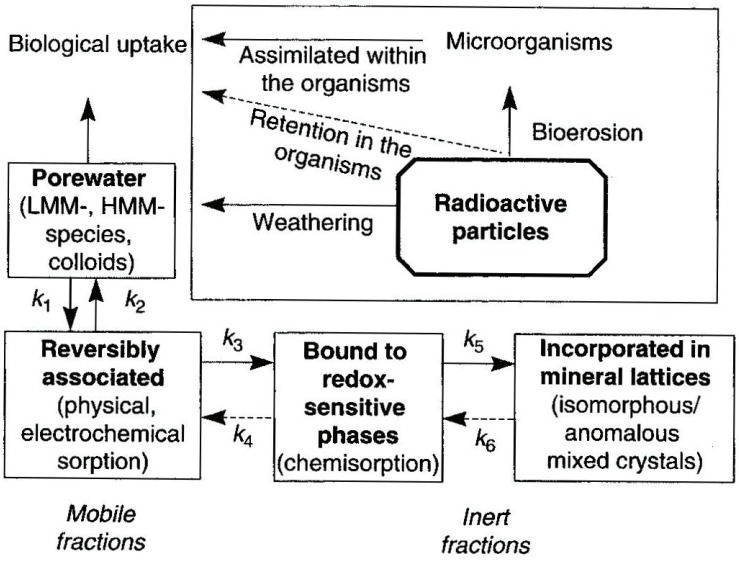

Figure 3. Processes affecting the speciation of radioactive debris deposited in soil-water and sediment-water systems. From Salbu (2000b).

1.1 Hypotheses and objectives of the current work

Following releases of radionuclides from nuclear weapons tests into the atmosphere of the Northern hemisphere, deposition of radionuclides have occurred in all European countries. Little information on Pu and ^{236}U deposition in the Norwegian environment is available. The working hypotheses (denoted H1 – H5) of the present work are presented below.

Based on the available information on the deposition of short lived radionuclides associated with global fallout during the 1950-1960ies, fallout should be relatively uniformly distributed, and follow the precipitation pathway.

H1: Pu originating from nuclear weapons tests should follow the precipitation pattern, and be enriched at the western coast of Norway.

Based on the available information on the deposition of short lived radionuclides associated with nuclear reactor accidents (e.g., Windscale, Chernobyl), Norwegian territories have been affected by the fallout. Deposition of refractory radionuclides (lanthanides, Zr etc.) from the Chernobyl accident has also been observed in Norway.

H2: Traces of Pu associated with reactor fallout should be more unevenly distributed than debris from weapons tests, and it should be possible to identify the signal at certain inland sites in Norway.

Following historical severe nuclear events, radioactive particles have been emitted into the atmosphere. Radioactive particles from the Chernobyl accident have been deposited in many countries in Europe, including Norway.

H3: Inert radioactive particles are expected to be present in samples affected by fallout from the nuclear weapon tests and from nuclear reactor accidents.

Following deposition of Pu and U, several processes will influence the concentrations presently observed in top soils, such as vertical transport and production of increasing humic substance layer.

H4: Over time the Pu and U in top soils will decrease.

Due to the fact that Pu isotopes and ^{236}U are almost exclusively anthropogenic, and formed by single and multiple neutron capture during nuclear weapon detonations (military sources) and reactor operations (civil sources), the isotopic signatures can be utilised to differentiate among military or civil sources.

H5: Pu and U isotopic composition or atom ratios can be utilized for source identification in environmental samples. If the time resolution is sufficiently good, single events contributing to the deposition of Pu and ^{236}U can be identified.

The objective of the current work is to quantify the activity concentrations and atom ratios of Pu isotopes and ^{236}U in available archive samples in order to:

- Estimate the inventory of Pu (^{239}Pu, ^{240}Pu, ^{241}Pu, ^{242}Pu, ^{242}Pu) and ^{236}U in samples from Norwegian territories; identify if the deposition followed the precipitation load and assess whether the top soils have been depleted with respect to these radionuclides over time (Papers I-III).
- Identify if radioactive particles are still present in fallout affected samples (Paper II, III).

- Utilise atom ratios of Pu (^{240}Pu, ^{241}Pu, ^{242}Pu, ^{242}Pu relative to ^{239}Pu) as well as the ^{137}Cs distribution pattern to distinguish between areas affected by military (global fallout) and civil (Chernobyl) sources (Paper I).
- Utilise atom ratios of Pu (^{240}Pu, ^{241}Pu, ^{242}Pu, ^{242}Pu relative to ^{239}Pu) and ^{236}U/^{239}Pu in combination with atmospheric dispersion modelling to obtain a plausible link between deposition and events such as single detonations or series of detonations. (Papers II and III).

The archive samples include soil surface samples collected at sites distributed across the Norwegian mainland in 1990 as well as in 2005 (same sites), an 28.6 m deep ice core from Nordaustlandet, Svalbard covering the period ~1950 – 2000 and selected air filter samples from 11 stations collected daily during 1957 until 1980.

To obtain qualitative (heterogeneous distributions and radioactive particles) and quantitative (activity concentrations) information on Pu isotopes and ^{236}U in environmental samples, advanced techniques such as digital autoradiography, ESEM-XRMA, ICP-MS and AMS have been utilized.

2 Sources of radioactive contamination to the atmosphere

The input from atmospheric nuclear weapons tests and major nuclear accidents has been of local, regional and global importance, albeit mainly restricted to the hemisphere where the events occurred. Most other sources contributing to the release of anthropogenic radionuclides to the environment have had local or regional influence. The deposition of Pu and U in Norwegian terrestrial environments are therefore attributed to severe events such as atmospheric nuclear weapons tests during 1950-1960ies and major nuclear accidents occurring within the Northern hemisphere, such as the Windscale and Chernobyl accidents. To distinguish between the military (nuclear weapon) and civil (nuclear energy) sources, Pu and $^{236}U/^{239}Pu$ atom ratios are considered useful tools.

The process of source identification requires knowledge of the different sources, and characteristics of these. This chapter summarises some of the available information on sources contributing to radioactive contamination of the environment of the northern hemisphere.

2.1 Characteristics of nuclear weapon devices relevant to source identification

Following the classifications of Barnaby (1992), nuclear weapons may be characterised as pure fission weapons (≤0.05 Mt), boosted fission weapons (0.05 – 0.5 Mt) and thermonuclear weapons (>0.5 Mt). These classes will briefly be discussed below. Pure fusion weapons and the fission cores of boosted and thermonuclear weapons are usually composed of a hollow sphere of highly enriched U (HEU, more than 90 % ^{235}U), Pu with a high abundance of ^{239}Pu (93 – 99 %) or a combination of the two (Hicks and Barr, 1984; Barnaby, 1992; Hansen, 1995; Grønhaug, 2001; Lind, 2006; Ranebo *et al.,* 2007). These U and Pu isotopes have a large fission cross section for both low and high energy neutrons and are suitable as weapons material. Additionally, the fission core is often surrounded by a tamper, i.e., an outer heavy metal sphere. The tamper has the dual purpose of reflecting stray neutrons from the fission back into the weapon material and keeping the fissionable mass together for a longer time, thus increasing the efficiency of the detonation (Glasstone and Dolan, 1980; Barnaby, 1992). Tamper materials can be made from natural or depleted U, W, Be, Pb or steel (Maxwell *et al.,* 1955; Lapp, 1970; Rhodes, 1995; DOE, 1996). Natural or depleted U provides ^{238}U as a secondary fissionable material when bombarded with high energy neutrons released in boosted or thermonuclear weapons, thus causing increased yield (Barnaby, 1992; Choppin *et al.,* 2002).

Boosting of nuclear weapons is accomplished through the presence of fusion material in the centre of the fission core (Barnaby, 1992). The high temperatures and pressures obtained during fission causes fusion to occur in this material and increase the yield by providing additional neutrons augmenting the on-going fission chain reactions.

Thermonuclear weapons can be classified as two stage (fission – fusion) devices or three stage (fission – fusion – fission) devices. In both categories the energy from the detonation of the first fission stage is released as high energy x-rays. This energy compresses and heats the fusion stage sufficiently to reach the very high temperatures and pressures necessary for initiating fusion. During fusion, heat and additional high energy neutrons are released. In three stage devices, these neutrons are utilised for fission of a natural or depleted U third stage / tamper (Izrael and Baxter (2002), and references therein).

2.1.1 Low yield weapons (<~0.05 Mt)

Pu in debris from low yield detonations has been reported in a number of publications. The $^{240}Pu/^{239}Pu$ atom ratios are most often found in the range of weapon material Pu (0.01 – 0.07), indicating that little neutron capture has taken place during the detonation. Similarly, the production of ^{236}U was modest and $^{236}U/^{239}Pu$ atom ratios in debris from low yield detonations are low, e.g. Hicks and Barr (1984), Beasley *et al.* (1998b), Lind *et al.* (2005), Lind *et al.* (2007).

2.1.2 High and very high yield weapons (0.05 – 58 Mt)

Literature data (e.g. Diamond *et al.* (1960), Yamamoto *et al.* (1996), Lindahl *et al.* (2011a)) clearly shows that the $^{240}Pu/^{239}Pu$ atom ratio in debris from three stage (fission – fusion – fission) devices approaches that of power producing reactors with long fuel irradiation time. Information on $^{240}Pu/^{239}Pu$ atom ratios in debris from two stage thermonuclear devices (fission – fusion) is scarce; however, the lack of a U tamper would imply lower production of Pu isotopes and lower $^{240}Pu/^{239}Pu$ atom ratios.

Debris from individual high yield tests at the US Eniwetak test site has shown a remarkable lack of correlation between yield and $^{240}Pu/^{239}Pu$ atom ratios. Recent work has been carried out on Eniwetak corals with a high and accurate time resolution (K. Fifield, pers. comm.). The $^{240}Pu/^{239}Pu$ atom ratios (~0.4) in debris from the very high yield Ivy Mike test (10 Mt) were found to be in agreement with published values (e.g. Diamond *et al.* (1960), Lindahl *et al.* (2011a)), while two high yield tests (~2 Mt) in 1956 and 1958 produced debris with $^{240}Pu/^{239}Pu$ atom ratios of ~0.18 and 0.09 respectively. It is likely that the relatively low Eniwetak atom ratios are due to design

differences between the different devices, more specifically differences in the content of ^{238}U from which heavier Pu isotopes are formed (K. Fifield, pers. comm.). Similarly, the lack of a pronounced $^{240}Pu/^{239}Pu$ atom ratio peak after the large FSU testing series in 1961 and 1962 seems to imply a lower production of heavier Pu isotopes in these detonations. Several of the very high yield atmospheric tests conducted by the FSU in 1961 and 1962 have been proposed to be two stage thermonuclear devices, thus without a fissionable uranium tamper, e.g. Lapp (1970), Grønhaug (2001), Barnaby (1992). If this was representative of FSU post moratorium testing it may explain the lack of a peak in $^{240}Pu/^{239}Pu$ atom ratios after the very high yield FSU testing series in 1961 and 1962.

Data on the production of ^{236}U in high yield detonations are scarce at best. However, the generation of ^{236}U should be enhanced by the high neutron fluxes and presence of ^{235}U and ^{238}U seen in high yield fission – fusion – fission devices.

2.1.3 Global (stratospheric) fallout

The term global fallout describes fallout of debris injected into the stratosphere by atmospheric detonations. This debris later deposited relatively homogeneously, mainly within the hemisphere of the injection. Global fallout is recognisable by a characteristic $^{240}Pu/^{239}Pu$ atom ratio, 0.18 ± 0.01 and 0.17 ± 0.02 within the northern and southern hemisphere respectively (Kelley *et al.,* 1999). The difference in the $^{240}Pu/^{239}Pu$ atom ratios of fallout observed between the northern and southern hemisphere likely reflect the relative influence of the detonations carried out. While northern hemisphere global fallout carried influence from FSU high yield polar detonations and US equatorial detonations, southern hemisphere global fallout originated mainly from US and UK equatorial detonations (initially high $^{240}Pu/^{239}Pu$ atom ratios, later lower (K. Fifield, pers. comm.).

Significant perturbations of the $^{240}Pu/^{239}Pu$ signal are found in areas affected by local fallout at testing sites (0.039 – 0.0435, Lind (2006), Beasley *et al.* (1998b)), in debris from accidents (0.055 – 0.53, e.g., Lind *et al.* (2007), Srncik *et al.* (2008), Salminen-Paatero *et al.* (2012)) and operational releases from reprocessing operations (0.03 – 0.24, Lindahl *et al.* (2011b)).

The $^{240}Pu/^{239}Pu$ atom ratio in stratospheric debris varies with the contemporary input. The dominant sources of stratospheric Pu in 1952 and 1954 were the very large US detonations at equatorial testing sites Enewetak and Bikini (Björklund and Goliath, 2009). These tests were conducted as surface detonations, spreading massive amounts of debris locally, tropospherically and stratospherically. The $^{240}Pu/^{239}Pu$ atom ratio in

debris from several of these tests have been determined, (e.g. Diamond *et al.* (1960), Yamamoto *et al.* (1996), Lindahl *et al.* (2011a)), $^{240}Pu/^{239}Pu$ ratios in the range 0.32 – 0.46 were been reported. High $^{240}Pu/^{239}Pu$ atom ratio debris from detonations at equatorial sites was also apparent in herbage samples from England in the years 1954 – 1956 (Warneke *et al.,* 2002), and in an ice core from Greenland (Koide *et al.,* 1985) in the estimated years 1956 and 1957. These findings indicate stratospheric transport of debris from equatorial latitudes.

While the isotopic signatures of Pu from different sources are well described, concentrations of ^{236}U in global fallout are underreported due to analytical challenges. Some publications on isotopic signatures of $^{236}U/^{239}Pu$ (or $^{236}U/^{239+240}Pu$) have emerged during the last few years. The $^{236}U/^{239}Pu$ atom ratio in integrated global fallout ranges between 0.05 and 0.5 (Ketterer *et al.,* 2007; Sakaguchi *et al.,* 2009), however, significantly higher ratios are indicated in more recent samples (Srncik *et al.,* 2011; Eigl *et al.,* 2013) (Paper II).

2.2 A brief history of atmospheric nuclear weapons testing

Atmospheric nuclear tests have been conducted by five nations: USA, FSU (FSU), UK, France and China (UNSCEAR, 2000a). Detonation sites of all known atmospheric nuclear tests, including safety tests are illustrated in Figure 4.

During 1945 – 1980, a total of 543 atmospheric nuclear tests with a total yield equivalent to 440 Mt TNT were conducted worldwide, causing local, regional and global contamination. Three main periods of atmospheric nuclear testing can be identified. The first period lasted from 1945 – 1958, and comprised US, UK and FSU testing at both hemispheres. In the period 1959 to September 1961, a moratorium was imposed during which no tests were conducted except for four French detonations in Algeria. During the second period (September 1961 through December 1962) tests were conducted by the FSU and US at north hemisphere test sites. The partial test ban treaty, signed by the Soviet Union, USA and the United Kingdom prohibited atmospheric nuclear testing by the signatory states from 1963 onwards (CTBTO, 2012). During the third period (1964 – 1980) atmospheric testing was conducted by China (north hemisphere test site Lop Nor) and France (south hemisphere test sites Mururoa and Fangataufa).

In addition, a number of peaceful nuclear detonations (PNEs) have been performed, primarily by the USA, 27 PNE detonations and the FSU, 124 PNEs and 32 tests for PNE devices (Carter and Moghissi, 1977; Cochran and Norris, 1996). These detonations were relatively low yield (<0.180 Mt) surface or underground tests

(Björklund and Goliath, 2009), and contamination should be insignificant beyond the local scale.

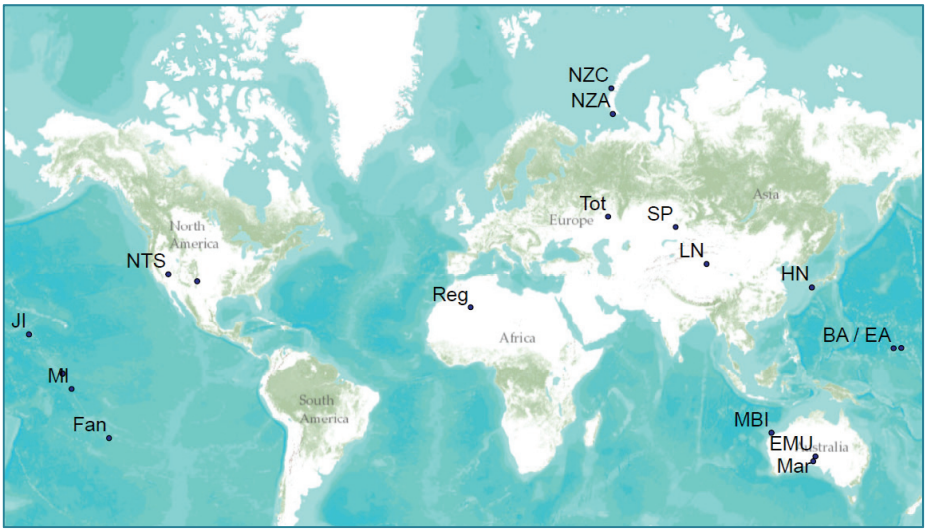

Figure 4. Detonation sites of atmospheric nuclear detonations worldwide in the period 1945 – 1980. NZ – Novaya Zemlya (NZ A – Chernaya Guba, NZ B- Sukhoy Nos); Tot – Totsk; SP – Semipalatinsk; HN – Hiroshima and Nagasaki; NTS – Nevada test site (and New Mexico); JI Johnston Island; BA / EA – Bikini and Eniwetak atolls; MI – Malden Island; REG – Reggane (Algeria); FAN – Fangataufa / Mururoa; MBI - Monte Bello Island; EMU – Emu desert; Mar – Maralinga.

Northern hemisphere test sites

According to Carter and Moghissi (1977) atmospheric nuclear detonations were conducted at six northern hemisphere test areas during 1945 – 1980. Detonations took place at Nevada test site and Pacific Proving Grounds (USA), Semipalatinsk and Novaya Zemlya (FSU) and Algeria (France) until the end of 1962. After 1962, northern hemisphere atmospheric testing took place at the Lop Nor test site (China) until 1980. A total of 445 atmospheric nuclear detonations with an accumulated yield of 428 Mt TNT equivalents were detonated at these sites (UNSCEAR, 2000a). During the most intensive period (1961 and 1962) 176 tests with a total yield of 274 Mt were conducted, mainly at the FSU test areas in Semipalatinsk and Novaya Zemlya (Björklund and Goliath, 2009). A summary of northern hemisphere atmospheric nuclear testing and gross beta activity concentrations measured in Norwegian ground level air is given in Figure 5.

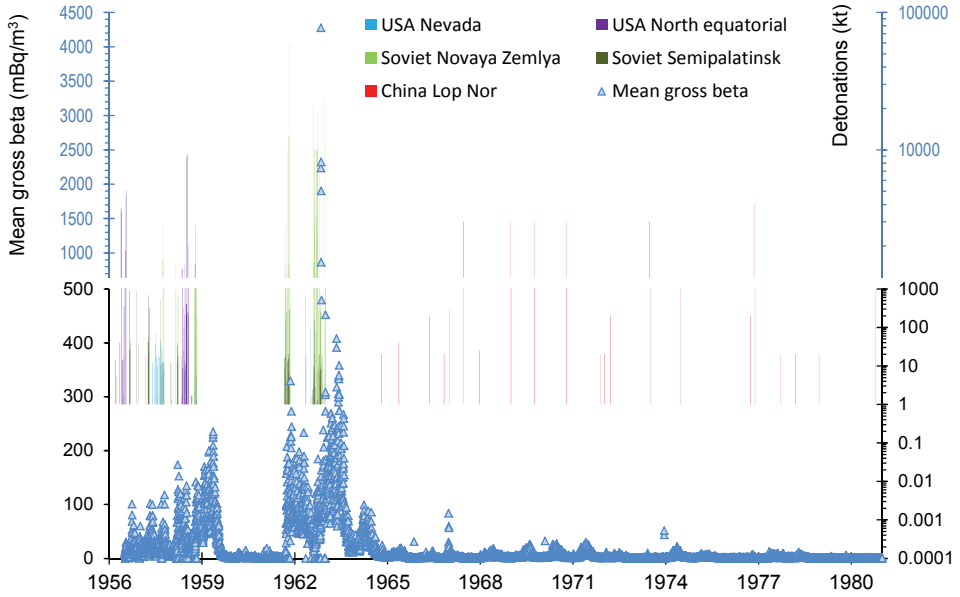

Figure 5. Northern hemisphere atmospheric nuclear detonations in the period 1959 – 1980 and mean gross beta activity concentrations measured in ground level air in Norway in the same period. Data from Björklund and Goliath (2009) and T. Bergan (pers. comm.).

2.2.1 Former Soviet Union test sites

Semipalatinsk Testing Site (STS)

The Semipalatinsk test site is situated in the North eastern part of Kazakhstan covering an area of 18500 km^2. Two main testing areas were in operation; Ground zero where atmospheric tests were conducted, and the Degelen Mountains where underground tests were conducted (Grosche, 2002).

The first soviet nuclear detonation took place at STS in August 1949, and the site was in operation until1989. In the period 1949 – 1962, 116 surface and air detonations with an accumulated yield of 6.6 – 6.9 Mt were carried out (Björklund and Goliath, 2009). Several tests are known to have caused considerable local and regional contamination (e.g. Gusev *et al.* (1997), Khalturin *et al.* (2005) and Gordeev *et al.* (2006)). Pu and U isotopes in local fallout have been well characterized (e.g. Beasley *et al.* (1998b), Yamamoto *et al.* (2004) and Lind (2006)). UNSCEAR (2000a) estimates that 8 of the atmospheric tests carried out at STS were thermonuclear. Nevertheless, the ^{240}Pu/^{239}Pu atom ratios in debris associated with tests at the site are generally low. Atom ratios of ^{240}Pu/^{239}Pu in a particle and soil samples collected at

STS ground zero were 0.039 ± 0.009 and 0.0438 ± 0.0001 respectively (Beasley *et al.,* 1998b; Lind, 2006).

Novaya Zemlya Testing Site (NZ)

Following concerns that fallout from high yield tests at STS could be severely detrimental to public health, decisions were made to conduct further large tests at the remote Novaya Zemlya testing site (e.g. Khalturin *et al.* (2005)). The Novaya Zemlya testing area is located in the high Arctic and consists of three testing sites; Chernaya Bay where underwater and surface detonations were conducted, Sukhoy Nos where atmospheric detonations were conducted and Matochkin Strait where underground detonations were carried out. FSU monitoring of debris from atmospheric tests at NZ revealed two main trajectories associated with significant radioactive fallout (tropospheric). One trajectory extends due South as far as the Caspian Sea, the other several thousand kilometres South East towards the Sea of Okhotsk (Khalturin *et al.,* 2005).

In the period September 1957 to late December 1962, 91 atmospheric nuclear test detonations were conducted above or on Novaya Zemlya with a total explosive yield equivalent to 240 – 255 Mt TNT (UNSCEAR, 2000a; Khalturin *et al.,* 2005; Björklund and Goliath, 2009). Detonations at NZ were large, and in combination with a large height of detonation (H_{det}) and the low polar tropopause this caused considerable contributions to the stratospheric inventory of radioactive debris.

Publications on the radiological condition of Novaya Zemlya are scarce, but local contamination has been documented after some of the detonations (e.g. AMAP (1998), Smith *et al.* (2000), Oughton *et al.* (2004)). Particles from detonations at Novaya Zemlya in October 1958 have been identified in samples from stratospheric air above central Sweden (Sisefsky, 1961). The debris in this filter originated from to two tests above Novaya Zemlya the 30. September 1958 with yields of 0.9 and 1.2 Mt. Parts of the same filter (bulked) has later been analysed by Warneke (2002), and a $^{240}Pu/^{239}Pu$ atom ratio of 0.101 was determined.

During the test series in 1961 and 1962, some very large atmospheric nuclear tests were conducted at this site. Six tests had yields exceeding 10 Mt, and the largest one of these, the Tsar Bomba, detonated the 30 October 1962, had a yield of 50 – 58 Mt (UNSCEAR, 2000a; Björklund and Goliath, 2009). The neutron fluxes in this device would have been very high. In the presence of ^{238}U as tamper, this device would have generated massive amounts of heavier Pu isotopes. However, it has been indicated that the device was downscaled from its original 100 Mt configuration by substituting

the original U tamper with a lead tamper (e.g. Lapp (1970), Grønhaug (2001) and references therein).

2.2.2 US test sites

Nevada test site

At the Nevada test site 86 atmospheric, air or surface detonations with an accumulated yield of 1.01 Mt took place in the period 1945 – 1962 (UNSCEAR, 2000a; Björklund and Goliath, 2009). Atmospheric tests at this site were generally small (less than 0.1 Mt), and $^{240}Pu/^{239}Pu$ and $^{241}Pu/^{239}Pu$ atom ratios (0.00015 – 0.08, and 0.00038 – 0.0072 respectively) in debris at site were low (Hicks and Barr, 1984; Hansen, 1995). The lowest ratios in debris were associated with detonation of pure U-devices. Furthermore, the detonation heights of the tests were relatively low. A majority of the devices detonated at the surface, from steel towers, in balloons or by airdrop. Particles associated with tower shots range from spherical air-detonation resembling particles to conglomerates of particles adhering to each other (Crocker *et al.,* 1966).

US equatorial tests (Bikini, Enewetak, Johnston Island, and Christmas Island).

At Bikini and Enewetak atolls 63 detonations were carried out at surface, placed on barges, mounted in towers, or by air drop by the US in the period 1946 – 1958 (Björklund and Goliath, 2009). Detonation heights were generally low and environmental materials were readily fused with debris from the detonations. Altogether 35 thermonuclear detonations were performed at the two atolls; most of these were surface detonations, including the first US thermonuclear device (Ivy Mike) and the largest (Castle Bravo). Severe local contamination has occurred on at least one occasion, Castle Bravo detonation, where flake like particulate debris was deposited up to 200 km eastwards from the detonation within hours after the detonation, affecting local residents, fishermen and US service men (e.g. Yamamoto *et al.* (1996), Cronkite *et al.* (1997), UNSCEAR (2000a)). Pu linked to high yield detonations at the Marshall Islands is associated with high atom ratios, e.g. Castle Bravo: $^{240}Pu/^{239}Pu$ 0.32 ± 0.03 (Yamamoto *et al.,* 1996), and Ivy Mike: $^{240}Pu/^{239}Pu$ 0.46 ± 0.01 (Lindahl *et al.,* 2012).

Tests at Johnston Island and Christmas Island were all detonated at sufficient height to avoid local fallout. At Johnston Island 7 high altitude (H_{det}>21000 m) and 5 atmospheric tests were conducted, while at Christmas island 24 atmospheric tests were conducted in the period August 1958 – November 1962 (Björklund and Goliath, 2009).

2.2.3 French test sites

A series of 17 low yield (0.0007 – 0.12 Mt) tests was carried out on ground or in tower (Reggane desert) and underground (Ekker) in the period 1960 – 1966 (Björklund and Goliath, 2009). The French aboveground testing in Algeria were carried out during the partial test ban treaty period (1958 – 1961). Air concentrations of radioactivity at this time were low, and debris from at least one of the tests was detected at distant locations (Hvinden, 1960; Patterson and Lockhart, 1960; Lindblom, 1961). Lindblom (1961) found that particles from the largest French atmospheric detonation in Algeria (13 February 1960, 0.07 Mt) had reached Sweden. Local contamination associated with close in fallout from the aboveground detonations and venting from underground tests has also been reported (IAEA, 2005).

2.3 Accidents during transport of nuclear weapons

UNSCEAR (1993) lists fourteen accidents involving the loss of nuclear devices, the two most severe were the Palomares (1966) and Thule (1968) aircraft accidents involving the disintegration of two and four thermonuclear devices, respectively. Later investigations (e.g. Lind *et al.* (2005), Jimenez-Ramos *et al.* (2007), Lind *et al.* (2007), Eriksson *et al.* (2008)) indicated the weapon material to be mixed U / Pu metal oxide with low $^{240}Pu/^{239}Pu$ atom ratios. There was no nuclear yield involved in any of the accidents, and contamination was limited to the local scale (Mitchell *et al.* (1997) and references therein).

2.4 Releases from the nuclear fuel cycle

Releases of radionuclides from the nuclear fuel cycle are associated with mining and milling, reactor operation, reprocessing and inadequate storage or dumping of waste. Releases from mining and milling operations are first and foremost associated with remnants of U and daughter products in the mine tailings, and give rise to higher than background releases of natural radionuclides in the vicinity of the sites (UNSCEAR, 1993). Nuclear reactor operation and post irradiation fuel handling have caused both operational and accidental releases of radionuclides to the environment. Reprocessing plants release fission products and transuranium elements, mainly to the aquatic (marine and rivers) environment. Long lived nuclides (e.g. ^{3}H, ^{14}C, ^{85}Kr, ^{99}Tc, ^{129}I and ^{137}Cs) are of major concern (UNSCEAR, 1993))

2.4.1 Nuclear reactor accidents

UNSCEAR (1993) states six accidents that have caused exposures of the general public at four installations handling nuclear fuel (two at the FSU Mayak production

centre; long term releases from the Windscale piles and the Windscale fire; the Three Mile Island accident, and the Chernobyl accident). The Fukushima accident in 2011 also caused the release of radionuclides to the atmosphere. The accident took place out of the range of the samples employed in the present work, and furthermore, Pu contamination in Norway from this accident is unlikely. Of the accidents mentioned in UNSCEAR (1993), only the Chernobyl accident and possibly the Windscale fire could be of significance to Norwegian territories.

Windscale

The Windscale piles were two air-cooled, graphite-moderated reactors in operation in the period 1950 – 1957. Major releases of radionuclides have happened at two occasions. Long term release occurred during normal operation in the period 1952 – 1957; fuel elements with broken cartridges and fuel elements jammed in the coolant stream were oxidised at low temperature resulting in the release of U-matrix particles with fission and activation products (Chamberlain, 1987; Salbu *et al.,* 1994; Smith *et al.,* 2007). Particles were described as large (10 – 250 μm), flake like and layered (Figure 6); the structure of the particles could lead to longer residence times in the atmosphere than comparable spherical particles (Salbu *et al.,* 1994).

During a routine operation of annealing Wigner energies stored in the graphite moderator of one of the reactors, the 7 October 1957, the moderator overheated resulting in a fire (UNSCEAR, 1993; Garland and Wakeford, 2007). Volatiles and particulates were released at several occasions during attempts to cool the moderator and extinguish the fire (UNSCEAR, 1993; Garland and Wakeford, 2007). An estimated 1 – 42 g Pu was released (Garland and Wakeford, 2007), and since the reactor was operated for weapon production purposes $^{240}Pu/^{239}Pu$ atom ratios can be assumed to be low.

Due to the high temperatures and low air flows during the accident the release of U particles would have been low (Chamberlain, 1996). The debris plume from the Windscale accident moved south – southeast towards central Europe before turning northwards and was observed to pass over Norway (Storebø, 1958; Hvinden and Lillegraven, 1963; UNSCEAR, 1993; Garland and Wakeford, 2007).

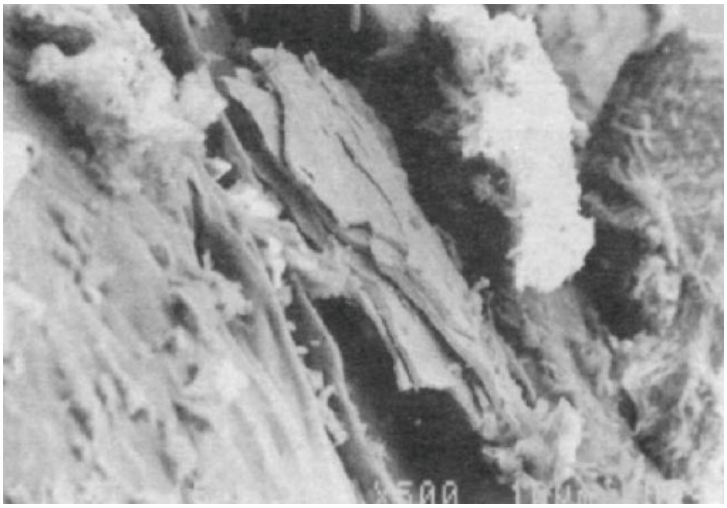

Figure 6. Fuel particle captured in the vicinity of the Windscale plant in 1956, demonstrating the flake like structure of the particles released during 1952 – 1957. From Salbu *et al.* (1994)

The Chernobyl accident

During system testing on Saturday 26 April 1986 one of the reactors at the Chernobyl power plant was run at low output. The reactor output became unstable due to a combination of design weaknesses and operator errors. The power level of the reactor increased rapidly and caused a release of the primary coolant and pressure loss within the reactor. The overheated coolant (light water) vaporized instantaneously. A fuel vapour explosion followed, disrupting the core and parts of the building, exposing the graphite moderator to the atmosphere (UNSCEAR, 2000b).

Radioactive debris was released in the initial explosions as well as from the subsequent fire, which lasted until the 5 May. Vast areas of Europe were severely affected, and both volatile species as well as particles originating from the accident have been identified at large distances from the plant, including Scandinavia, 2000 km away from the accident site (e.g. Devell *et al.* (1986), Backe *et al.* (1987) Salbu (1988a), Pöllänen *et al.* (1997) and references therein, UNSCEAR (2000b) and references therein, Salminen-Paatero *et al.* (2012)). About 6 – 8 tons of uranium based fuels with an estimated 20 kg of Pu isotopes (^{239}Pu – ^{242}Pu) were released during the Chernobyl accident (UNSCEAR, 2000b).

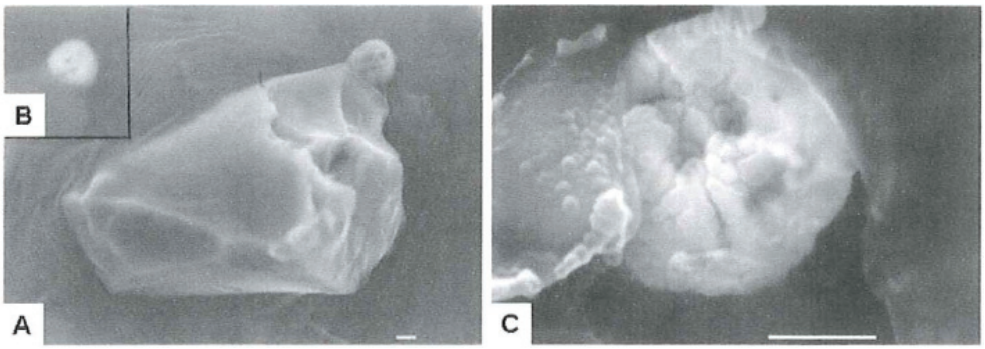

Figure 7. Ru-particle originating from the Chernobyl accident attached to a carrying silicon particle. The particle was retrieved in Valdres Norway in 1987 (Salbu, 1988b; Lind, 2006). A) General overview of the Ru – silicon conglomerate B) BEI image of the Ru-particle C) High magnification image of the Ru-particle. Bar = 1 µm.

Isotope ratios calculated from core inventory estimates differ significantly from global fallout ratios. A $^{236}U/^{239}Pu$ atom ratio of 9.3 was estimated while for Pu isotope ratios, estimates range considerably (UNSCEAR, 2000b). The $^{240}Pu/^{239}Pu$ ratios was estimated to range between 0.34 and 0.44, $^{241}Pu/^{239}Pu$ between 0.134 and 0.273, and $^{242}Pu/^{239}Pu$ between 0.046 and 0.042 (UNSCEAR, 2000b). Measured $^{240}Pu/^{239}Pu$ atom ratios within the exclusion zone and in air in Vilnius (Lithuania) during passage of the plume from the accident ranged between 0.38 – 0.41, and fits well with the estimates (Muramatsu *et al.,* 2000; Lujaniene *et al.,* 2009).

Publications addressing debris from the Chernobyl accident deposited in Fenno-Scandinavia indicate highly varying $^{240}Pu/^{239}Pu$ atom ratios. Lindahl *et al.* (2004) found atom ratios in the range 0.16 – 0.44, mainly due to mixing with global fallout. Salminen-Paatero *et al.* (2012) on the other hand found ratios in the range 0.13 – 0.53 in samples associated with fresh deposition (hot particles, commercially exploited peats, and lichens). The large variation in Pu atom ratios observed in the latter work likely reflects the Chernobyl core included U fuels with varying (low and high) burn up.

Debris from the Chernobyl accident moving towards Fenno-Scandinavia was vertically divided into two main air layers. Materials in the upper layer mainly affected Finland, while materials from the lower layers affected Sweden and Norway (Saltbones, 1986; Persson *et al.,* 1987; Pöllänen *et al.,* 1997). Deposition of debris from the Chernobyl accident is addressed in paper I and II.

Nuclear fuel reprocessing

Several reprocessing plants have been in operation in the northern hemisphere. According to Skipperud (2004), three Former Soviet union weapon production plants: Chelyabinsk-65 (Mayak) since 1948, Tomsk-7 since 1953 and Krasnoyarsk-27 since 1958; two UK weapon production and later reprocessing plants: Windscale, since 1951, Dounreay, since 1955; and the French COGEMA la Hague plant (in operation since 1965) are or have been in operation. The main releases of radionuclides from these plants have been to rivers or the ocean. The Ob and Yenisei Rivers, which were contaminated by FSU weapon production plants eventually discharge into the Kara Sea and the Arctic. Similarly, effluents from the Sellafield, Dounreay and La Hague have been discharged into surface waters in the Irish Sea and the English Channel, respectively, ultimately leading to the North Sea. Several papers have addressed the transport of effluents from European and FSU reprocessing and weapon production into the Arctic (e.g. Raisbeck *et al.* (1995), Beasley *et al.* (1998a) and Herrmann *et al.* (1998)). The isotopic composition of Pu in sediment profiles collected close to the Sellafield reprocessing plant represent a crude history of the reprocessing activities at the site. Pu from the early period (~1960) of weapons grade Pu (~0.06), later $^{240}Pu/^{239}Pu$ in the effluents increased, and peaked around 1980 with a $^{240}Pu/^{239}Pu$ ratio of ~0.25 (Kershaw *et al.,* 1995).

2.5 Satellite accidents

Six satellites carrying radioisotope thermal generators (RTG) have been destroyed during launch and re-entry in the period 1964 – 1983 (Krey *et al.,* 1979; Leifer *et al.,* 1987; UNSCEAR, 1993). For three of these cases the RTG or reactors have been recovered entirely or lost at sea without further releases of radionuclides. Two of the three remaining satellites disrupted completely during re-entry, while the last satellite disintegrated partially or completely upon re-entry (UNSCEAR, 1993).

SNAP-9A

In 1964, a Transit navigational satellite equipped with a SNAP-9A RTG disintegrated upon re-entry into the atmosphere causing the release of 950 g ^{238}Pu into the southern hemisphere stratosphere (Hardy *et al.,* 1973; UNSCEAR, 1993). Due to the low ^{238}Pu background, the input of ^{238}Pu from this accident was considerable. The inventory of ^{238}Pu in the environment increased threefold with a 20 : 80 distribution between the northern and southern hemisphere (Hardy *et al.,* 1973).

Cosmos-954

In 1978, the FSU Cosmos 954 satellite partially burned during re-entry. Following disintegration volatiles were largely released in the stratosphere, while large shrapnel and refractories scattered over vast areas in Canada. The power source of this satellite has been indicated to contain enriched U (Krey *et al.,* 1979). Uranium isotopes and an estimated 120 g of ^{239}Pu was released during the accident (UNSCEAR (1993) and references therein).

Cosmos-1402

In 1983 the FSU Cosmos 1402 satellite re-entered the atmosphere and disintegrated over the South Atlantic Ocean. This accident caused releases of 50 kg of U highly enriched in ^{235}U (Leifer *et al.,* 1987). In 1984 and 1985, altered ^{235}U/^{238}U activity ratios (Bakhtiar *et al.,* 1985) and $^{239+240}$Pu elevated activity concentrations (Salaymeh *et al.,* 1987) in rainwater in Fayetteville (36 ºN) indicated that debris from the Cosmos 1402 had reached the northern hemisphere.

3 Transport and atmospheric behaviour

Transport and deposition of radioactive debris released to the atmosphere depends on a number of factors. Both source related characteristics like chemical reactivity, hygroscopicity, particle size and release height, as well as environmental conditions like wind direction, humidity, land topography and precipitation affect residence time and deposition.

This chapter will briefly summarise source related and environmental factors affecting the atmospheric transport and deposition of radioactive aerosols and gases.

3.1 Plume rise

During nuclear detonations very large amounts of energy were released within a very short time range. Consequently, the device, supporting materials and environmental materials close to the detonation reached temperatures of $10^6 – 10^7$ K (Glasstone and Dolan, 1980). The extremely hot gases and vapours formed a rapidly rising and expanding fireball containing device remnants, supporting materials and incorporated environmental materials. The height to which the debris cloud rose depended on the detonation height, detonation yield, and meteorological conditions (Glasstone and Dolan, 1980). Atmospheric compartments and cloud rise observations according to Peterson (1970) are given in Figure 8 and Figure 9.

Low yield detonations released the main part of their debris into the troposphere, (Figure 9). Debris injected in the troposphere had a mean residence half-life of 72 days (Holloway and Hayes, 1982), and although it has been postulated that the debris was deposited mainly at the latitude bands in which the detonation took place, debris have been shown to spread significantly (Machta *et al.,* 1956; Hvinden *et al.,* 1964) (paper II).

Insertion of debris above the tropopause started to occur for detonations larger than 0.4 Mt in polar regions and 1 Mt in equatorial regions (Peterson, 1970). Debris injected into the stratosphere is indicated to have had residence times in the range 5 months to 2 years, depending on latitude, injection height and season (Junge, 1963; Telegadas and List, 1969; Peterson, 1970). The distribution of debris between the compartments of the stratosphere had significance not only for the residence time, but also the distribution of debris between the hemispheres. Debris injected into the lower polar stratosphere (9 – 17 km) had estimated residence half-lives of 5 months before being deposited in a 20:1 distribution between northern and southern hemisphere respectively. Debris injected in the upper north polar stratosphere on the other hand

had estimated residence half-lives of 2 years and was deposited in a 4:1 distribution between the northern and southern hemispheres (Peterson, 1970).

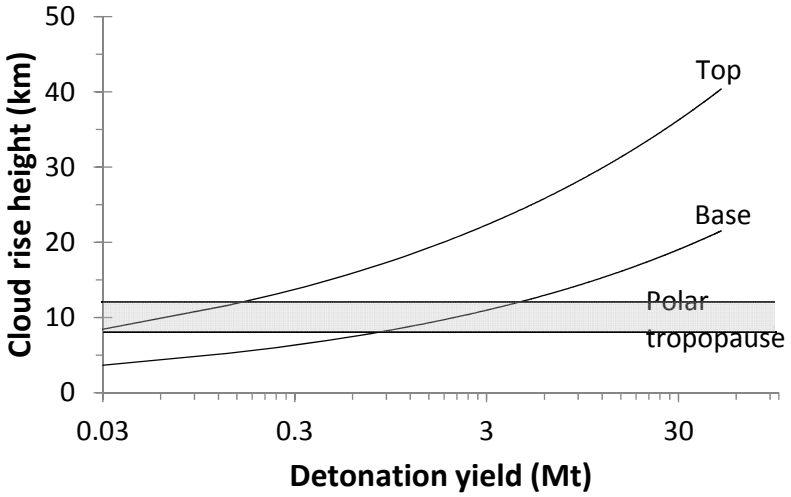

Figure 8. Elevation of base and top of mushroom cloud caps from nuclear detonations as a function of detonation yield in polar regions according to Peterson (1970). The shaded box represents approximate locations of the summer (upper confinement) and winter (lower confinement) polar troposphere.

The stratosphere is assumed to serve as a relatively well mixed inventory of radionuclides from diverse high yield and high elevation detonations, likely due to mixing effect in the lower stratosphere prior to transfer to the troposphere. Nevertheless, it has been indicated that clouds of concentrated activity existed in the stratosphere for months after detonations (Storebø, 1959).

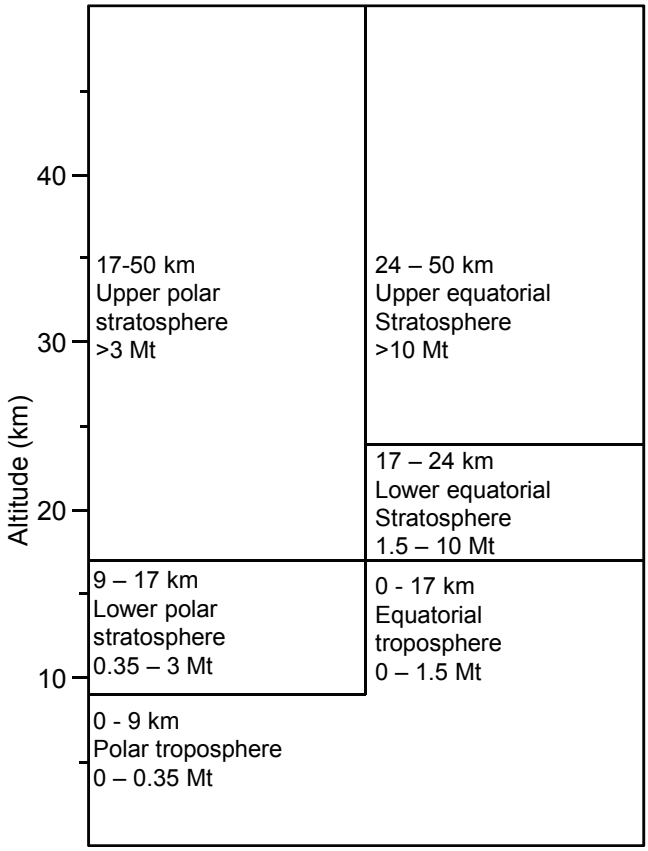

Figure 9. Atmospheric compartments modified from Peterson (1970). Yield numbers indicate the size of detonations estimated to inject more than 50 % of its debris in the respective compartments. Polar latitudes defined as latitudes above 30 °N or S.

3.2 Atmospheric circulation

The general atmospheric circulation is based on three idealized large circulation patterns: the Hadley cell, Ferrel cell and the polar cell (Figure 10). Chapters 3.2.1 through 3.2.4 give a brief presentation of the circulation patterns and the effects on a regional scale. The description is based on Ahrens (2003), unless otherwise stated.

3.2.1 Hadley cell

The highest energy transfer by solar irradiation is usually at tropical latitudes, near equator. This causes the formation of warm moist air which rises until it reaches the tropopause where it is deflected polewards (the tropopause represents a barrier through which tropospheric air generally does not penetrate). The increased elevation and the adiabatic cooling of the air (also possibly the encountering of cold tropopause

air) cause the formation of precipitation, and the rising air keeps the tropopause suspended here at a higher elevation than further north and south. The air deflects and moves polewards while losing heat by radiation on the way south / north. Subsidence patterns starts to emerge around 30 °N/S (the subtropics). The subsidence and convergence of winds from equator causes high pressure areas of surface air to emerge at these latitudes. The higher air pressure forces surface air to move towards equator and the poles, due south or north; however, the Coriolis Effect deflects the wind towards its right and causes surface winds between equator and 30 °N/S to be moving in an easterly direction.

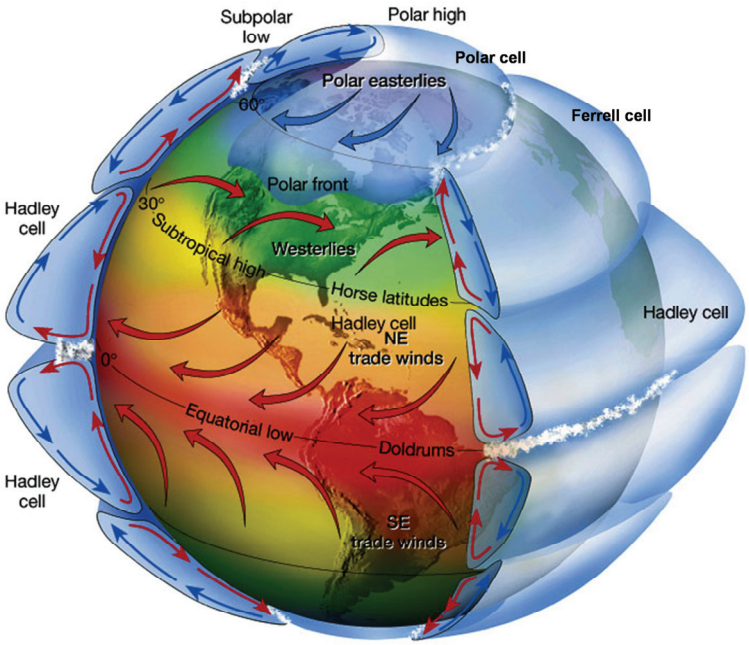

Figure 10. Atmospheric circulation patterns according to Lutgens and Tarbuck (2001).

3.2.2 Ferrel cell

The increased surface pressure at subtropical latitudes (30 – 60 ° N / S) caused by the Hadley cell forces mild air to be shifted northwards. Due to the Coriolis effect the prevailing wind direction in this cell is westerly. Further north, at latitudes depending on season and local circumstances the northwards moving air encounters cold polar southwards moving air and forms the polar front of low pressure at approximately 60 °N. At the polar front air masses rise and again move towards the subtropics and the poles.

3.2.3 Polar cell

Driven partially by the northwards moving air from the polar front and partially by the subsiding air (and high pressure) at the poles, the polar cell cause easterly winds. As mentioned above the polar front is not stationary and the polar cell may extend as far south as 40 °N covering substantial areas of snow covered continental Eurasia and North America in winter (Barrie, 1986; Warneke, 2002).

3.2.4 Arctic contamination

Several authors have indicated that continental Eurasia is an important contributor to arctic pollution (e.g. Barrie and Hoff (1984); Barrie (1986), Barrie *et al.* (1992), Stohl (2006)). During winter the arctic air mass extends as far south as 40 °N over continental Eurasia and Northern America; the air mass form an isolated dome limited southwards by the polar front. A semi-permanent high pressure area over Siberia forces transport of tropospheric air on its west side towards the Arctic, while a high pressure ridge above North America extracts air southwards from the arctic (Barrie, 1986; Barrie *et al.,* 1992; MacDonald *et al.,* 2000). Fluctuations in the transport have been observed to depend on the North Atlantic Oscillation (NAO) defined as the pressure difference between a permanent low pressure area above Iceland and a permanent high pressure above the Azores / south-west Europe (Walker and Bliss, 1932). Transport of tropospheric air masses from Eurasia and Northern America towards the Arctic is stronger during periods of a positive North Atlantic Oscillation index, defined as a large difference in the atmospheric pressure at the mentioned locations. The effect is largest for transport from Europe and least for transport from Asia (Eckhardt *et al.,* 2003).

3.3 Importance of particle characteristics

During the course of an atmospheric nuclear detonation unspent weapon material, fission products, activation products, and device remnants are evaporated by the energy released in the detonation, and form a fireball. Upon expansion and interaction with the surrounding atmosphere the fireball cools and eventually reach the condensation temperature of the different elements present (Junge, 1963).

For particle categorisation, important distinctions arise between surface detonations and air detonations. Air detonations were those detonations carried out at sufficient height to avoid large amounts of surface materials being incorporated into the fireball. Usually the limit between a surface detonation and an air detonation is set by the expression $H=55w^{0.4}$, where H is the height above ground of the detonation and w is the yield in kt (Peterson, 1970). Detonations carried out below this height are denoted

surface detonations, as the fireball from the detonations is in contact with the surface. Local deposition of debris is higher, and in addition larger particles with a higher incorporation of environmental materials are produced. High yield tests, especially FSU tests at Novaya Zemlya were usually performed sufficiently high above ground to avoid interactions between the fireball and the ground (UNSCEAR, 2000a). According to Grønhaug (2001), most FSU air detonations took place above a height of $H=100w^{0.33}$, thus ensuring very little interaction with ground materials.

Air detonation particles formed after condensation of device remnants alone or onto atmospheric particulates. The resulting particles were predominately spherical in shape and with a uniform distribution of radioactivity throughout (Crocker *et al.,* 1966; Heft, 1970; Peterson, 1970). Particle diameters in the range 0.01 - 20 μm were frequently reported, e.g. Sisefsky (1961), Sisefsky (1966), Glasstone and Dolan (1980). The particle population after surface detonations tended to form two distinct groups. One group which resembled the air detonation particles mentioned above, and the other group formed from surface materials directly affected by, or drawn into the fireball. The latter group of particles were generally larger and more irregular in shape following condensation of debris onto unmelted or partially melted environmental materials (Heft, 1970). Furthermore, the distribution of radioactivity was more uneven in this group, the activity tended to be higher on the surface of the particles (Crocker *et al.,* 1966; Glasstone and Dolan, 1980).

3.4 Factors affecting atmospheric residence time and deposition

The residence time of particles in the atmosphere is determined by the injection height, particle characteristics and meteorological conditions during release and deposition. Larger particles (>20 μm) are deposited relatively rapidly to form local fallout (Junge, 1963). Reports of larger particles transported over a long range are rare e.g. Mamuro *et al.* (1965), Pöllänen *et al.* (1997). Most particles detected at some distance from the detonation or accident site are substantially smaller than 20 μm (e.g. Sisefsky (1966), Kemmochi (1966), Persson and Sisefsky (1971), Pöllänen *et al.* (1997)).

Small particles are not efficiently removed from the atmosphere by gravity alone, e.g. Storebø (1960). Instead, such particles have been found to be subject to considerable wind transport, and have been retrieved at long distances from the detonation sites (Sisefsky, 1961; Mamuro *et al.,* 1962; Mamuro *et al.,* 1963). Sisefsky (1961) located and described more than 900 particles from high yield detonations at Novaya Zemlya in September and October 1958. These highly radioactive particles were captured in the low stratosphere above central Sweden some 17 days after the detonation. They

were found to be spherical, and in the size range 0.2 – 5 μm, the lower limit being set by the resolution of the optical microscope used. Fallout particles with diameters up to 14 μm originating from detonations at Semipalatinsk or Novaya Zemlya have also been retrieved in Japan, some 4000 - 6000 km from the detonation sites (Mamuro *et al.,* 1962). Debris from Chinese nuclear tests was retrieved in Sweden on several occasions, e.g. Sisefsky (1966), (1967), Sisefsky and Persson (1971) and Persson and Sisefsky (1971). Particles were captured above and below the tropopause as well as on ground level after transit times as short as 8 days. A range of different particles were described, from dense relatively small (0.2 – 5 μm) particles originating from air detonations to larger less dense and insoluble particles from surface detonations. Finally, particles from the Chernobyl accident were transported and deposited far from the accident site. Pöllänen *et al.* (1997) A comprehensive review of Chernobyl particles retrieved at various sites in Europe can be found in Pöllänen *et al.* (1997).

Atmospheric particles generated in nuclear detonations rapidly become a part of the atmospheric particle population. As such, they are subjected to the same processes as natural and other anthropogenic particles. The most important mechanism for the removal of tropospheric particles is wet deposition, in which the particles act as cloud condensation nuclei (CCN), onto which atmospheric moisture condenses. Water insoluble particles larger than ~0.1 μm and water soluble particles larger than 0.01 μm may serve as CCN (Wallace and Hobbs, 2006). Further, particles may be incorporated into existing water droplets by diffusion (diffusional collection) or by impact with falling precipitation (inertial collection) (Wallace and Hobbs, 2006). Precipitation thus removes (radioactive) particles from the atmosphere and deposits these on the ground, i.e., there is a correlation between mean precipitation loads and deposition of radioactive debris (Storebø, 1959; Storebø, 1968; Lee *et al.,* 1997; Palsson *et al.,* 2013).

3.5 Post depositional processes of relevance to the present thesis

Humic surface soil

Refractory radionuclides released during high temperature events like nuclear weapon detonations and power plant accidents are assumed to be deposited as particles or fragments (IAEA, 2011). No publications have been found which directly addresses the mobility of radioactive particles in natural soils. However, several publications have shown that a major proportion of GFO-related Pu and Cs still resided within the upper 10 - 15 cm of undisturbed soils, and that the concentration decrease exponentially with depth (e.g. (Bunzl *et al.,* 1995; Lee and Lee, 2000; Lee and Lee,

2001)). Cs and Pu seem to be strongly bound to both organic and mineral soils (Bunzl *et al.,* 1998; Lee and Lee, 2001; Skipperud, 2004).

Ice core

Contaminants are deposited onto the glacier surface with precipitation (wet deposition) or directly (dry deposition). Meltwater percolation occurs for glaciers in which melting during the warm seasons exceeds the infiltration capacity of the annual layer. Consequently, meltwater containing contaminants percolate past the annual layer potentially disturbing the stratigraphy. The estimated melt index of Svalbard glaciers ranges within 15 – 25 %, and the effective percolation depth of the Austfonna glacier is estimated to range within 2 – 5 years (Tarussov, 1992). Pinglot *et al.* (2003) estimates a downward migration corresponding to between 0 and 1.6 year for the AUS-99 ice core investigated in the present work. The Austfonna ice core has been dated based on the ^{3}H concentration profile, with the 1963 ^{3}H peak at 21.3 m physical depth (Watanabe *et al.,* 2001). However, ^{3}H is incorporated in the glacier as water, and may behave more conservatively than particular radionuclides upon infiltration of meltwater.

4 Materials and methods

Atmospheric radioactive debris can be characterised by the activity concentrations, radionuclide speciation and atom ratios. Particle diameter, shape and density reveal important information on the release scenario, while the nuclide and isotopic composition serves source and age identification purposes. During the course of the present work, digital autoradiography has been employed in order to locate and isolate individual particles captured in air filters, ESEM (Environmental Scanning Electron Microscope) has been applied for further isolation of potential particles, while synchrotron based x-ray microtechniques (Hasylab) has been attempted for speciation analysis of hotspots identified by autoradiography. Concentrations of U and Pu, and respective atom ratios in the samples have been determined by SF-ICP-MS and AMS. Chapter 4 describes the sample preparation and analytical methods used in the present work.

4.1 Samples investigated

Humic surface soil samples

The Humic surface soil samples were collected in 1990 and 2005 (courtesy of Eiliv Steinnes) at 45 locations across Norway, representing all regions (Figure 11). An area of 330 cm^2 to a depth of 7 cm was sampled from the surface soil layer at each location. Assuming that global fallout has been retained within the sampling depth, the samples represent the accumulated deposition of radionuclides released to the atmosphere. Although great care was taken in order to sample exactly the same locations in 1990 and 2005, minor deviations could occur due to problems with relocating the exact position. The samples were air dried at room temperature prior to storage.

Ice core samples

The ice core was drilled at the summit of the Austfonna glacier (79.8333 °N, 24.0167 °E, and 750 m a.s.l.) in 1999 to a depth of 289 m (Figure 12). The ice core was cut into appropriate sections based on information available from previous studies of the ice core (Pinglot *et al.,* 2001; Watanabe *et al.,* 2001; Pinglot *et al.,* 2003) combined with gross beta activity concentrations in Norwegian ground level air (T. Bergan, pers. comm.).

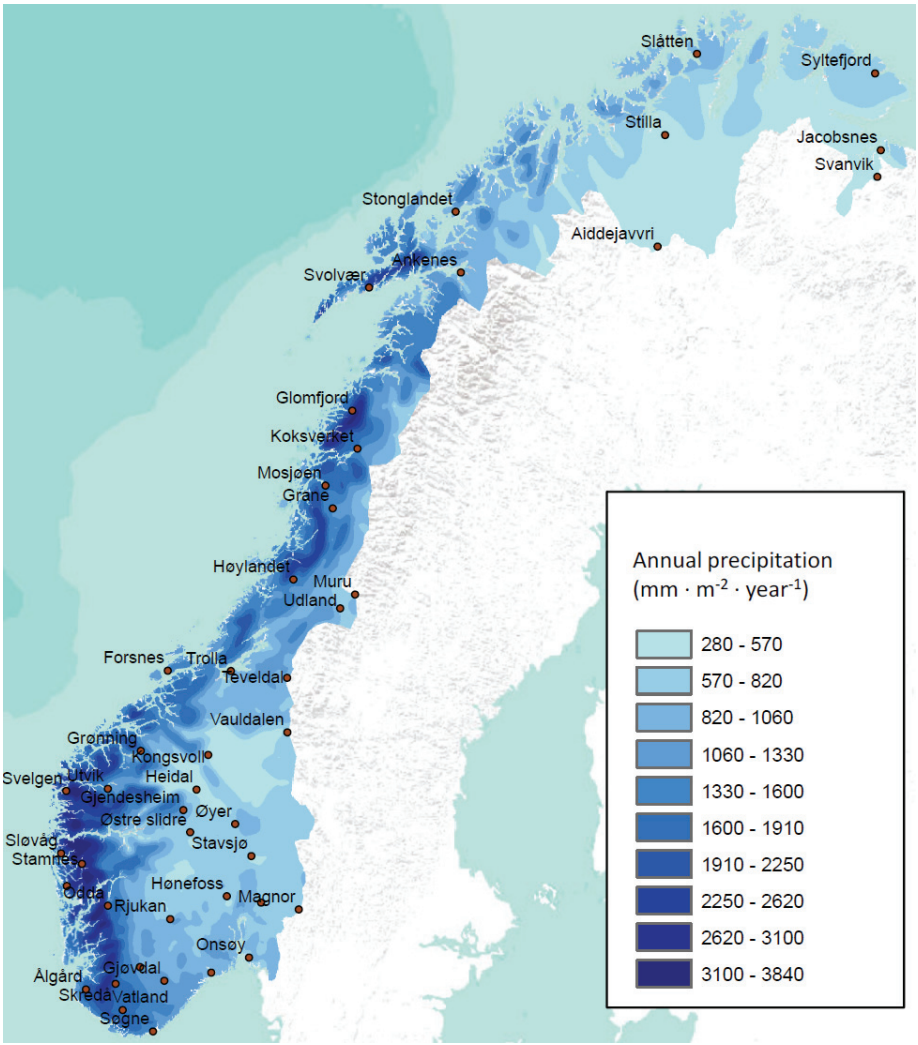

Figure 11. The sampling locations for humic surface soil samples (paper III). Mean annual precipitation indicated.

Air filter samples

As a consequence of atmospheric nuclear weapons testing from 1945 onwards, the Norwegian Defence Research Establishment (FFI) operated a surveillance and monitoring program for radioactive fallout (Njølstad, 2006). Gross beta activities were measured in deposition (wet and dry deposition), milk and surface air from 1957 until the mid-1980s. Radioactivity in ground level air was monitored through the operation of 2 – 10 air filter stations nationwide (cf. Figure 12). According to Lockhart *et al.* (1964) the filters were specified to retain 99.9 % of atmospheric

particulates larger than 0.3 μm at the flow rates used (18 m^3 h^{-1}). The filters were changed every 24 h, and gross beta activities were analysed 48 – 72 h after the collection (Hvinden, 1958).

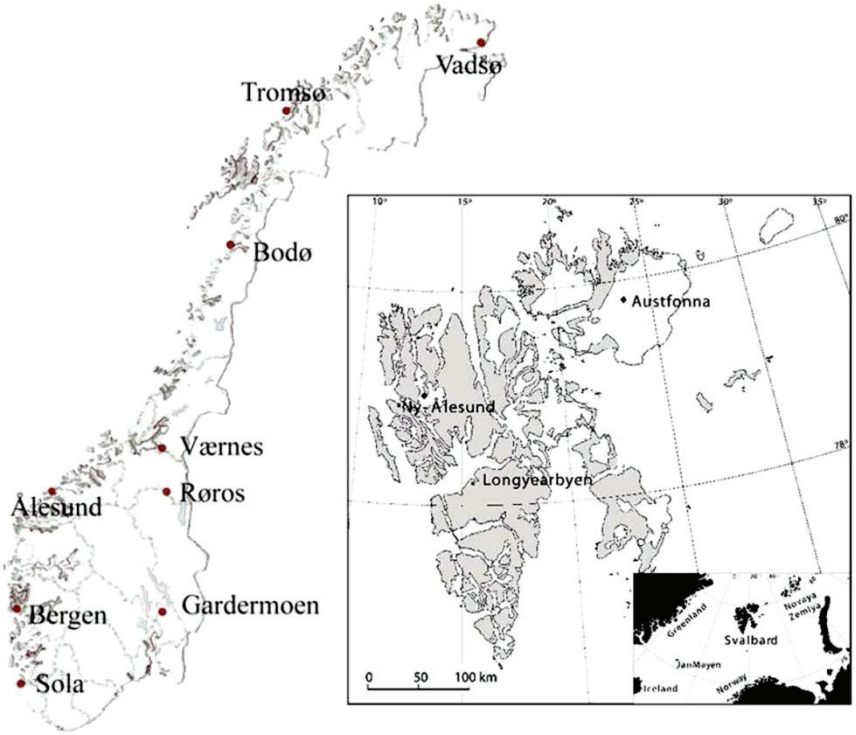

Figure 12. Map of and air filter stations in mainland Norway (right), Svalbard with the sampling location of the AUS-99 ice core on Austfonna (left).

Air filters were primarily selected from Bergen, representing a southern coastal site, Røros representing an inland site and Vadsø for its proximity to the NZ testing site. The sample selection was designed to identify periods of atmospheric nuclear testing, hence filters from the pre-moratorium (1957 and 1958), immediately after the cessation of the moratorium (September 1961 and onwards) and filters form the periods of spring maximum deposition in 1962 and 1963 were analysed. Filters were also selected when high gross beta activities indicated the arrival of debris from atmospheric nuclear weapon testing. Finally three samples were prepared representing ten consecutive days of air filter sampling at Bergen (1957) and Røros (1961 and 1962); these samples were prepared without the use of yield monitor, in order to measure $^{242}Pu/^{239}Pu$, and $^{244}Pu/^{239}Pu$ atom ratios.

An overview of the samples analysed in the present work is given in Table 2.

Table 2. Overview of the samples analysed in the present work

Sample type	Time period	Main purpose and limitations	Analytes	Key sources
Humic surface soils, mainland Norway, samples from 45 sites in 1990 and 2005, (n=87)	1945 – 2005	Geographical distributions, fallout inventories, source identification and wash out.	^{137}Cs, ^{238}Pu ^{239}Pu, ^{240}Pu, ^{241}Pu, ^{242}Pu	Integrated fallout: NWT, satellite accidents, Windscale and Chernobyl accidents
Ice core, Nordaustlandet, Svalbard (n=9)	~1949 – 1999	Temporal distribution, source assessment. Low time resolution	^{234}U, ^{236}U, ^{239}Pu, ^{240}Pu, ^{241}Pu	Chronology, all sources. NWT, satellite accidents, reactor accidents
Air filters, mainland Norway, 2 – 10 stations (n=58)	1957 – 1963	Source identification and transport assessment. Good temporal and spatial resolution. No representation of high yield PPG test period (1952, 1954).	^{234}U, ^{236}U, ^{239}Pu, ^{240}Pu, ^{241}Pu, ^{242}Pu, ^{244}Pu	High time resolution chronology. NWT at Northern hemisphere test sites and global fallout, Windscale accident

4.2 Sample preparation

Sample preparation in mass spectrometry includes all steps necessary to prepare the analytes which are to be measured in a form suitable for the specific instrument. Some important steps are common for several instruments.

Interfering elements is a common problem in most analytical instruments due to mass or energy overlap. This is usually reduced or eliminated by reducing the presence of the interfering species or elements through proper chemical separation. Interferences cannot always be resolved, and an important example is the energy overlap between ^{239}Pu and ^{240}Pu in alpha-spectrometry; this interference arises from the very similar alpha-energies of the two isotopes, and insufficient energy resolution of the spectrometers. Since the two plutonium isotopes have identical chemical properties it is not possible to separate them prior to analysis, leading to ^{239}Pu and ^{240}Pu activities being reported as a sum in alpha spectrometry. Computer based spectral deconvolution techniques may be applied to resolve the individual activities of ^{239}Pu and ^{240}Pu analysed by alpha-spectrometry (e.g. Vintró *et al.* (1996); Pollanen *et al.* (2012)), however, this requires that the samples have sufficient activity. For low activity samples, it is still necessary to apply mass spectrometric methods in order to measure the individual activities of ^{239}Pu and ^{240}Pu. Combined methods which samples are first prepared for and analysed by alpha spectrometry, and thereafter re-dissolved or otherwise liberated from alpha-spectrometry planchets and analysed by mass-spectrometric methods provide additional information in the ^{238}Pu/$^{239+240}$Pu activity ratio (e.g. Skipperud (2004); Michel *et al.* (2007); Cizdziel *et al.* (2008)).

Mass spectrometric methods do not suffer from spectral interferences, as these techniques base the separation on mass differences rather than alpha energy differences. The main interference problem for mass spectrometric techniques arises from the presence of species with the same (mass · energy) / charge ratio as the analyte of interest. Molecular interferences as mentioned above could easily be a problem for ICP-MS, and proper measures must be taken to detect and correct for interferences arising from undissociated molecular species.

Humic surface soil samples

Pebbles and conifer cones were removed from the dried samples, and the samples were ground to a fine powder. Aliquots of ~25 g were analysed for ^{137}Cs by gamma spectrometry. After addition of yield monitor (^{242}Pu) the samples were covered by watch glasses and dry ashed. The ashing temperature was gradually increased to 500 °C to avoid ignition of the samples causing cross contamination and the

formation of refractory species (Vintró and Mitchell, 2006). A temperature of 500 °C was kept for at least 8 h or until the samples were completely ashed. The ashed samples were then leached in aqua regia (3:1 mixture of concentrated HCl and HNO_3), filtered, and the filtrate was taken to dryness by careful evaporation.

Anion exchange of the samples were performed according to the procedure described by Clacher (1995): the dried sample residue was taken up in 50 – 100 ml 8 M HNO_3, and Pu was reduced to Pu(III) by addition of $FeSO_4$ and thereafter oxidised to Pu(IV) by adding $NaNO_2$. The samples were then loaded onto pre cleaned DOWEX 1 x 8 anion exchange columns. Pu and Th are selectively bound to the resin, while U, Am and Po pass through. The column was further cleaned by passing 50 – 75 ml 8M HNO_3. Th was then stripped from the column with 50 ml 9 M HCl and finally Pu was eluted with a 40 ml 1:100 mixture of 50 % HI in 9M HCl. The Pu eluate was evaporated to dryness and re-dissolved in 20 ml 0.5 M HNO_3 for analysis by ICP-MS.

Ice core and air filter samples

The ice core was cut into sample segments (1.5 – 5 kg) covering different fallout periods, as illustrated in Figure 13. In order to preserve the samples uncontaminated, the cutting was performed in a clean room facility at low temperature (-20 °C). The samples were then melted in room temperature in closed pre-cleaned HDPE bottles, and filtrated with a cut-off of 50 nm (Nucleopore 0.05 µm, Whatman Schleicher&Schuell). The filters were dried and subjected to digital autoradiography as described below, while the filtrates were evaporated to dryness. After completed autoradiography the filters were weighed directly into PTFE ultraclave tubes and yield monitors (~17 pg ^{233}U and ^{242}Pu) were added. The ice core filters were digested in 5 ml sub boiled ultrapure HNO_3 (conc.) at high temperature and pressure in an ultraclave unit. The digested filters were recombined with the residues from the dried filtrates, and the sample solutions were diluted to an acid concentration of 8 M.

Most of the air filter were treated as individual samples, and sections corresponding to 110 – 220 m^3 air (1/4 – 1/2 filter) were weighed directly into PTFE ultraclave tubes. Yield monitors (^{233}U and ^{242}Pu, ~17 pg each) were added for quantitative analysis. For the analysis of $^{241}Pu/^{239}Pu$, $^{242}Pu/^{239}Pu$ and $^{244}Pu/^{239}Pu$, grouped air filters were selected from ten consecutive days from October 1957 (filters from Bergen) and during spring peak deposition in 1962 and 1963 (filters from Røros). As it was of interest to analyse the $^{242}Pu/^{239}Pu$ and $^{244}Pu/^{239}Pu$ atom ratios in the grouped sample, a yield monitor was not added to the latter samples.

Pu and U retained on the filters was leached in sub boil ultrapure HNO_3 (conc.) at high temperature and pressure in an ultraclave unit (UltraCLAVE 3, Milestone Ltd). After leaching, the sample solutions were diluted to an acid concentration of 8 M, and filtered.

Separation of Pu from the sample solution followed the procedure described for humic surface soils above. The U fraction was further purified according to the procedure described by Wilcken (2006): the dried U and Am eluate was dissolved in 15 ml 3 M HNO_3 with 0.5 M $Al(NO_3)_3$, and loaded onto pre-cleaned columns containing 2 ml UTEVA ion-exchange resin. The columns were rinsed with an additional 5 ml 3 M HNO_3, and converted to the chloride form with 5 ml 9 M HCl. Am and Po was stripped off the columns with 20 ml 5 M HCl with 0.05 M $(COOH)_2$. U was eluted with 30 ml 0.01 M HCl.

The Pu and U eluates were evaporated to dryness and taken up in 2 ml concentrated HNO_3 with 2 mg Fe as $Fe(NO_3)_3$, and evaporated to dryness again. The residues were baked at 500 ºC overnight. For final target preparation, the Fe / U and Fe / Pu precipitates were pressed into Al sample holders using silver powder as a electric and thermal conductor / binder.

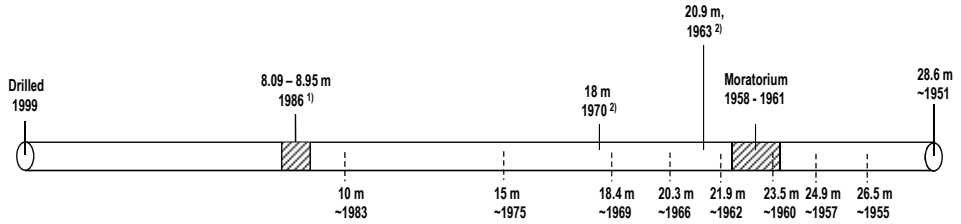

Figure 13 Illustration of the AUS-99 ice core with sample segments indicated.

4.2.1 Location of radioactive heterogeneities

Digital autoradiography

The filters (ice core filtration membranes and air filters) were mounted on paper and subjected to digital autoradiography. During exposure, the background was reduced by placing the imaging plate (Molecular dynamics, GE Healthcare) and the samples in a protective cassette which was again put in a radiation shielding box of lead. Exposure times of four weeks were routinely used, and the exposed plates were scanned in an image plate scanner (Typhoon 8600, Molecular dynamics) within two hours after termination of the exposure. Indications of radioactive heterogeneities were often encountered, and repeated sample splitting and re-exposures resulted in the isolation of small areas of filter (on the order of a few

mm^2) which were mounted onto Al stubs with sticky carbon tape and prepared for ESEM-XRMA-analysis.

Environmental scanning electron microscopy with X-ray micro-analysis (ESEM-XRMA)

Samples isolated by digital autoradiography were analysed by ESEM-XRMA to elaborate the exact position of fallout particles. The samples were run uncoated in the microscope as sample coating may cause interferences in subsequent speciation analysis (Lind, 2006). In order to remediate electrostatic charging of the samples, analyses were performed with the presence of low amounts of atmospheric gas in the sample chamber. To obtain satisfactory specimen penetration depth, counting statistics and detection limits, high acceleration voltages (30 kV) and beam currents (1 – 10 nA) were used.

4.2.2 Determination of concentrations and atom ratios

Determination of ^{137}Cs

Aliquots of the humic surface soil samples, weighed directly into 200 ml NUNC boxes, were measured by low energy (LEGe) gamma spectrometry (Canberra, Meriden CT, USA, relative efficiency 25 % using a purposebuilt geometry setup). The energy resolution (full width at half maximum, FWHM) was 1.76 keV at 1.33 MeV. Counting times ranging between 0.5 and 40 h were used depending on activity to ensure a counting uncertainty below 5 %.

Concentration and atom ratios of Pu isotopes by ICP-MS

Plutonium atom ratios (^{239}Pu, ^{240}Pu and ^{242}Pu (yield monitor)) were determined by SF-ICP-MS (Thermo Finnegan Element 2) in low resolution mode ($R = m / \Delta m = 300$). The sample solutions were introduced to the instrument by self-aspiration at a rate of 1.8 ml min^{-1}. Concentrations of ^{239}Pu and ^{240}Pu were determined through the obtained $^{239}Pu/^{242}Pu$ and $^{240}Pu/^{242}Pu$ ratios. Procedural and analytical blanks as well as standard reference materials (IAEA 384, IAEA 300, NIST 4353a) were analysed for method verification.

Determination of Pu and U isotopes by AMS

The relative abundances of Pu (^{239}Pu, ^{240}Pu, ^{241}Pu, ^{242}Pu and ^{244}Pu) were determined using the 14 UD tandem accelerator at the Australian National University (ANU), Canberra. Three isotopes (e.g. ^{239}Pu, ^{240}Pu and ^{242}Pu (yield monitor)) were counted sequentially in each set up, and the count rates were normalised against the most abundant isotope (^{242}Pu for samples with added yield monitor, otherwise ^{239}Pu). Counting times varied between 60 and 300 seconds were used, depending on

concentrations. A certified reference material for Pu atom ratios (UKAEA No. UK Pu 5/92138) was measured repeatedly during analyses. The $^{242}Pu/^{239}Pu$ atom ratio precision for the reference material was 3.1 % (standard deviation, n=13). Detection limits were calculated based on analytical blanks spiked with 17 pg ^{242}Pu. The detection limits were 4.2 and 1.3 fg for ^{239}Pu and ^{240}Pu respectively. Some samples were prepared without yield monitor in order to analyse ^{241}Pu, ^{242}Pu and ^{244}Pu. For these samples a quantitative detection limit cannot be established. However, blanks without yield monitor run for ^{241}Pu, ^{242}Pu and ^{244}Pu had very low count rates corresponding to 0, 0.48 and 0.1 counts per minutes for the three isotopes, respectively. Due to the low background, blank corrections were not applied to these results.

Similarly to the Pu analysis, three U isotopes (^{233}U (yield monitor), ^{234}U and ^{236}U) were measured sequentially, and the concentrations of ^{234}U and ^{236}U were established based on the measured $^{234}U/^{233}U$ and $^{236}U/^{233}U$ atom ratios. Analytical blanks spiked with 20 pg ^{233}U gave 115 and 17.5 counts of ^{234}U and ^{236}U for counting times of 0.5 and 3 minutes respectively, corresponding to detection limits of 0.9 pg and 24 fg of ^{234}U and ^{236}U respectively. Blank corrections were applied to the results of all U samples.

4.3 Methods employed in the present thesis

Radionuclides can be identified and quantified based on radiometric as well as mass spectrometric methods. A range of different methods exhibiting different advantages and drawbacks are available for the purpose. Radiometric methods include α, β and γ spectrometry, while mass spectrometric methods include inductively coupled plasma – mass spectrometric methods (ICP-MS), Accelerator Mass Spectrometry (AMS), Thermal Ionisation Mass Spectrometry (TIMS) and Resonance Ionisation Mass Spectrometry (RIMS).

Radiometric methods, e.g. alpha spectrometry offers low detection limits (e.g. $\sim 1 \times 10^{-14}$ g ^{239}Pu). However, long counting times, and insufficient resolution for quantifying ^{239}Pu and ^{240}Pu individually is a serious drawback (e.g. Hou and Roos (2008) and Skipperud (2004)). Mass spectrometry on the other hand offers more than sufficient resolution, and provides an important tool for source identification, namely the $^{240}Pu/^{239}Pu$ atom ratio.

The rest of the chapter focus on the instrumental techniques used in the present thesis. The isobaric interference from ^{238}U precludes the determination of ^{238}Pu. A combined sample preparation for alpha spectrometry and mass spectrometry is frequently used in order to reveal the $^{238}Pu/^{239+240}Pu$ activity ratio and $^{240}Pu/^{239}Pu$

atom ratio in the same sample, e.g. Ketterer *et al.* (2004), Lujaniene *et al.* (2009), Salminen-Paatero *et al.* (2012).

4.3.1 Mass spectrometry

In mass spectrometry, different elements and isotopes of the elements are separated from each other by the mass to charge ratio. A multitude of different mass spectrometers are in use, their general working principle is to accelerate analyte ions to high energies, and separate the different masses by applying magnetic and / or electrostatic fields.

Interferences in mass spectrometry arise from species with the same (mass · energy)/ charge ratio as the analyte of interest. Molecular, poly charged or isobaric interferences may cause problems for precise determination of concentrations and atom ratios. Different strategies are available for the remediation of these interferences. Matrix separation (ion exchange or solvent extraction) resolves a range of interferences, but is labour intensive and time consuming.

Inductively coupled plasma – mass spectrometry (ICP-MS)

ICP-MS is a versatile and relative inexpensive technique offering good precision and high throughput of samples for measurements of both isotope ratios and concentrations in a range of sample types. Sample introduction systems for the direct volatilisation of solid samples exists, as does ultra-low volume methods, and absolute detection limits in the attogram-range for U and Pu has been reported for the latter (Schaumlöffel *et al.,* 2005).

The analytes are introduced to the instrument as an aerosol or as gas and transported by an argon carrier gas to a hot plasma (6000 - 8000 K) where the sample atoms are ionized to a high degree. The ionised analyte ions are then accelerated and subjected to separation by electrostatic and / or magnetic fields. A variety of mass separation configurations of ICP-MS are in use, including quadrupole, sector field, double focussing sector field and multi-collectors.

ICP-MS is a multi-elemental method, thus complex samples can be introduced and the concentrations of several elements or isotopes of elements can be determined in rapid scans. Short reading times and rapid switching between masses reduce problems associated with signal drift. Consequently, the precision of isotope ratio analysis with ICP-MS is good. Hou and Roos (2008) states precisions in the range 0.1 – 0.5 % for isotope ratio determination using common ICP-MS instruments (double focussing sector field and quadrupole), and even better for multi-collector

ICP-MS instruments. However, isotope ratio precision is ultimately sensitive to the concentrations presented to the instrument.

ICP-MS instruments are inherently more sensitive to interferences and background than AMS-systems (Fifield, 2008), impairing both detection limits and abundance sensitivities. Poor abundance sensitivity is a problem when analysing isotopes with low abundance when there are high abundance isotopes of similar atomic mass present in the sample (e.g. ^{235}UH interfering with ^{236}U). Good chemical separation and the reduction of water in the aerosol can resolve some of these problems. However, analysis of ^{236}U by ICP-MS has an abundance sensitivity of ^{236}U/^{238}U around 1×10^{-7} (Boulyga and Heumann, 2006) and is still superseded by AMS in which ratios as low as 1×10^{-12} may be measured (Fifield, 2008).

The primary worry in Pu analysis by ICP-MS is mass interferences due to the presence of ^{238}U. U may be present in in considerable concentrations in the final sample solutions as a result of incomplete separation, or from post separation contamination. Mass overlaps on mass 239 may arise both from the $^{238}U^{1}H^{+}$ peak as well as shoulder overlap from the prominent ^{238}U peak. During the present work, the count rates at mass 239 and 240 was monitored during the analysis of a strong U solution (1 µg l^{-1}), and used for establishing a mathematical correction factor based on the ^{238}U count rates in the samples. This correction was applied to both ^{239}Pu and ^{240}Pu, though the effect was negligible at mass 240.

Accelerator mass spectrometry (AMS)

AMS is superior to other mass spectrometric techniques in its high sensitivity, high resolution, low detection limits and insensitivity to molecular interferences (Fifield, 2008; Hou and Roos, 2008). Sufficient sample quantities can be obtained through isotope dilution followed by precipitation with silver, e.g. Englund *et al.* (2007) or co-precipitation with iron oxide, e.g. Fifield (2008). The final sample target is prepared by mixing the sample preparates with an appropriate binder / conductor, and pressed into appropriate sample holders.

The principle of the method is similar to ICP-MS; the masses are separated by electric and magnetic fields, and lead to a detector where high concentration analyte atoms are measured as currents, and less abundant analyte atoms are counted individually. The major difference is that in AMS atoms are accelerated to MeV energies as opposed to KeV energies in ICP-MS. The higher energies facilitate the distinction of elements too close in mass to be resolved by ICP-MS.

The ANU AMS system is described essentially as two mass spectrometers separated by a molecule dissociating accelerator stage (Fifield, 2008), and the main

distinctions from other more conventional mass spectrometric methods arises from the high energy obtained in the accelerator and the double mass spectrometer. As described by Fifield (2008), the AMS facility at ANU consists of five main parts (Figure 14):

- The ion source and pre accelerator of -5 kV generating and forcing negative PuO^- and UO^- molecular ions towards an pre accelerator
- Accelerating the analyte ions through 100 kV in the pre accelerator and directing them towards the positive terminal of the tandem accelerator
- Molecule splitting and ionization by removing electrons forming Pu^+ and U^+ ions in a low pressure gas stripper
- Accelerating the positive ions towards the ground potential in the second part of the tandem accelerator. Selection of Pu and U ions with the correct mE/q ratio
- A detection system sorting out remaining interfering species by mass or energy

PuO^- and UO^- ions are generated in the ion source and pre-accelerated by the negative potential (5 kV) of the ion source and then by a 150 kV pre accelerator before the specific analyte (Pu or U) are inserted into the accelerator by the inflection magnet. The inflection magnet has a resolution of $M/\Delta M \sim 1000$, whereas a resolution of 300 would be sufficient to distinguish UO from PuO (Fifield, 2008). Thus, the beam should be sufficiently pure in either U or Pu in the first part of the acceleration. The PuO^- or UO^- molecules are further accelerated towards the high voltage terminal where a stripping gas (O_2 or Ar at 0.002 mbar) dissociates the molecules and change the charge by removing electrons. The positive Pu or U ions are then further accelerated towards the ground terminal of the tandem accelerator. Pu^{5+} ions are selected in the analysing magnet and are passed through a velocity filter (Wien filter). The detector used depends on the species being analysed. For Pu potential interfering elements which may reach the detector have significantly lower momentum than Pu and are easily distinguished by an ionization chamber detector. For ^{236}U, on the other hand, the high abundance of natural U isotopes (^{234}U, ^{235}U and ^{238}U) necessitates the employment of a time-of-flight (TOF) detector in addition to the ionisation chamber detector (Fifield, 2008).

Generally the AMS detection is vulnerable to any species which, after the stripping and the second part of the acceleration, have obtained the same ME/q^2 as the Pu or U isotope analysed. This may be the case for $^{238}U^{17}O^-$ and $^{238}U^{18}O^-$ formed in the ion source and which is stripped off their O-atoms early in the acceleration process, interfering with ^{239}Pu and ^{240}Pu, these are probably the most prevalent interfering species in Pu analyses, and the situation is impaired by insufficient separation chemistry prior to analysis as well insufficient vacuum in the early accelerator stages (Fifield, 2008). Poly-atomic molecules of lighter elements (e.g. $^{191}Pt^{16}O_4$,

$^{191}Pt^{4+}$, $^{143}Sm^{3+}$, $^{96}Mo^{2+}$ and $^{48}Ti^{+}$) may also cause interference. On the other hand, the probability of any of these to reach the detector is low given their low natural abundance and the complexity of the initial poly-atomic molecules (Fifield, 2008)

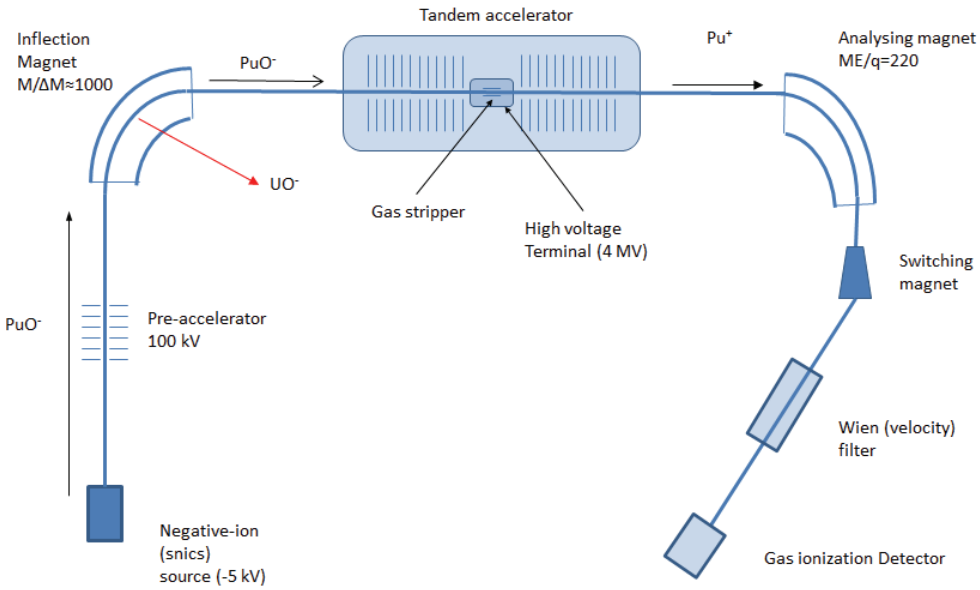

Figure 14. The ANU 14 UD accelerator as inferred from (Fifield, 2008) and (Winkler, 2007).

4.3.2 Environmental Scanning Electron microscope (ESEM)

A scanning electron microscope operates under the principle of a focussed electron beam interacting with the sample. The electron beam penetrates the surface of the sample, generating a semi spherical or pear shaped interaction volume, depending on specimen density and accelerating voltage of the incident beam. As a result of the interactions between the electron beam and the sample, several different signal types are generated. Elastic or inelastic scattering of incident electrons causes the emission of backscattered and secondary electrons respectively. Energy deposited by inelastic scattering causes excitation of sample atoms, and later emission of auger electrons or characteristic x-rays (Postek *et al.,* 1980). Backscattered and secondary electrons serve to reveal the topography of the sample, while characteristic x-rays can be used for qualitative or semiquantitative analysis of sample composition.

The backscattered electrons from the sample are particularly useful in the search for actinides as backscattering increases proportionally with atomic number of the sample atoms. A sample with high atomic number will thus appear brighter in the

microscope than a sample of low atomic number, and it is recognized that two elements differing in atomic number by more than three can be distinguished from each other in in the electron microscope using BEI mode (Postek *et al.,* 1980). Problems arise when particles are smaller than the resolution of the electron microscope and when high atomic number elements appear with low concentrations embedded in particles of lighter elements. Electron microscope run on well prepared samples should be able to give sub-micrometre resolution (Lind, 2006). However, this requires the instrument to be run under high vacuum. The presence of even minute concentration of air impairs the resolution of the microscope by diffusing the beam. Furthermore, the penetration depth into the sample is low, and the method has relatively high detection limits.

Normally samples prepared for SEM are coated with a material with good electrical conductivity in order to carry away charging effects brought upon the sample by the electron beam. For the case of particle characterisation, sample coating is unfavourable since the coating may interact with later speciation analysis of the particles (Lind, 2006). To overcome the problem of electrostatic charging of the specimen the examination is carried out with a slightly higher pressure in the sample chamber of the electron microscope. Furthermore, beam currents and accelerating voltages were kept high in order to reduce detection limits and increase electron beam penetration depth in the sample (Lind, 2006). Both the presence of air in the sample chamber and the high beam current impairs resolution to such a degree that particles below ~2 μm cannot be distinguished.

X-ray micro analysis (XRMA)

X-Ray micro-analysis allows for the semi quantitative determination of individual elements in a sample on a microscopic level. An electron beam excites sample atoms by removing electrons from the atom; upon de-excitation characteristic x-rays are emitted (Parrish and Mantler; Postek *et al.,* 1980). The penetration depth is low, on the order of 1 μm for electron beam excitation (Parrish and Mantler), consequently detection of inclusions of Pu or U trapped behind other particles or as inclusions in larger particles could prove difficult. During the present work, ESEM-XRMA served the purpose of examining hotspots identified by digital autoradiography. Substantial effort was put into locating and identifying actinide carrying particles for further examination by μ-x-ray fluorescence, however these attempts were futile due to small particle size or a complex matrix.

High intensity micro x-ray techniques (synchrotron)

The intense, well collimated and polarised x-ray radiation produced in synchrotron facilities used permits non-destructive analysis of elemental composition, structure

and speciation. As opposed to XRMA, the penetration depth of the beam is large, permitting the investigation of internal composition and structure (Lind, 2006). The method has been successfully applied to characterize U and Pu containing particles (Salbu *et al.,* 2001). In the present work the method was tested for radioactive particles contained in the air filters, however it was not found to be useful, likely due to low concentrations.

4.3.3 Digital autoradiography

Digital autoradiography has got several advantages over conventional film based autoradiography and track-etch techniques in offering high sensitivity and a large dynamic range. The primary detector (image plate) is composed of a highly photostimulable phosphor supported by thin plastic sheet, and in most cases protected by a thin protective layer (Lind, 2006). During exposure the sample is brought in close contact with the imaging plate, and placed within a protective box. Detection limits on the order of 0.002 Bq has been reported for a ^{238}Pu particle in a autoradiography system similar to the one used in the present work (Zeissler, 1997). The appliance of shielding as described by (Mori *et al.,* 1996) reduces the background and hence the detection limit. During the exposure, the phosphor (BaFBr: Eu^{2+}) captures and stores the irradiated energy until scanned by an image plate scanner. The energy is then released as luminescence, which is detected by the instrument (Lind, 2006).

4.3.4 Atmospheric dispersion modelling

In this work an atmospheric dispersion model (HYSPLIT) has been used to model releases from selected atmospheric and underground detonations at Novaya Zemlya and Semipalatinsk. Hysplit is a Lagrangian dispersion model in which transport and dispersion of particles or puffs of air are simulated based on forecast or historical meteorological data. The model encompasses simple trajectory calculations, as well as more complex dispersion and deposition simulations with puffs or particles or a combination of the two as an input term for the simulation (Draxler and Hess, 1997). Transport and deposition calculations are performed in a Lagrangian framework, while concentrations are calculated within a fixed grid (Eulerian).

Hysplit has not been designed specifically for modelling nuclear detonations, and does not include calculations of cloud stabilisation height and particle distributions. Thus, this information must be acquired from other sources and included in the model prior to the simulations. Furthermore, the model is sensitive to the quality of the meteorological data forming the basis of the simulations. Available archived

meteorological data improved after the international geophysics year in 1957 – 1958, and this applies in particular to data released from the former Soviet Union.

Geographical location, release heights and particle sizes are factors that have significant influence on transport times and deposition times and locations (Pöllänen *et al.,* 2006; J. Bartnicki, Pers. Comm.). The starting points of the simulations may be one or several geographical points separated by horizontal and / or vertical distance, and several classes of particles with individual densities, size and gravitational settling may be defined into the model alongside gaseous releases.

The removal of radioactive debris on the time scales simulated in this work is assumed to take place through two processes: wet and dry deposition. Large particles are affected by gravity and deposit rapidly after the detonation, whereas smaller particles and gaseous debris have considerable residence times in the troposphere and are subject to transport over large distances. Wet deposition is assumed to be the most efficient deposition mechanism for these particles.

5 Summary of findings

Paper I - Levels and trends of deposition and concentrations of Pu and Cs in Humic surface soils

To differentiate between sources contributing to Pu contamination, Pu concentration and atom ratios were determined in humic surface soil samples from 45 geographically well distributed sites across the Norwegian mainland using SF-ICP-MS and AMS. The $^{239+240}$Pu activity concentrations ranged within 4 – 149 Bq m^{-2} (1990) and 0.7 – 63 Bq m^{-2} (2005), with the higher concentrations predominantly found at coastal locations. To identify any migration of Pu from the upper 5-7 cm of the surface soils, Pu activity concentrations in samples collected at the same sites in 1990 and 2005 were compared. On average, about 35 % of the $^{239+240}$Pu activity concentrations in the 1990 samples remained in the humic soil samples collected in 2005. The ^{240}Pu/^{239}Pu atom ratios ranged within 0.164 to 0.211 (1990) and 0.161 to 0.195 (2005), predominantly within the range of global fallout. Results based on the ^{240}Pu/^{239}Pu atom ratio, as well as levels of heavier Pu isotopes (^{241}Pu and ^{242}Pu) indicated a slight (8 to 13 %) contribution of Pu from the Chernobyl accident in some inland areas of Norway.

Paper II - Chronology of Pu isotopes and ^{236}U in an arctic ice core

In the present work, state of the art isotopic fingerprinting techniques are applied to an Arctic ice core in order to quantify deposition of U and Pu, and to identify possible tropospheric transport of debris from former Soviet Union test sites Semipalatinsk (Central Asia) and Novaya Zemlya (Arctic Ocean). An ice core chronology of ^{236}U, ^{239}Pu, and ^{240}Pu concentrations, and atom ratios, measured by accelerator mass spectrometry in a 28.6 m deep ice core from the Austfonna glacier at Nordaustlandet, Svalbard is presented. The ice core chronology corresponds to the period 1949 to 1999. The main sources of Pu and ^{236}U contamination in the Arctic were the atmospheric nuclear detonations in the period 1945 to 1980, as global fallout, and tropospheric fallout from the former Soviet Union test sites Novaya Zemlya and Semipalatinsk. Activity concentrations of $^{239\ +\ 240}$Pu ranged from 0.008 to 0.254 mBq cm^{-2} and ^{236}U from 0.0039 to 0.053 μBq cm^{-2}. Concentrations varied in concordance with ^{137}Cs concentrations in the same ice core. In contrast to previous published results, the concentrations of Pu and ^{236}U were found to be higher at depths corresponding to the pre-moratorium period (1949 to 1959) than to the post-moratorium period (1961 and 1962). The ^{240}Pu/^{239}Pu ratio ranged from 0.15 to 0.19, and ^{236}U/^{239}Pu ranged from 0.18 to 1.4.

The Pu atom ratios ranged within the limits of global fallout in the most intensive period of nuclear atmospheric testing (1952 to 1962). To the best knowledge of the authors the present work is the first publication on biogeochemical cycles with respect to ^{236}U concentrations and $^{236}U/^{239}Pu$ atom ratios in the Arctic and in ice cores.

Paper III - Long-range tropospheric transport of uranium and plutonium weapons fallout from Semipalatinsk nuclear test site to Norway

A combination of state-of-the-art isotopic fingerprinting techniques and atmospheric transport modelling using real-time historical meteorological data has been used to demonstrate direct tropospheric transport of radioactive debris from specific nuclear detonations at the Semipalatinsk test site in Kazakhstan to Norway via large areas of Europe. A selection of archived air filters collected at ground level at 9 stations in Norway during the most intensive atmospheric nuclear weapon testing periods (1957–1958 and 1961–1962) has been screened for radioactive particles and analysed with respect to the concentrations and atom ratios of plutonium (Pu) and uranium (U) using accelerator mass spectrometry (AMS). Digital autoradiography screening demonstrated the presence of radioactive particles in the filters. Concentrations of ^{236}U (0.17–23 nBq m^{-3}) and $^{239+240}Pu$ (1.3–782 μBq m^{-3}) as well as the atom ratios $^{240}Pu/^{239}Pu$ (0.0517–0.237) and $^{236}U/^{239}Pu$ (0.0188–0.7) varied widely indicating several different sources. Filter samples from autumn and winter tended to have lower atom ratios than those sampled in spring and summer, and this likely reflects a tropospheric influence in months with little stratospheric fallout. Very high ^{236}U, $^{239+240}Pu$ and gross beta activity concentrations, as well as low $^{240}Pu/^{239}Pu$ (0.0517–0.077), $^{241}Pu/^{239}Pu$ (0.00025–0.00062) and $^{236}U/^{239}Pu$ (0.0188–0.046) atom ratios, characteristic of close-in and tropospheric fallout, were observed in filters collected at all stations in Nov 1962, 7–12 days after three low-yield detonations at Semipalatinsk (Kazakhstan). Atmospheric transport modelling (NOAA HYSPLIT_4) using real-time meteorological data confirmed that long range transport of radionuclides, and possibly radioactive particles, from Semipalatinsk to Norway during this period was plausible. The present work shows that direct tropospheric transport of fallout from atmospheric nuclear detonations periodically may have had much larger influence on radionuclide air concentrations and deposition than previously anticipated.

6 Results and discussion

In the present work, concentrations, atom- and activity ratios of U, Pu and ^{137}Cs have been determined using several chemical and instrumental techniques. In order to assure the quality of the obtained data, blanks (analytical and procedural), standard reference materials and in-house standards have been processed and analysed along with the samples and are presented in

Table **4**. Standard reference materials and in house standards represent common samples for ICP-MS and AMS and permit the intercomparison of the results from the two instruments (Figure 15).

Detection limits

Instrumental and procedural detection limits in the present work are based on repeated measurements of analytical and procedural blanks. Detection limits for both instruments were based on the analysis of procedural blanks and are presented in Table 3. ICP-MS analysis suffers higher and more variable background than AMS analysis. The detection limits for ICP-MS was calculated as the average intensities for the blank samples + 3 σ. For AMS analysis, background counts were low, and the detection limit was calculated as the blank count rates (cps) on the respective mass.

Table 3. Detection limits (g) based on repeated analysis of blank samples.

	^{234}U	^{236}U	^{239}Pu	^{240}Pu
ICP-MS	-	-	2.65×10^{-13}	7.45×10^{-14}
AMS	9.00×10^{-12}	2.40×10^{-14}	4.20×10^{-15}	1.30×10^{-15}

Accuracy

Repeated analyses of Pu concentrations and atom ratios in certified reference materials and in-house standards were performed throughout the course of the present work for quality assurance and quality control; the results are presented in Table 4.

Table 4. Concentrations and atom ratios of plutonium in certified reference materials and in house standards analysed in the present work. The UKAEA Pu 5/92138 has certified $^{239}Pu/^{240}Pu$:^{242}Pu atom ratios close to unity and is used for instrumental calibration, for this reason it is analysed without yield monitor addition. Consequently, concentrations are unavailable for this material. Certified or recommended values from reference sheet when available, literature values included for comparison.

Reference material	^{239}Pu conc. pg g^{-1}	^{240}Pu conc. pg g^{-1}	$^{239+240}Pu$ Bq kg^{-1}	$^{240}Pu/^{239}Pu$ atom ratio	Reference
IAEA 384	46 ± 6	2.2 ± 0.5	125 ± 18	0.0501 ± 0.0008	This work (n=5)
(Fangataufa sediment)	42 ± 4*	2.1 ± 0.2*	107 ± 2	0.048 ± 0.006	Povinec *et al.* (2007)
	41.2 ± 0.3	2.06 ± 0.01	112.02 ± 0.74	0.0501 ± 0.0005*	Godoy *et al.* (2009)
NIST 4353	4.9 ± 0.3	0.29 ± 0.01	13.8 ± 0.7	0.058 ± 0.002	This work (n=3)
(Rocky flats soil)	6.1 ± 0.7**	0.34 ± 0.04**	16.8 ± 1.8	0.053 – 0.060**	Reference sheet
	3.97 ± 0.02	0.218 ± 0.001	10.65 ± 0.04	0.055 ± 0.001	Cizdziel *et al.* (2008)
	2.1 ± 0.1	0.14 ± 0.02	5.88 ± 0.28	0.065 ± 0.009	Child *et al.* (2008)
IAEA 300	1.17 ± 0.04	0.20 ± 0.01	4 ± 1	0.22 ± 0.03	This work (n=4)
(Baltic sea sediment)	-	-	3.44 – 3.65	-	Reference sheet
	1.05 ± 0.04	0.18 ± 0.01	3.9 ± 0.1	0.17 ± 0.01	Child *et al.* (2008)
	0.97 ± 0.06	0.19 ± 0.01	3.8 ± 0.2*,†	0.19 ± 0.003	Nygren *et al.* (2003)
in-house standard	-	-		0.127 ± 0.004	This work (ICP-MS) (n=3)
2626 (sediment)				0.115 ± 0.007	L. Skipperud (Pers. Comm).
in-house standard	-	-		0.019 ± 0.003	This work ICP-MS and AMS (n=5)
3516 (soil)				0.0194±0.0008	L. Skipperud (Pers. Comm).
UKAEA Pu5/92138	-	-		0.97 ± 0.014	This work (n=16)
				0.966 ± 0.001	Reference sheet

* - information / uncertified value, ** - Calculated from reference sheet, † - Nygren *et al.* (2003) reports considerable inhomogeneities in the IAEA-300 reference material affecting both Pu concentrations and atom ratios.

Precision

A certified reference material for Pu atom ratios (UKAEA Pu5/92138) was analysed repeatedly during AMS-analysis in the present work. Atom ratio precisions of 2.5, 2.7 and 1.4 % was calculated for $^{240}Pu/^{239}Pu$, $^{239}Pu/^{242}Pu$ and $^{240}Pu/^{242}Pu$, respectively (relative standard deviation, n=16). The precisions for $^{240}Pu/^{239}Pu$ atom ratios, determined by SF-ICP-MS in repeated measurements of reference materials IAEA 300, IAEA284 and in house standards 2626 (sediment) and 2516 (soil) was below 7 % RSD (0.4 – 7 %).

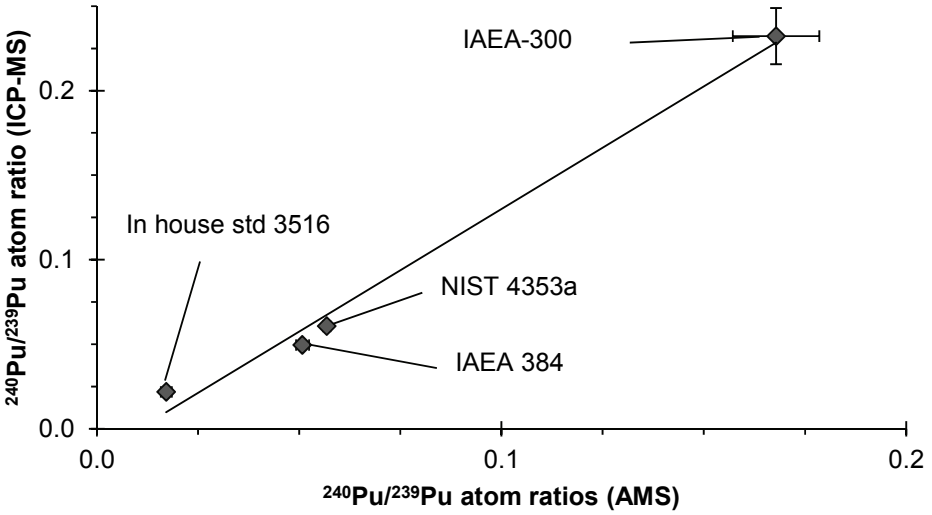

Figure 15. Comparison of 240Pu/239Pu atom ratios in standard reference materials and in house standards (IAEA300, IAEA384, NIST4353a and in-house standard 3516) analysed by AMS and SF-ICP-MS.

Activity concentrations of ^{238}Pu and $^{239+240}Pu$ ratios were determined in selected humic surface soil samples. The activity concentrations were well correlated (R^2=0.97 n=25) between the two instruments, as shown in Figure 16.

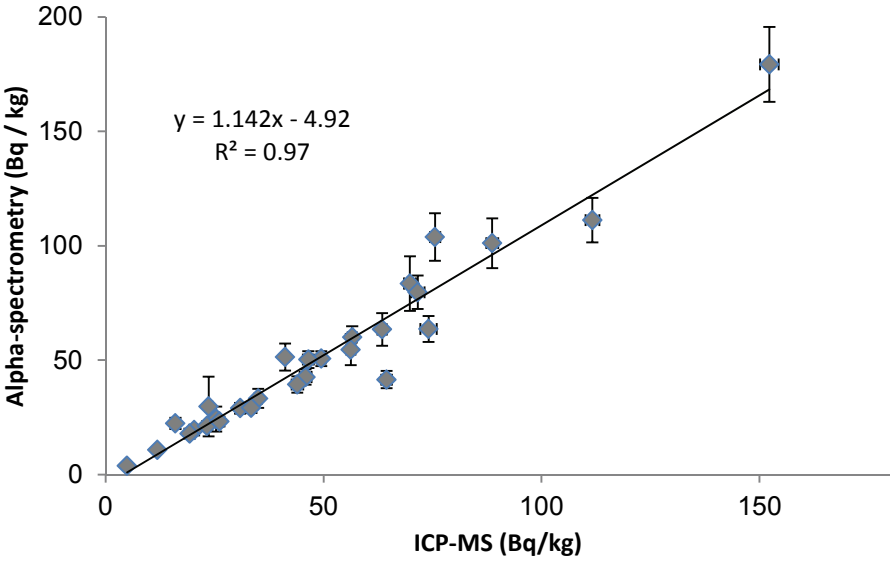

Figure 16. The correlation between concentrations of $^{239+240}$Pu determined in humic surface soil samples with ICP-MS and alpha-spectrometry respectively.

6.1 Plutonium deposition in the terrestrial environment of Norway

6.1.1 Concentrations of Pu in the terrestrial environment

Deposition of $^{239+240}$Pu in the humic surface soils (Paper I) were found within the ranges 4 – 149 Bq m^{-2} (1990) and 0.63 – 63 Bq m^{-2} (2005). The $^{239+240}$Pu activity concentrations were largely within the range of 14 – 135 Bq m^{-2} for soil samples collected at similar latitudes in 1970 (Hardy *et al.,* 1973; Kelley *et al.,* 1999). Thus a substantial proportion of the Pu deposition during the main period of deposition (1945 - 1963) still seems to be present within the upper 7 cm of humic surface soil layers in Norway.

The calculated integrated deposition in the Austfonna ice core was 8.2 ± 0.1 Bq m^{-2} for $^{239+240}$Pu and 0.151 ± 0.005 mBq m^{-2} for ^{236}U. The $^{239+240}$Pu values were in accordance with the value stated by Hardy *et al.* (1973) (average value for latitudes 78 – 80 and 80 – 90 °N).

6.1.2 Geographical distribution of Pu

The highest concentrations of $^{239+240}$Pu in the humic surface soil samples were found at coastal sites with high annual precipitation (Figure 17 and Paper I). Significant variations were observed between sites with similar precipitation levels. Orographic precipitation (Storebø, 1959; Storebø, 1968) and washout due to precipitation rates and chemistry (Steinnes and Njastad, 1993) may explain some of

this variation. Similarly, the lowest activity concentrations were found at inland locations with low annual precipitation. This is generally in agreement with the global fallout theory. However, a good correlation between precipitation and activity concentrations could not be established. This may be attributed to soil chemistry, precipitation chemistry and precipitation rates in the years following the initial deposition.

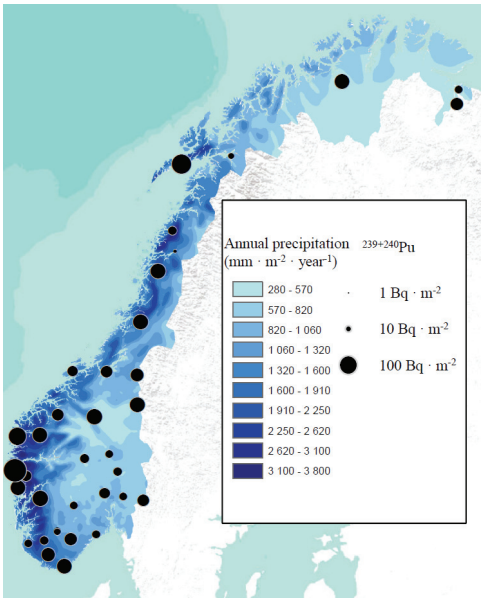

Figure 17. Activity concentrations of $^{239+230}$Pu in humic surface soils in Norway (Paper I) and annual precipitation levels.

In contrast to Pu, the highest concentrations of ^{137}Cs were found at inland locations associated with high precipitation in the first few days after the Chernobyl accident (Figure 18). The deposition of ^{137}Cs from the Chernobyl accident depended heavily on the location of the plume and the precipitation pattern in the days after the accident. Thus heterogeneous distributions should be expected. The main deposition of debris from the Chernobyl accident in Norway originated from the releases during the initial explosion the 26 March 1986. This debris reached central Scandinavia and Norway the 29 and 30 April 1986 (Saltbones, 1986), elevated concentrations of ^{131}I and ^{137}Cs in air were observed until 9 May 1986 (Sæbø *et al.,* 1998). Furthermore, radioactive particles containing Chernobyl origin Zr, Ru, I, Cs, Ba and Ce isotopes were observed in rain water collected in Oslo on 6 May 1986 and in environmental samples collected in 1987 (Salbu, 1988a; Salbu, 1988b).

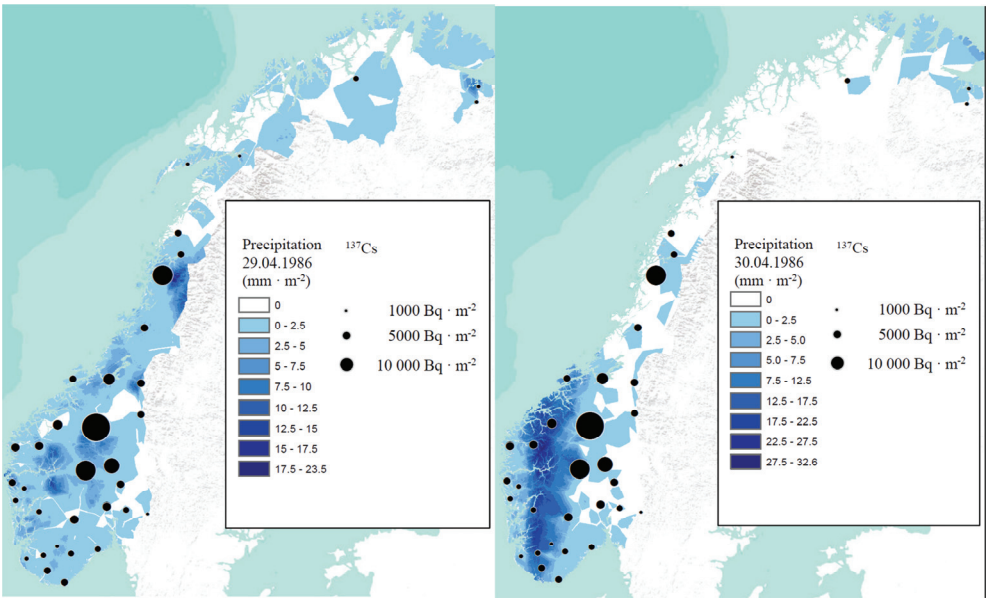

Figure 18. Measured activity concentrations of ^{137}Cs, samples collected in 1990 in Norway (Paper I) plotted along levels of precipitation in the days following the Chernobyl accident (McInnes).

6.1.3 *Trends in deposition of Pu*

Concentrations of $^{239+240}$Pu and ^{236}U in the Austfonna ice core ranged within 0.008 – 0.254 mBq cm^{-2} and 0.0039 – 0.053 µBq cm^{-2}, respectively (paper II). The concentrations were found to be higher at depths corresponding to the pre-moratorium period 1956 – 1959 than the post-moratorium period (cf. Figure 19). This is in contrast to previously published values (e.g. Warneke *et al.* (2002), Koide *et al.* (1985), UNSCEAR (2000a) and Olivier *et al.* (2003)), in which the highest deposition of radionuclides were reported to have taken place in the period 1962–1964. The Pu and ^{236}U deposition profile is supported by ^{137}Cs deposition profiles in the same core and several other ice cores from the same glacier (Pinglot *et al.,* 2003). A few possible reasons for this anomaly will be presented below.

- Variations in the ice core accumulation rates, reflected in annual precipitation or melting. This could cause $^{239+240}$Pu and ^{236}U concentrations to be higher in those segments of the core corresponding to 1955 – 1958 than in the segments corresponding to 1959 - 1962 and 1962 – 1962 without reflecting variations in actinide deposition.
- Fluctuations in the south – north tropospheric transport in combination with a higher number of detonations at Semipalatinsk and tropospheric debris from US equatorial detonations. Several papers have addressed long range transport of

pollutants from Eurasia and north America reaching the Arctic, particularly during winter, e.g. Barrie and Hoff (1984), Barrie (1986), Stohl (2006) and (Warneke *et al.,* 2010). According to Barrie (1986), the arctic winter air mass extends as far south as 40 °N over continental Eurasia and a persistent high pressure area forces air pollutants from Central Europe and Eurasia towards the Arctic. Tropospheric transport towards the Arctic is enhanced during positive North Atlantic Oscillation phases (Eckhardt *et al.,* 2003).

- A post deposition redistribution of radionuclides embedded glacier ice may arise from infiltration and percolation of meltwater. Tritium (^{3}H), which is used to establish the 1963 maximum deposition in the ice core is bound in water molecules, and is likely to behave more conservatively in the ice profile than debris particles. This could cause Pu and ^{236}U to be depleted in layers corresponding to 1963, and enhanced in in deeper layers, leaving ^{3}H relatively unaffected.

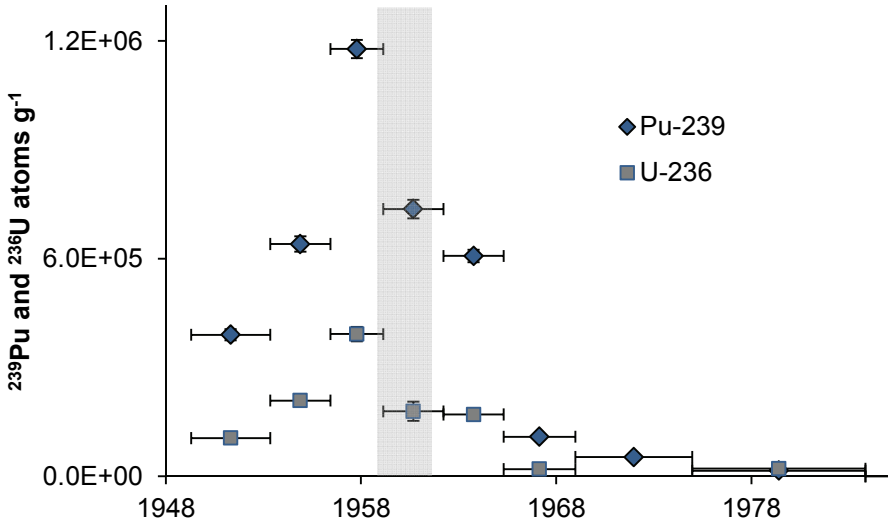

Figure 19. Concentrations of ^{239}Pu and ^{236}U (atoms kg^{-1}) in the Austfonna ice core. The shaded grey box indicates the moratorium period (November 1958 – September 1961).

6.1.4 *Wash-out* (humic surface soil samples)

By comparing the $^{239+240}Pu$ and ^{137}Cs concentrations in the upper 7 cm of humic surface soil samples collected in 1990 with those from 2005, the average retention of $^{239+240}Pu$ was found to be 35 %, ranging within 2 and 78 % when obvious outliers had been removed from the dataset (appendix 2). The outliers included samples with identical or higher activity concentrations in 2005 than in 1990, and 4

samples where the humic layer in 2005 had an insufficient depth. Similarly, the average retention of ^{137}Cs in the samples was 35 %, and ranging within 9.2 and 92%.

The long-term bioavailability and mobility of radionuclides released to the environment depends primarily on the release scenario, speciation and interactions between the radionuclides and environmental materials after deposition. Depending on the chemical conditions in the recipient medium, the mobility of the deposited radionuclides may change over time. Weathering and bio-erosion increase the mobility of the deposited radionuclides, while sorption, chemisorption and incorporation into mineral lattices decrease the mobility (Salbu, 2000b). Both Pu and Cs are assumed to be relatively immobile in organic rich and mineral soils and sediments (Skipperud, 2004; Qiao *et al.,* 2012).

6.2 Radioactive particles in surface air and ice core samples

Results from digital autoradiography of the air filters (Paper III) and the AUS-99 ice core (Paper II) indicated the presence of radioactive particles in samples from periods with atmospheric nuclear testing at the FSU test sites Novaya Zemlya and Semipalatinsk. In periods without atmospheric nuclear testing radioactive few particles could be identified, despite high concentrations of actinides in the filters (Paper III and Appendix 1). Since refractory radionuclides released from atmospheric nuclear detonations are assumed to form particles (Heft, 1970; Salbu, 2008), it is likely that these filters contain particles too deeply embedded in the filter material to be detected by digital autoradiography. Filters with high activities (gross beta, Pu, U,) were usually darker than the background in the autoradiographs, even in the absence of hotspots.

Fallout particles as large as 20 μm have been reported in fresh fallout. However, large particles are assumed to be rapidly removed from the atmosphere by gravitational settling and particle diameters larger than 6 μm are seldom found in debris transported over longer distances, e.g. Mamuro *et al.* (1962), Sisefsky (1966), and Sisefsky (1966). Stratospheric radioactive debris particles tended to be larger in periods with atmospheric testing than in periods without, e.g. Chagnon and Junge (1965), Feely *et al.* (1966), Telegadas and List (1969). Figure 20 shows autoradiographs of a selection of air filters collected in the period 1961 – 1963.

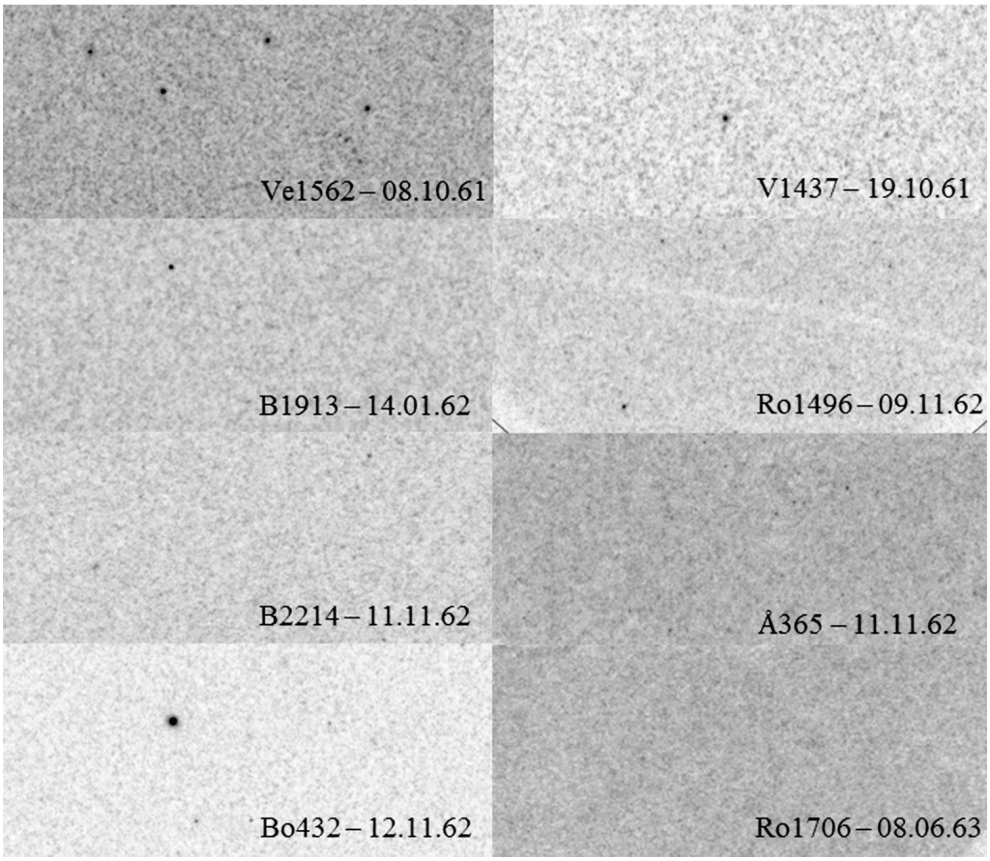

Figure 20. Autoradiographs of selected air filters with radioactive heterogeneities. The filters with highest associated Pu and U concentrations were from November 1962. Hotspots indicating the presence of particles can be seen in the filters from the autumn and winter of 1961 and 1962, but were absent or ambiguous in filters associated with spring peak deposition as illustrated by the autoradiograph of the filter from Røros, the 8 June 1963 (lower right). Location codes: B – Bergen, Ro – Røros, V – Vadsø, Ve – Værnes and Å – Ålesund.

A selection of digital autoradiographs of ice core filters is shown in Figure 21. These indicate the presence of low activity particles at depth ranges corresponding to the atmospheric nuclear testing periods at Novaya Zemlya and Semipalatinsk (1951 – 1962). Radioactive heterogeneities were also seen at depths corresponding to the time period 1986 – 1989. These particles may originate from the Chernobyl accident in 1986 or a vented underground detonation at Novaya Zemlya in 1987. The vented underground detonation at Novaya Zemlya is further described in Mikhailov (2004) as a situation in which highly radioactive gases escaped through fissures and into the open atmosphere and lingered over the area for several days. Both volatiles and refractory nuclides escaped; the escaped gases were detected as far south as Risø in Denmark (Bjurman *et al.,* 1990).

Radioactive particles were frequently sampled and characterised during the atmospheric nuclear testing periods e.g. Sisefsky (1961), Mamuro *et al.* (1962), Edvarson and Sisefsky (1966), Sisefsky (1966). However, to the author's best knowledge this is the first time fallout particles from atmospheric nuclear weapon tests have been localised in ice core samples.

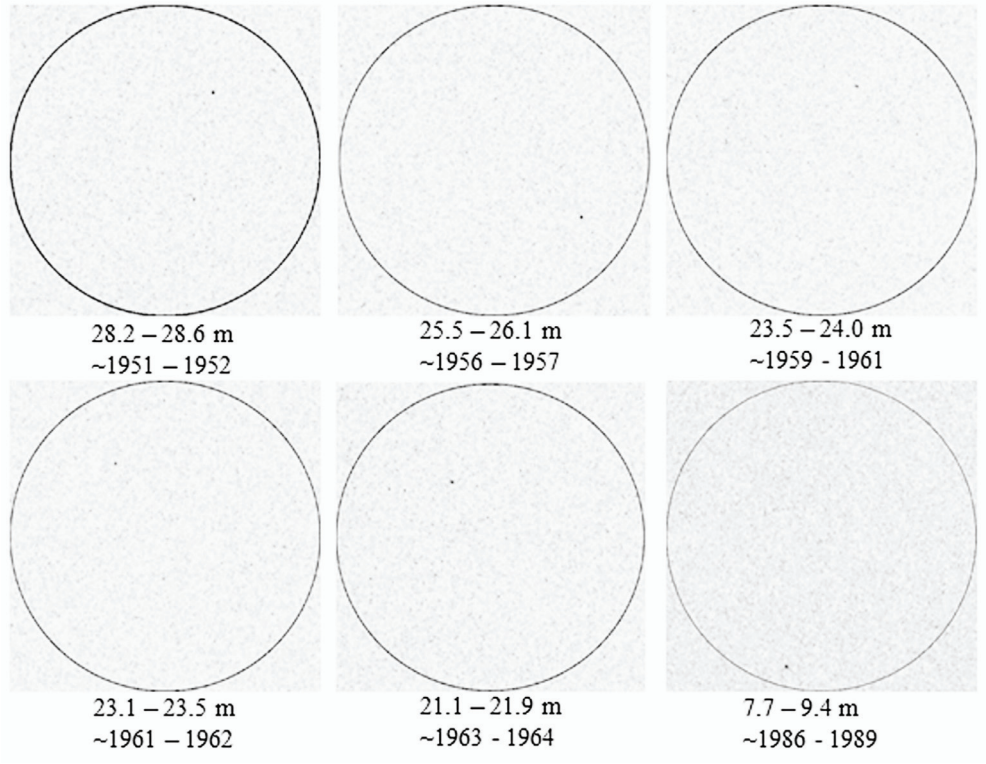

Figure 21. Digital autoradiographs of ice core filters with radioactive heterogeneities. The size of the filters are indicated by the outer circle (ø=47 mm) whereas autoradiography hotspots indicating the presence of radioactive particles are inscribed in smaller circles.

Attempts were made to isolate and characterise individual particles using ESEM-XRMA and the x-ray microprobe, beamline L, HASYLAB. However, the Pu and U signals could not be observed, probably due to the complex sample matrix (cellulose asbestos filters), and that concentrations of Pu and U in the particles were below the detection limits for these methods. Fallout particles have been reported to consist mainly of Fe, Al, Ca, Si and Pb, i.e., materials associated with bomb casing, tamper and environmental materials, (Sisefsky, 1964; Crocker *et al.,* 1966; Kemmochi, 1966). Thus, the relative concentration of actinides in particles may prove too low to be directly detected by ESEM-XRMA.

6.3 Atom and activity ratios

Source identification of radioactive contamination is important in order to reveal transport routes and transit times of pollution as well as predicting the extent of future accidental or operational releases. In the present work Pu atom and activity ratios were utilised in combination with atmospheric dispersion modelling for source identification and source assessment purposes.

6.3.1 $^{238}Pu/^{239+240}Pu$ activity ratios

Activity ratios of $^{238}Pu/^{239+240}Pu$ were determined in a subset of the humic surface soil samples; ratios were found to range within 0.022 and 0.07 (0.04 ± 0.01, n=27). The activity ratios were in general higher than the $^{238}Pu/^{239+240}Pu$ atom ratio established by Hardy *et al.* (1973) (0.026 ± 0.04, 25 northern hemisphere locations with latitude higher than 30 ºN decay corrected to 01.01.2012). This might indicate an influence from Chernobyl debris. Activity ratios of $^{238}Pu/^{239+240}Pu$ in debris from the Chernobyl accident were substantially higher than global fallout, Lujaniene *et al.* (2009) observed ratios in the range 0.44 – 0.5 in air in Vilnius in the days following the accident, while ratios in the range 0.03 – 0.70 and 0.04 – 0.57 were found in debris deposited in Finland and Sweden respectively (Lindahl *et al.,* 2004; Salminen-Paatero *et al.,* 2012). However, the distribution of elevated $^{238}Pu/^{239+240}Pu$ atom ratios did not reflect known deposition of Chernobyl debris. It is conceivable that the ^{238}Pu derived from the SNAP-9A breakdown have had different chemical properties than the $^{239+240}Pu$ deposited after nuclear weapon tests. A lower wash-out of SNAP-derived ^{238}Pu in the soils could then possibly offer an explanation of the higher activity ratios found.

6.3.2 $^{240}Pu/^{239}Pu$ atom ratios

The $^{240}Pu/^{239}Pu$ atom ratios obtained in the present thesis varied within 0.161 – 0.211 in humic surface soil samples, (paper I), 0.15 – 0.19 the Austfonna ice core, (paper II), and 0.0517 – 0.237 in air filters from the period 1957 - 1963, (paper III). Figure 22 and Figure 23 shows summary plots of the $^{240}Pu/^{239}Pu$ isotopic composition of the samples analysed in (paper III) along with literature values for comparison.

Radionuclides deposited at a site represent a mixture of fallout from regional and global fallout from atmospheric nuclear tests, reactor accidents and any locally deposited radionuclides. The $^{240}Pu/^{239}Pu$ atom ratios observed in the humic surface soils samples were used to assess the relative impact of fallout from atmospheric nuclear detonations and the Chernobyl accident in Norway. The $^{240}Pu/^{239}Pu$ atom ratios found (0.164 – 0.211 in samples from 1990 and 0.161 – 0.195 in samples

from 2005) indicated integrated global fallout to be the most important source. However, high atom ratios at some inland locations were attributed to a slight Chernobyl influence.

The ice core samples (Paper II) offer poorer time resolution and less secure dating than the air filters (Paper III). The time resolution is 1 - 3 years at best, depending on in core concentrations and post – depositional processes. Downward migration due to melting and infiltration disturb the isotopic signal (e.g. Tarussov (1992), Pinglot *et al.* (2003)). Despite the close geographical and climatological proximity of the Austfonna glacier, from which the core was extracted, to Former Soviet Union test sites Novaya Zemlya and Semipalatinsk, no significant deviations from global fallout levels of the $^{240}Pu/^{239}Pu$ atom ratios were observed. In Figure 22 $^{240}Pu/^{239}Pu$ atom ratios observed in the air filter samples (paper III) are compared with literature values. The $^{240}Pu/^{239}Pu$ atom ratios observed in the air filter samples (paper III) were found to be in agreement with ratios observed by Warneke *et al.* (2002) and Salminen-Paatero *et al.* (2012) in periods with coherent sampling times (1957, 1958 and 1963). In the remaining periods, autumn 1961 and 1962, the atom ratio of Pu in air reflected weapon debris from low and intermediate yield detonations.

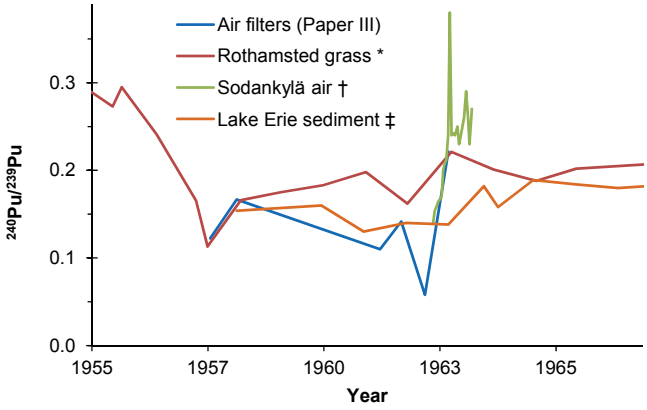

Figure 22. Summary plot of $^{240}Pu/^{239}Pu$ atom ratios discussed. Activity weighted yearly mean values for all stations have been used for the air filter samples (Paper III); 1962 split into spring (March and April) and winter (November). Literature values included for comparison: * - Rothamsted herbage archive, Warneke *et al.* (2002), † - Surface air Sodankylä from Salminen-Paatero *et al.* (2012), ‡ - Lake Erie sediment from Winkler (2007).

During time periods associated with atmospheric nuclear testing at Novaya Zemlya and Semipalatinsk the air filters from all stations had $^{240}Pu/^{239}Pu$ atom ratios of 0.06 ± 0.01 (activity weighted mean ± 1 s.d.), i.e., significantly lower than global

fallout ratios. This is opposed to periods without atmospheric nuclear testing wherein the $^{240}Pu/^{239}Pu$ atom ratios of 0.18 ± 0.04 approached stratospheric fallout ratios (cf. Figure 23 and appendix 1). Similar tendencies have been reported elsewhere, e.g. Salminen-Paatero *et al.* (2012) and Warneke *et al.* (2002) (Figure 22). The results of Pu isotope measurements in air filter samples (Paper III) suggest that debris from low yield detonations has had a strong influence on actinide concentrations in ground level air during periods of atmospheric testing at FSU test sites Semipalatinsk and Novaya Zemlya. The higher $^{240}Pu/^{239}Pu$ atom ratios seen in periods without atmospheric nuclear testing and in connection with spring peak deposition indicate influence of debris from high yield detonations, originally injected into the stratosphere.

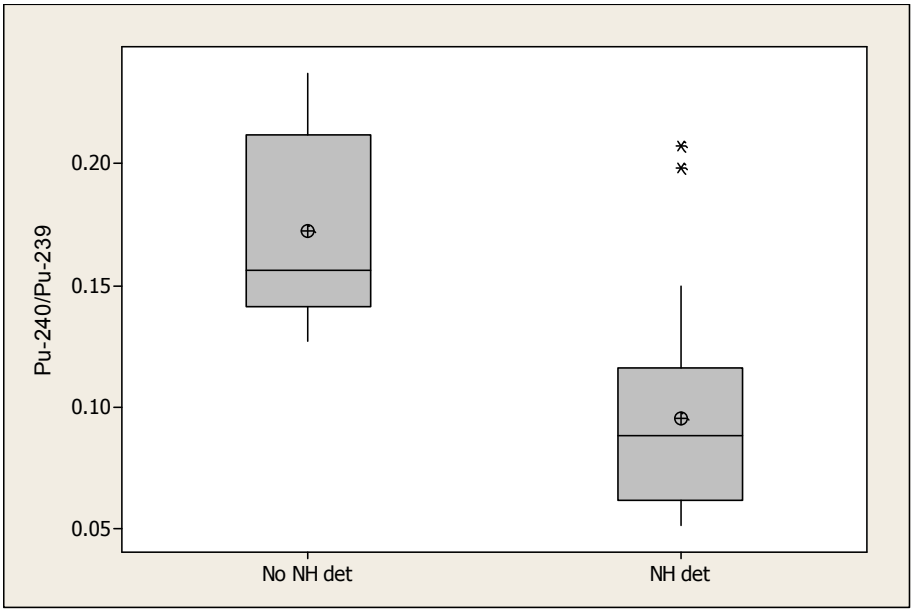

Figure 23. Summary plot of $^{240}Pu/^{239}Pu$ atom ratios during 1957 – 1963. The data are grouped into filters from periods with northern hemisphere atmospheric testing (NH det) versus periods without northern hemisphere atmospheric testing (no NH det). Ringed cross – mean of observations within the category. * - outliers.

Debris from low yield detonations generally characterised by low $^{240}Pu/^{239}Pu$ and $^{241}Pu/^{239}Pu$ atom ratios (e.g. Hicks and Barr (1984), Beasley *et al.* (1998b), Lind (2006)), while high yield detonations generally yielded high $^{240}Pu/^{239}Pu$, $^{241}Pu/^{239}Pu$ atom ratios (e.g. Diamond *et al.* (1960), Yamamoto *et al.* (1996), Lindahl *et al.* (2012)). Debris from reactors features a range of different $^{240}Pu/^{239}Pu$ atom ratios, depending on burn up and the history of the fuel. Characteristic for fuels from power production reactors and recycled fuels is, however, elevated $^{240}Pu/^{239}Pu$

atom ratios due to accumulation of heavier Pu isotopes and fission of ^{239}Pu (Lovins, 1980). Publications stating the ^{236}U/^{239}Pu atom ratios in debris from nuclear detonations are rare, and mostly concerning local fallout from low yield detonations (Beasley *et al.,* 1998b) and global fallout (Ketterer *et al.,* 2007; Sakaguchi *et al.,* 2009). Information on this ratio in debris from high yield detonations has not been found. However, the ratio is expected to be higher than in global fallout.

Detonations at STS were generally of low yield (average 59 kt, range 0.001 – 1600 kt). (UNSCEAR, 2000a; Björklund and Goliath, 2009). In contrast detonations at NZ were of high and very high yield (average 2900 kt, range 2 – 5800 kt) (UNSCEAR, 2000a; Björklund and Goliath, 2009). The arctic location of NZ would cause most of the debris from atmospheric nuclear detonations conducted here to be apportioned to the stratosphere, and thus to be dispersed and deposited as global fallout (Peterson, 1970; UNSCEAR, 2000a). Furthermore, it has been indicated that most detonations at NZ were carried out under wind directions that would cause tropospheric debris to be deposited onto FSU territories (Khalturin *et al.,* 2005).

Previous work on high time resolution samples has been done by Warneke *et al.* (2002) and Salminen-Paatero *et al.* (2012). Like the air filter samples analysed in Paper III, the samples analysed by Salminen-Paatero *et al.* (2012) permit a time resolution down to 24 hours, while the herbage archive used by Warneke *et al.* (2002) has been collected biannually (spring and autumn) to annually, with a time resolution down to three months at best. The air filter samples were collected daily, and the fine time resolution and secure dating allows for observation of short term trends and episodes which is not possible in other sample types like ice cores, sediment cores or soil samples.

6.3.3 ^{236}U/^{239}Pu atom ratios in ice core samples and air filter samples

In the present work ^{236}U/^{239}Pu atom ratios have been determined an Arctic ice core from Nordaustlandet and in selected air filter samples; ^{236}U/^{239}Pu atom ratios in the range 0.0188 – 0.7 (air filters) and 0.18 – 1.4 (ice core) were found.

The ^{236}U/^{239}Pu atom ratio in the Austfonna ice core was predominately found within the global fallout range reported by Ketterer *et al.* (2007). There was a tendency of higher ^{236}U/^{239}Pu atom ratios at depths corresponding to pre-moratorium deposition than at depths corresponding to post-moratorium deposition; however, uncertainties were high. The ^{236}U/^{239}Pu atom ratio observed at depths corresponding to the period 1975 – 1983 is very high (1.4 ± 0.4), however,

this is in agreement with reports of $^{236}U/^{239}Pu$ in riverine- and sea-water (Eigl *et al.,* 2013) and soil samples (Srncik *et al.,* 2011; Ketterer *et al.,* 2013).

The $^{236}U/^{239}Pu$ atom ratios observed in the air filters (Paper III) were predominately within the range of global fallout reported by Ketterer *et al.* (2007). During the passage over Norway of a radioactive cloud attributed to low yield tests at STS in October / November 1962 (further discussed in chapter 6.5), very low $^{236}U/^{239}Pu$ atom ratios were observed. These ratios were significantly different from the values reported by Ketterer *et al.* (2003) to be representative of global fallout, but largely in agreement with ratios observed in local fallout at STS by (Beasley *et al.,* 1998b).

The $^{236}U/^{239}Pu$ atom ratios obtained from the analysis of the ice core and the air filters samples (paper II and paper III) are illustrated in Figure 24, along with literature data for comparison. Soil US and Sediment FSU refers to $^{236}U/^{239}Pu$ atom ratios in soil samples from Washington state (US), and the Pechora region in the FSU calculated from the data presented by Ketterer *et al.* (2013); Soil Las Palmas refers to bulk analysis of soil samples from La Palma, Canary Islands, as reported in Srncik *et al.* (2011).

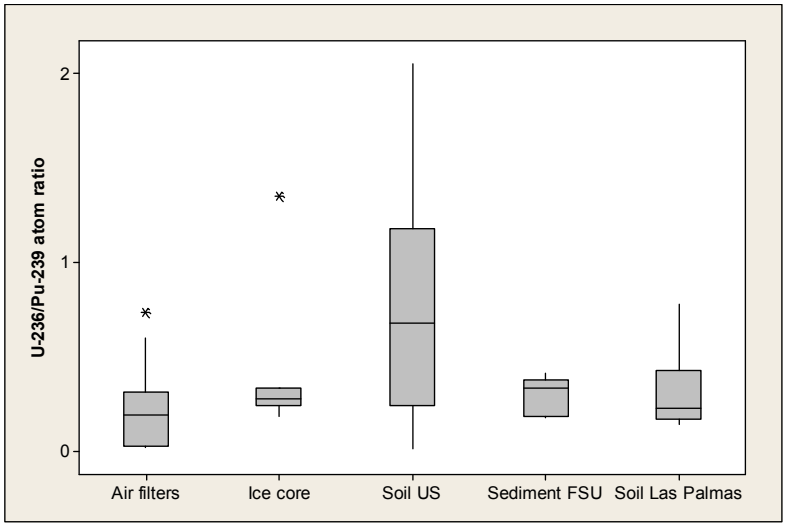

Figure 24. Boxplot of $^{236}U/^{239}Pu$ atom ratios observed in the present thesis. Air filter samples from Norway during 1957 – 1963 (Paper III), the ice core from Nordaustlandet (Paper II). * denotes outliers. Literature values included for comparison: Soil US – soil samples from Washington state USA and Sediment FSU – lake sediments from the Pechora region (Ketterer *et al.,* 2013). Bulk soil samples (0 – 5 cm) from La Palma, Canary Islands Srncik *et al.* (2011).

The observed variations in the $^{236}U/^{239}Pu$ atom ratio likely reflect variations in weapon design. The main source of ^{236}U in nuclear weapon debris is thermonuclear fission – fusion – fission reactions in which fast neutrons released from a fusion

secondary stage induces fission in a tertiary tamper stage of natural or depleted U (Winkler *et al.,* 2012). In this process ^{236}U is produced in neutron capture in ^{235}U or the reaction ^{238}U (n, 3n) ^{236}U. Nuclear weapon material in pure fission weapons or thermonuclear primaries has been indicated to consist of pure U, Pu or a combination of the two (e.g. Bukharin (1998), Eriksson *et al.* (2005), Ranebo *et al.* (2007), Lind *et al.* (2007)). The production of ^{236}U in pure fission and fission - fusion detonations is likely lower than in fission – fusion – fission detonations, and the $^{236}U/^{239}Pu$ atom ratio in debris from low yield detonations has been indicated to be low (Paper III and Beasley *et al.* (1998b)).

6.4 Plutonium isotopes heavier than ^{240}Pu

Analysis of Plutonium isotopes heavier than ^{240}Pu were performed in selected humic surface soil samples (paper I), pooled air filters from 1957 (Sola 9 – 21 October 1957), 1962 (Røros 16 – 26 march 1962) and 1963(Røros 1 – 11 June 1963), and selected filters from November 1962 (paper III). The results are presented in Table 5 and Figure 25.

The $^{242}Pu/^{239}Pu$ atom ratio observed in the pooled air filter samples and the humic surface soil samples ranged within 1.3 $\times 10^{-3}$ and 10 $\times 10^{-3}$. The lowest ratios were found in pooled air filter samples from 1961, and the highest atom ratios were found in the humic surface soil samples.

A higher $^{242}Pu/^{239}Pu$ atom ratio was found in the pooled filter sample from 1957 than from 1962. The same tendency is observed in the $^{242}Pu/^{239}Pu$ atom ratios in a time resolved sediment core from Lake Erie, wherein substantially higher ratios (5.36 $\times 10^{-3}$) were found the moratorium than after (3.20$\times 10^{-3}$ for the years 1961 to 1964) (Winkler *et al.,* 2004). The pooled filters from 1957 would have collected debris from atmospheric detonations in the few months preceding the sampling. Transfer of debris from the stratosphere to the troposphere is at its lowest during the months September through October (UNSCEAR, 2000a), and contemporary atmospheric testing activities would likely easily overwhelm the Pu atom ratio signatures of stratospheric debris. The pooled filters from 1962 would have captured almost exclusively stratospheric debris for the following reasons:

- The sampling period was during the peak transfer of debris from the stratosphere to the troposphere as defined in (UNSCEAR, 2000a)
- Only the US detonation the 05.03.1962 was close enough geographically to affect the filters. However, this detonation was as small cratering detonation (Björklund and Goliath, 2009), depositing most of its debris close to the detonation site. Debris from the detonation conducted above Christmas Island

the 25.04.1962 is unlikely to have reached Norway soon enough to influence Pu concentrations and atom ratios in the air filters from the sampling period.

The most likely origin of the debris in the pooled air filters from 1962 is then FSU test series in September through November 1961. This test series encompassed small, large and very large detonations injecting debris into different parts of the atmosphere. The stratospheric residence time of debris from the largest detonations were long, and peak deposition of this debris would not be expected to take place until the spring of 1963 (Peterson, 1970). Thus the radionuclide composition in the troposphere in the first half of 1962 should be dominated by debris from detonations in the range 0.7 – 4 Mt. Eight detonations performed in 1961 had a yield in the size range suitable for inserting debris into the lower polar stratosphere. The $^{240}Pu/^{239}Pu$ and $^{242}Pu/^{239}Pu$ atom ratios measured in the spring of 1962, 0.145 and 1.3×10^{-3} is likely representative of the mixed debris from these detonations.

Table 5. Atom ratios obtained in paper I (upper part, humic surface soil samples) and paper III (lower part, air filter samples).

Site	Date / year	$^{240}Pu/^{239}Pu$	$^{241}Pu/^{239}Pu$ $\times 10^{-3}$	$^{242}Pu/^{239}Pu$ $\times 10^{-3}$	$^{244}Pu/^{239}Pu$ $\times 10^{-4}$
Glomfjord	2005	0.20 ± 0.02	2.3 ± 0.8	10 ± 2	n.a.
Trolla	2005	0.17 ± 0.01	1.5 ± 0.6	4.5 ± 0.7	n.a.
Fyllingsdalen	2005	0.17 ± 0.01	1.4 ± 0.4	5.1 ± 0.9	n.a.
Kløfta	2005	0.19 ± 0.02	0.9 ± 0.5	6 ± 1	n.a.
Svolvær	2005	0.17 ± 0.01	1.3 ± 0.3	3.8 ± 0.5	n.a.
Røros	09.11.1962	0.0605 ± 0.0008	0.46 ± 0.06	n.a.	n.a.
Bergen	11.11.1962	0.0517 ± 0.0009	0.62 ± 0.09	n.a.	n.a.
Ålesund	11.11.1962	0.0574 ± 0.0006	0.37 ± 0.04	n.a.	n.a.
Ålesund	12.11.1962	0.061 ± 0.001	0.25 ± 0.05	n.a.	n.a.
Bergen	9.10-21.10.57	0.116 ± 0.007	n.a.	2.8 ± 0.5	n.a.
Røros	16.4 - 26.4.62	0.145 ± 0.003	0.4 ± 0.1	1.3 ± 0.1	b.d.
Røros	1.6 - 11.6.63	0.220 ± 0.003	1.6 ± 0.2	4.5 ± 0.2	1.7 ± 0.5

n.a. – not analysed, b.d. – below the detection limit
reference date 01.01.2012.

The pooled air filter sample from 1963 had a $^{242}Pu/^{239}Pu$ atom ratio higher than established integrated global fallout (Kelley *et al.,* 1999) and contemporary levels (Winkler, 2007). However, consistently high gross beta activities indicate that

these filters were deployed during the spring peak deposition of stratospheric fallout. The fallout thus captured would include debris from the high yield detonations from 1961 and possibly 1962, and high Pu atom ratios should be expected. It should also be mentioned that the $^{240}Pu/^{239}Pu$ atom ratio in this sample agrees well with ratios reported by Warneke *et al.* (2002) and Salminen-Paatero *et al.* (2012) for the same time period.

The $^{240}Pu/^{239}Pu$ and $^{242}Pu/^{239}Pu$ atom ratios in the humic surface soil samples were well correlated (R^2_{adj}=0.85 and p=0.01). The higher $^{242}Pu/^{239}Pu$ atom ratios found at Glomfjord and Kløfta may reflect a slight deposition of Chernobyl-related plutonium. The calculated $^{242}Pu/^{239}Pu$ atom ratio in the fuel of the Chernobyl reactor at the time of the accident ranged within 0.039 – 0.048 (UNSCEAR (2000b), and references therein), i.e., approximately 10 times the global fallout ratio of 0.0039 ± 0.0007 (Kelley *et al.,* 1999).

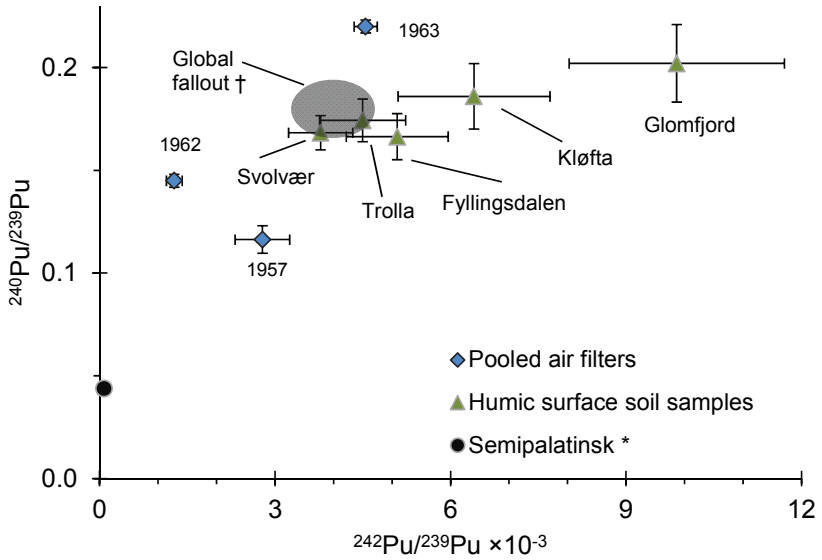

Figure 25. Atom ratios of $^{240}Pu/^{239}Pu$ and $^{242}Pu/^{239}Pu$ in the present work, reference date 01.01.2012. The pooled air filter samples are based on ten consecutive days of sampling in Bergen in autumn 1957 and Røros in spring 1962 and 1963. Literature values included for comparison, * Beasley *et al.* (1998b), † Kelley *et al.* (1999).

6.5 Source identification

6.5.1 *Debris from the Windscale accident*

Pu activity concentrations and $^{240}Pu/^{239}Pu$ atom ratios were determined in air filters from Sola, 9th, 16th, 17th, 22nd October 1957. In addition $^{240}Pu/^{239}Pu$ atom ratios were determined in grouped air filters from Bergen covering the period 9 to 21 October. The $^{240}Pu/^{239}Pu$ atom ratios were found to range within 0.09 – 0.12 in this period. Atmospheric dispersion modelling (e.g. Bergan *et al.* (2008)) and elevated gross beta activities in the air filters indicate that the debris cloud from the Windscale fire arrived to the Norwegian West coast the 16 October. The highest gross beta concentrations were measured at Sola and Bergen (321 and 249 mBq m^{-3} respectively, the 16 October), however, the Pu concentrations did not peak on the same day as the gross beta concentrations. The $^{240}Pu/^{239}Pu$ atom ratio observed in the filter from the 16th October was lower than the other filters from the same period, however, it is not likely that the low $^{249}Pu/^{239}Pu$ atom ratio reflects Windscale Pu. The releases of Pu from the Windscale fire have been estimated to be low, assuming an $^{240}Pu/^{239}Pu$ below 0.07 for weapons grade Pu, the total estimated releases of Pu would be less than 45 g (Garland and Wakeford, 2007).

Between 22 August and 10 October 1957, 7 nuclear detonations with yields in the range 0.006 – 2.9 Mt were conducted at FSU test sites NZ and STS. Pu in debris from these detonations should be expected to overwhelm the non-local fallout from the Windscale accident. Thus, the Pu captured in these filters likely originates from nuclear weapons rather than the Windscale plant.

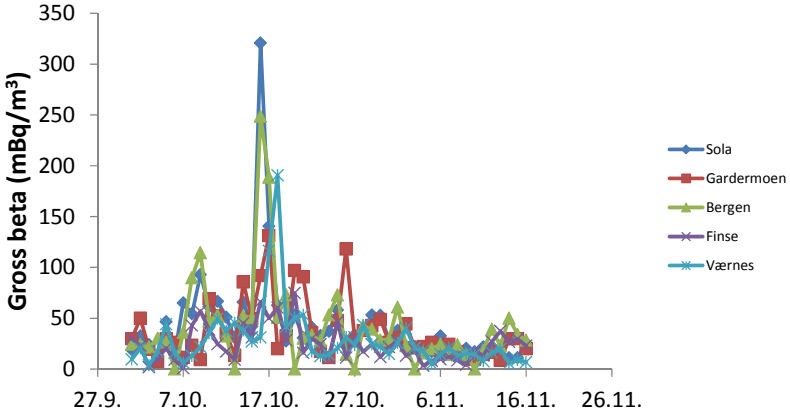

Figure 26. Gross beta activities in Norwegian ground level air measured during the first few days after the Windscale accident in 1957 (Bergan). Peak activities were seen at the west coastal stations Sola and Bergen before proceeding east / northeast to Gardermoen and Værnes.

6.5.2 Debris from the Chernobyl accident

In Paper I, the $^{240}Pu/^{239}Pu$ atom ratios (0.161 – 0.211) for both series of the humic surface soil samples were mainly reflecting global fallout. Significant deviations from global fallout atom ratios were found for some inland locations (Kongsvoll, Skredå, Vauldalen, Kløfta, Stavsjø and Øystre Slidre) indicating influence of Chernobyl related debris. A selection of $^{240}Pu/^{239}Pu$ atom ratios obtained in this work and in southern Sweden and Finland is shown in Figure 27.

Lower variation was observed in the results from this work compared to the results from Sweden (Lindahl *et al.,* 2004) and Finland (Salminen-Paatero *et al.,* 2012). Lichens, as used by both authors, absorbs most of its nutrients and hence contaminants, from the air (Lindahl *et al.,* 2004; Steinnes, 2008). Chernobyl derived Pu deposited onto lichens is thus less likely to be diluted by global weapons fallout Pu. Similarly, peats from commercially exploited peatlands, as used by Salminen-Paatero *et al.* (2012), are also likely to represent less diluted Chernobyl fallout, provided that harvest of the peat layer was conducted between the main deposition of global fallout and the Chernobyl accident. Additionally, as reviewed by Pöllänen *et al.* (1997), deposition of Chernobyl related debris was highly heterogeneous with numerous hot spots ranging in size from 30 cm up to several kilometres.

The influence of debris from the Chernobyl accident on $^{240}Pu/^{239}Pu$ atom ratios in the humic surface soil samples was assessed in (paper I) using the formula:

$$X = \frac{(R_{Sample} - R_{GFO})}{(R_{Chb} - R_{GFO})} * 100\%$$

where R_{GFO} is the $^{240}Pu/^{239}Pu$ atom ratio in global fallout, (0.18 according to Kelley *et al.* (1999)) and R_{Chb} (0.40 ± 0.07 is the estimated $^{240}Pu/^{239}Pu$ atom ratio given in UNSCEAR (2008)). The calculated Chernobyl debris influence on the $^{239+240}Pu$ concentrations at sites Kongsvoll, Skredå, Vauldalen, Kløfta, Stavsjø and Øystre Slidre was calculated to range within 8 and 13 %.

The $^{241}Pu/^{239}Pu$ atom ratios in the humic surface soil samples suffered from large uncertainties as a consequence of low concentrations. Nevertheless, the Glomfjord sample displayed a $^{241}Pu/^{239}Pu$ atom ratio higher than global fallout indicating a Chernobyl influence of the deposition at this site. The indication of a Chernobyl influence at Glomfjord was further corroborated by the $^{242}Pu/^{239}Pu$ atom ratio, which also indicated that the Kløfta sample had been influenced by Chernobyl derived Pu. The $^{134}Cs/^{137}Cs$ activity ratio measured in soils from 1986 from areas close to Kløfta and Glomfjord (Ullensaker (0.43) and Rana (0.35)) , indicated that

both Kløfta and Glomfjord were within municipalities that received a substantial deposition of Chernobyl debris (Backe *et al.,* 1986).

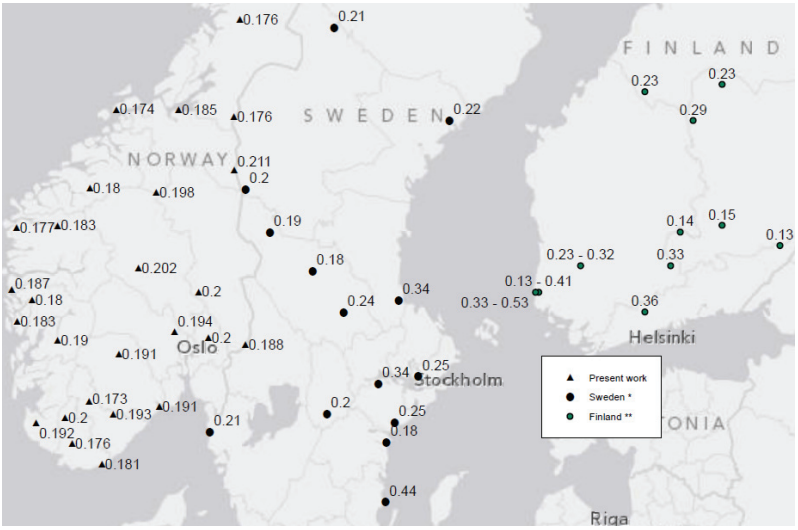

Figure 27. Pu-240/Pu239 atom ratios measured in this work (values from the series collected in 1990), southern Finland and Sweden following the Chernobyl accident. * Lindahl *et al.* (2004), ** Salminen-Paatero *et al.* (2012). Lindahls work is based on lichen samples collected in the period June 1986 – September 1988, Salminen-Paateros work is based on peat samples, lichen samples and hot particles collected through the summer and autumn of 1986.

6.5.3 Direct tropospheric transport from Semipalatinsk

During 7.11.1962 – 13.11.1962, pronounced peaks in gross activities in air filters were registered at all stations (Paper III). Elevated activities were first observed at , Gardermoen, Røros and Værnes the 8 November, however, the highest activity concentrations were observed in Ålesund the . Analysis of the filters revealed low $^{240}Pu/^{239}Pu$ (0.0517 – 0.077), $^{241}Pu/^{239}Pu$ (2.5 – 6.2) $\times 10^{-4}$ and $^{236}U/^{239}Pu$ (0.0188 – 0.046) atom ratios consistent with debris from low yield detonations. Based on activity ratios of short lived beta emitters, Hvinden *et al.* (1964) estimated that the debris originated from a detonation the 31.10 or 01.11.1962. Two low yield atmospheric detonations (0.003 and 0.01 Mt) were performed at STS the 31.10 and 01.11.62. These detonations would have produced debris in which the $^{240}Pu/^{239}Pu$, $^{241}Pu/^{239}Pu$ or $^{236}U/^{239}Pu$ atom ratios would be very similar to undetonated weapon material. Three detonations in the yield range 0.24 – 0.28 Mt were performed at NZ in the same period; however, $^{240}Pu/^{239}Pu$ and $^{236}U/^{239}Pu$ atom ratios in debris from these detonations is expected to be higher than those found in the air filters from November 1962.

Hysplit simulations were performed simulating the transport of debris from detonations at Semipalatinsk and Novaya Zemlya. The results indicate that the elevated activity concentrations seen in surface air in Norway during 7 to 13 November 1962 originated from one or more of the three atmospheric nuclear detonations above Novaya Zemlya in the period 30 October to 1 November 1962. Figure 28 shows the HYSPLIT simulation of a release above Semipalatinsk test sited the 31 November 1962.

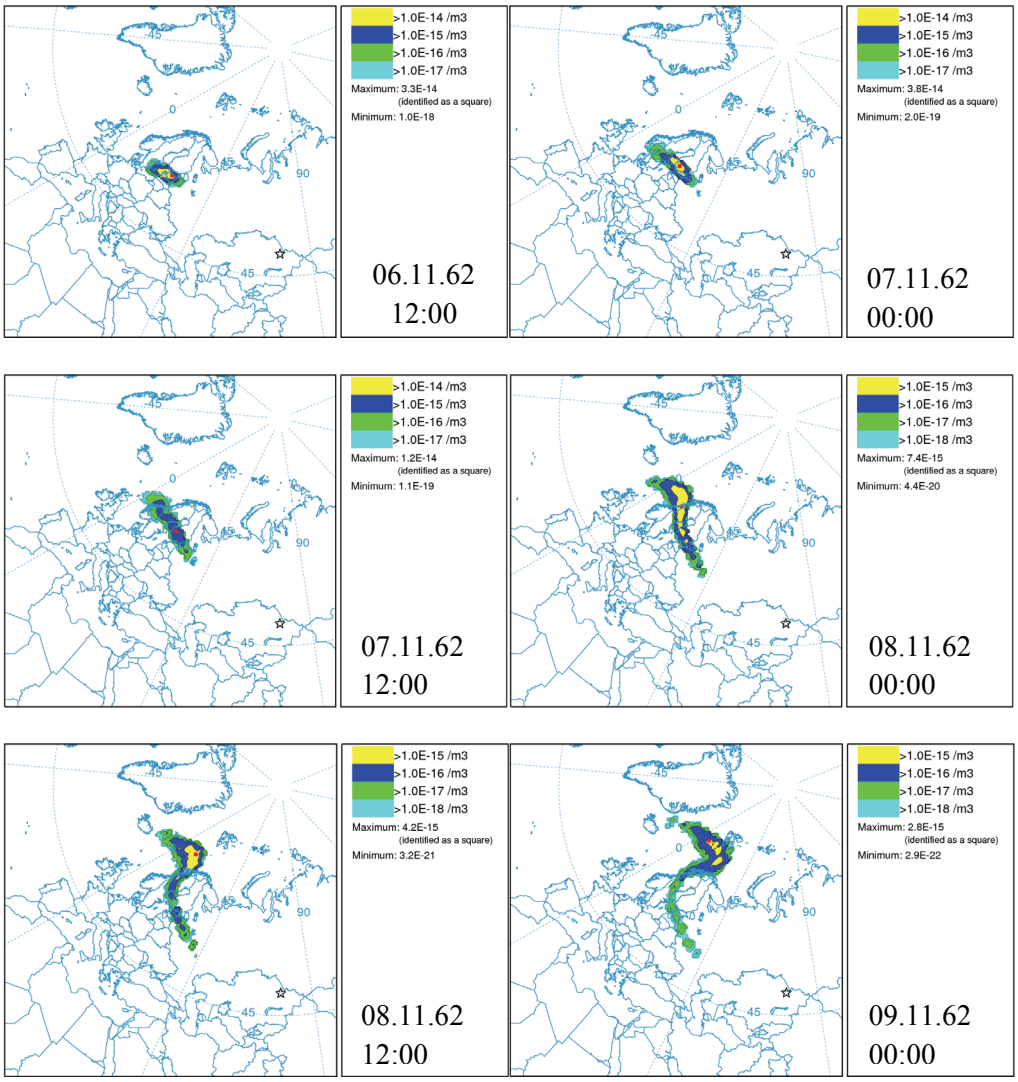

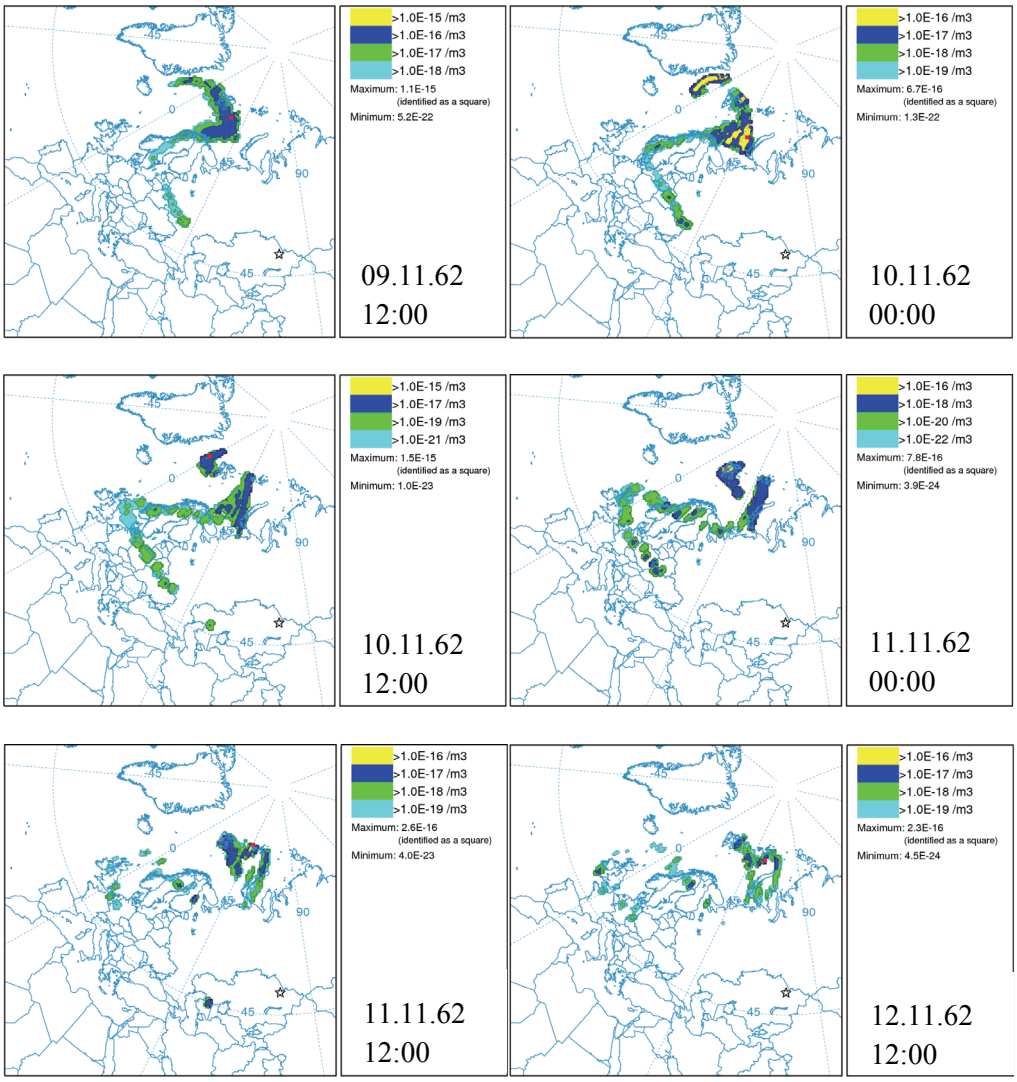

Figure 28. Summary of a selected HYSPLIT simulation of the radioactive cloud from a low yield detonation above Semipalatinsk the 31.10.1962. Release heights between 1750 – 5000 m were simulated, and post detonation debris concentrations in air between 0 and 75 m above ground were simulated. The figure shows the position of the plume from 6.11.1962 at 12:00 and with 12 hour increments thereafter.

Air concentrations of Pu and ^{236}U concentrations during this episode were exceptionally high (11.7 - 782 µBq m^{-3} and 4.6 – 20.1 nBq m^{-3} respectively). However, it is unlikely that this would affect integrated fallout. Deposition is strongly correlated to precipitation (e.g. Storebø (1968), Pálsson *et al.* (2012)),

which was very low during the passage of the plume (www.eklima .no; D.R. Kristoffersen, pers. comm.).

The time resolution of Pu in the ice core (Paper II), was insufficient for the direct identification of detonations. High pre moratorium $^{240}Pu/^{239}Pu$ atom ratios indicative of fallout from the US thermonuclear detonations in 1952 and 1954, documented in other publications (e.g. Koide *et al.* (1985), Olivier *et al.* (2004), Warneke *et al.* (2002)) were not observed. Positive inflections in the $^{240}Pu/^{239}Pu$ atom ratio caused by fallout from the large Former Soviet Union test series in 1961 and 1962 could not be identified either. The difference between the current results and the results of Warneke *et al.* (2002) are easily explained by the poorer resolution of the Austfonna ice core, and the fact that the highest atom ratios observed by Warneke *et al.* (2002) were associated with low deposition rates. The high atom ratio observations made by Koide *et al.* (1985) and Olivier *et al.* (2004) on the other hand are associated with high deposition rates, and the reason for the discrepancy must be sought elsewhere. As reviewed by Barrie (1986), the arctic winter air mass covers large areas of continental Europe and Central Asia as far south as 40 °N. Pollutants tropospherically transported from Europe and Central Asia enters the Arctic from South-East (Barrie, 1986; Stohl *et al.,* 2000). Furthermore, the deposition profile observed at Nordaustlandet contrasts with deposition profiles established for other sites (Koide *et al.,* 1985; Warneke *et al.,* 2002; Olivier *et al.,* 2004). This indicates a different deposition regime at Svalbard. The mixture of debris from low yield, low $^{240}Pu/^{239}Pu$ atom ratio debris from STS with debris from high yield, high $^{240}Pu/^{239}Pu$ atom ratio debris from NZ could offer an explanation.

7 Concluding remarks

In the present thesis source identification and source assessment have been conducted based on Pu and U atom and activity ratios in radioactive debris in humic surface soil samples from mainland Norway (Paper I); an arctic ice core covering the period 1949 - 1999(Paper II); and air filter samples from Norway during 1957 - 1963(Paper III). Radioactive particles have been searched for and identified in the air filter samples the ice core samples (Paper II) and (Paper III). Atmospheric dispersion modelling (NOAA HYSPLIT_4) has been used for source identification purposes in (Paper III).

The main objectives of the present work have been to assess the inventory and provenance of Pu from atmospheric nuclear weapon detonations and reactor accidents deposited on Norwegian territories. A combination of advanced mass spectrometry techniques and atmospheric dispersion modelling has been applied.

In the following section the working hypotheses of the present work will be answered based on the obtained results.

H1. *Pu originating from nuclear weapons tests should follow the precipitation pattern, and be enriched at the western coast of Norway*

- Based on concentrations and atom ratios of Pu in humic surface soils, the dominant source was found to be global fallout. Deposition was found to be highest along the western coast in accordance with high annual precipitation rates.

H2. *Traces of Pu associated with reactor fallout should be more unevenly distributed than debris from weapons tests, and it should be possible to identify the signal at certain inland sites in Norway.*

- Pu in integrated fallout samples like surface soils is largely attributed to global fallout Pu. Thus the impact of deposition from a source must be substantial in order to be detected by means of isotope ratio measurements. Nevertheless, higher than global fallout $^{240}Pu/^{239}Pu$ atom ratios were observed at some eastern inland sites in Norway. Further analysis on the abundances of heavier Pu isotopes (^{241}Pu and ^{242}Pu) for a sub-selection of the soils confirmed influence of Chernobyl related Pu at several inland sites.

H3. Inert radioactive particles are expected to be present in samples affected by fallout from the nuclear weapons tests and nuclear reactor accidents

- Autoradiography hotspots indicated the presence of radioactive particles on filters collected during periods associated with atmospheric nuclear tests at

FSU test sites Novaya Zemlya and Semipalatinsk. Autoradiography of air filters revealed the presence of radioactive particles almost exclusively in periods during and after atmospheric nuclear weapons detonations, while there were very few particle indications during periods of high stratospheric deposition (spring peak deposition). Hotspots were also observed in ice core filtrates, during time periods associated with FSU atmospheric testing activities (1949 – 1965) and the Chernobyl accident or a vented underground test at Novaya Zemlya (1985 - 1989).

H4. Over time the Pu concentrations in soil will decrease

- Pu concentrations in parallel samplings of humic surface soils in 1990 and 2005 were analysed. A clear decrease in $^{239+240}$Pu concentrations was found.

H5. Pu and U isotopic composition or atom ratios can be utilized for source identification. If the time resolution is sufficiently good, single events contributing to the deposition of Pu and ^{236}U can be identified.

- Source identification and source assessment was performed both for high time resolution samples and integrated fallout samples. Pu and U isotopes captured in archive air filters (time resolution 24 h) allowed for the identification of tropospherically transported fallout from FSU test site Semipalatinsk. Global fallout was found to be the dominant source of Pu deposition in mainland Norway. However, an impact from the Chernobyl accident was shown as well.

In summary, the following conclusions can be drawn:

- Pu deposition in the terrestrial environment of Norway was found to be primarily caused by global fallout. However, a slight Chernobyl influence was found at several inland sites.
- Pu and ^{236}U concentration profiles in an ice core from Austfonna (Svalbard) showed higher concentrations at depths corresponding to pre-moratorium deposition (1956 – 1959) than post-moratorium (1959 – 1962). This is in contrast to timer resolved sampling from other locations, and indicates either the influence of post depositional processes altering concentration profiles of particulate radionuclides in the glacier, or a different deposition pattern at this site compared to other sites.
- Pu in air showed a clear influence of debris from FSU test sites NZ and STS during periods associated with testing at these sites, attaining ^{240}Pu/^{239}Pu atom ratios significantly lower than global fallout. Similarly, the presence of radioactive particles was much higher during these periods. During periods without atmospheric nuclear testing at NZ and STS, ^{240}Pu/^{239}Pu atom ratios reflected global (stratospheric fallout).

Appendix 1. Summary of gross β activities, Pu concentrations, $^{240}Pu/^{239}Pu$ atom ratios and particle indications in the air filters analysed in paper III

Site	Date	Gross β mBq m^{-3}	Particles	$^{240}Pu/^{239}Pu$ atom ratio	$^{239+240}Pu$ μBq m^{-3}
Sola	09.10.1957	93	0	0.13 ± 0.01	7.4 ± 0.2
Sola	16.10.1957	321	0	0.09 ± 0.02	3.0 ± 0.2
Sola	17.10.1957	141	0	0.115 ± 0.006	3.5 ± 0.2
Bergen	08 - 20.10.1957	941	-	0.116 ± 0.007	n.d.
Sola	22.10.1957	41	0	0.15 ± 0.02	2.2 ± 0.1
G.moen	01.06.1958	127	0	0.169 ± 0.008	22.1 ± 0.5
G.moen	02.06.1958	152	0	0.170 ± 0.007	24.9 ± 0.5
G.moen	03.06.1958	155	0	0.162 ± 0.007	28.4 ± 0.6
Sola	27.09.1961	235	1	0.090 ± 0.008	6.9 ± 0.2
G.moen	28.09.1961	327	0	0.09 ± 0.01	1.96 ± 0.08
Røros	06.10.1961	207	2	0.088 ± 0.005	2.86 ± 0.05
Bergen	19.10.1961	428	2	0.086 ± 0.009	3.2 ± 0.1
Røros	19.10.1961	98	0	0.20 ± 0.07	15 ± 3
Vadsø	19.10.1961	130	1	0.14 ± 0.03	1.3 ± 0.1
Bergen	27.10.1961	65	0	0.09 ± 0.02	1.8 ± 0.1
Røros	27.10.1961	35	0	b.d.	b.d.
Vadsø	27.10.1961	83	0	0.15 ± 0.02	1.73 ± 0.09
Bodø	10.11.1961	1093	0	0.093 ± 0.014	14.9 ± 0.7
Tromsø	11.11.1961	888	0	0.07 ± 0.002	1.7 ± 0.1
Tromsø	12.11.1961	1747	7	0.067 ± 0.006	16.3 ± 0.5
Ålesund	17.11.1961	305	1	0.100 ± 0.007	4.3 ± 0.1
Røros	11.01.1962	199	0	0.13 ± 0.01	2.25 ± 0.09
Bergen	17.01.1962	297	0	0.110 ± 0.007	18.1 ± 0.5
Røros	04.03.1962	58	0	0.127 ± 0.005	12.3 ± 0.2
Bergen	15.04.1962	209	0	0.138 ± 0.006	26.7 ± 0.5
Bergen	16.04.1962	205	0	0.137 ± 0.005	27.8 ± 0.4
Bergen	17.04.1962	263	0	0.142 ± 0.003	30.3 ± 0.4
Bergen	18.04.1962	104	0	0.148 ± 0.006	15.4 ± 0.3
Bergen	19.04.1962	157	0	0.138 ± 0.007	21.4 ± 0.5
Bergen	20.04.1962	252	0	0.141 ± 0.004	36.0 ± 0.5
Bergen	21.04.1962	219	0	0.152 ± 0.005	29.1 ± 0.4
Bergen	22.04.1962	207	0	0.140 ± 0.005	27.8 ± 0.4

Bergen	23.04.1962	222	0	0.156 ± 0.005	34.0 ± 0.5
Bergen	24.04.1962	154	0	0.152 ± 0.006	19.7 ± 0.4
Vadsø	25.04.1962	78	0	0.14 ± 0.01	3.2 ± 0.1
Røros	15 - 25.04.1962	1992	2	0.145 ± 0.003	n.d.
Sola	09.11.1962	3142	15	0.060 ± 0.001	169 ± 2
G.moen	09.11.1962	9092	15	0.0614 ± 0.0007	575 ± 5
Røros	09.11.1962	11527	22	0.0574 ± 0.0006	487 ± 4
Bodø	09.11.1962	8132	2	0.054 ± 0.001	301 ± 3
Tromsø	10.11.1962	2050	4	0.063 ± 0.003	116 ± 2
Bergen	11.11.1962	6327	8	0.059 ± 0.001	267 ± 2
Ålesund	11.11.1962	15467	9	0.0517 ± 0.0009	782 ± 7
Værnes	11.11.1962	2362	3	0.062 ± 0.002	121 ± 1
Vadsø	11.11.1962	464	8	0.077 ± 0.004	11.7 ± 0.2
Ålesund	12.11.1962	8781	9	0.061 ± 0.0008	631 ± 5
Ålesund	13.11.1962	1762	0	0.064 ± 0.003	87 ± 1
Ålesund	17.11.1962	48	1	0.21 ± 0.01	2.48 ± 0.09
Bergen	28.05.1963	162	0	0.190 ± 0.006	20.1 ± 0.3
Bergen	29.05.1963	130	0	0.195 ± 0.007	27.1 ± 0.5
Bergen	30.05.1963	307	0	0.23 ± 0.01	18.2 ± 0.4
Bergen	31.05.1963	499	0	0.204 ± 0.007	26.3 ± 0.5
Bergen	01.06.1963	394	1	0.237 ± 0.005	53.9 ± 0.7
Bergen	03.06.1963	332	0	0.227 ± 0.0.007	35.3 ± 0.6
Bergen	06.06.1963	376	0	0.221 ± 0.005	20.3 ± 0.3
Røros	08.06.1963	817	0	0.225 ± 0.004	157 ± 2
Røros	31.05-10.06.1963	4681	0	0.227 ± 0.004	n.d.

Appendix 2. Summary of some results from the humic surface soil samples in paper I, the $^{238}Pu/^{239+240}Pu$ activity ratio and retention of $^{239+240}Pu$ and ^{137}Cs. Numbers in brackets are outliers, cf. chapter 6.1.4.

			Retention			
	$^{238}Pu/^{239+240}Pu$ 1990		^{137}Cs		$^{239+240}Pu$	
Site	Activity ratio	±	%	±	%	±
Onsøy	0.049	0.004	n.a.	n.a.	n.a.	n.a.
Kløfta	0.040	0.005	(136)	(4)	60	6
Magnor	0.07	0.03	46	4	2.84	0.2
Stavsjø	0.043	0.007	39	2	52	4
Østre slidre	0.059	0.006	76	2	16	2
Øyer	n.a.	n.a.	50	2	75	17
Gjendesheim	n.a.	n.a.	n.a.	n.a.	n.a.	n.a.
Heidal	0.030	0.003	n.a.	n.a.	n.a.	n.a.
Hønefoss	n.a.	n.a.	13.2	0.9	5.61	0.7
Langesund	0.063	0.005	65	2	(90)	(7)
Rjukan	0.045	0.003	16.8	0.7	(218)	(11)
Gjøvdal	0.027	0.002	23	1	66	9
Hylestad	0.040	0.004	n.a.	n.a.	n.a.	n.a.
Søgne	0.045	0.005	18	1	5.52	0.5
Vatland	0.046	0.004	47	2	65	13
Skredå	n.a.	n.a.	27	2	28	2
Ålgård	0.06	0.01	33	2	(158)	(9)
Odda	0.039	0.005	33	1	57	11
Fyllingsdalen	0.043	0.003	54	4	(98)	(3)
Stamnes	0.025	0.002	20	1	(1.9)	(0.3)
Sløvåg	0.036	0.004	43	2	4	1
Svelgen	n.a.	n.a.	35	2	71	2
Utvik	0.036	0.002	37	1	2.10	0.1
Grønning	0.022	0.001	21	1	78	8
Kongsvoll	n.a.	n.a.	n.a.	n.a.	n.a.	n.a.
Vauldalen	n.a.	n.a.	38	2	10.98	0.6
Trolla	n.a.	n.a.	20.9	0.9	44	3
Forsnes	0.040	0.006	n.a.	n.a.	n.a.	n.a.
Teveldal	n.a.	n.a.	15.0	0.4	5.39	0.9

Udland	n.a.	n.a.	n.a.	n.a.	n.a.	n.a.
Muru	0.043	0.009	n.a.	n.a.	n.a.	n.a.
Høylandet	n.a.	n.a.	45	1	51	3
Grane	0.034	0.004	n.a.	n.a.	n.a.	n.a.
Mosjøen	0.052	0.003	9.2	0.5	3	1
Koksverket	0.036	0.003	28	2	(497)	(91)
Glomfjord	0.055	0.005	38	2	73	14
Ankenes	0.038	0.006	59	4	(157)	(8)
Svolvær	n.a.	n.a.	92	5	34	2
Stonglandet	n.a.	n.a.	n.a.	n.a.	n.a.	n.a.
Stilla	n.a.	n.a.	9.9	0.6	21	1
Slåtten	n.a.	n.a.	n.a.	n.a.	n.a.	n.a.
Aiddejavvri	n.a.	n.a.	n.a.	n.a.	n.a.	n.a.
Syltefjord	0.033	0.002	n.a.	n.a.	n.a.	n.a.
Jakobsnes	n.a.	n.a.	23	1	(98)	(10)
Svanvik	n.a.	n.a.	20	1	6.93	0.5

References

Ahrens CD. Meteorology today: an introduction to weather, climate, and the environment. South Melbourne: Thomson/Brooks/Cole, 2003.

AMAP. Radioactivity, Oslo, 1998.

Backe S, Bjerke H, Rudjord A, Ugletveit F. 1986. Nedfall av cesium i Norge etter tsjernobylulykken. NRPA. Østerås.

Backe S, Bjerke H, Rudjord AL, Ugletveit F. Fall-out Pattern in Norway after the Chernobyl Accident Estimated from Soil Samples. Radiat. Prot. Dosim. 1987; 18: 105-107.

Bakhtiar N, Lee SC, Kuroda PK. U-235 fallout from the nuclear-powered satellite Cosmos-1402. Journal of Radioanalytical and Nuclear Chemistry 1985; 91: 403-409.

Barnaby F. Plutonium and security. London: Macmillan, 1992.

Barrie LA. Arctic air-pollution - an overview of current knowledge. Atmospheric Environment 1986; 20: 643-663.

Barrie LA, Gregor D, Hargrave B, Lake R, Muir D, Shearer R, *et al.* Arctic contaminants - sources, occurrence and pathways. Science of the Total Environment 1992; 122: 1-74.

Barrie LA, Hoff RM. The oxidation rate and residence time of sulfur-dioxide in the arctic atmosphere. Atmospheric Environment 1984; 18: 2711-2722.

Bartnicki J, Salbu B, Saltbones J, Foss A, Lind OC. 2001. Gravitational settling of particles in dispersion model simulations using the Chernobyl accident as a test case. The norwegian meteorological institute. Oslo.

Bartnicki J, Salbu B, Saltbones J, Foss A, Lind OC. Long-range transport of large particles in case of nuclear accident or explosion. 26th NATO/CCMS International Technical Meeting on Air Pollution Modelling and its Application. Istanbul Technical University, Istanbul, Turkey, 2003, pp. 53 - 60.

Beasley T, Cooper L, Grebmeier J, Aagaard K, Kelley J, Kilius L. Np-237/I-129 atom ratios in the Arctic Ocean: Has Np-237 from western European and Russian fuel reprocessing facilities entered the Arctic Ocean? Journal of Environmental Radioactivity 1998a; 39: 255-277.

Beasley T, Kelley J, Orlandini K, Bond L, Aarkrog A, Trapeznikov A, *et al.* Isotopic Pu, U, and Np signatures in soils from Semipalatinsk-21, Kazakh Republic and the Southern Urals, Russia. Journal of Environmental Radioactivity 1998b; 39: 215-230.

Bergan T, Dowdall M, Selnaes OG. On the occurrence of radioactive fallout over Norway as a result of the Windscale accident, October 1957. Journal of Environmental Radioactivity 2008; 99: 50-61.

Bjurman B, Degeer LE, Vintersved I, Rudjord AL, Ugletveit F, Aaltonen H, *et al.* The detection of radioactive material from a venting underground nuclear-explosion. Journal of Environmental Radioactivity 1990; 11: 1-14.

Björklund L, Goliath M. 2009. Kärnladdningars skadeverkningar. Totalförsvarets forskningsinstitut (Swedish Defence Research Agency).

Boulyga SF, Heumann KG. Determination of extremely low U-236/U-238 isotope ratios in environmental samples by sector-field inductively coupled plasma mass spectrometry using high-efficiency sample introduction. Journal of Environmental Radioactivity 2006; 88: 1-10.

Bukharin OA. Securing Russia's HEU stocks. Science and global security 1998; 7: 311-331.

Bunzl K, Kracke W, Schimmack W, Zelles L. Forms of fallout Cs-137 and Pu239+240 in successive horizons of a forest soil. Journal of Environmental Radioactivity 1998; 39: 55-68.

Bunzl K, Kracke W, Shimmack W, Auerswald K. Migration of fallout Pu-239+240, Am-241 and Cs-137 in the various horizons of a forest soil under pine. Journal of Environmental Radioactivity 1995; 28: 17-34.

Carlson J, Bardsley J, Bragin V, Hill J. Plutonium Isotopics - Non-Proliferation And Safeguards Issues. Australian Safeguards Office, Canberra, ACT, Australia, 1988.

Carter MW, Moghissi AA. 3 decades of nuclear testing. Health Phys. 1977; 33: 55-71.

Chagnon CW, Junge CE. The Size Distribution of Radioactive Aerosols in the Upper Troposphere. Journal of Applied Meteorology 1965; 4: 329-333.

Chamberlain AC. Environmental impact of particles emitted from Windscale piles, 1954-7. Science of the Total Environment 1987; 63: 139-160.

Chamberlain AC. Emissions from Sellafield and activities in soil. Science of the Total Environment 1996; 177: 259-280.

Child DP, Hotchkis MAC, Williams ML. High sensitivity analysis of plutonium isotopes in environmental samples using accelerator mass spectrometry (AMS). J. Anal. At. Spectrom. 2008; 23: 765-768.

Choppin GR, Liljenzin JO, Rydberg J. Radiochemistry and nuclear chemistry. Oxford: Butterworth-Heinemann, 2002.

Cizdziel JV, Ketterer ME, Farmer D, Faller SH, Hodge VF. Pu-239,Pu-240,Pu-241 fingerprinting of plutonium in western US soils using ICPMS: solution and laser ablation measurements. Anal. Bioanal. Chem. 2008; 390: 521-530.

Clacher AP. 1995. Development and application of analytical methods for environmental radioactivity. PhD thesis. University of Manchester.

Cochran T, Norris RS. 1996. Nuclear weapons tests and peaceful nuclear explosions by the soviet union, August 29, 1949 to october 24, 1990. Natural resources defence council inc.

Cooper LW, Kelley JM, Bond LA, Orlandini KA, Grebmeier JM. Sources of the transuranic elements plutonium and neptunium in arctic marine sediments. Marine Chemistry 2000; 69: 253-276.

Crocker GR, Oconnor JD, Freiling EC. Physical and radiochemical properties of fallout particles. U.S. naval radiological defense laboratory, San Francisco, 1966.

Cronkite EP, Conard RA, Bond VP. Historical events associated with fallout from Bravo Shot - Operation Castle and 25 Y of medical findings. Health Phys. 1997; 73: 176-186.

CTBTO. Partial test ban treaty http://www.ctbto.org/index.php?id=280&no_cache=1&letter=p#partial-test-ban-treaty- 2013

Devell L, Tovedal H, Bergstrom U, Appelgren A, Chyssler J, Andersson L. Initial observations of fallout from the reactor accident at chernobyl. Nature 1986; 321: 192-193.

Diamond H, Fields PR, Stevens CS, Studier MH, Fried SM, Inghram MG, *et al.* Heavy Isotope Abundances in Mike Thermonuclear Device. Physical Review 1960; 119: 2000.

DOE. U.S. Department of Energy. OpenNet www.osti.gov/opennet/forms.jsp?formurl=document/guidline/pubgd.html 2011

Draxler RR, Hess GD. 1997. Description of the HYSPLIT 4 modeling system. Air Resources Laboratory. Silver spring, Maryland.

Eckhardt S, Stohl A, Beirle S, Spichtinger N, James P, Forster C, *et al.* The North Atlantic Oscillation controls air pollution transport to the Arctic. Atmospheric Chemistry and Physics 2003; 3: 1769-1778.

Edvarson K, Sisefsky J. Observations on particle properties of nuclear debris in upper atmosphere. Tellus 1966; 18: 457-&.

Eigl R, Srncik M, Steier P, Wallner G. 236U/238U and 240Pu/239Pu isotopic ratios in small (2 L) sea and river water samples. Journal of Environmental Radioactivity 2013; 116: 54-58.

Englund E, Aldahan A, Possnert G, Alfimov V. A routine preparation method for AMS measurement of I-129 in solid material. Nucl. Instrum. Methods Phys. Res. Sect. B-Beam Interact. Mater. Atoms 2007; 259: 365-369.

Entwistle JA, Flowers AG, Nageldinger G, Greenwood JC. Identification and characterization of radioactive 'hot' particles in Chernobyl fallout-contaminated soils: the application of two novel approaches. Mineralogical Magazine 2003; 67: 183-204.

Eriksson M, Lindahl P, Roos P, Dahlgaard H, Holm E. U, Pu, and Am nuclear signatures of the Thule hydrogen bomb debris. Environmental Science & Technology 2008; 42: 4717-4722.

Eriksson M, Osan J, Jernstrom J, Wegrzynek D, Simon R, Chinea-Cano E, *et al.* Source term identification of environmental radioactive Pu/U particles by their characterization with non-destructive spectrochemical analytical techniques. Spectrochimica Acta Part B-Atomic Spectroscopy 2005; 60: 455-469.

Feely HW, Seitz H, Lagomarsino RJ, Biscaye PE. Transport and fallout of stratospheric radioactive debris. Tellus 1966; 18: 316-328.

Fifield LK. Accelerator mass spectrometry of the actinides. Quaternary Geochronology 2008; 3: 276-290.

Garland JA, Wakeford R. Atmospheric emissions from the Windscale accident of October 1957. Atmospheric Environment 2007; 41: 3904-3920.

Glasstone S, Dolan PJ. The Effects of nuclear weapons. [Washington]: U.S. Government Printing Office, 1980.

Godoy M, Godoy JM, Roldao LA, Tauhata L. Determination of total content and isotopic compositions of plutonium and uranium in environmental samples for safeguards purposes by ICP-QMS. Journal of Environmental Radioactivity 2009; 100: 613-625.

Gordeev K, Shinkarev S, Ilyin L, Bouville A, Hosh M, Luckyanov N, *et al.* Retrospective dose assessment for the population living in areas of local fallout from the Semipalatinsk Nuclear Test Site - Part II: Internal exposure to thyroid. J. Radiat. Res. 2006; 47: A137-A141.

Grosche B. Semipalatinsk test site: Introduction. Radiation and Environmental Biophysics 2002; 41: 53-55.

Grønhaug K. 2001. Atmosfæriske prøvesprengninger i Sovietunionen - en oversikt. Norwegian Defence Research Establishment (FFI).

Gusev BI, Abylkassimova ZN, Apsalikov KN. The Semipalatinsk Nuclear Test Site: a first assessment of the radiological situation and the test related radiation doses in the surrounding territories. Radiation and Environmental Biophysics 1997; 36: 201-204.

Hansen C. The swords of Armageddon, U.S. nuclear weapons development since 1945. In: Hansen C, editor. The swords of Armageddon. VII, 1995.

Hardy EP, Krey PW, Volchok HL. Global Inventory and Distribution of Fallout Plutonium. Nature 1973; 241: 444-445.

Heft RE. The Characterization of Radioactive Particles from Nuclear Weapons Tests. Radionuclides in the Environment. 93. American Chemical Society, 1970, pp. 254-281.

Herrmann J, Nies H, Goroncy I. Plutonium in the deep layers of the Norwegian and Greenland Seas. Radiat. Prot. Dosim. 1998; 75: 237-245.

Hicks H, Barr D. 1984. Nevada test site fallout atom ratios: Pu-240 / Pu-239 and Pu-241 / Pu-239. Lawrence Livermore National Laboratory.

Holloway RW, Hayes DW. Mean Residence Time of Plutonium in the Troposphere. Environmental Science & Technology 1982; 16: 127-129.

Hou XL, Roos P. Critical comparison of radiometric and mass spectrometric methods for the determination of radionuclides in environmental, biological and nuclear waste samples. Analytica Chimica Acta 2008; 608: 105-139.

Hvinden T. 1958. Radioaktivt nedfall i Norge i 1957. Norwegian Defence Research Establishment (FFI). Kjeller.

Hvinden T. 1960. Radioactive fallout in Norway, july 1959 to july 1960. Norwegian Defence Research Establishment (FFI).

Hvinden T, Lillegraven A. Caesium-137 in Air and Precipitation in Norway During October 1957. Nature 1963; 199: 366-&.

Hvinden T, Lillegraven A, Lillesæter O. Passage of Radioactive Cloud over Norway November 1962. Nature 1964; 202: 950-&.

IAEA. 2005. Radiological conditions at the former french nuclear test sites in Algeria: Preliminary assessment and recommendations. Wien.

IAEA. 2011. Radioactive particles in the environment: Sources, particle characterization and analytical techniques.

Izrael JA, Baxter MS. Radioactive fallout after nuclear explosions and accidents: (translated from the original russian work). Amsterdam: Elsevier, 2002.

Jia G, Triulzi C, Marzano FN, Belli M, Sansone U, Vaghi M. Plutonium, Am-241, Sr-90, and Cs-137 concentrations in some Antarctic matrices, 1999, pp. 349-357.

Jimenez-Ramos MC, Barros H, Garcia-Tenorio R, Garcia-Leon M, Vioque I, Manjon G. On the presence of enriched amounts of U-235 in hot particles from the terrestrial area affected by the Palomares accident (Spain). Environmental Pollution 2007; 145: 391-394.

Jones SR, Willans SM, Smith AD, Cawse PA, Baker SJ. Deposition of actinides in the vicinity of Sellafield, Cumbria: Accounting for historical discharges to atmosphere from the plant. Science of the Total Environment 1996; 183: 213-229.

Junge CE. Air chemistry and radioactivity. New York: Academic Press, 1963.

Kelley JM, Bond LA, Beasley TM. Global distribution of Pu isotopes and Np-237. Science of the Total Environment 1999; 238: 483-500.

Kemmochi M. Analysis of highly radioactive fallout particles from Chinese nuclear test (I). Journal of Nuclear Science and Technology-Tokyo 1966; 3: 106-&.

Kershaw PJ, Sampson KE, McCarthy W, Scott RD. The measurement of the isotopic composition of plutonium in an Irish Sea sediment by mass spectrometry. Journal of Radioanalytical and Nuclear Chemistry-Articles 1995; 198: 113-124.

Ketterer ME, Groves AD, Strick BJ. U-236 inventories, U-236/U-238, and U-236/Pu-239: The stratospheric fallout signature. Geochim. Cosmochim. Acta 2007; 71: A480-A480.

Ketterer ME, Groves AD, Strick BJ, Asplund CS, Jones VJ. Deposition of U-236 from atmospheric nuclear testing in Washington state (USA) and the Pechora region (Russian Arctic). Journal of Environmental Radioactivity 2013; 118: 143-149.

Ketterer ME, Hafer KM, Link CL, Royden CS, Hartsock W. Anthropogenic U-236 at Rocky Flats, Ashtabula river harbor, and Mersey estuary: three case studies by sector inductively coupled plasma mass spectrometry. Journal of Environmental Radioactivity 2003; 67: 191-206.

Ketterer ME, Hafer KM, Mietelski JW. Resolving Chernobyl vs. global fallout contributions in soils from Poland using Plutonium atom ratios measured by inductively coupled plasma mass spectrometry. Journal of Environmental Radioactivity 2004; 73: 183-201.

Khalturin V, Rautian T, Richards P, Leith W. A review of nuclear testing by the Soviet Union at Novaya Zemlya, 1955 - 1990. Science and global security 2005; 13: 1 - 42.

Koide M, Bertine KK, Chow TJ, Goldberg ED. The Pu-240 Pu-239 Ratio, a Potential Geochronometer. Earth and Planetary Science Letters 1985; 72: 1-8.

Krey PW. Plutonium-238 from SNAP-9A burnup. Transactions of the American Nuclear Society 1967; 10: 1-&.

Krey PW, Leifer R, Benson WK, Dietz LA, Coluzza JL, Hendrikson HC. Atmospheric Burnup of the Cosmos-954 Reactor. Science 1979; 205: 583-585.

Lapp RE. Nuclear weapons - past and present. Science and Public Affairs-Bulletin of the Atomic Scientists 1970; 26: 103-106.

Lee MH, Lee CW. Association of fallout-derived Cs-137, Sr-90 and Pu-239,Pu-240 with natural organic substances in soils. Journal of Environmental Radioactivity 2000; 47: 253-262.

Lee MH, Lee CW. Characteristics of cumulative deposition of fallout Pu in environmental samples collected in South Korea. Vol 1, 2001.

Lee MH, Lee CW, Boo BH. Distribution and characteristics of Pu-239,Pu-240 and Cs-137 in the soil of Korea. Journal of Environmental Radioactivity 1997; 37: 1-16.

Leifer R, Juzdan ZR, Kelly WR, Fassett JD, Eberhardt KR. Detection of uranium from Cosmos-1402 in the stratosphere. Science 1987; 238: 512-514.

Lind OC. 2006. Characterisation of radioactive particles in the environment using advanced techniques. PhD-thesis. The Norvegian University of Life Sciences, Ås.

Lind OC, Nygren U, Thaninc L, Ramebäck H, Sidhu S, Roos P, *et al.* 2008. Overview of sources of radioactie particles of Nordic relevance as well as a short description of available particle characterisation techniques. Nordic nuclear safety research (nks).

Lind OC, Salbu B, Janssens K, Proost K, Dahlgaard H. Characterization of, uranium and plutonium containing particles originating from the nuclear weapons accident in Thule, Greenland, 1968. Journal of Environmental Radioactivity 2005; 81: 21-32.

Lind OC, Salbu B, Janssens K, Proost K, Garcia-Leon M, Garcia-Tenorio R. Characterization of U/Pu particles originating from the nuclear weapon accidents at Palomares, Spain, 1966 and Thule, Greenland, 1968. Science of the Total Environment 2007; 376: 294-305.

Lindahl P, Andersen MB, Keith-Roach M, Worsfold P, Hyeong K, Choi MS, *et al.* Spatial and temporal distribution of Pu in the Northwest Pacific Ocean using modern coral archives. Environment International 2012; 40: 196-201.

Lindahl P, Asami R, Iryu Y, Worsfold P, Keith-Roach M, Choi MS. Sources of plutonium to the tropical Northwest Pacific Ocean (1943-1999) identified using a natural coral archive. Geochim. Cosmochim. Acta 2011a; 75: 1346-1356.

Lindahl P, Roos P, Eriksson M, Holm E. Distribution of Np and Pu in Swedish lichen samples (Cladonia stellaris) contaminated by atmospheric fallout. Journal of Environmental Radioactivity 2004; 73: 73-85.

Lindahl P, Worsfold P, Keith-Roach M, Andersen MB, Kershaw P, Leonard K, *et al.* Temporal record of Pu isotopes in inter-tidal sediments from the northeastern Irish Sea. Science of the Total Environment 2011b; 409: 5020-5025.

Lindblom G. Advection over Sweden of radioactive dust from the 1st French nuclear test explosion. Tellus 1961; 13: 106-112.

Lockhart LB, Patterson RL, Anderson WL. 1964. Characteristics of Air Filter Media Used For Monitoring Airborne Radioactivity. U.S. Naval Research Laboratory. Washington DC.

Lovins AB. Nuclear-weapons and power-reactor plutonium. Nature 1980; 283: 817-823.

Lujaniene G, Aninkevicius V, Lujanas V. Artificial radionuclides in the atmosphere over Lithuania. Journal of Environmental Radioactivity 2009; 100: 108-119.

Lutgens FK, Tarbuck EJ. The atmosphere : an introduction to meteorology. Upper Saddle River, N.J.: Prentice Hall, 2001.

MacDonald RW, Barrie LA, Bidleman TF, Diamond ML, Gregor DJ, Semkin RG, *et al.* Contaminants in the Canadian Arctic: 5 years of progress in understanding sources, occurrence and pathways. Science of the Total Environment 2000; 254: 93-234.

Machta L, List RJ, Hubert LF. World-wide travel of atomic debris. Science 1956; 124: 474-477.

Mamuro T, Fujita A, Seiyama T, Matsunami T, Yoshikawa K. Electron microscopic examination of highly radioactive fall-out particles. Nature 1963; 197: 478-&.

Mamuro T, Fujita A, Yoshikawa K, Matsunami T. Microscopic examination of highly radioactive fall-out particles. Nature 1962; 196: 529-&.

Mamuro T, Matsunami T, Maki N. Solubility of fallout particles. Health Phys. 1965; 11: 316-&.

Maxwell RD, Paine RW, Shea TE. 1955. Evaluation of radioactive fallout (Extracted version). ARMED FORCES SPECIAL WEAPONS PROJECT. Washington D.C.

Michel H, Ketterer ME, Barci-Funel G. ICP-MS analysis of plutonium activities and Pu-240/Pu-239 ratio in alpha spectrometry planchet deposits. Journal of Radioanalytical and Nuclear Chemistry 2007; 273: 485-490.

Mikhailov VE. 2004. Nuclear explosions in the USSR: the north test site reference material. IAEA. Vienna, Austria.

Mitchell PI, Vintro LL, Dahlgaard H, Gasco C, SanchezCabeza JA. Perturbation in the Pu-240/Pu-239 global fallout ratio in local sediments following the nuclear accidents at Thule (Greenland) and Palomares (Spain). Science of the Total Environment 1997; 202: 147-153.

Mori C, Suzuki T, Koido S, Uritani A, Miyahara H, Yanagida K, *et al.* Effect of background radiation shielding on natural radioactivity distribution measurement with imaging plate, 1996, pp. 544-546.

Muramatsu Y, Ruhm W, Yoshida S, Tagami K, Uchida S, Wirth E. Concentrations of Pu-239 and Pu-240 and their isotopic ratios determined by ICP-MS in soils collected from the Chernobyl 30-km zone. Environmental Science & Technology 2000; 34: 2913-2917.

Njølstad O. Atomic intelligence in Norway during the Cold War. Journal of Strategic Studies 2006; 29: 653-673.

Nygren U, Rodushkin I, Nilsson C, Baxter DC. Separation of plutonium from soil and sediment prior to determination by inductively coupled plasma mass spectrometry. J. Anal. At. Spectrom. 2003; 18: 1426-1434.

Olivier S, Bajo S, Fifield LK, Gaggeler HW, Papina T, Santschi PH, *et al.* Plutonium from global fallout recorded in an ice core from the Belukha glacier, Siberian Altai. Environmental Science & Technology 2004; 38: 6507-6512.

Olivier S, Schwikowski M, Brutsch S, Eyrikh S, Gaggeler HW, Luthi M, *et al.* Glaciochemical investigation of an ice core from Belukha glacier, Siberian Altai. Geophysical Research Letters 2003; 30.

Oughton DH, Day P, Fifield LK. Plutonium measurement using accelerator mass spectrometry: methodology and applications. Plutonium in the environment 2001.

Oughton DH, Fifield LK, Day JP, Cresswell RC, Skipperud L, Di Tada ML, *et al.* Plutonium from Mayak: Measurement of isotope ratios and activities using accelerator mass spectrometry. Environmental Science & Technology 2000; 34: 1938-1945.

Oughton DH, Salbu B, Brand TL, Day JP, Aarkrog A. Under-determination of Sr-90 in soils containing particles of irradiated uranium oxide fuel. Analyst 1993; 118: 1101-1105.

Oughton DH, Skipperud L, Fifield LK, Cresswell RG, Salbu B, Day P. Accelerator mass spectrometry measurement of Pu-240/Pu-239 isotope ratios in Novaya Zemlya and Kara Sea sediments. Applied Radiation and Isotopes 2004; 61: 249-253.

Palsson SE, Howard BJ, Bergan TD, Paatero J, Isaksson M, Nielsen SP. A simple model to estimate deposition based on a statistical reassessment of global fallout data. J Environ Radioact 2013; 121: 75-86.

Pálsson SE, Howard BJ, Bergan TD, Paatero J, Isaksson M, Nielsen SP. A simple model to estimate deposition based on a statistical reassessment of global fallout data. Journal of Environmental Radioactivity 2012.

Parrish W, Mantler M. X-ray fluorescence analysis www.accessscience.com/content.aspx?searchStr=parrish&id=750700

Patterson RL, Lockhart LB. LONG-RANGE DETECTION OF FRENCH NUCLEAR TESTS OF 1960. Science 1960; 132: 474-474.

Persson C, Rodhe H, Degeer LE. The Chernobyl accident - a meteorological analysis of how radionuclides reached and were deposited in Sweden. Ambio 1987; 16: 20-31.

Persson G, Sisefsky J. Radioactive particles from eighth chinese nuclear test. Health Phys. 1971; 21: 421-&.

Peterson KR. An empirical model for estimating world-wide deposition from atmospheric nuclear detonations. Health Phys. 1970; 18: 357-&.

Pinglot JF, Hagen JO, Melvold K, Eiken T, Vincent C. A mean net accumulation pattern derived from radioactive layers and radar soundings on Austfonna, Nordaustlandet, Svalbard. Journal of Glaciology 2001; 47: 555-566.

Pinglot JF, Vaikmae RA, Kamiyama K, Igarashi M, Fritzsche D, Wilhelms F, *et al.* Ice cores from Arctic sub-polar glaciers: chronology and post-depositional processes deduced from radioactivity measurements. Journal of Glaciology 2003; 49: 149-158.

Pollanen R, Siiskonen T, Ihantola S, Toivonen H, Pelikan A, Inn K, *et al.* Determination of Pu-239/Pu-240 isotopic ratio by high-resolution alpha-particle spectrometry using the ADAM program. Applied Radiation and Isotopes 2012; 70: 733-739.

Postek MT, Howard KS, Johnson AH, McMichael KL. Scanning electron microscopy: a student's handbook, 1980.

Povinec PP, Pham MK, Sanchez-Cabeza JA, Barci-Funel G, Bojanowski R, Boshkova T, *et al.* Reference material for radionuclides in sediment IAEA-384 (Fangataufa Lagoon sediment). Journal of Radioanalytical and Nuclear Chemistry 2007; 273: 383-393.

Pöllänen R. 2002. Nuclear fuel particles in the environment - characteristics, atmospheric transport and skin doses. Helsinki.

Pöllänen R, Ketterer ME, Lehto S, Hokkanen M, Ikaheimonen TK, Siiskonen T, *et al.* Multi-technique characterization of a nuclear bomb particle from the Palomares accident. Journal of Environmental Radioactivity 2006; 90: 15-28.

Pöllänen R, Valkama I, Toivonen H. Transport of radioactive particles from the Chernobyl accident. Atmospheric Environment 1997; 31: 3575-3590.

Qiao JX, Hansen V, Hou XL, Aldahan A, Possnert G. Speciation analysis of I-129, Cs-137, Th-232, U-238, Pu-239 and Pu-240 in environmental soil and sediment. Applied Radiation and Isotopes 2012; 70: 1698-1708.

Raisbeck GM, Yiou F, Zhou ZQ, Kilius LR. I-129 from nuclear-fuel reprocessing facilities at sellafield (uk) and la hague (france) - potential as an oceanographic tracer. Journal of Marine Systems 1995; 6: 561-570.

Ranebo Y, Eriksson M, Tamborini G, Niagolova N, Bildstein O, Betti M. The use of SIMS and SEM for the characterization of individual particles with a matrix originating from a nuclear weapon. Microscopy and Microanalysis 2007; 13: 179-190.

Rhodes R. Dark sun: the making of the hydrogen bomb. New York: Simon & Schuster, 1995.

Rokop D, Efurd D, Benjamin T, Cappis J, Chamberlin J, Poths H, *et al.* 1995. Isotopic signatures, an important tool in today's world. Chemical Science and Technology Division, Los Alamos National Laboratory. Los Alamos.

Sakaguchi A, Kawai K, Steier P, Quinto F, Mino K, Tomita J, *et al.* First results on U-236 levels in global fallout. Science of the Total Environment 2009; 407: 4238-4242.

Salaymeh S, Lee SC, Kuroda PK. Plutonium fallout from the nuclear-powered satellite Cosmos-1402. Journal of Radioanalytical and Nuclear Chemistry-Articles 1987; 111: 147-155.

Salbu B. Radionuclides associated with colloids and particles in rainwaters, Oslo, Norway. In: Philipsborn F, Steinhausler F, editors. Proceedings of an International Workshop. Bergbau and industriemuseums, Theuern, 1988a, pp. 83 - 84.

Salbu B. Radionuclides associated with colloids and particles in the Chernobyl Fallout. Joint meeting OECD(NEA)/CEC Recent Advances in Reactor Accident Consequence Assessment, Rome, 1988b.

Salbu B. Source-related characteristics of radioactive particles: A review. Nuclear Technology Publ, 2000a, pp. 49-54.

Salbu B. Speciation of radionuclides in the environment. Encyclopedia of analytical chemistry. John Wiley & Sons Ltd, 2000b, pp. 12993 - 13016.

Salbu B. Actinides associated with particles. In: Kudo A, editor. Plutonium in the environment. Elsevier, Oxford, 2001, pp. 121-138.

Salbu B. Radioactive particles released from different nuclear sources: With focus on nuclear weapons tests. In: Salbu B, Skipperud L, editors. Nuclear Risks in Central Asia, 2008, pp. 7-17.

Salbu B, Krekling T, Lind OC, Oughton DH, Drakopoulos M, Simionovici A, *et al.* High energy X-ray microscopy for characterisation of fuel particles. Nuclear Instruments & Methods in Physics Research Section a-Accelerators Spectrometers Detectors and Associated Equipment 2001; 467: 1249-1252.

Salbu B, Krekling T, Oughton DH, Ostby G, Kashparov VA, Brand TL, *et al.* Hot particles in accidental releases from Chernobyl and Windscale nuclear installations. Analyst 1994; 119: 125-130.

Salbu B, Nikitin AI, Strand P, Christensen GC, Chumichev VB, Lind B, *et al.* Radioactive contamination from dumped nuclear waste in the Kara sea - results from the joint Russian-Norwegian expeditions in 1992-1994. Science of the Total Environment 1997; 202: 185-198.

Salminen-Paatero S, Nygren U, Paatero J. 240Pu/239Pu mass ratio in environmental samples in Finland. Journal of Environmental Radioactivity 2012; 113: 163-170.

Saltbones J. 1986. Kjernekraft-ulykken i Chernobyl: Atmosfærisk transport og spredning av radioaktivt materiale. The norwegian meteorological institute (met.no). Oslo.

Schaumlöffel D, Giusti P, Zoriy MV, Pickhardt C, Szpunar J, Lobinski R, *et al.* Ultratrace determination of uranium and plutonium by nano-volume flow injection double-focusing sector field inductively coupled plasma mass spectrometry (nFI-ICP-SFMS). J. Anal. At. Spectrom. 2005; 20: 17-21.

Sisefsky J. Debris from tests of nuclear weapons - activities roughly proportional to volume are found in particles examined by autoradiography and microscopy. Science 1961; 133: 735-&.

Sisefsky J. Investigation of nuclear weapon debris with x-ray microanalyser. Nature 1964; 203: 708-&.

Sisefsky J. 1966. Studies of debris particles from the third chinese nuclear test. Totalförsvarets forskningsinstitut (Swedish Defence Research Agency). Stockholm.

Sisefsky J. 1967. Studies of debris particles from the fourth and fifth chinese nuclear tests. Totalförsvarets forskningsinstitut (Swedish Defence Research Agency). Stockholm.

Sisefsky J, Persson G. Debris over Sweden from the Chinese nuclear weapon test September 1969. Health Phys. 1971; 21: 463-&.

Skipperud L. 2004. Plutonium in the environment: sources and mobility. PhD-thesis. The Norwegian University of Life Sciences, Ås.

Smith AD, Jones SR, Gray J, Mitchell KA. A review of irradiated fuel particle releases from the Windscale Piles, 1950-1957. Journal of Radiological Protection 2007; 27: 115-145.

Smith JN, Ellis KM, Polyak L, Ivanov G, Forman SL, Moran SB. (PU)-P-239,240 transport into the Arctic Ocean from underwater nuclear tests in Chernaya Bay, Novaya Zemlya. Cont. Shelf Res. 2000; 20: 255-279.

Srncik M, Hrnecek E, Steier P, Wallner A, Wallner G, Bossew P. Vertical distribution of Pu-238, Pu-239(40), Am-241, Sr-90 and Cs-137 in Austrian soil profiles. Radiochimica Acta 2008; 96: 733-738.

Srncik M, Steier P, Wallner A. Depth profile of 236U/238U in soil samples in La Palma, Canary Islands. Journal of Environmental Radioactivity 2011; 102: 614-619.

Steinnes E. Use of mosses to study atmospheric deposition of trace elements: contributions from investigations in Norway. International Journal of Environment and Pollution 2008; 32: 499-508.

Steinnes E, Njastad O. Use of mosses and lichens for regional mapping of Cs-137 fallout from the Chernobyl accident. Journal of Environmental Radioactivity 1993; 21: 65-73.

Stohl A. Characteristics of atmospheric transport into the Arctic troposphere. Journal of Geophysical Research-Atmospheres 2006; 111.

Stohl A, Seibert P, Wotawa G, Arnold D, Burkhart JF, Eckhardt S, *et al.* Xenon-133 and caesium-137 releases into the atmosphere from the Fukushima Dai-ichi nuclear power plant: determination of the source term, atmospheric dispersion, and deposition. Atmospheric Chemistry and Physics 2012; 12: 2313-2343.

Stohl A, Spichtinger-Rakowsky N, Bonasoni P, Feldmann H, Memmesheimer M, Scheel HE, *et al.* The influence of stratospheric intrusions on alpine ozone concentrations. Atmospheric Environment 2000; 34: 1323-1354.

Storebø PB. 1958. Advection of radioactive dust over Noway after the Windscale accident in England October 1957. Norwegian Defence Research Establishment (FFI).

Storebø PB. Orographical and climatological influences on deposition of nuclear-bomb debris. Journal of Meteorology 1959; 16: 600-608.

Storebø PB. The exchange of air between stratosphere and troposphere. Journal of Meteorology 1960; 17: 547-554.

Storebø PB. Precipitation formation in a mountainous coast region. Tellus 1968; 20: 239-&.

Sæbø A, Høibråten S, Engøy T. Måling av radioaktive stoffer i nedfall over Norge 1982-1997. Norwegian Defence Research Establishment (FFI), Kjeller, 1998.

Tarussov A. The arctic from Svalbard to Severnaya Zemlya: climatic reconstructions from ice cores. In: Bradley RS, Jones PD, editors. Climate since A.D. 1500. Routledge, London, 1992, pp. xv, 679 s. : ill.

Telegadas K, List RJ. Are particulate radioactive tracers indicative of stratospheric motions? Journal of Geophysical Research 1969; 74: 1339-&.

UNSCEAR. Annex B, Exposures from man-made sources of radiation. United nations scientific comitte on the effects of ionizing radiation, New York, 1993.

UNSCEAR. 2000a. Annex C, sources and effects of ionizing radiation. United Nations Scientific Committee on the Effects of Atomic Radiation. Vienna.

UNSCEAR. 2000b. Annex J, Exposures and effects of the Chernobyl accident. United Nations Scientific Committee on the Effects of Atomic Radiation. Vienna.

UNSCEAR. 2008. Annex J, Exposures and effects of the Chernobyl accident. United Nations Scientific Committee on the Effects of Atomic Radiation. Vienna.

Vintró LL, Mitchell PI. Actinides and Other Alpha-Emitters, Determination of. Encyclopedia of Analytical Chemistry. John Wiley & Sons, Ltd, 2006.

Vintró LL, Mitchell PI, Condren OM, Moran M, Vives i Batlle J, Sánchez-Cabeza JA. Determination of the 240Pu/239Pu atom ratio in low activity environmental samples by alpha spectrometry and spectral deconvolution. Nuclear Instruments and Methods in Physics Research Section A: Accelerators, Spectrometers, Detectors and Associated Equipment 1996; 369: 597-602.

Walker GT, Bliss EW. World weather V. Memoirs of the Royal Meteorological Society 1932; IV: 53 - 84.

Wallace JM, Hobbs PV. Atmospheric science : an introductory survey. Amsterdam: Elsevier, 2006.

Warneke C, Froyd KD, Brioude J, Bahreini R, Brock CA, Cozic J, *et al.* An important contribution to springtime Arctic aerosol from biomass burning in Russia. Geophysical Research Letters 2010; 37.

Warneke T. 2002. High-precision isotope ratio measurements of uranium and plutonium in the environment. PhD-thesis. Southampton.

Warneke T, Croudace IW, Warwick PE, Taylor RN. A new ground-level fallout record of uranium and plutonium isotopes for northern temperate latitudes. Earth and Planetary Science Letters 2002; 203: 1047-1057.

Watanabe O, Motoyama H, Igarashi M, Kamiyama K, Matoba S, Goto-Azuma K, *et al.* Studies on climatic and environmental changes during the last few hundred years using ice cores from various sites in Nordauslandet, Svalbard. Memoirs of National Institute of Polar Research 2001; 54: 227 - 242.

Wilcken K. 2006. Accelerator mass spectrometry of natural U-236 and Pu-239 with emphasis on nucleogenic isotope production. PhD-thesis. The Australian National University, Canberra.

Winkler S. 2007. Accelerator mass spectrometry of heavy radionuclides with special focus on Hf-182. PhD-thesis. The Australian National University, Canberra.

Winkler S, Ahmad I, Golser R, Kutschera W, Orlandini KA, Paul M, *et al.* Anthropogenic Pu-244 in the environment. New Astron. Rev. 2004; 48: 151-154.

Winkler S, Steier P, Carilli J. Bomb fall-out 236U as a global oceanic tracer using an annually resolved coral core. Earth and Planetary Science Letters 2012; 359–360: 124-130.

Yamamoto M, Hoshi M, Takada J, Sakaguchi A, Apsalikov KN, Gusev BI. Distributions of Pu isotopes and Cs-137 in soil from Semipalatinsk Nuclear Test Site detonations throughout southern districts. Journal of Radioanalytical and Nuclear Chemistry 2004; 261: 19-36.

Yamamoto M, Ishiguro T, Tazaki K, Komura K, Ueno K. Np-237 in Hemp-palm leaves of Bontenchiku for fishing gear used by the fifth Fukuryu-Maru: 40 years after "Bravo". Health Phys. 1996; 70: 744-748.

Yassi A. Basic environmental health. Oxford: Oxford University Press, 2001.

Zeissler CJ. Comparison of semiconductor pixel array, phosphor plate, and track-etch detectors for alpha autoradiography. Nuclear Instruments & Methods in Physics Research Section a-Accelerators Spectrometers Detectors and Associated Equipment 1997; 392: 249-253.

Paper I

Levels and trends of Pu deposited on humic surface soils

C.C. Wendel[a,*], L. Skipperud[a], O.C. Lind[a], E. Steinnes[b], S. Lierhagen[b], B. Salbu[a]

[a]*Isotope Laboratory, Department of Plant and Environmental Sciences, Norwegian University of Life Sciences, P.O. Box 5003, N-1432 Aas, Norway*
[b]*Department of Chemistry, Norwegian University of Science and Technology, Trondheim, Norway*

Abstract

To differentiate between sources contributing to Pu contamination, Pu concentration and atom ratios were determined in humic surface soil samples from 45 geographically well distributed sites across the Norwegian mainland using SF-ICP-MS and AMS. The $^{239+240}$Pu activity concentrations ranged within 4 – 149 Bq m^{-2} (1990) and 0.7 – 63 Bq m^{-2} (2005), with the higher concentrations predominantly found at coastal locations. To identify any migration of Pu from the upper 5-7 cm of the surface soils, Pu activity concentrations in samples collected at the same sites in 1990 and 2005 were compared. On average, about 35 % of the $^{239+240}$Pu activity concentrations in the 1990 samples remained in the humic soil samples collected in 2005. The ^{240}Pu/^{239}Pu atom ratios ranged within 0.164 to 0.211 (1990) and 0.161 to 0.195 (2005), predominantly within the range of global fallout. Results based on the ^{240}Pu/^{239}Pu atom ratio, as well as levels of heavier Pu isotopes (^{241}Pu and ^{242}Pu) indicated a slight (8 to 13 %) contribution of Pu from the Chernobyl accident in some inland areas of Norway.

*Corresponding author:
Cato Wendel
P.O. box 5003
Norwegian University of Life Sciences
1432 Ås, Norway
Phone: +47 69 96 60 13
Email: catow@umb.no

1. Introduction

The presence of the anthropogenic radionuclides ^{137}Cs and $^{239+240}$Pu in the environment is a result of planned and accidental releases. The most prominent sources were the 543 atmospheric nuclear test detonations carried out in the period 1945 to 1980, resulting in the release of an estimated 3300 kg of $^{239+240}$Pu, and 296 kg of ^{137}Cs (UNSCEAR, 2000a). In this period, 445 atmospheric detonations with a total yield of equivalent to 428 Mt TNT took place at the northern hemisphere test sites (UNSCEAR, 2000a). Debris from atmospheric nuclear detonations were distributed in the different compartments of the atmosphere according to detonation yield, detonation height and meteorological conditions; giving rise to local, regional and global fallout. Terrestrial radioactive contamination in the northern hemisphere is usually attributed to stratospheric deposition, and the concentrations are largely dependent on variations in mean annual precipitation. However, the origin of nuclear weapon debris in surface air during 1957 to 1963 tests has been shown to be of both tropospheric and stratospheric origin (Wendel *et al.*, 2013).

Releases of radioactive debris from the Chernobyl accident in 1986 were different in both nature and amount from the releases from atmospheric nuclear detonations (UNSCEAR, 2000b). The estimated releases from this accident (18 kg $^{239+240}$Pu and 26 kg ^{137}Cs) were deposited over a much shorter time period and distributed over a smaller area (UNSCEAR, 2000b). Fuel fragments and particles of refractory radionuclides were mainly deposited close to the accident site, while smaller particles were deposited over vast areas of Europe (Salbu, 2000; UNSCEAR, 2000b; Paatero *et al.*, 2010; Salminen-Paatero *et al.*, 2012), including Sweden, Finland and Norway (Devell *et al.*, 1986; Reponen *et al.*, 1993; Salbu, 1994; Lindahl *et al.*, 2004) about 2000 km from the site. An overview of particles deposition following the Chernobyl accident is given in Pöllänen *et al.* (1997). The major deposition of debris from the Chernobyl accident took place in a short period during the accident and the first few weeks after the accident. Consequently, the deposition was strongly affected by short- term precipitation patterns along the pathway of the plume. Large variations in the spatial distribution is seen, both on regional scales as well as on the local scale such and within sampling areas of 1 × 1 m (Backe *et al.*, 1986; Lindahl *et al.*, 2004; Salminen-Paatero *et al.*, 2012). In contrast global fallout, lasting decades, is relatively homogeneously distributed largely reflecting the precipitation pattern (e.g. Pálsson *et al.* (2006), Pálsson *et al.* (2012), Palsson *et al.* (2013)).

The isotopic composition of plutonium is a tool well suited for source identification. Global fallout Pu is a mixture of debris from low and high yield weapons and its characteristic atom ratio of ^{240}Pu/^{239}Pu is 0.180 ± 0.014 (Kelley *et al.*, 1999). Civil reactor derived Pu is usually characterised by higher ^{240}Pu/^{239}Pu atom ratios depending on the burn up time of the fuel. Estimates of fuel composition in the Chernobyl reactor given in UNSCEAR (2000b), and indicate an ^{240}Pu/^{239}Pu atom ratio of 0.40, and $^{239+240}$Pu/^{137}Cs of 1.4×10^{-3} (reference date January 2010) which is well in accordance with other

literature data (Muramatsu *et al.*, 2000; Srncik *et al.*, 2008; Lujaniene *et al.*, 2009). However, the Chernobyl reactor at the time of the accident contained fuel of various degrees of burn up, and substantial variations in atom and activity ratios have been found (e.g. Salminen-Paatero *et al.* (2012)). The variable burn up of the Chernobyl debris is particularly evident in Finland, where atom ratios ranging from 0.13 – 0.53 were measured in lichen samples, commercially exploited peats and isolated hot particles (Salminen-Paatero *et al.*, 2012). The $^{242}Pu/^{239}Pu$ atom ratio is an order of magnitude higher in average Chernobyl debris compared to global fallout. In contrast, the $^{240}Pu/^{239}Pu$ atom ratios is an order of two higher in Chernobyl debris than in global fallout (Kelley *et al.*, 1999; UNSCEAR, 2000b)). Thus the $^{242}Pu/^{239}Pu$ atom ratio is a more sensitive indicator of Chernobyl fallout influence.

The objectives of the present work were to utilize the activity concentrations of ^{239}Pu, ^{240}Pu, ^{241}Pu, ^{242}Pu and ^{137}Cs as well as the respective atom and activity ratio distribution patterns in surface humic soil layers to distinguish between sources contributing to radioactive fallout in Norway, and to evaluate to what extent changes in activity concentrations in humic surface soils had occurred over a time span of 15 years, based on sampling taking place at the same sites in 1990 and 2005.

2. Materials and methods

2.1. Samples and pre-treatment

Samples of the humus layer from forested areas from a total of 45 locations across Norway (Figure 5) collected in 1990 and 2005 were included in the analytical program. Approximately 330 cm^2 of soil were taken from the various locations to a depth of 5-7 cm, roughly representing the humus-layer. Although care was taken to sample exactly the same site in both 1990 and 2005 the sampling sites may have differed slightly at some locations. The samples were air dried at room temperature before storage, and were ground to a fine powder and homogenised prior to analysis.

2.2. Radiocaesium determination

Subsamples of ~25 g were analysed to determine the ^{137}Cs activity concentrations using a low energy (LEGe) gamma spectrometry (Canberra Meriden CT, USA, FWHM 1.76 keV at 1.33 MeV). A relative efficiency of 25 % was obtained using a purposebuilt geometry setup. Counting times of 0.5 – 40 h were used depending on activity to ensure a counting uncertainty below 5 %.

2.3. Sample dissolution and radiochemical separation

After addition of plutonium tracer ^{242}Pu as yield monitor, the samples were covered by watch glasses and ashed at 500 °C overnight for small samples (~10 g) or until completely combusted for the larger combined Cs /Pu samples (~25 g). The ashes were then digested in Aqua Regia (dissolution time 6 h), filtered through Whatman GF/C glass fibre filters and evaporated to dryness. Plutonium was separated from other actinides by anion exchange chromatography (Clacher, 1995). The Pu eluate was evaporated to dryness and taken up in 20 ml 0.5 M HNO_3 for analysis by ICP-MS.

A subset of the samples (Svolvær, Trolla, Fyllingsdalen, Kløfta and Glomfjord) was prepared for AMS analysis of heavier Pu isotopes. These samples were prepared without the use of a yield monitor in order to determine $^{241}Pu/^{239}Pu$ and $^{242}Pu/^{239}Pu$ atom ratios. Approximately 0.8 – 1.1 g of sample material was weighed directly into PTFE ultraclave tubes. The samples were then digested under high temperature and pressure in sub-boiling ultrapure nitric acid (conc.), in an ultraclave unit (UltraCLAVE 3, Milestone Ltd). After digestion the acid concentrations were diluted to 8M, and filtered. Following anion exchange separation, the Pu eluates were evaporated to dryness, taken up in 2 ml ultrapure HNO_3 with 2 mg Fe as $Fe(NO_3)_3$ and evaporated to dryness again before being baked at 500 °C overnight. Final preparations for AMS analysis were done by mixing the Fe/Pu precipitates with silver powder at a ratio of 1:4 before pressing the samples into Al holders. The silver powder provides sufficient bulk and electrical conductivity for the analysis.

2.4. Determination of Pu

Concentrations and atom ratios of ^{239}Pu and ^{240}Pu were determined by SF-ICP-MS (Thermo Finnegan Element 2). All measurements were performed in the low-resolution mode $R=m/\Delta m=300$ (full width at 10 % maximum). The count rate at mass 238 was measured in order to account for the $^{238}U^{1}H^{+}$ interference originating from uranium still present in the solutions after ion exchange. Sample solutions were introduced to the instrument by self-aspiration at a rate of ~1.8 ml/min. The procedure was verified by the analysis of standard reference materials (Table 4) and procedural and analytical blanks. Results for the reference materials were found to be in good agreement with certified and information values. Due to high uncertainties, likely due to low Pu concentrations in the sample solutions measurements giving less than 100 cps for ^{240}Pu were disregarded.

Atom ratios of $^{241}Pu/^{239}Pu$ and $^{242}Pu/^{239}Pu$ in a selection of the samples were determined using the 14 UD tandem accelerator at the Australian National University (ANU), Canberra. The method is described in detail by Fifield (2008), and only a short summary will be given here. Pu isotopes ^{239}Pu, ^{240}Pu and ^{242}Pu were counted sequentially with counting times of 1, 1 and 3 minutes, respectively. Pu-241 was counted separately, with 5 minutes counting time, and normalised to ^{239}Pu. Blanks without

added yield monitor were run for all Pu isotopes, and a count rate corresponding to 0.67, 0.17, 0 and 0.48 counts per minute were measured for ^{239}Pu, ^{240}Pu, ^{241}Pu and ^{242}Pu, respectively. Based on analytical blanks with added yield monitor, the count rates obtained here corresponds to procedural detection limits at the sub-fg range (Wendel *et al.*, 2013). A certified reference material for Pu atom ratios (UKAEA certified nuclear reference material No: UK Pu5/92138) was measured repeatedly during the run. The precision of the ^{240}Pu/^{239}Pu, ^{239}Pu/^{242}Pu and ^{240}Pu/^{242}Pu atom ratios was 2.1, 2.4 and 2.1 % respectively (relative standard deviation, n=3).

3. Results and discussion

All results obtained in the current work are presented in Table 5 and Table 6. A wide variation in both activity concentrations and ratios were observed. Activity concentrations of ^{137}Cs, 674 – 41065 Bq m^{-2} (1990) and 173 – 57481 (2005) were generally higher in inland regions than in coastal areas. The $^{239+240}$Pu activity concentrations (Table 5 and Figure 6) ranged between 4.3 and 149 Bq m^{-2} (1990) and 0.7 and 63 Bq m^{-2} (2005), with the highest concentrations occurring in coastal areas associated with high annual precipitation. The $^{239+240}$Pu/^{137}Cs activity ratios ranged between 0.0012 and 0.108 (1990) and 0.00025 – 0.112 (2005), and ^{240}Pu/^{239}Pu atom ratios ranged between 0.164 and 0.211 (1990) and 0.161 and 0.195 (2005). The Pu atom ratios were generally within the range of global fallout as reported by Kelley *et al.* (1999).

3.1. Variation in the $^{239+240}$Pu activity concentrations

A general south to north trend in deposition as would be expected according to the global fallout model was not seen, and this is in agreement with the results of Bergan (2002). The highest concentrations of Pu were predominately found along the west coast of Norway. Prevailing wind directions in Norway are westerly causing moist and relatively warm Atlantic air to rise and cool over land. Coastal air masses moving inland from are gradually depleted in debris causing the highest deposition of radioactive debris to take place during the first precipitation events over land (Storebø, 1968). The seven sites with the highest Pu concentrations (Sløvåg, Fyllingsdalen, Odda, Svelgen, Høylandet, Mosjøen and Svolvær) are all situated along the west coast of Norway and have been affected by high precipitation rates (Figure 6). Conversely, sites with low annual precipitation tend to have lower Pu concentrations in the humic soil layers. Still, Pu concentrations were also high at some typical inland sites such as Kongsvoll with low annual precipitation but high ^{137}Cs deposition.

The generalized precipitation pattern described above and illustrated in Figure 6 cannot explain all site-to-site variations seen in the Pu concentration data. The retention of Pu in humic layers will depend on the degree of interactions (sorption, complexation) and on the composition of the

precipitation, being influenced by sea spray along the coast. Thus, local washout effects brought about by the increased ion concentrations in coastal rainwater can therefore be expected to reduce the activity concentrations in humic layers (Steinnes and Gjelsvik, 2008). Furthermore, apparent dilution effects brought about by continued deposition of organic matter on top of the humus layer should be expected. This effect would depend on the amount of litter deposited on top of the humic layer per year, and is likely to be stronger in a heavily forested area than in arctic and alpine areas.

Based on the samples collected in 1990, the deposition pattern of $^{239+240}$Pu and its dependence on mean annual precipitation indicate that global fallout from nuclear weapon tests is the major source of Pu in Norway.

3.1.1. Trends: comparison of Pu data from samples collected in 1990 and 2005

The results show that at most sites the $^{239+240}$Pu activity concentrations in 1990 were higher than in the samples collected in 2005. Thus, wash-out processes seem to affect the Pu levels in humic layers, especially in samples from sites affected by high precipitation. By calculating the relative retention of Pu in soils (activity concentration in 2005/activity concentration in 1990 × 100 %), the overall retention of $^{239+240}$Pu in the samples was found to be 31 %, after having removed obvious outliers. The outliers included 4 samples for which the humic layers were not sufficiently deep in 2005, and 7 samples in which the 2005 concentration level exceeded or were near identical to that of 1990. Similarly, the average retention of ^{137}Cs was found to be 34 %.

3.2. Variation in the $^{240}Pu/^{239}Pu$ atom ratio

The $^{240}Pu/^{239}Pu$ atom ratios were generally within the limits of global fallout (0.18 ± 0.01) established by Kelley *et al.* (1999) (Table 5 and Figure 7). The atom ratios obtained at certain sites were, however, somewhat higher (especially Vauldalen, Stavsjø, Øystre Slidre, Skredå and Kløfta) and somewhat lower (especially Svolvær) than the global fallout signal.

The highest $^{240}Pu/^{239}Pu$ atom ratios (0.20 – 0.211) were obtained in humic samples from inland sites (Skredå, Vauldalen, Kløfta, Stavsjø and Øystre Slidre). The $^{134}Cs/^{137}Cs$ activity ratios measured within the respective districts of these sites shortly after the Chernobyl accident ranged from 0.34 – 0.51 (Backe *et al.*, 1986). These $^{134}Cs/^{137}Cs$ ratios are close to that estimated for the Chernobyl reactor (UNSCEAR, 2000b), and indicate moderate to strong deposition signal of Chernobyl fallout related Cs, and possibly Pu at these sites. Based on the $^{240}Pu/^{239}Pu$ atom ratios obtained for these sites, a simple estimation of the proportion of Chernobyl Pu deposited can be calculated based on the respective Pu atom ratios and the formula:

$$X = \frac{\left(R_{Sample} - R_{Global\ fallout}\right)}{\left(R_{Chernobyl} - R_{Global\ fallout}\right)} * 100\%$$

Here a $^{240}Pu/^{239}Pu$ atom ratio of 0.40 was assumed to be representative for Chernobyl fallout($R_{chernobyl}$), and 0.180 to be representative of global fallout ($R_{global\ fallout}$), (Kelley *et al.*, 1999; UNSCEAR, 2000b)

The $^{240}Pu/^{239}Pu$ atom ratios of the abovementioned sites reflect a Pu contribution from Chernobyl ranging within 8 – 13 %.

In contrast, the $^{240}Pu/^{239}Pu$ atom ratio (0.164 ± 0.001 and 0.161 ± 0.004 for the 1990 and 2005 sample respectively) obtained for Svolvær, a northern coastal area, was lower than the global fallout range stated by Kelley *et al.* (1999). Observed $^{240}Pu/^{239}Pu$ atom ratios in ground level air during periods of atmospheric testing and a few months thereafter remained substantially lower than global fallout $^{240}Pu/^{239}Pu$ levels (Salminen-Paatero *et al.*, 2012; Wendel *et al.*, 2013). This likely reflects debris from low and intermediate yield nuclear weapon detonations transported through the troposphere or the lower stratosphere from the Former Soviet Union test sites. It is possible that the low $^{240}Pu/^{239}Pu$ atom ratios observed at coastal sites with high annual precipitation, such as Svolvær, can be attributed to a stronger deposition of debris from low and intermediate yield detonations.

Based on the $^{240}Pu/^{239}Pu$ atom ratio, the global fallout signal dominated at most sites, while a Pu Chernobyl signal was indicated at Vauldalen, Stavsjø, Øystre Slidre, Skredå and Kløfta (inland) and a low yield nuclear test signal was indicated at Svolvær (coastal area).

3.3. The variations in the $^{241}Pu/^{239}Pu$ and $^{242}Pu/^{239}Pu$ atom ratios

Heavier Pu atom ratios were determined for a subset of the samples (Svolvær, Trolla, Fyllingsdalen, Kløfta, Glomfjord). The $^{241}Pu/^{239}Pu$ atom ratios ranged within 0.0009 – 0.0023 and $^{242}Pu/^{239}Pu$ atom ratios ranged within 0.0038 – 0.0098 (Figure 8). Two samples (Kløfta and Glomfjord) were found to have a $^{242}Pu/^{239}Pu$ atom ratio significantly higher than that from global fallout indicating a Chernobyl fallout influence. Both sites belongs to districts where the $^{134}Cs/^{137}Cs$ ratios activity ratios were found be high (0.40 and 0.37 respectively) after the Chernobyl accident (Backe *et al.*, 1986) but only Kløfta had a $^{240}Pu/^{239}Pu$ atom ratio exceeding that of global fallout. The $^{242}Pu/^{239}Pu$ atom ratio is potentially a more sensitive signal / indicator of Chernobyl fallout than the $^{240}Pu/^{239}Pu$ ratio; primarily due to the higher concentration of ^{242}Pu in a civil reactor compared to low and moderate yield nuclear weapon debris. The $^{242}Pu/^{239}Pu$ atom ratio in Chernobyl debris is an order of magnitude higher than in global fallout, in contrast to the $^{240}Pu/^{239}Pu$ atom ratio which is a factor of 2 higher in Chernobyl debris than in global fallout (Kelley *et al.*, 1999; UNSCEAR, 2000a; b).

4. Conclusions

Concentrations and atom ratios of plutonium were determined in humus samples from 45 geographically well distributed sites in Norway in 1990 and 2005. Plutonium concentrations (1 – 149 Bq m^{-2}) were higher in coastal regions with high annual precipitation reflecting global fallout, while caesium deposition (170 – 57500 Bq m^{-2}) reflected fallout from the Chernobyl accident.

At the west coastal areas where the Chernobyl fallout signal was weak the, $^{239+240}Pu/^{137}Cs$ activity ratios approached that of global fallout. The $^{240}Pu/^{239}Pu$ atom ratios (0.161 – 0.211) mainly reflected a global fallout origin of plutonium deposited in Norway, however, deviations in the $^{240}Pu/^{239}Pu$ atom ratio indicating influence from deposition of debris form the Chernobyl accident were found at 5 sites in the central eastern inland part of Norway. The $^{241}Pu/^{239}Pu$ and $^{242}Pu/^{239}Pu$ atom ratios determined for a subset of the samples from 2005 varied widely (0.0009 – 0.00023 and 0.0038 – 0.0099), but indicated that samples from two sites (Kløfta and Glomfjord) were influenced by a Chernobyl derived Pu signal. These results should encourage the future use of the $^{242}Pu/^{239}Pu$ atom ratio for source identification purposes.

The Pu activity concentrations in the humic surface soil samples collected in 1990 was found to be reduced by an average of 31 % compared to 15 years later, and no significant differences were found between coastal and inland regions. Caesium activity concentrations (173 – 57481 Bq m^{-2}) were found to be highest in inland locations reflecting the arrival of the Chernobyl plume in combination with local precipitation in the days following the accident.

Acknowledgements

The authors gratefully acknowledge the support provided by the Research Council of Norway (Project no. 421048). We are indebted to Signe Dahl for kind assistance with the layout. Keith Fifield, Stephen G. Tims and Deborah Oughton for AMS beam time and assistance the analysis of heavier Pu isotopes in the humic surface soil samples.

References

Backe, S. *et al.*, 1986.Nedfall av cesium i Norge etter tsjernobylulykken, NRPA. Østerås

Beasley, T. *et al.*, 1998. Isotopic Pu, U, and Np signatures in soils from Semipalatinsk-21, Kazakh Republic and the Southern Urals, Russia. Journal of Environmental Radioactivity 39, 215-230.

Bergan, T.D., 2002. Radioactive fallout in Norway from atmospheric nuclear weapons tests. Journal of Environmental Radioactivity 60, 189-208.

Child, D.P. *et al.*, 2008. High sensitivity analysis of plutonium isotopes in environmental samples using accelerator mass spectrometry (AMS). J. Anal. At. Spectrom. 23, 765-768.

Clacher, A.P., 1995. Development and application of analytical methods for environmental radioactivity.PhD thesis, University of Manchester, Manchester.

Devell, L. *et al.*, 1986. Initial observations of fallout from the reactor accident at chernobyl. Nature 321, 192-193.

Fifield, L.K., 2008. Accelerator mass spectrometry of the actinides. Quaternary Geochronology 3, 276-290.

Kelley, J.M. *et al.*, 1999. Global distribution of Pu isotopes and Np-237. Science of the Total Environment 238, 483-500.

Kirchner, G., Noack, C.C., 1988. Core history and nuclide inventory of the Chernobyl core at the time of accident. Nuclear Safety 29, 1-5.

Lindahl, P. *et al.*, 2004. Distribution of Np and Pu in Swedish lichen samples (Cladonia stellaris) contaminated by atmospheric fallout. Journal of Environmental Radioactivity 73, 73-85.

Lujaniene, G. *et al.*, 2009. Artificial radionuclides in the atmosphere over Lithuania, pp. 108-119.

McInnes, H., Personal communication, Personal communication.

Muramatsu, Y. *et al.*, 2000. Concentrations of Pu-239 and Pu-240 and their isotopic ratios determined by ICP-MS in soils collected from the Chernobyl 30-km zone. Environmental Science & Technology 34, 2913-2917.

Paatero, J. *et al.*, 2010. Airborne and deposited radioactivity from the Chernobyl accident - a review of investigations in Finland. Boreal Environment Research 15, 19-33.

Pálsson, S.E. *et al.*, 2012.New simple deposition model based on reassessment of global fallout data 1954 – 1976. Final report from the NKS-B activity DepEstimates

Denmark

Palsson, S.E. *et al.*, 2013. A simple model to estimate deposition based on a statistical reassessment of global fallout data. J Environ Radioact 121, 75-86.

Pálsson, S.E. *et al.*, 2006. Prediction of spatial variation in global fallout of Cs-137 using precipitation. Science of the Total Environment 367, 745-756.

Povinec, P.P. *et al.*, 2007. Reference material for radionuclides in sediment IAEA-384 (Fangataufa Lagoon sediment). Journal of Radioanalytical and Nuclear Chemistry 273, 383-393.

Pöllänen, R. *et al.*, 1997. Transport of radioactive particles from the Chernobyl accident. Atmospheric Environment 31, 3575-3590.

Reponen, A. *et al.*, 1993. Plutonium fallout in southern finland after the chernobyl accident. Journal of Environmental Radioactivity 21, 119-130.

Salbu, B., 1994. Determination of physicho-chemical forms of radionuclides in natural aquatic systems, in: Holm, E. (Ed.), Radioecology. World Scientific, Singapore, p. 352

Salbu, B., 2000. Source-related characteristics of radioactive particles: A review. Nuclear Technology Publ, pp. 49-54.

Salminen-Paatero, S. *et al.*, 2012. 240Pu/239Pu mass ratio in environmental samples in Finland. Journal of Environmental Radioactivity 113, 163-170.

Srncik, M. *et al.*, 2008. Vertical distribution of Pu-238, Pu-239(40), Am-241, Sr-90 and Cs-137 in Austrian soil profiles. Radiochimica Acta 96, 733-738.

Steinnes, E., Gjelsvik, R., 2008. Geograpical trends in Cs-137 fallout from the Chernobyl accident and leaching from natural surface soil in Norway, International conference on radioecology and environmental radiation. Norwegian Radiation Protection Authority, Bergen, p. 4 b.

Storebø, P.B., 1968. Precipitation formation in a mountainous coast region. Tellus 20, 239-&.

UNSCEAR, 2000a.Annex C, sources and effects of ionizing radiation, United Nations Scientific Committee on the Effects of Atomic Radiation. Vienna

UNSCEAR, 2000b.Annex J, Exposures and effects of the Chernobyl accident, United Nations Scientific Committee on the Effects of Atomic Radiation. Vienna

Wendel, C.C. *et al.*, 2013. Long-range tropospheric transport of uranium and plutonium weapons fallout from Semipalatinsk nuclear test site to Norway. Environment International 59, 92-102.

Captions

Table 1. Plutonium concentrations and atom ratios in certified reference materials measured with SF-ICP-MS in the present work. * Data refers to $^{239+240}$Pu activity concentrations.

Table 2. Activity concentrations, atom ratios and activity ratios of ^{239}Pu, ^{240}Pu and ^{137}Cs in Norwegian humic surface soils. Stated uncertainties are couting uncertainties for ^{137}Cs activity concentrations, $^{239+240}$Pu and ^{240}Pu/^{239}Pu based on aliquots of the samples. All uncertainties are 1 σ. Literature data included for comparison (Beasley *et al.*, 1998; Kelley *et al.*, 1999; UNSCEAR, 2000a, b), $^{239+240}$Pu/^{137}Cs data decay corrected to the reference date of this work (01.01.2009), * - decay corrected from 01.01.1963, ** - decay corrected from 01.05.1986.

Table 3. Atom ratios of ^{240}Pu/^{239}Pu, ^{241}Pu/^{239}Pu and ^{242}Pu/^{239}Pu in samples collected in 2005. Stated uncertainties are counting uncertainties (1 σ).

Figure 1. Overview of the sampling sites in 1990 and 2005.

Figure 2. Map of the sampling sites with ^{239}Pu activity concentrations (Bq m^{-2}) concentrations , and mean annual precipitation in the period 1961 – 1990 (mm year^{-1} m^{-2}) (McInnes, Personal communication)

Figure 3. Atom and activity ratios measured in the humus samples collected in 1990. Upper figure: ^{240}Pu/^{239}Pu atom ratios, the shaded region indicates the range of global fallout according to Kelley *et al.* (1999), with ±1 σ error. The indicated uncertainties are based on parallel samples (3 – 5) for the ^{240}Pu/^{239}Pu atom ratios and counting uncertainties for the $^{239+240}$Pu/^{137}Cs ratios. Lower figure: $^{239+240}$Pu/^{137}Cs activity ratios in the same samples. The lower boundary of the shaded areas indicates the calculated $^{239+240}$Pu/^{137}Cs ratio measured in ground level air in Lithuania during the Chernobyl accident (Lujaniene *et al.*, 2009) and the upper boundary indicates the same ratio in global fallout (UNSCEAR, 2000a). Reference date 01.01.2009.

Figure 4. The $^{241}Pu/^{239}Pu$ vs. $^{242}Pu/^{239}Pu$ in humic surface soil layer samples, the indicated uncertainties are based on the counting uncertainties of the instrument. Literature values included for comparison (Kirchner and Noack, 1988; Beasley *et al.*, 1998; Kelley *et al.*, 1999). The $^{241}Pu/^{239}Pu$ atom ratios are decay corrected to the reference date of this work (01.01.2009).

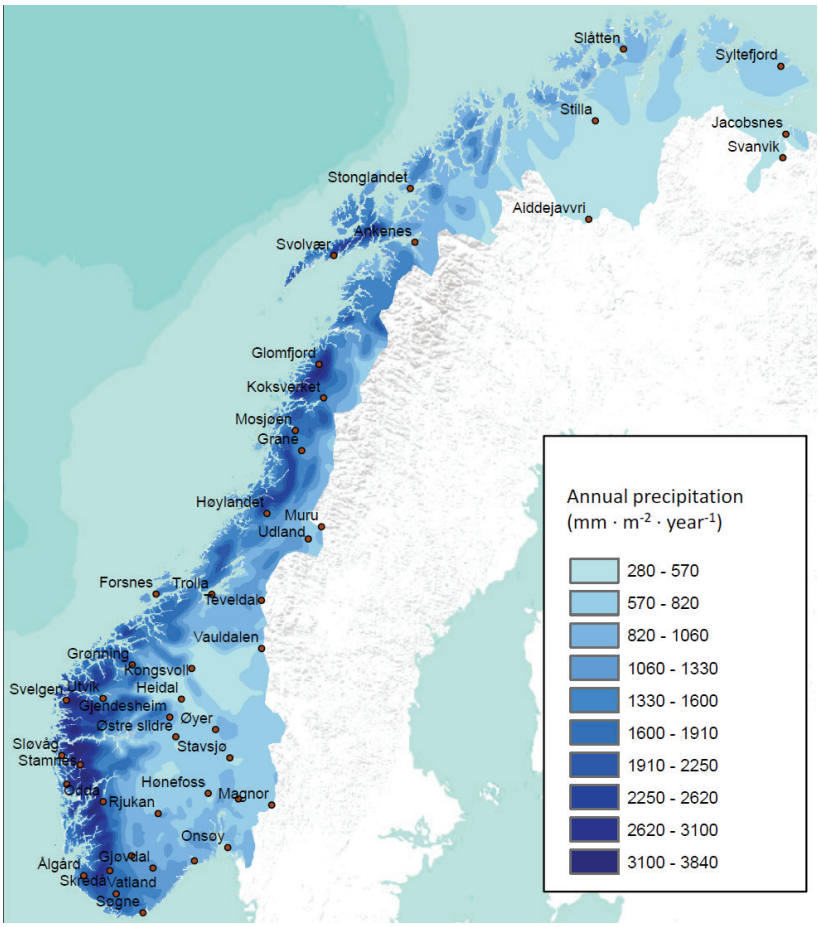
Slåtten
Syltefjord
Stilla
Jacobsnes
Svanvik
Stonglandet
Aiddejavvri
Svolvær
Ankenes
Glomfjord
Koksverket
Mosjøen
Grane
Høylandet
Muru
Udland
Forsnes
Trolla
Tevelda
Vauldalen
Grønning
Kongsvoll
Svelgen
Utvik
Heidal
Gjendesheim
Øyer
Østre slidre
Sløvåg
Stavsjø
Stamnes
Hønefoss
Odda
Rjukan
Magnor
Onsøy
Gjovdal
Ålgård
Skreda
Vatland
Sogne
Annual precipitation
(mm · m-2 · year-1)
280 - 570
570 - 820
820 - 1060
1060 - 1330
1330 - 1600
1600 - 1910
1910 - 2250
2250 - 2620
2620 - 3100
3100 - 3840

Figure 5.

Table 4.

Reference material	$^{239+240}$Pu activity Bq kg^{-1}	^{240}Pu/^{239}Pu atom ratio	Reference
IAEA 384	125 ± 18	0.0501 ± 0.0008	This work (n=5)
Fangataufa sediment	107 ± 2	0.049 ± 0.001	Povinec *et al.* (2007)
NIST 4353	13.8 ± 0.7	0.058 ± 0.002	This work (n=3)
Rocky flats soil	16.8 ± 2	0.053 – 0.060	Reference sheet
IAEA 300	4 ± 1	0.22 ± 0.03	This work (n=4)
Baltic sea sediment	3.09 – 3.90	-	Reference sheet
	3.92 ± 0.1	0.17 ± 0.01	Child *et al.* (2008)

Table 5.

	^{137}Cs Bq m^{-2}		$^{239+240}$Pu Bq m^{-2}		^{240}Pu/^{239}Pu		$^{239+240}$Pu/^{137}Cs	
Site	1990	2005	1990	2005	1990	2005	1990	2005
Onsøy	n.a.	920 ± 20	n.a.	2.7 ± 0.1	n.a.	0.178 ± 0.009	n.a.	0.003 ± 0.0002
Kløfta	2020 ± 54	2800 ± 60	19 ± 2	11.3 ± 0.3	0.20 ± 0.01	0.183 ± 0.006	0.009 ± 0.001	0.0041 ± 0.0001
Magnor	670 ± 34	300 ± 26	42 ± 1	1.18 ± 0.08	0.188 ± 0.005	b.d.	0.062 ± 0.004	0.0038 ± 0.0004
Stavsjø	3300 ± 114	1300 ± 35	24 ± 1	12.5 ± 0.7	0.2 ± 0.01	b.d.	0.0073 ± 0.0004	0.0096 ± 0.0006
Øystre Slidre	20500 ± 511	15500 ± 225	25 ± 4	3.9 ± 0.2	0.202 ± 0.008	b.d.	0.0012 ± 0.0002	0.00025 ± 0.00001
Øyer	12900 ± 236	6500 ± 157	18 ± 4	13.3 ± 0.3	b.d.	0.189 ± 0.005	0.0014 ± 0.0003	0.00205 ± 0.00007
Gjendesheim	n.a.	25500 ± 427	n.a.	24.7 ± 0.7	n.a.	0.195 ± 0.003	n.a.	0.00097 ± 0.00003
Heidal	n.a.	33300 ± 539	n.a.	8.5 ± 0.5	n.a.	b.d.	n.a.	0.00026 ± 0.00002
Hønefoss	3800 ± 188	510 ± 24	36 ± 2	2.0 ± 0.2	0.194 ± 0.005	b.d.	0.0095 ± 0.0006	0.004 ± 0.0005
Langesund	2290 ± 49	1500 ± 32	20.4 ± 0.9	18 ± 1	0.191 ± 0.009	0.19 ± 0.01	0.0089 ± 0.0004	0.0123 ± 0.0008
Rjukan	4540 ± 77	760 ± 31	18.6 ± 0.9	40.5 ± 0.8	0.191 ± 0.009	0.184 ± 0.003	0.0041 ± 0.0002	0.053 ± 0.002
Gjøvdal	2080 ± 74	490 ± 20	48 ± 6	32.0 ± 0.7	0.193 ± 0.007	0.178 ± 0.004	0.023 ± 0.003	0.066 ± 0.003
Hylestad	900 ± 25	n.a.	15 ± 2	n.a.	0.173 ± 0.006	n.d.	0.017 ± 0.002	n.a.
Søgne	2900 ± 98	520 ± 27	65 ± 3	3.6 ± 0.3	0.181 ± 0.009	b.d.	0.023 ± 0.001	0.0069 ± 0.0006
Vatland	3100 ± 67	1440 ± 58	53 ± 10	35 ± 1	0.176 ± 0.007	0.177 ± 0.006	0.017 ± 0.003	0.024 ± 0.001
Skredå	1880 ± 34	510 ± 28	23.3 ± 0.6	6.6 ± 0.3	0.200 ± 0.004	b.d.	0.0123 ± 0.0004	0.0128 ± 0.0009
Ålgård	1190 ± 63	400 ± 16	17.8 ± 0.9	28 ± 1	0.192 ± 0.007	0.176 ± 0.006	0.015 ± 0.001	0.071 ± 0.004
Odda	1900 ± 39	620 ± 25	70 ± 13	40.0 ± 0.9	0.190 ± 0.005	0.181 ± 0.004	0.037 ± 0.007	0.065 ± 0.003
Fyllingsdalen	1710 ± 65	920 ± 52	64 ± 1	63 ± 1	0.183 ± 0.004	0.184 ± 0.004	0.037 ± 0.002	0.068 ± 0.004
Stamnes	1410 ± 51	280 ± 11	34 ± 2	0.7 ± 0.1	0.18 ± 0.01	b.d.	0.024 ± 0.002	0.0024 ± 0.0004
Sløvåg	3100 ± 65	1320 ± 44	149 ± 4	6 ± 2	0.187 ± 0.005	b.d.	0.048 ± 0.002	0.005 ± 0.001

Svelgen	3700 ± 148	1300 ± 26	89 ± 2	63.4 ± 0.9	0.177 ± 0.006	0.177 ± 0.003	0.024 ± 0.001	0.049 ± 0.001
Utvik	3800± 81	1400 ± 28	62 ± 1	1.31 ± 0.08	0.183 ± 0.004	b.d.	0.0166 ± 0.0005	0.00094 ± 0.00006
Grønning	5100 ± 149	1070 ± 45	44 ± 4	35 ± 2	0.18 ± 0.01	0.178 ± 0.002	0.0087 ± 0.0007	0.033 ± 0.003
Kongsvoll	41000 ± 1103	n.a.	71 ± 4	n.a.	0.198 ± 0.009	n.a.	0.0017 ± 0.0001	n.a.
Vauldalen	2910 ± 68	1110 ± 52	69 ± 2	7.5 ± 0.3	0.211 ± 0.008	0.162 ± 0.006	0.024 ± 0.001	0.0068 ± 0.0004
Trolla	7300 ± 155	1520 ± 54	42 ± 3	18.2 ± 0.4	0.185 ± 0.007	0.174 ± 0.005	0.0057 ± 0.0004	0.012 ± 0.0005
Forsnes	2910 ± 76	n.a.	32 ± 2	n.a.	0.174 ± 0.006	n.a.	0.0109 ± 0.0006	n.a.
Teveldal	3490 ± 79	520 ± 10	52 ± 8	2.8 ± 0.2	0.176 ± 0.003	b.d.	0.015 ± 0.002	0.0053 ± 0.0004
Udland	n.a.	18100 ± 349	n.a.	15.9 ± 0.5	n.a.	0.174 ± 0.005	n.a.	0.00088 ± 0.00003
Muru	n.a.	57500 ± 736	n.a.	16 ± 2	n.a.	b.d.	n.a.	0.00029 ± 0.00003
Høylandet	3330 ± 79	1490 ± 34	68 ± 4	35.2 ± 0.7	0.176 ± 0.009	0.176 ± 0.004	0.021 ± 0.001	0.0237 ± 0.0007
Grane	n.a.	15600 ± 435	n.a.	3.9 ± 0.2	n.a.	b.d.	n.a.	0.00025 ± 0.00001
Mosjøen	21400 ± 736	1970 ± 73	67 ± 12	2.2 ± 0.5	0.190 ± 0.006	b.d.	0.0032 ± 0.0006	0.0011 ± 0.0003
Koksverket	2620 ± 71	740 ± 40	4.3 ± 0.8	21.4 ± 0.6	0.186 ± 0.008	0.168 ± 0.005	0.0016 ± 0.0003	0.029 ± 0.002
Glomfjord	2520 ± 51	950 ± 40	23 ± 5	17 ± 0.4	0.184 ± 0.006	0.176 ± 0.004	0.009 ± 0.002	0.0179 ± 0.0008
Ankenes	760 ± 48	440 ± 12	11.0 ± 0.4	17.2 ± 0.5	0.182 ± 0.009	0.172 ± 0.005	0.014 ± 0.001	0.039 ± 0.002
Svolvær	1020 ± 22	950 ± 50	111 ± 2	38 ± 3	0.164 ± 0.001	0.161 ± 0.004	0.108 ± 0.003	0.04 ± 0.003
Stonglandet	n.a.	170 ± 12	n.a.	2.2 ± 0.2	n.a.	b.d.	n.a.	0.012 ± 0.001
Stilla	1760 ± 53	173 ± 9	63 ± 2	13 ± 0.7	0.178 ± 0.003	b.d.	0.036 ± 0.002	0.075 ± 0.005
Slåtten	n.a.	300 ± 18	n.a.	34 ± 1	n.a.	b.d.	n.a.	0.112 ± 0.008
Aiddejavvri	n.a.	230 ± 14	n.a.	21 ± 1	n.a.	0.19 ± 0.009	n.a.	0.093 ± 0.007
Syltefjord	n.a.	1120 ± 39	n.a.	33 ± 1	n.a.	0.189 ± 0.008	n.a.	0.03 ± 0.002
Jakobsnes	890 ± 18	203 ± 8	18.5 ± 0.9	18 ± 2	0.181 ± 0.007	b.d.	0.021 ± 0.001	0.09 ± 0.009
Svanvik	1030 ± 30	210 ± 13	47 ± 2	3.3 ± 0.1	0.19 ± 0.01	b.d.	0.046 ± 0.003	0.016 ± 0.001
Semipalatinsk					0.0438 ± 0.00001		-	

Global fallout	-	-	-	-	0.18 ± 0.01	-	0.033*	-
Chernobyl	-	-	-	-	0.40	-	0.0016**	-

n.a. - not analysed

b.d. - below detection limit

Table 6.

Site	$^{240}Pu/^{239}Pu$	$^{241}Pu/^{239}Pu$ $\times 10^{-3}$	$^{242}Pu/^{239}Pu$ $\times 10^{-3}$
Glomfjord	0.20 ± 0.02	2.3 ± 0.8	9.9 ± 1.8
Trolla	0.17 ± 0.01	1.5 ± 0.6	4.5 ± 0.7
Fyllingsdalen	0.17 ± 0.01	1.4 ± 0.4	5.1 ± 0.9
Kløfta	0.19 ± 0.02	0.9 ± 0.5	6.4 ± 1.3
Svolvær	0.17 ± 0.01	1.3 ± 0.3	3.8 ± 0.5

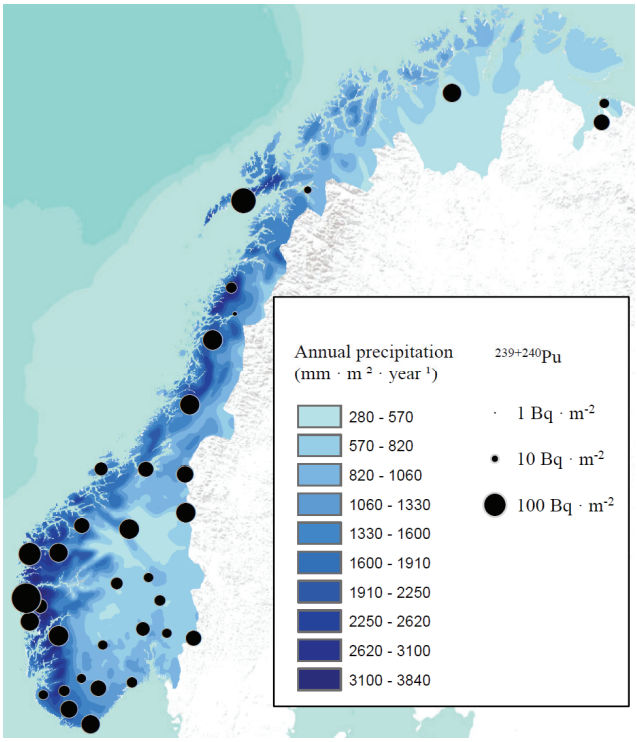
Annual precipitation
(mm · m ² · year ¹)
280 - 570
570 - 820
820 - 1060
1060 - 1330
1330 - 1600
1600 - 1910
1910 - 2250
2250 - 2620
2620 - 3100
3100 - 3840
239+240Pu
1 Bq · m-2
10 Bq · m-2
100 Bq · m-2

Figure 6.

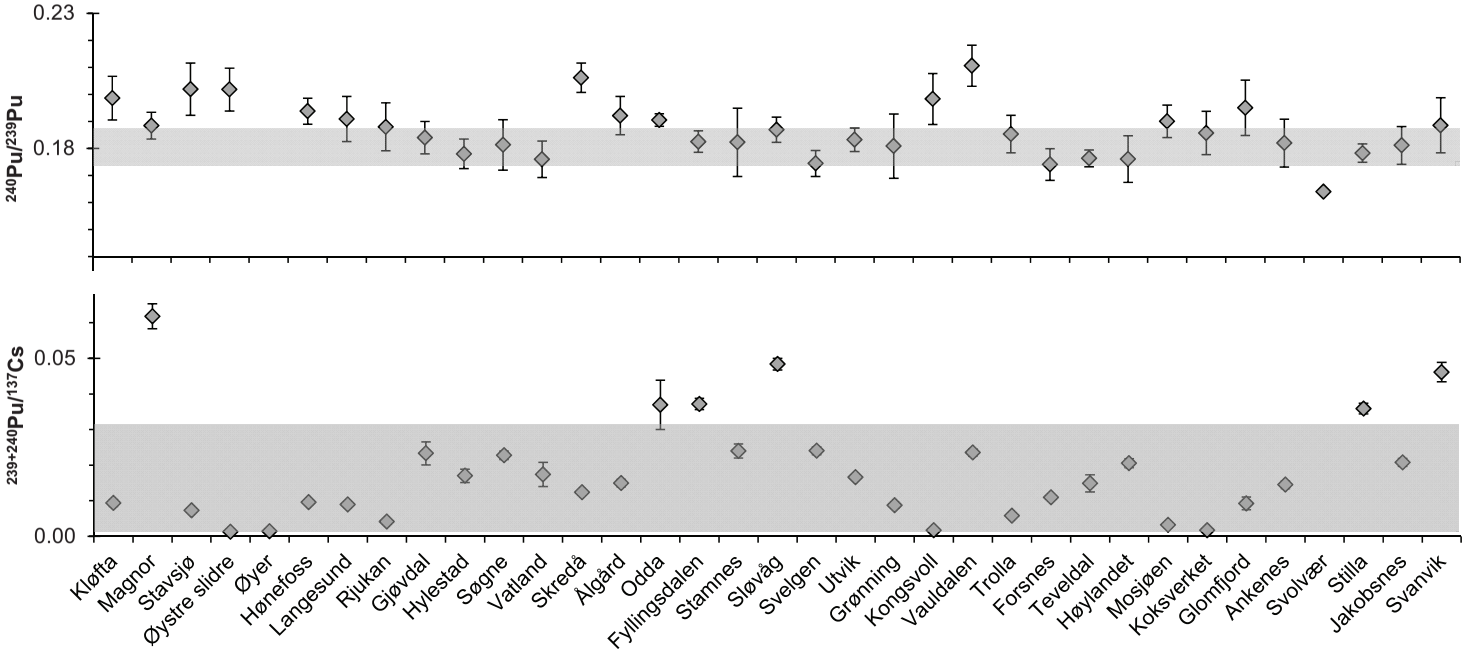

Figure 7. Atom and activity ratios measured in the humus samples collected in 1990. Upper figure: $^{240}Pu/^{239}Pu$ atom ratios, the shaded region indicates the range of global fallout according to Kelley *et al.* (1999), with ±1 σ error. The indicated uncertainties are based on parallel samples (3 – 5) for the $^{240}Pu/^{239}Pu$ atom ratios and counting uncertainties for the $^{239+240}Pu/^{137}Cs$ ratios. Lower figure: $^{239+240}Pu/^{137}Cs$ activity ratios in the same samples. The lower boundary of the shaded areas indicates the calculated $^{239+240}Pu/^{137}Cs$ ratio measured in ground level air in Lithuania during the Chernobyl accident (Lujaniene *et al.*, 2009) and the upper boundary indicates the same ratio in global fallout (UNSCEAR, 2000a). Reference date 01.01.2009.

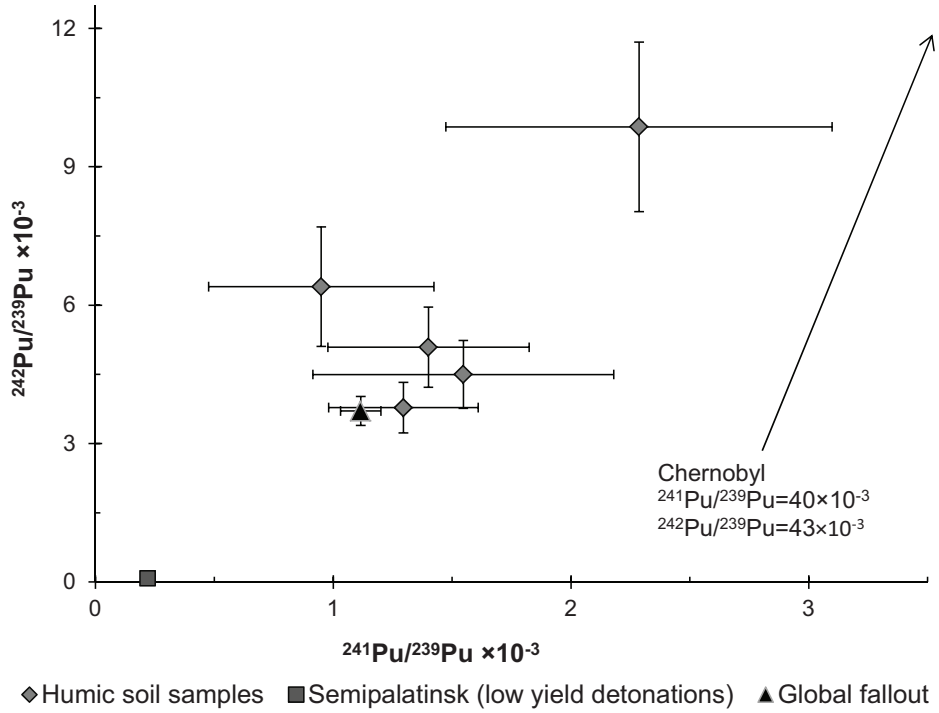

Figure 8. The $^{241}Pu/^{239}Pu$ vs. $^{242}Pu/^{239}Pu$ in humic surface soil layer samples, the indicated uncertainties are based on the counting uncertainties of the instrument. Literature values included for comparison (Kirchner and Noack, 1988; Beasley *et al.*, 1998; Kelley *et al.*, 1999). The $^{241}Pu/^{239}Pu$ atom ratios are decay corrected to the reference date of this work (01.01.2009).

Paper II

Science of the Total Environment 461–462 (2013) 734–741

Contents lists available at SciVerse ScienceDirect

Science of the Total Environment

journal homepage: www.elsevier.com/locate/scitotenv

Chronology of Pu isotopes and ^{236}U in an Arctic ice core

C.C. Wendel [a,*], D.H. Oughton [a,1], O.C. Lind [a,2], L. Skipperud [a,3], L.K. Fifield [b,4], E. Isaksson [c,5], S.G. Tims [b,6], B. Salbu [a,7]

[a] Isotope Laboratory, Department of Plant and Environmental Sciences, Agricultural University of Norway, P.O. Box 5003, N-1432 Aas, Norway
[b] Department of Nuclear Physics, Australian National University, Canberra ACT 0200, Australia
[c] Norwegian Polar Institute, Fram Centre, Hjalmar Johansens Gate 14, N9296 Tromsø, Norway

HIGHLIGHTS

- Concentrations and atom ratios of Pu and 236U determined in an Arctic ice core.
- Concentrations of U and Pu found to be higher pre- than post-moratorium.
- U and Pu concentrations found to vary in concordance with 137Cs concentrations.
- Particles indicated at depths corresponding to atmospheric nuclear testing.

ARTICLE INFO

Article history:
Received 4 January 2013
Received in revised form 16 May 2013
Accepted 18 May 2013
Available online xxxx

Editor: Mae Sexauer Gustin

Keywords:
^{236}U/^{239}Pu
^{240}Pu/^{239}Pu
Atom ratio
AMS
Arctic
Ice core

ABSTRACT

In the present work, state of the art isotopic fingerprinting techniques are applied to an Arctic ice core in order to quantify deposition of U and Pu, and to identify possible tropospheric transport of debris from former Soviet Union test sites Semipalatinsk (Central Asia) and Novaya Zemlya (Arctic Ocean). An ice core chronology of ^{236}U, ^{239}Pu, and ^{240}Pu concentrations, and atom ratios, measured by accelerator mass spectrometry in a 28.6 m deep ice core from the Austfonna glacier at Nordaustlandet, Svalbard is presented. The ice core chronology corresponds to the period 1949 to 1999. The main sources of Pu and ^{236}U contamination in the Arctic were the atmospheric nuclear detonations in the period 1945 to 1980, as global fallout, and tropospheric fallout from the former Soviet Union test sites Novaya Zemlya and Semipalatinsk. Activity concentrations of $^{239+240}$Pu ranged from 0.008 to 0.254 mBq cm^{-2} and ^{236}U from 0.0039 to 0.053 μBq cm^{-2}. Concentrations varied in concordance with ^{137}Cs concentrations in the same ice core. In contrast to previous published results, the concentrations of Pu and ^{236}U were found to be higher at depths corresponding to the pre-moratorium period (1949 to 1959) than to the post-moratorium period (1961 and 1962). The ^{240}Pu/^{239}Pu ratio ranged from 0.15 to 0.19, and ^{236}U/^{239}Pu ranged from 0.18 to 1.4. The Pu atom ratios ranged within the limits of global fallout in the most intensive period of nuclear atmospheric testing (1952 to 1962). To the best knowledge of the authors the present work is the first publication on biogeochemical cycles with respect to ^{236}U concentrations and ^{236}U/^{239}Pu atom ratios in the Arctic and in ice cores.

1. Introduction

Atmospheric nuclear testing took place through four decades from 1945 to 1980, cf. Table 1. Three periods can easily be identified. The first period (1945 to 1958) was dominated by US testing at equatorial sites (Bikini, Eniwetok and Johnston Island). This period ended in 1958 with the implementation of a moratorium (1959 to 1961). Except for four French detonations the moratorium was largely respected until September 1961 (1961-9). In the second period (1961 and 1962) former Soviet Union testing at Novaya Zemlya (Arctic Ocean) and Semipalatinsk (Kazakhstan) dominated. United States of America (USA) atmospheric testing followed in the spring of 1962 until the limited test ban treaty was implemented in 1963, terminating all atmospheric nuclear testing by the USA and the former Soviet Union (FSU). The

* Corresponding author. Tel.: +47 976 659 48.
E-mail addresses: cato.wendel@umb.no (C.C. Wendel), deborah.oughton@umb.no (D.H. Oughton), ole-christian.lind@umb.no (O.C. Lind), lindis.skipperud@umb.no (L. Skipperud), keith.fifield@anu.edu.au (L.K. Fifield), elisabeth.isaksson@npolar.no (E. Isaksson), steve.tims@anu.edu.au (S.G. Tims), brit.salbu@umb.no (B. Salbu).
[1] Tel.: +47 6496 5544.
[2] Tel.: +47 6496 5545.
[3] Tel.: +47 6496 5546.
[4] Tel.: +61 2 6125 2095.
[5] Tel.: +47 77 75 05 15.
[6] Tel.: +61 2 6125 2086.
[7] Tel.: +47 6496 5541.

0048-9697/$ – see front matter © 2013 Elsevier B.V. All rights reserved.
http://dx.doi.org/10.1016/j.scitotenv.2013.05.054

Table 1
Atmospheric nuclear tests within the northern hemisphere during 1945–1980, based on Björklund and Goliath (2009).

Test site	Period	Sum yield (kt)	Mean yield (kt)	Number of tests
Algerie (France)	1960–1961	92	23	4
Lop Nor (China)	1966–1979	13,785	1149	12
Nevada test site (USA)	1945–1958	1018	10	101
	1962	107	18	6
US equatorial (Bikini, Eniwetok and Johnston Island)	1946–1958	116,091	1707	68
	1961–1962	14,216	1421	10
Semipalatinsk (FSU)[a]	1949–1958	6237	127	49
	1961–1962	639	10	67
Novaya Zemlya (FSU)[a]	1957–1958	20,682	766	27
	1961–1962	235,148	3855	61
Orenburg, Aralsk and Kapustin Yar (FSU) [a]	1954–1961	121	17	7

[a] FSU — former Soviet Union.

third period started with the first Chinese detonation in 1964-10, and lasted until 1980-10. This period included Chinese (Lop Nor) and French (Mururoa and Fangataufa) tests (UNSCEAR, 2000; Björklund and Goliath, 2009).

Former Soviet Union nuclear testing sites, Novaya Zemlya and Semipalatinsk, and the USA Pacific proving grounds (Bikini, Eniwetok, Johnston Island) along with the Nevada Nuclear Test site were the dominant locations in the northern hemisphere during the first period 1945 to 1962 (UNSCEAR, 2000; Björklund and Goliath, 2009). More than 320 atmospheric tests were carried out at these sites, with a yield of 86 and 247 Mt partitioned between fission and total yield, respectively. The largest detonations in the northern hemisphere took place over Novaya Zemlya in 1961 to 1962 giving massive contribution to the stratospheric inventory of artificial radionuclides (Table 1). The accumulated yield of all FSU detonations above Novaya Zemlya in 1961 and 1962 amounts to some 57% of all atmospheric nuclear weapons detonated during 1945 to 1980 (UNSCEAR, 2000).

Debris from nuclear detonations may be divided into three impact classes: local, regional (tropospheric), and global (stratospheric). This will depend on local and synoptic meteorological conditions, and the yield of the detonation. Detonations on the ground or sea surface give rise to large amounts of contaminated ground material and agglomerates of ground material and bomb remnants as relatively large particles that are deposited from the atmosphere within hours or days.

All detonations within the troposphere generate fine particulate debris that largely remains in the troposphere until removed from the atmosphere by precipitation or dry deposition. This is thought to occur mainly in the hemisphere of the detonation (UNSCEAR, 2000). The residence half-life of tropospheric debris has been estimated to 70 days (Holloway and Hayes, 1982). The troposphere extends from 0 to 9 km above sea level at polar latitudes (above 60°N or S) and from 0 to17 km above sea level at equatorial latitudes (Peterson, 1970). For polar detonations larger than 300 kt, and equatorial detonations larger than 3000 kt the centre of the debris cloud penetrates into the stratosphere (Peterson, 1970). Debris thus injected into the stratosphere has a residence half-life there of between 8 months and 2 years depending on the height at which it is deposited and the latitude (Peterson, 1970). Stratospheric debris falls out more evenly than tropospheric debris and the deposition rate is usually found to vary with latitude and precipitation (e.g. Pálsson et al. (2006); Pálsson et al. (2013)).

The $^{240}Pu/^{239}Pu$ atom ratio of weapon debris depends on the yield and the design of the bomb. Low yield detonations (0 to ~300 kt) produce debris which differs little from undetonated weapon material (Cooper et al., 2000). Very large detonations (above 5 Mt) have been reported to produce high $^{240}Pu/^{239}Pu$ atom ratio debris. Typical weapon grade plutonium has atom ratios in the order of 0.01 to 0.07, while debris from civil reactor accidents and very large detonations are in the 0.3 to 0.45 range (Diamond et al., 1960; Warneke et al., 2002; Lindahl et al., 2011). Debris captured in the lower stratosphere above Sweden the 1958-10-17 had a reported $^{240}Pu/^{239}Pu$ atom ratio of 0.101 (Warneke, 2002). This debris originated from two large detonations above Novaya Zemlya on the 1958-09-30 (0.9 and 1.2 Mt) (Sisefsky, 1961; Björklund and Goliath, 2009). Plutonium recovered in sediments of the Chernaya Bay, southern Novaya Zemlya, yielded low $^{240}Pu/^{239}Pu$ (0.0304 to 0.0324) atom ratios reflecting low yield atmospheric and underwater tests in the area (Smith et al., 1995, 2000). Except for these results, little information is available regarding the plutonium atom ratios for debris from high yield Novaya Zemlya atmospheric detonations, and the area still remains off limits.

Uranium-236 is an almost entirely anthropogenic isotope of uranium, with a half-life of 2.34×10^7 years. In the terrestrial environment, a natural $^{236}U/^{238}U$ ratio of 3×10^{-14} has been estimated (Srncik (2011), and references therein). However, bomb fallout during the atmospheric nuclear testing era significantly altered this ratio. Pre-nuclear $^{236}U/^{238}U$ atom ratios in the oceans were in the range 3 to 8×10^{-12}, the ratio peaked in 1964 with values of ~2×10^{-9} (Winkler et al., 2012). Particularly contaminated sites have $^{236}U/^{238}U$ ratios as high as 4×10^{-5} (Irish Sea sediment, Srncik et al. (2011a)). No similar chronology has been found for terrestrial environments; present day global fallout affected areas have $^{236}U/^{238}U$ ratios ranging within 10^{-7} to 10^{-9} (Sakaguchi et al., 2009; Srncik et al., 2011b), ratios as high as 6.7×10^{-4} have been reported for sites severely contaminated by local fallout (Boulyga et al., 2002). Sakaguchi et al. (2009) state two main origins for ^{236}U in fallout; in the atmosphere formation from ^{240}Pu ($t_{1/2}$ = 6564 years) or the production from ^{238}U by ^{238}U decay through the loss of two neutrons (n, 3n) to ^{236}U. The isotope can also be produced naturally by the decay of ^{235}U through the loss of a neutron and gamma radiation described as the following reaction: ^{235}U (n,γ)^{236}U. Steier et al. (2008) estimated the natural terrestrial and marine inventories of ^{236}U to be 34 kg and that produced in reactors until 2003 to be 10^6 kg, of which only a small proportion would have been released to the open environment. Releases from atmospheric nuclear detonations on the other hand, are unconfined. Sakaguchi et al. (2009) estimated that up to 900 kg of ^{236}U was dispersed in atmospheric nuclear detonations.

Publications on ^{236}U concentrations and $^{236}U/^{239}Pu$ atom ratios are limited, and published $^{236}U/^{239}Pu$ ratios range between 0.05 and 0.5 in areas which have received mainly global fallout (Ketterer et al., 2007; Sakaguchi et al., 2009). Beasley et al. (1998b) reported $^{236}U/^{239}Pu$ atom ratios of 0.0224 in debris from low yield detonations at ground zero at the Semipalatinsk test site.

Ice cores from glaciers provide valuable information on historical deposition of natural and anthropogenic components from the atmosphere, (e.g. Koide et al. (1985); Warneke et al. (2002); Olivier et al. (2004)). The high annual snow accumulation of a glacier compared with other environmental compartments (e.g. soil) increases the time resolution and may allow for identification of time periods of deposition with accuracy down to less than a year. However, depending on the meteorological conditions, pollutants may be subject to redistribution due to melting and infiltration that would alter the stratigraphy of the glacier.

The objectives of the current work were to establish concentrations and atom ratio chronologies of ^{236}U, ^{239}Pu and ^{240}Pu in an ice core from Nordaustlandet (Svalbard) and to use this information for source identification and assessment purposes. Our hypothesis was that tropospheric transport of debris from detonation sites at Novaya Zemlya and Semipalatinsk (Kazakhstan) influenced the radionuclide deposition at this location.

2. Materials and methods

The ice core investigated in this work (AUS99) has been thoroughly described elsewhere (Pinglot et al., 2001; Watanabe et al., 2001; Hermanson et al., 2005), and only a short summary will be given here.

The core was drilled from the summit of Austfonna, Nordaustlandet 79.83°N, 24.02°E 750 m a.s.l. in 1999-04/1999-05, to a depth of 289 m (Isaksson et al., 2003). The Austfonna ice cap is located in the north-eastern part of the Svalbard archipelago on the island of Nordaustlandet (Fig. 1). Winds in the area are predominately easterly or north-easterly, and an extension of the North Atlantic Current results in winter temperatures that are relatively mild. Through the retrieval of the 1963 ^{3}H and ^{137}Cs peaks at 20.9 m physical depth, the mean annual accumulation rate was estimated to be 0.37 to 0.45 m water equivalent (Watanabe et al., 2001; Pinglot et al., 2003). Based on this an estimated time/depth relationship was set up and confirmed based on variation in electrical conductivity corresponding with volcano eruption fallout (Watanabe et al., 2001). Furthermore, oxygen atom ratios ($^{18}O/^{16}O$) were used to confirm the dates based on the general trend in temperature fluctuations measured at nearby stations (Watanabe et al., 2001).

We were allotted ~20 to 25% of the original ice core cross section of 70 cm^2, and this reduced the potential time resolution for U and Pu analysis of the ice core. Sample sizes for analyses were based on anticipated plutonium concentrations from deposition history and gross beta measurements in air in the 1950s and 1960s (Tone Bergan, personal communication, 2008). As such, the ice core was cut into samples ranging in mass from 1.5 to 5 kg (supplementary material Fig. S1) in a cold room (−20 °C). The samples were melted at room temperature and filtered through membrane filters with a cut-off of 50 nm (Nucleopore 0.05 μm, Whatman Schleicher &Schuell). Filtered solutions were then evaporated to dryness while the filters were subjected to digital autoradiography to detect particles embedded in the ice.

2.1. Digital autoradiography

Dried filters were mounted sequentially on paper and placed in close contact with a cleared and cleaned autoradiography imaging plate (Imaging plate, Molecular dynamics), and placed in a protective cassette to reduce the impact of external radiation. To further reduce the radiation background, the autoradiography cassettes containing the image plate and samples were placed in a custom-built low-activity lead box. To allow for the detection of the low activities, anticipated for the polar ice, an exposure time of 28 days was used, after which the imaging plate was scanned in an image plate scanner (Typhoon 8600, Molecular dynamics) at a resolution of 100 μm.

Fig. 1. Map of the sampling site at Nordaustlandet, Svalbard. The AUS-99 core was drilled at the summit of Austfonna (79.83°N, 24.02°E).

2.2. Sample preparation for accelerator mass spectrometry (AMS)

Unless stated otherwise all chemicals used were of analytical grade. Ultrapure HNO_3 and HCl were produced in the laboratory using a sub-boiling distillation unit (Milestone SubPure) and used for digestion, ion separation and final sample preparation. Deionised water (18 MΩ) was obtained from a MilliQ apparatus (Barnstead B-pure).

Following autoradiography the filters and high purity yield monitors (~17 pg each of ^{233}U (National proficiency laboratory (NPL) UBP10020, <0.24% ^{234}U and 0.00% ^{236}U) and ^{242}Pu (NPL R15-00, <0.0003% ^{241}Pu)) were placed in Poly Tetra Fluor Ethylene (PTFE) ultraclave tubes and digested under high temperature and pressure in nitric acid (conc.) in an ultraclave unit (UltraCLAVE 3, Milestone Ltd.). After digestion the filter digests were recombined with the respective evaporates to ensure the best possible signal. The solutions were diluted to 8 M HNO_3 and plutonium was separated from the sample matrix by anion exchange (DOWEX 1 × 8) (Clacher, 1995). The uranium eluate was further purified with uranium tetravalent specific resin (UTEVA) according to the procedure suggested by Wilcken (2006). Following separation the respective Pu and U eluates were evaporated to dryness, taken up in 2 ml concentrated HNO_3 with 2 mg Fe as $Fe(NO_3)_3$ and evaporated to dryness again before being baked at 500 °C overnight. Prior to AMS analysis the Fe/Pu and Fe/U precipitates were mixed with silver powder at a ratio of 1:4, and pressed into Al holders. The silver powder has the dual purposes of providing sufficient bulk and electrical conductivity for analysis.

2.3. Analysis

Concentrations and atom ratios of plutonium and uranium were determined by accelerator mass spectrometry using the 14 UD (units double i.e. 14 essentially identical units at the low and high energy side of the accelerator) pelletron tandem accelerator at the Australian National University (ANU), as described by Fifield (2008).

2.3.1. Plutonium analysis

Three plutonium isotopes (^{242}Pu (yield monitor), ^{240}Pu and ^{239}Pu) were counted sequentially with counting times ranging from 1 to 3 min according to their abundance. The sequence was repeated twice with a third ^{242}Pu count at the end. Concentrations of ^{239}Pu and ^{240}Pu were calculated from the measured $^{239}Pu/^{242}Pu$ and $^{240}Pu/^{239}Pu$ atom ratios. The results are presented in Table 3 and Figs. 2 and 4. The accuracy of the atom ratios was confirmed through repeated measurements of a certified reference material for plutonium atom ratios (UKAEA certified nuclear reference material No: UK Pu5/92138). The UKAEA (United Kingdom Atomic Energy Authority) reference material was prepared in advance, and is used for instrumental calibration purposes. It was precipitated directly with Fe_2O_3 without prior chemical separation. The measured $^{240}Pu/^{239}Pu$ (0.966 ± 0.001), $^{242}Pu/^{239}Pu$ (0.975 ± 0.002) and $^{242}Pu/^{239}Pu$ (0.943 ± 0.002) in the material is by design close to unity. Count rates were high, comparable to count rates of the ^{242}Pu tracer used, i.e. 17 pg ^{242}Pu giving ~200 cps.

The precision for the $^{242}Pu/^{239}Pu$ atom ratio was 2.7% (relative standard deviation, n = 16). Analytical blanks, spiked with 17 pg ^{242}Pu gave at most 1 count of ^{239}Pu and ^{240}Pu in any given 2 or 3 minute counting interval, respectively.

With count rates for ^{242}Pu of 12,000 counts min^{-1}, this corresponds to conservative procedural detection limits of 0.7 and 0.5 fg for ^{239}Pu and ^{240}Pu respectively. At these concentrations, no background corrections were required.

2.3.2. Uranium analysis

Like plutonium, three uranium isotopes (^{233}U (yield monitor), ^{234}U and ^{236}U) were counted sequentially with counting time ranging from 0.5 to 3 min according to their abundances. The sequence was repeated twice with a third ^{233}U count at the end. Concentrations of ^{236}U were calculated from the $^{236}U/^{233}U$ atom ratios. In contrast to the sub-fg backgrounds observed in the plutonium case, measurements of the analytical blanks indicated a significant background of ^{236}U. This most likely arose from analyses of a set of three depleted-uranium (DU) samples with unexpectedly high ^{236}U concentrations. One of these was run in the ion source prior to the measurement of the ice-core samples, while all three were pressed into sample holders at the same time as the ice-core samples. Analysis of blank pressed before and after the DU sample together with instrument blanks showed that the background was largely due to memory effects in the ion source. We found no evidence of cross-contamination during the sample-pressing process. The average ^{236}U counting rate from the two blanks was 5 counts min^{-1}, and this was reasonably stable during analyses. This count rate has been subtracted from all of the ice-core samples with an assumed uncertainty of ±2.5 $countsmin^{-1}$. The corresponding 2 σ detection limit in the present work is then ~20 fg of ^{236}U, based upon typical ^{233}U count rates of 4800/min from the 20 pg spike.

Concentrations of natural uranium in the samples were deduced from the $^{234}U/^{233}U$ ratios assuming the natural abundance of 5.5×10^{-5} for ^{234}U. Based on the two analytical blanks, the observed ratios corresponded to ~20 ng of uranium. The blanks consisted of ~2 mg of iron oxide mixed with 6 to 10 mg of silver powder. This was the matrix housing the sample. Potential sources of this background uranium are the analytical reagents, the silver powder, the aluminium sample holders, and more generally from the ion source. It is evident from Table 3 that the ^{238}U concentrations in the ice-core samples are in many cases comparable with the blanks. Hence the uranium concentrations in the original ice were at or below a few ppt.

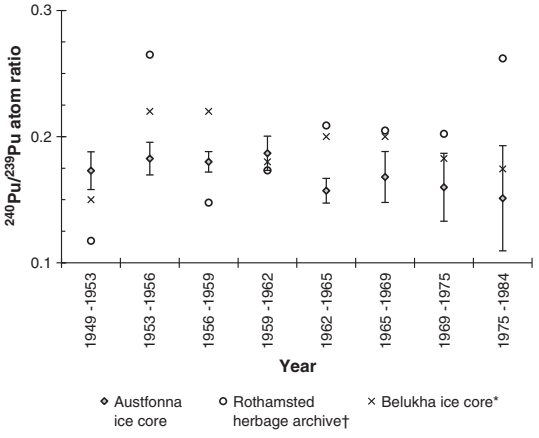

Fig. 2. $^{240}Pu/^{239}Pu$ atom ratios recorded in the Austfonna ice core. Uncertainties are counting statistics (1σ). Activity-weighted averages of literature data included for comparison: † Rothamsted herbage archive (UK) (Warneke et al., 2002); * ice core extracted from the Belukha glacier (Siberian Altai) (Olivier et al., 2004).

3. Results and discussion

3.1. Autoradiography

Digital autoradiography serves as a technique for detecting and isolating natural or anthropogenic radioactive particles in a sample. Detailed identification of nuclides, concentrations, particle size and isotopic composition rely on other methods (scanning electron microscope with X-ray microanalysis in combination with Synchrotron radiation based micro X-ray fluorescence (μ-SRXRF) at HASYLAB beam line L.). Indications of radioactive heterogeneities were observed at several depths in the ice core, most notably at 7 to 9.4 m (~1985 to 1989, associated with Chernobyl fallout and/or venting Novaya Zemlya

underground detonation the 1987-08-02) and 20 to 28 m core depth (~1949 to 1965, associated with atmospheric nuclear testing) (Table 2 and supplementary material, Fig. S2).

3.2. $^{240}Pu/^{239}Pu$ atom ratio

The $^{240}Pu/^{239}Pu$ atom ratios (Fig. 2) were found to range from 0.15 ± 0.04 to 0.19 ± 0.01. All stated uncertainties are based on the counting statistics (1σ). The uncertainties were in general too high to distinguish the results from global fallout. Neither the very low atom ratios (0.06) reported for 1952 by Warneke et al. (2002) in Rothamsted herbage archive and by Olivier et al. (2004) in an alpine ice core (0.08), nor the high ratios found by Warneke et al. (2002) in an alpine ice core and Rothamsted herbage archive (0.26 to 0.31), Koide et al. (1985) in two ice cores from Greenland (0.28) and in surface air in Finland in 1963 (0.38) (Salminen-Paatero et al., 2012) were found in the Austfonna ice core. The high atom ratios measured in samples from 1954 to 1956 (Warneke et al., 2002) (0.261) and 1955 to 1958 (Koide et al., 1985) (0.28) are attributed to fallout from US equatorial (Bikini and Eniwetok) testing of high yield devices. All the above mentioned works are based on sampling sites much further south than the Austfonna ice core; the air filter samples from Sodankylä (67°N, 26°E) employed by Salminen-Paatero et al. (2012) were the geographically closest. Both Warneke et al. (2002) and Olivier et al. (2004) suggested their results are more likely to be influenced by tropospheric fallout from the Nevada testing sites in USA and Semipalatinsk testing site in Kazakhstan. Measurements of debris from both sites have been shown to have characteristically low $^{240}Pu/^{239}Pu$ atom ratios (e.g. Hicks and Barr, 1984; Beasley et al., 1998b). It is important to keep in mind that the very low and very high atom ratios (0.06, 0.306 and 0.295) observed by Warneke et al. (2002) in 1952, 1954 and 1955, respectively, were associated with low concentrations over a short time span. If the time resolution in the sampling is insufficient, such transient signals may be lost due to prior and subsequent deposition of Pu with a different $^{240}Pu/^{239}Pu$ atom ratio.

Deposition of artificial radionuclides at Austfonna would be constituted by global fallout, and tropospheric fallout mainly from the former Soviet Union test sites Novaya Zemlya (Fig. 1), and Semipalatinsk located currently in Kazakhstan. The sampling site is situated some 1000 to 1200 km from the Novaya Zemlya test sites, and 3800 km from the Semipalatinsk test site. Most tests at the Novaya Zemlya main test site exhibited high yields and would have injected a large proportion of debris into the stratosphere, unavailable for local and regional deposition (Peterson, 1970; UNSCEAR, 2000). In contrast tests performed at the Semipalatinsk test site were of lower yield, and more debris would be available for local and regional deposition.

The detection of fine variations in the isotopic signature in an ice core relies heavily on sufficient time resolution. The sample sizes necessary for quantification limited the time resolution of the present ice core to 3 years. In addition surface melting and infiltration of meltwater during the summer have disturbed the stratigraphy of the Austfonna glacier. Pinglot et al. (2003) estimate the downward migration of particulate radionuclides in the Austfonna glacier to be between 0 and 0.72 m water equivalent, corresponding to between 0 and 1.6 years, although this migration is likely to vary from year to year. Consequently the measured signal represents a mixture of debris from different stratospheric and tropospheric origin, particularly in the period 1954 to 1958 when several test sites were in operation simultaneously.

The lack of a pronounced peak in $^{240}Pu/^{239}Pu$ atom ratios (Koide et al., 1985; Warneke et al., 2002) after the very large former Soviet Union testing series in 1961 and 1962 is remarkable. However, several authors (e.g. Lapp (1970), Barnaby (1992), Grønhaug (2001), Bukharin and Podvig (2004), Winkler (2007)) have indicated that, in contrast to the early USA thermonuclear detonations, several of the former Soviet Union detonations were conducted without the presence of a fissionable natural or depleted U tamper. The fissionable U tamper constitutes an important source of Pu isotopes through single or multiple neutron captures in ^{238}U (Diamond et al., 1960; Bell, 1965; Barnaby, 1992; Winkler, 2007; Fifield, Personal communication). Such detonations, when conducted at sufficient height above ground, would not only produce less radioactive fallout, the production of Pu isotopes heavier than ^{239}Pu would also be lower, resulting in lower $^{240}Pu/^{239}Pu$ atom ratios.

3.3. $^{236}U/^{239}Pu$ atom ratio

With one exception, the $^{236}U/^{239}Pu$ values obtained in this work (Table 3 and Fig. 3) fall within a narrow range of 0.18 to 0.33. Due to low activity concentrations the uncertainties were in general high. Ranges of $^{236}U/^{239}Pu$ in global fallout are relatively underreported, Ketterer et al. (2007) state a relatively wide range of 0.05 to 0.5, while Sakaguchi et al. (2009) state a more narrow range of 0.218 to 0.252. Due to the scarcity of results, it is difficult to infer $^{236}U/^{239}Pu$ atom ratios representative for the Arctic and Nordaustlandet based on the literature. The integrated value for the main period of stratospheric deposition (1949 to 1969) is 0.27 ± 0.05. This is slightly higher than the value found in surface soil samples by Sakaguchi et al. (2009), but well within the range measured in soils, sediments and peat cores by Ketterer et al. (2007). Detonations at the Novaya Zemlya test site were generally of high yield, and likely to have produced high $^{236}U/^{239}Pu$ fallout, while fallout from the Semipalatinsk test site has been documented to have low $^{236}U/^{239}Pu$ atom ratios (Beasley et al., 1998b).

Count rates of ^{236}U and ^{239}Pu in the 1975 to 1983 segment were low, but nevertheless significant. The $^{236}U/^{239}Pu$ atom ratio observed in this segment (1.4 ± 0.4) is very high compared to the ratios obtained from the period 1949 to 1969, however, it is comparable to $^{236}U/^{239}Pu$ atom ratios reported by Srncik et al. (2011b) for surface soils from La Palma (0.04 to 14), and by Eigl et al. (2013) for marine and riverine waters (1–12). The similarity between the results in Austfonna and those of Srncik et al. (2011b) reflects the fact that these samples are primarily affected by global atmospheric fallout

Table 2
Radioactive particles retained by membrane filters (Nucleopore 0.05 μm) in the Austfonna ice core by depth. Layers without indications of radioactive heterogeneities have been omitted.

Depth	Depth (m.w.e.)	Estimated time	No. of particles	Mass of ice (g)	Events
28.2–28.6	20.8–21.1	1949	2	688	Atm. tests (USA/FSU)[a]
26.1–26.5	19.2–19.5	1953	2	499	Atm. tests (USA/FSU)[a]
25.5–26.1	18.7–19.2	1953–1954	1	509	Atm. tests (USA/FSU)[a]
23.5–23.9	17.2–17.5	1957–1958	1	547	Atm. tests (USA/FSU)[a]
23.1–23.5	16.3–17.2	1958–1959	2	504	Atm. tests (USA/FSU)[a]
21.1–21.9	15.3–15.9	1961–1962	1	483	Atm. tests (USA/FSU)[a]
7–9.4	4.6–6.4	1985–1989	2	1412	Chernobyl accident/FSU vented underground test[b]

[a] Atm. tests — atmospheric nuclear tests, FSU — former Soviet Union.
[b] Vented underground detonation at Novaya Zemlya as described in Bjurman et al. (1990) and Mikhailov (2004).

Table 3
Concentrations, atom and activity ratios of ^{137}Cs, ^{236}U, ^{238}U and $^{239+240}$Pu in the Austfonna ice core. Stated uncertainties are counting statistics (1σ). Cs-137 activities at time of deposition according to Pinglot et al. (2003).

Time	$^{239+240}$Pu (mBq cm^{-2})	^{236}U (μBq cm^{-2})	^{240}Pu/^{239}Pu atom ratio	^{236}U/^{239}Pu atom ratio	^{236}U/^{238}U[a] atom ratio × 10^{-6}	^{238}U[a] ng sample^{-1}	^{137}Cs[b] mBq kg^{-1}	$^{239+240}$Pu/^{137}Cs activity ratio [b]
1984–1999	b.d.	b.d.	b.d.	b.d.	b.d.	6.8 ± 0.9	1.8	
1975–1984	0.008 ± 0.001	0.008 ± 0.001	0.15 ± 0.04	1.4 ± 0.4	4.5 ± 0.9	9 ± 1		
1969–1975	0.018 ± 0.001	b.d.	0.16 ± 0.03	b.d.	b.d.	b.d.	2.5	0.031
1965–1969	0.033 ± 0.001	0.0039 ± 0.0009	0.17 ± 0.02	0.18 ± 0.06	4 ± 1	5.1 ± 0.7	5.9	0.027
1962–1965	0.132 ± 0.003	0.024 ± 0.002	0.16 ± 0.01	0.28 ± 0.06	b.d.	b.d.	41.8	0.021
1959–1962	0.165 ± 0.005	0.025 ± 0.002	0.19 ± 0.01	0.24 ± 0.05	4.6 ± 0.5	32 ± 2	40.4	0.028
1956–1959	0.254 ± 0.004	0.053 ± 0.004	0.180 ± 0.008	0.33 ± 0.07	106 ± 24	2.3 ± 0.5	77.6	0.023
1953–1956	0.108 ± 0.003	0.022 ± 0.002	0.18 ± 0.01	0.33 ± 0.07	b.d.	b.d.	29	0.034
1949–1953	0.098 ± 0.004	0.017 ± 0.001	0.17 ± 0.02	0.27 ± 0.06	13 ± 2	8.6 ± 0.8	23.8	0.024

b.d. — below detection limit.
[a] Calculated from the analysed ^{236}U/^{234}U ratio assuming the natural abundance of 5.5 × 10^{-5} for ^{234}U.
[b] Cs-137 activity concentrations inferred from (Pinglot et al., 2003), at time of fallout. The uncertainties are not available.

from nuclear weapons detonations. In Srncik et al. (2011b) ^{236}U/^{239}Pu ratios in the uppermost layers of surface soils were in the range 3.3 to 14, and this was attributed to selective downward migration of Pu-isotopes. U and Pu are expected to be present in the ice core as fine particulates, with similar and low mobility in the ice core.

The reasons for the high ^{236}U/^{239}Pu ratios found in the 1975 to 1983 segment is then likely to be found in more recent releases of anthropogenic radionuclides. The main sources of radioactive debris in the atmosphere in this period were Chinese atmospheric nuclear detonations. Eight atmospheric detonations were conducted in the period 1974 to 1980 (Björklund and Goliath, 2009). Other sources which may have had influence were discharges from nuclear reprocessing activities in Europe. Marine discharges of radionuclides from the European nuclear waste reprocessing plants (Sellafield and La Hague) have been traced in the Arctic Ocean (e.g. Beasley et al. (1998a), Cooper et al. (1998)), and this could potentially have had influence on radionuclide deposition on the Austfonna glacier. Little is known about the ^{236}U/^{239}Pu atom ratio in releases from the Sellafield reprocessing plant; however in Irish Seawater collected in 1993 a ratio of 2.3 was found (Povinec et al., 2002).

3.4. Concentrations of ^{239}Pu and ^{236}U

Activity concentrations of $^{239+240}$Pu and ^{236}U were found to range from 0.008 to 0.254 mBq cm^{-2} and 0.0039 to 0.053 μBq cm^{-2}, respectively (Table 3). The integrated ice core inventory of $^{239+240}$Pu was 0.82 ± 0.01 mBq cm^{-2}, and 0.151 ± 0.005 μBq cm^{-2} for ^{236}U.

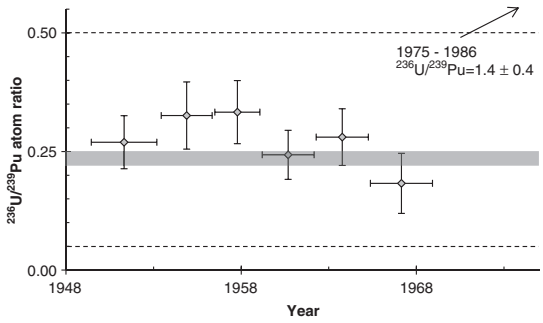

Fig. 3. Atom ratios of ^{236}U/^{239}Pu in a profile of the Austfonna ice core, estimated time interval 1951–1966. The ^{236}U/^{239}Pu atom ratio for the 1974–1983 indicated by arrow for clarity of the remaining results. Instrumental counting uncertainties included. Shaded area — global fallout according to Sakaguchi et al. (2009), upper and lower dashed lines — global fallout according to Ketterer et al. (2007).

The $^{239+240}$Pu integrated deposition compares well with the 0.85 ± 0.06 mBq cm^{-2} estimated by Hardy et al. (1973) (average of values for 70 to 80°N and 80 to 90°N latitudinal bands), but somewhat higher than the 0.552 mBq cm^{-2} obtained by Kudo et al. (1998) on the Agassiz ice cap. Publications reporting the ^{236}U deposition density are limited. Sakaguchi et al. (2010) report inventories ranging between 0.036 and 0.87 μBq cm^{-2} in Japanese surface soil samples mainly affected by global fallout.

The activity concentrations of $^{239+240}$Pu and ^{236}U peaked at the same depth (Table 3), and were well correlated throughout the profile ($r^2 = 0.95$, $p = 0.0001$). Interestingly, the concentrations of these nuclides in the ice core were found to be higher in the pre-moratorium period, as defined by the ^{3}H peak, than in the post-moratorium period. This is in contrast with observations at other sites where the highest deposition of Pu is found to have taken place in 1963 (Koide et al., 1982, 1985; Warneke et al., 2002; Olivier et al., 2004). It is, however, in agreement with the observations done by Pinglot et al. (2003) in this ice core and several other ice cores extracted from Austfonna. It is also in agreement with observations of ^{137}Cs deposition in Bodø (Bergan (2002), and references therein). Some possible reasons for the higher concentrations of ^{137}Cs, $^{239+240}$Pu and ^{236}U will be discussed in the following paragraphs.

After release to the atmosphere ^{3}H quickly enters the hydrological cycle as a natural constituent of water as ^{3}H^{1}HO. Since tritium is bound in water molecules it tends to behave more conservatively in a glacier than radionuclides deposited onto the glacier as particles. The primary causes of redistribution of tritium in a glacier are isotope diffusion and meltwater percolation (Van der Wel et al., 2011). Particulate radionuclides on the other hand have a larger tendency to be transported downwards by meltwater percolation (Pinglot et al., 2003). The infiltration of particulate radionuclides in deeper layers of the glacier could cause a depletion of particulate radionuclides in periods associated with higher melt, and simultaneously enhanced concentrations in deeper layers. Van der Wel et al. (2011) observed the formation of firn layers preserving the annual stratigraphy for ^{3}H in a glacier with high annual melting. It is not clear whether this applies to the Austfonna glacier, and it is unlikely that it affects particulate contaminants in the same way. It cannot be ruled out that the discordance between ^{3}H deposition and actinide and fission product deposition at this site could be related to the source rather than post depositional processes. The coherence between the $^{239+240}$Pu, ^{236}U and ^{137}Cs concentration profiles a (cf. Table 3 and Fig. 4), and the discordance between the ^{3}H and the ^{137}Cs concentration profiles (Pinglot et al., 2003) seem to indicate that a differential redistribution has taken place post deposition. However, the very high yield thermonuclear detonations above Novaya Zemlya in 1961 and 1962 should have released very large amounts of ^{3}H to the atmosphere without increasing the amount of weapon debris and fission products

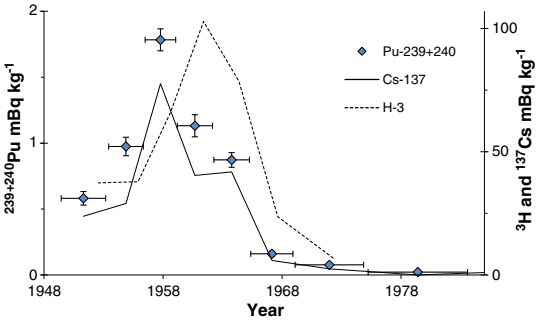

Fig. 4. Activity concentrations of $^{239+240}$Pu, ^{3}H and ^{137}Cs in the Austfonna-99 ice core. The error bars on the time axis refers to the estimated time span of each subsample, error bars on the concentration axis refers to one standard deviation counting error of the measurement. Caesium and tritium data modified from Pinglot et al. (2003) to fit the sampling periods of the present work.

proportionally. This is evident from the data of Koide and Goldberg (1985).

Enhanced transport of contaminants from central Eurasia to the Arctic during the winter months has been described in several works, e.g. Barrie and Hoff (1984), Barrie (1986) and Stohl (2006). At this time an air mass forms an isolated dome extending southwards as far as 40°N over continental Eurasia and Northern America, limited by the polar front (Barrie, 1986). A semi-permanent (winter) high pressure area above Siberia causes enhanced transport of air contaminants from central Siberia and Kazakhstan towards the Arctic (Barrie and Hoff, 1984; Barrie, 1986; Stohl, 2006). Tropospheric debris from detonations carried out at the Semipalatinsk test site could thus be transported effectively to the Arctic and Austfonna (Fig. 1). The total detonated yield at the Semipalatinsk test site in 1957 and 1958 was significantly higher (1.7 to 2.1 Mt) than in 1961 and 1962 (0.33 to 0.7 Mt) (UNSCEAR, 2000; Björklund and Goliath, 2009). However, as discussed in Section 3.2, ^{240}Pu/^{239}Pu atom ratios are indistinguishable from global fallout, and it cannot be concluded whether debris from low yield tests at the Semipalatinsk test site has had such an influence.

The presence of ^{137}Cs at shallow depths (8.05 to 8.95 m, ~1986 to 1988) likely originates either from the Chernobyl accident or a vented underground detonation that occurred at Novaya Zemlya 1987-08-02 (Bjurman et al., 1990; Pinglot et al., 2001, 2003; Mikhailov, 2004) (Table 3). Plutonium concentrations in the layer were below the detection limit, thus the source cannot be verified in the present work.

4. Conclusions

Atom ratios and concentrations of ^{236}U, ^{239}Pu and ^{240}Pu were obtained for an ice core from the high Arctic. The ^{240}Pu/^{239}Pu atom ratios fell within a tight range between 0.15 and 0.19, and are close to the global fallout ratio of 0.18. The ^{236}U/^{239}Pu atom ratios were also found to be within a narrow range of 0.18 to 0.33 throughout most of that part of the core corresponding to the nuclear testing era. Integrated deposition of $^{239+240}$Pu and ^{236}U were 0.82 ± 0.01 mBq cm^{-2}, and 0.151 ± 0.005 μBq cm^{-2}, respectively. In contrast with time-resolved measurements of deposition at other sites, Pu and ^{236}U were found to have higher concentrations at depths corresponding to the pre-moratorium period than at depths corresponding to the post-moratorium period. This may suggest either an ice core chronology disturbed by meltwater percolation or the influence of a tropospheric source different from global fallout and testing at the geographically close Novaya Zemlya test site. The discrepancy between Pu and U concentration profiles in this work and ^{3}H concentration profiles obtained in other works may reflect different mobility of particulate and dissolved contaminants in the glacier.

Supplementary data to this article can be found online at http://dx.doi.org/10.1016/j.scitotenv.2013.05.054.

Acknowledgements

The authors gratefully acknowledge the support provided by the Research Council of Norway (Project no. 421048). We are thankful to the Norwegian Defence Research Establishment (FFI) for giving us access to their collection of air filters and letting us (destructively) analyse some of them. We are indebted to Signe Dahl for kind assistance with the layout.

References

Barnaby F. Plutonium and security. London: Macmillan; 1992.
Barrie LA. Arctic air-pollution — an overview of current knowledge. Atmos Environ 1986;20:643–63.
Barrie LA, Hoff RM. The oxidation rate and residence time of sulfur-dioxide in the arctic atmosphere. Atmos Environ 1984;18:2711–22.
Beasley T, Cooper LW, Grebmeier JM, Aagaard K, Kelley JM, Kilius LR. Np-237/I-129 atom ratios in the Arctic Ocean: has Np-237 from western European and Russian fuel reprocessing facilities entered the Arctic Ocean? J Environ Radioact 1998a;39:255–77.
Beasley TM, Kelley JM, Orlandini KA, Bond LA, Aarkrog A, Trapeznikov AP, et al. Isotopic Pu, U, and Np signatures in soils from Semipalatinsk-21, Kazakh Republic and the Southern Urals, Russia. J Environ Radioact 1998b;39:215–30.
Bell GI. Production of heavy nuclei in Par and Barbel devices. Phys Rev 1965;139:1207.
Bergan TD. Radioactive fallout in Norway from atmospheric nuclear weapons tests. J Environ Radioact 2002;60:189–208.
Björklund L, Goliath M. Kärnladdningars skadeverkningar. Totalförsvarets forskningsinstitut (Swedish Defence Research Agency); 2009.
Bjurman B, Degeer LE, Vintersved I, Rudjord AL, Ugletveit F, Aaltonen H, et al. The detection of radioactive material from a venting underground nuclear-explosion. J Environ Radioact 1990;11:1–14.
Boulyga SF, Matusevich JL, Mironov VP, Kudrjashov VP, Halicz L, Segal I, et al. Determination of U-236/U-238 isotope ratio in contaminated environmental samples using different ICP-MS instruments. J Anal At Spectrom 2002;17:958–64.
Bukharin OA, Podvig PL. Russian strategic nuclear forces. Cambridge, Mass: MIT Press; 2004.
Clacher AP. Development and application of analytical methods for environmental radioactivity. Manchester: Manchester University; 1995 [PhD-thesis].
Cooper LW, Beasley TM, Zhao XL, Soto C, Vinogradova KL, Dunton KH. Iodine-129 and plutonium isotopes in Arctic kelp as historical indicators of transport of nuclear fuel-reprocessing wastes from mid-to-high latitudes in the Atlantic Ocean. Mar Biol 1998;131:391–9.
Cooper LW, Kelley JM, Bond LA, Orlandini KA, Grebmeier JM. Sources of the transuranic elements plutonium and neptunium in arctic marine sediments. Mar Chem 2000;69:253–76.
Diamond H, Fields PR, Stevens CS, Studier MH, Fried SM, Inghram MG, et al. Heavy isotope abundances in Mike thermonuclear device. Phys Rev 1960;119:2000.
Eigl R, Srncik M, Steier P, Wallner G. 236U/238U and 240Pu/239Pu isotopic ratios in small (2 L) sea and river water samples. J Environ Radioact 2013;116:54–8.
Fifield LK. Accelerator mass spectrometry of the actinides. Quat Geochronol 2008;3:276–90.
Fifield K. Personal communication.
Grønhaug K. Atmosfæriske prøvesprengninger i Sovietunionen - en oversikt. Norwegian Defence Research Establishment (FFI); 2001.
Hardy EP, Krey PW, Volchok HL. Global inventory and distribution of fallout plutonium. Nature 1973;241:444–5.
Hermanson MH, Isaksson EH, Teixeira C, Muir DCG, Compher KM, Li YF, et al. Current-use and legacy pesticide history in the Austfonna ice cap, Svalbard, Norway. Environ Sci Technol 2005;39:8163–9.
Hicks H, Barr D. Nevada test site fallout atom ratios: Pu-240/Pu-239 and Pu-241/Pu-239. Lawrence Livermore National Laboratory; 1984.
Holloway RW, Hayes DW. Mean residence time of plutonium in the troposphere. Environ Sci Technol 1982;16:127–9.
Isaksson E, Hermanson M, Sheila HC, Igarashi M, Kamiyama K, Moore J, et al. Ice cores from Svalbard — useful archives of past climate and pollution history. Phys Chem Earth 2003;28:1217–28.
Ketterer ME, Groves AD, Strick BJ. U-236 inventories, U-236/U-238, and U-236/Pu-239: the stratospheric fallout signature. Geochim Cosmochim Acta 2007;71:A480.
Koide M, Goldberg ED. The historical record of artificial radioactive fallout from the atmosphere in polar glaciers. In: Langway CC, Oeschger H, Dansgaard W, editors. Greenland ice core: geophysics, geochemistry and the environment; 1985.
Koide M, Michel R, Goldberg ED, Herron MM, Langway CC. Characterization of radioactive fallout from pre-moratorium and post-moratorium tests to polar ice caps. Nature 1982;296:544–7.
Koide M, Bertine KK, Chow TJ, Goldberg ED. The Pu-240 Pu-239 ratio, a potential geochronometer. Earth Planet Sci Lett 1985;72:1–8.

Kudo A, Zheng J, Koerner RM, Fisher DA, Santry DC, Mahara Y, et al. Global transport rates of Cs-137 and Pu239 + 240 originating from the Nagasaki A-bomb in 1945 as determined from analysis of Canadian Arctic ice cores. J Environ Radioact 1998;40:289–98.
Lapp RE. Nuclear weapons — past and present. Science and public affairs. Bull At Sci 1970;26:103–6.
Lindahl P, Asami R, Iryu Y, Worsfold P, Keith-Roach M, Choi MS. Sources of plutonium to the tropical Northwest Pacific Ocean (1943–1999) identified using a natural coral archive. Geochim Cosmochim Acta 2011;75:1346–56.
Mikhailov VE. Nuclear explosions in the USSR: the north test site reference material. Vienna: IAEA; 2004.
Olivier S, Bajo S, Fifield LK, Gaggeler HW, Papina T, Santschi PH, et al. Plutonium from global fallout recorded in an ice core from the Belukha glacier, Siberian Altai. Environ Sci Technol 2004;38:6507–12.
Pálsson SE, Howard BJ, Wright SM. Prediction of spatial variation in global fallout of Cs-137 using precipitation. Sci Total Environ 2006;367:745–56.
Pálsson SE, Howard BJ, Bergan TD, Paatero J, Isaksson M, Nielsen SP. A simple model to estimate deposition based on a statistical reassessment of global fallout data. J Environ Radioact 2013;121:75–86.
Peterson KR. An empirical model for estimating world-wide deposition from atmospheric nuclear detonations. Health Phys 1970;18:357.
Pinglot JF, Hagen JO, Melvold K, Eiken T, Vincent C. A mean net accumulation pattern derived from radioactive layers and radar soundings on Austfonna, Nordaustlandet, Svalbard. J Glaciol 2001;47:555–66.
Pinglot JF, Vaikmae RA, Kamiyama K, Igarashi M, Fritzsche D, Wilhelms F, et al. Ice cores from Arctic sub-polar glaciers: chronology and post-depositional processes deduced from radioactivity measurements. J Glaciol 2003;49:149–58.
Povinec PP, Badie C, Baeza A, Barci-Funel G, Bergan TD, Bojanowski R, et al. Certified reference material for radionuclides in seawater IAEA-381 (Irish Sea Water). J Radioanal Nucl Chem 2002;251:369–74.
Sakaguchi A, Kawai K, Steier P, Quinto F, Mino K, Tomita J, et al. First results on U-236 levels in global fallout. Sci Total Environ 2009;407:4238–42.
Sakaguchi A, Kawai K, Steier P, Imanaka T, Hoshi M, Endo S, et al. Feasibility of using U-236 to reconstruct close-in fallout deposition from the Hiroshima atomic bomb. Sci Total Environ 2010;408:5392–8.
Salminen-Paatero S, Nygren U, Paatero J. 240Pu/239Pu mass ratio in environmental samples in Finland. J Environ Radioact 2012;113:163–70.
Sisefsky J. Debris from tests of nuclear weapons — activities roughly proportional to volume are found in particles examined by autoradiography and microscopy. Science 1961;133:735.
Smith JN, Ellis KM, Naes K, Dahle S, Matishov D. Sedimentation and mixing rates of radionuclides in Barents Sea sediments off Novaya Zemlya. Deep-Sea Res. Part II-Top. Stud. Oceanography 1995;42:1471–93.
Smith JN, Ellis KM, Polyak L, Ivanov G, Forman SL, Moran SB. (PU)-P-239,240 transport into the Arctic Ocean from underwater nuclear tests in Chernaya Bay, Novaya Zemlya. Cont Shelf Res 2000;20:255–79.
Srncik M. Investigation of the ^{236}U occurrence in the environment. Vienna: University of Vienna; 2011 [PhD-thesis].
Srncik M, Hrnecek E, Steier P, Wallner G. Determination of U, Pu and Am isotopes in Irish Sea sediment by a combination of AMS and radiometric methods. J Environ Radioact 2011a;102:331–5.
Srncik M, Steier P, Wallner A. Depth profile of 236U/238U in soil samples in La Palma, Canary Islands. J Environ Radioact 2011b;102:614–9.
Steier P, Bichler M, Fifield LK, Golser R, Kutschera W, Priller A, et al. Natural and anthropogenic U-236 in environmental samples. Nucl Instr Meth B-Beam Interact Mater Atoms 2008;266:2246–50.
Stohl A. Characteristics of atmospheric transport into the Arctic troposphere. J Geophys Res—Atmos 2006;111.
UNSCEAR. Annex C, sources and effects of ionizing radiation. Vienna: United Nations Scientific Committee on the Effects of Atomic Radiation; 2000.
Van der Wel LG, Streurman HJ, Isaksson E, Helsen MM, de Wal RSW, Martma T, et al. Using high-resolution tritium profiles to quantify the effects of melt on two Spitsbergen ice cores. J Glaciol 2011;57:1087–97.
Warneke T. High-precision isotope ratio measurements of uranium and plutonium in the environment. Southampton: University of Southampton; 2002 [PhD-thesis].
Warneke T, Croudace IW, Warwick PE, Taylor RN. A new ground-level fallout record of uranium and plutonium isotopes for northern temperate latitudes. Earth Planet Sci Lett 2002;203:1047–57.
Watanabe O, Motoyama H, Igarashi M, Kamiyama K, Matoba S, Goto-Azuma K, et al. Studies on climatic and environmental changes during the last few hundred years using ice cores from various sites in Nordauslandet, Svalbard. Mem Natl Inst Polar Res Spec Issue 2001;54:227–42.
Wilcken K. Accelerator mass spectrometry of natural U-236 and Pu-239 with emphasis on nucleogenic isotope production. Canberra: The Australian National University; 2006 [PhD-thesis].
Winkler S. Accelerator mass spectrometry of heavy radionuclides with special focus on Hf-182. Canberra: The Australian National University; 2007 [PhD-thesis].
Winkler S, Steier P, Carilli J. Bomb fall-out 236U as a global oceanic tracer using an annually resolved coral core. Earth Planet Sci Lett 2012;359–360:124–30.

Paper III

Environment International 59 (2013) 92–102

Contents lists available at SciVerse ScienceDirect

Environment International

journal homepage: www.elsevier.com/locate/envint

Long-range tropospheric transport of uranium and plutonium weapons fallout from Semipalatinsk nuclear test site to Norway

Cato Christian Wendel [a,*], L. Keith Fifield [b], Deborah H. Oughton [a], Ole Christian Lind [a], Lindis Skipperud [a], Jerzy Bartnicki [c], Stephen G. Tims [b], Steinar Høibråten [d], Brit Salbu [a]

[a] Isotope Laboratory, Department of Plant and Environmental Sciences, Agricultural University of Norway, P.O. Box 5003, N-1432 Aas, Norway
[b] Department of Nuclear Physics, Australian National University, Canberra, ACT 0200, Australia
[c] Norwegian Meteorological Institute (met.no), Oslo, Norway
[d] Norwegian Defence Research Establishment (FFI), Kjeller, Norway

ARTICLE INFO

Article history:
Received 21 December 2012
Accepted 27 May 2013
Available online xxxx

Keywords:
Atmospheric dispersion modelling
Source identification
Plutonium
Uranium-236
Atom ratio

ABSTRACT

A combination of state-of-the-art isotopic fingerprinting techniques and atmospheric transport modelling using real-time historical meteorological data has been used to demonstrate direct tropospheric transport of radioactive debris from specific nuclear detonations at the Semipalatinsk test site in Kazakhstan to Norway via large areas of Europe. A selection of archived air filters collected at ground level at 9 stations in Norway during the most intensive atmospheric nuclear weapon testing periods (1957–1958 and 1961–1962) has been screened for radioactive particles and analysed with respect to the concentrations and atom ratios of plutonium (Pu) and uranium (U) using accelerator mass spectrometry (AMS). Digital autoradiography screening demonstrated the presence of radioactive particles in the filters. Concentrations of ^{236}U (0.17–23 nBq m^{-3}) and $^{239+240}$Pu (1.3–782 μBq m^{-3}) as well as the atom ratios ^{240}Pu/^{239}Pu (0.0517–0.237) and ^{236}U/^{239}Pu (0.0188–0.7) varied widely indicating several different sources. Filter samples from autumn and winter tended to have lower atom ratios than those sampled in spring and summer, and this likely reflects a tropospheric influence in months with little stratospheric fallout. Very high ^{236}U, $^{239+240}$Pu and gross beta activity concentrations as well as low ^{240}Pu/^{239}Pu (0.0517–0.077), ^{241}Pu/^{239}Pu (0.00025–0.00062) and ^{236}U/^{239}Pu (0.0188–0.046) atom ratios, characteristic of close-in and tropospheric fallout, were observed in filters collected at all stations in Nov 1962, 7–12 days after three low-yield detonations at Semipalatinsk (Kazakhstan). Atmospheric transport modelling (NOAA HYSPLIT_4) using real-time meteorological data confirmed that long range transport of radionuclides, and possibly radioactive particles, from Semipalatinsk to Norway during this period was plausible. The present work shows that direct tropospheric transport of fallout from atmospheric nuclear detonations periodically may have had much larger influence on radionuclide air concentrations and deposition than previously anticipated.

1. Introduction

The primary sources of anthropogenic radionuclides in the environment are the atmospheric nuclear tests that were carried out during the period 1945 to 1980. A total of 543 atmospheric detonations were conducted worldwide, with a total yield of 440 Mt (megatons TNT equivalents) distributed as local (~15%), tropospheric (~8.5%) and stratospheric (~76%) fallout (UNSCEAR, 2000a). The apportionment of debris into the different atmospheric compartments depended primarily on the yield of the detonation, the detonation height and the latitude at which the tests took place. Debris from low-yield detonations remained almost completely in the troposphere and deposited downwind of the detonations, while high-yield detonations injected most of the debris into the lower or upper stratosphere. Debris inserted into the stratosphere was removed by atmospheric exchange processes and deposited essentially uniformly on the surface of the hemisphere on which the detonation took place.

The most intensive period was 1951–1962 interrupted by a moratorium between the United States, the Soviet Union and the United Kingdom banning testing between November 1958 and September 1961. During the period 1951–1958, 252 tests were conducted, with a total yield of 152 Mt and a calculated distribution of 35%, 9% and 56% between local, tropospheric and stratospheric compartments, respectively. From 1960 to 1962, 180 tests were conducted with a total yield of 257 Mt and a distribution of 0.1%, 7% and 93% among the abovementioned compartments (UNSCEAR, 2000a).

Four factors impact on the Pu and U fallout signal from a nuclear weapon: the fissile material, the type of device, the tamper, and the fission yield. Nuclear weapon material is assumed to consist in general of high purity ^{235}U and/or ^{239}Pu (Bukharin, 1998; Choppin et al., 2002; Forsberg et al., 1998). The ^{240}Pu/^{239}Pu atom ratio is primarily

* Corresponding author. Tel.: +47 64 96 6013; fax: +47 64 94 8359.
E-mail address: Cato.Wendel@umb.no (C.C. Wendel).

0160-4120/$ – see front matter
http://dx.doi.org/10.1016/j.envint.2013.05.017

affected by the yield of the detonation, where a higher yield gives higher atom ratios. There is an important difference between nuclear weapons and reactors in the way heavier isotopes are formed. In UO_2 reactors Pu isotopes are formed from neutron irradiation of ^{238}U yielding ^{239}U followed by double beta decay to ^{239}Pu. Heavier isotopes are formed from continued neutron capture in the ^{239}Pu, and the proportion of heavier Pu isotopes formed increases with irradiation time and neutron flux (burn up). Since the half-life of ^{243}Pu (4.956 h) is short, the production of ^{244}Pu is insignificant in reactors (Bodansky, 2004; Winkler, 2007). In thermonuclear devices on the other hand, irradiation times are short and neutron fluxes are high, and U-isotopes up to ^{255}U are generated before beta decay (Diamond et al., 1960). Thus, the presence of ^{244}Pu above the environmental background can be regarded as a clear signal of debris from thermonuclear detonations. An overview of the abundances of ^{236}U, ^{240}Pu, ^{241}Pu, ^{242}Pu and ^{244}Pu relative to ^{239}Pu associated with different sources is summarized in Table 1.

During the period 1957–1982 the Norwegian Defence Research Establishment (FFI) measured gross beta activities in ground level air on a daily basis. There were 2–11 air filter stations in operation nationwide (Njølstad, 2006; Sæbø et al., 1998). While the collected gross beta data show clear indications of influences from nuclear weapons tests, they do not provide information on the specific source of the fallout.

Tropospherically transported debris from atmospheric nuclear detonations has been assumed to follow the prevailing wind directions at the test site latitude, and air concentrations and deposition to be the strongest downwind of the test site. Deposition of debris at areas distant from the test sites is thus assumed to be dominated by stratospheric fallout. The prevailing wind direction at the Semipalatinsk test site in Kazakhstan is westerly carrying debris westwards over Asia and USA before reaching Western Europe. In addition it is known that Former Soviet Union atmospheric nuclear tests were carried out under wind directions that would lead the debris cloud over Former Soviet Union territories (Khalturin et al., 2005). The long transit caused by the eastward route would cause dilution of the debris, and substantial sedimentation of large refractory particles. However, particles from detonations at both Semipalatinsk, Novaya Zemlya and the Chinese test site Lop Nor have been detected in Sweden, e.g. Sisefsky (1961, 1964, 1967). We here hypothesize that tropospheric direct transport of debris from Former Soviet Union test sites Novaya Zemlya and Semipalatinsk to Western Europe and Norway has occurred on several occasions. Such transport would be recognized by characteristic perturbations in the $^{240}Pu/^{239}Pu$ atom ratios reflecting the yield of the detonations carried out at the respective test sites. The aim of this study has been to determine $^{240}Pu/^{239}Pu$ and $^{236}U/^{239}Pu$ atom ratios in debris from atmospheric nuclear detonations captured in surveillance air filters from the period 1957–1963 by accelerator mass spectrometry (AMS). Furthermore, to use the obtained results in combination with atmospheric dispersion modelling, NOAA HYSPLIT and NCEP reanalysis data were provided by the NOAA/OAR/ESRL PSD, Boulder Colorado (www.esrl.noaa.gov/psd/), to determine the main sources of radioactive debris in ground level air in Western Europe in this time period.

2. Materials and methods

2.1. Archive air filters

The Norwegian air monitoring programme covered the time period of 1956–1982. During this period air filters were sampled daily at 2–10 stations (Fig. 1) (Njølstad, 2006). At the air filter stations, 430 m^3 of air was pumped through cellulose asbestos filters (Draeger, Draegerwerk, Lübeck Germany) over a period of 24 h (Small, 1959). The filters were specified to retain more than 99.9% of particles larges than 0.3 μm at the flow rates used (Lockhart et al., 1964). The air intake of the filter stations was positioned 2 m above the ground, and the filters were changed every 24 h. After sampling, the filters were sent for analysis at a central lab, and the gross beta activity was determined 48–72 h after the collection (T. Bergan personal communication; Hvinden, 1958).

Air filters from 1957 and onwards were available for this work. The air filters selected were collected from the time before and after the moratorium, from 9 October 1957 (Sola) through 8 June 1963 (Røros). The samples were collected at seven coastal locations (Bergen, Sola, Ålesund, Værnes, Bodø, Tromsø and Vadsø) and two inland locations (Gardermoen and Røros). Vadsø was the northernmost sampling site, situated some 850 km southwest of Chernaya Bay, which was the southernmost testing site for nuclear devices at Novaya Zemlya. Air sampling performed in this way offers an exact geographical location and unique time resolution that is ideal for the purpose of this work.

2.2. Selection of filters

Filters were primarily chosen from three locations:

- Bergen representing a southern coastal site,
- Røros representing an inland site and
- Vadsø for its proximity to Novaya Zemlya and being the northernmost site.

In addition, filters from the other sites (Fig. 1) were chosen based on high gross beta activities. An episode with particularly high gross beta activities occurred in November 1962. It has previously been assumed that the high activities registered in this episode originated from a detonation at Novaya Zemlya in October/November 1962 (Hvinden et al., 1964). Hence, filters from all stations during this episode were selected for analysis. Finally, four filters from 1957 (October) and

Table 1
Atom ratios from various sources. Reference date: 01.01.2012.

Source	$^{240}Pu/^{239}Pu$	$^{241}Pu/^{239}Pu$	$^{242}Pu/^{239}Pu$	$^{236}U/^{239}Pu$	$^{244}Pu/^{239}Pu$
Undetonated weapons plutonium	0.01–0.07[a]	–	–	–	–
Low-yield detonations U-based[b]	0.00015–0.053[b]	$(0.2–2.3) \times 10^{-4}$[b]	–	–	–
Low-yield detonations Pu based[b]	0.01–0.08[b]	$(0.2–6.7) \times 10^{-4}$[b]	–	–	–
Low-yield detonations GZ Semipalatinsk	0.0438 ± 0.0001[c]	$(2.21 \pm 0.035) \times 10^{-4}$[c]	$(7.89 \pm 0.26) \times 10^{-5}$[c]	0.0244 ± 0.001[c]	–
Global fallout N. hemisphere	0.182 ± 0.005[d]	$(1.14 \pm 0.85) \times 10^{-3}$[d]	$(3.71 \pm 0.3) \times 10^{-3}$[d]	0.235 ± 0.014[e]	1.44×10^{-4}[i]
Castle Bravo, Ivy Mike	0.32–0.367[f]	$(2.27 \pm 0.029) \times 10^{-3}$[f]	0.019 ± 0.003[f]	–	$(1.18 \pm 0.07) \times 10^{-4}$[f]
Bikini atoll Various	0.06–0.32[g]	$(0.7–5.5) \times 10^{-3}$[g]	$(2.5–5.7) \times 10^{-4}$[g]	–	$(4.18 \pm 1.25) \times 10^{-4}$[g]
Reactor debris Chernobyl	0.43[h]	0.12[h]	0.047[h]	8.53[h]	–

[a] Warneke et al. (2002), Rokop et al. (1995), Eriksson et al. (2008).
[b] Hicks and Barr (1984), Hansen (1995), Oughton et al. (2000), Smith et al. (2000).
[c] Beasley et al. (1998).
[d] Kelley et al. (1999).
[e] Sakaguchi et al. (2009).
[f] Yamamoto et al. (1996), Diamond et al. (1960).
[g] Lachner et al. (2010).
[h] UNSCEAR (2000b).
[i] Based on Winkler (2007) results from Lake Erie, years 1963 and 1964.

Fig. 1. The air filter stations in Norway, 1956–1982, and the approximate location of the Novaya Zemlya test site C.

three from 1958 (June) with relatively high gross beta activities were chosen to represent the activity concentrations and atom ratios associated with pre-moratorium tests.

2.3. Autoradiography

In order to identify radioactive heterogeneities on air filters, archived filters were subjected to digital autoradiography (Molecular Dynamics storage phosphor screen). The storage phosphor screens were exposed to filters for 30 days in a (low activity) lead chamber, whereupon the plates were scanned within 1 h with a Typhoon 8600 digital image scanner (resolution 100 μm).

2.4. Sample dissolution and radiochemical separations

Unless stated otherwise all chemicals used were of analytical grade. Ultra-pure HNO_3 and HCl were produced in the laboratory using a sub-boiling distillation unit (Milestone SubPure), and used for digestion, ion separation and final sample preparation. Deionised water (18 Ω) was obtained from a MilliQ apparatus (Barnstead B-pure).

Approximately 0.4–0.7 g of each filter (corresponding to 1/4–1/2 of each filter) was weighed directly into PTFE ultraclave tubes, and for most samples high-purity tracers (20 pg ^{233}U and 17 pg ^{242}Pu) were added as yield monitors prior to digestion. Three samples were prepared with filter material from ten consecutive days at filter stations Bergen (1957) and Røros (1962, 1963). These samples were prepared without yield monitor for determination of $^{242}Pu/^{239}Pu$ and $^{244}Pu/^{239}Pu$ atom ratios. All samples were digested under high pressure and temperature in nitric acid (conc.) in an ultraclave (UltraCLAVE 3, Milestone Ltd). After digestion of the samples the acid concentrations were diluted to 8 M and actinides were separated by anion exchange (DOWEX 1 × 8) (Clacher, 1995). The U eluate was further purified by UTEVA extraction chromatography according to the procedure suggested by Wilcken (2006). After separation the eluates were evaporated to dryness, taken up in 2 ml HNO_3 (conc.) with 2 mg Fe as $Fe(NO_3)_3$ and evaporated to dryness again before being ashed at 500 °C to give final preparates for AMS analysis of Pu and U.

2.5. Determination of Pu and U

Concentration and atom ratios of U and Pu were determined by accelerator mass spectrometry using the 14 UD pelletron tandem accelerator at the Australian National University (ANU), Canberra as described in detail by Fifield (2008).

2.5.1. Plutonium analysis

Three plutonium isotopes (^{242}Pu (yield monitor), ^{240}Pu and ^{239}Pu or ^{241}Pu and ^{239}Pu) were counted sequentially with counting times ranging from 1 to 3 min according to their abundance. The sequence was repeated twice with a third ^{242}Pu count at the end. Concentrations of ^{239}Pu, ^{240}Pu and ^{241}Pu were calculated from the measured $^{239}Pu/^{242}Pu$, $^{240}Pu/^{242}Pu$ and $^{241}Pu/^{242}Pu$ atom ratios. For the samples without added yield monitor, Pu isotopes ^{239}Pu, ^{240}Pu, ^{241}Pu, ^{242}Pu and ^{244}Pu were measured in sequence, with counting times of 3 and 5 min being used for the least abundant isotopes ^{241}Pu and ^{244}Pu, respectively.

Analytical blanks spiked with 17 pg ^{242}Pu gave less than 4 and 2 counts of ^{239}Pu and ^{240}Pu for 2 and 3 minute counting times, respectively. With count rates for ^{242}Pu (yield monitor) of 8000 counts in 1 min this corresponds to procedural detection limits of 4.2 and 1.3 fg for ^{239}Pu and ^{240}Pu respectively. Blank calculations for ^{239}Pu and ^{240}Pu were based on both chemical blanks and air filters through which very little air had passed due to technical difficulties. Even though it cannot be ruled out that the blank filters did capture a little fallout during their short operating time, they showed very low Pu concentrations and were assumed to be representative of the upper limit of the background

levels of Pu and U in the air filters. Blanks without yield monitor were run for ^{241}Pu, ^{242}Pu and ^{244}Pu. A count rate corresponding to 0, 0.48 and 0.1 counts per minute was measured for the three isotopes respectively. A certified reference material for Pu atom ratios (UKAEA No. UK Pu 5/92138) was measured repeatedly in each run. The ^{242}Pu/^{239}Pu atom ratio precision for the reference material was 2.7% (standard deviation, n = 13).

2.5.2. Uranium analysis

Three U isotopes (^{233}U, ^{234}U and ^{236}U) were measured sequentially similar to the Pu isotopes and the concentrations of ^{234}U and ^{236}U were calculated based on the measured ^{234}U/^{233}U and ^{236}U/^{233}U atom ratios. Analytical blanks spiked with 20 pg ^{233}U gave 115 and 17.5 counts of ^{234}U and ^{236}U for counting times of 0.5 and 3 min respectively. With count rates of 5000 counts in 1 min for ^{233}U (yield monitor) this corresponds to a detection limit of 24 fg ^{236}U and 0.9 pg of ^{234}U. Due to the higher blank levels in the U samples, it was necessary to apply a blank correction based on tracer count rates and blank levels of ^{234}U and ^{236}U.

2.6. HYSPLIT air transport modelling

The use of the HYSPLIT model in simulating dispersion of debris from nuclear detonations and accidents has been well documented (e.g. Draxler and Hess, 1997, 1998; Kinser, 2001; Moroz et al., 2010). HYSPLIT does not simulate the dynamics of the debris cloud prior to stabilisation; therefore releases were simulated from the vertical axis of the stabilized mushroom cloud at several release heights following the work by Moroz et al. (2010). Several particle classes and vertical velocities were incorporated into the model (Saltbones et al., 2003). The vertical extent of the stabilized mushroom cloud cap was estimated according to Peterson (1970). Concentrations of post detonation debris in the layers 0–75 m above ground level were simulated throughout the transport simulation.

3. Results and discussion

3.1. Gross beta activities

The mean gross beta activities (3–9 stations) obtained in air filters collected in the period 1956–1964 are illustrated in Fig. 2. Furthermore, atmospheric detonations larger than 1 kt performed within the northern hemisphere are shown. The most important test sites in the northern hemisphere during the sampling period were the former Soviet Union test sites Novaya Zemlya and Semipalatinsk and the US test sites in the Pacific (Bikini, Eniwetok, Johnston Island and Christmas island), and Nevada. In addition, four small atmospheric nuclear detonations took place in the Reggane desert in Algeria (France). The largest detonations took place at Novaya Zemlya with a total yield of 255 Mt between 1957 and 1962. The total yield at Semipalatinsk was 6.6 Mt between 1949 and 1962. US testing sites in the Pacific had a total yield of 149 Mt between 1946 and 1962 in 94 underwater, surface and atmospheric bursts. Finally there were 101 detonations with a total yield of 1.1 Mt at the Nevada test site in the period 1951–1962 (Björklund and Goliath, 2009; UNSCEAR, 2000a).

The gross beta activities in air filters were generally higher in spring and early summer. After the passage of the spring maximum in 1959 (early May), the gross beta activities decreased rapidly and remained consistently low during the remaining moratorium period (1959–1961). Following the resumption of Former Soviet Union nuclear testing in September 1961, a substantial increase is observed 12–14 days later. An event with particularly high gross beta activity concentrations is seen in November 1962, and will be discussed in Section 3.6.1.

3.2. Radioactive heterogeneities in filters—Autoradiography

Radioactive heterogeneities indicating the presence of particles were observed as hotspots in digital autoradiographs in filters from periods with atmospheric nuclear detonations. Digital autoradiographs of selected filters are shown in Fig. 3. Even though the largest numbers

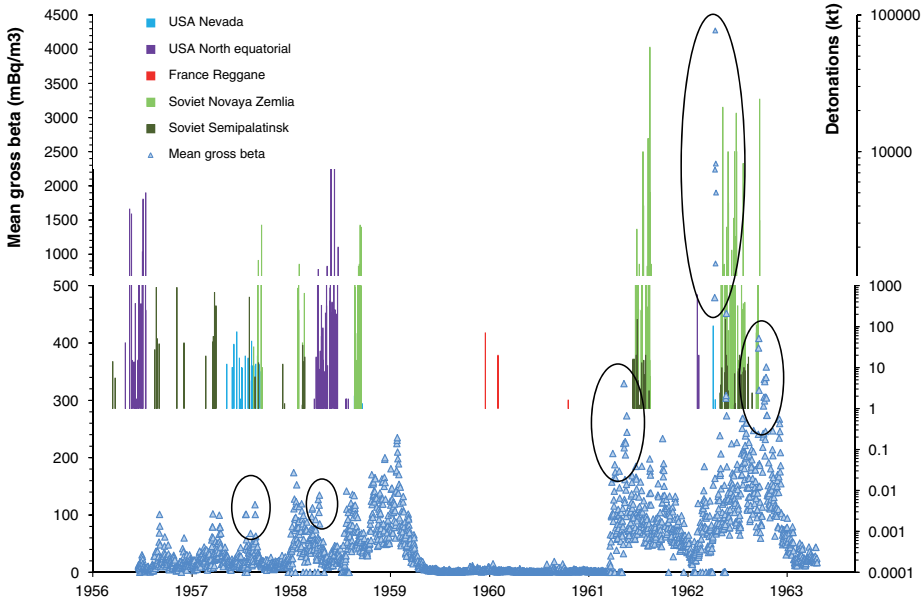

Fig. 2. Mean gross beta activities (N = 3–11 stations) and northern hemisphere detonations larger than 1 kt in the period 1956–1964. Gross beta activities from FFI and T. Bergan (personal communication), detonation data from Björklund and Goliath (2009). Sampling periods are indicated by black ellipses. North equatorial test sites are US test sites Bikini, Eniwetok, Johnston Island and Christmas Island.

of particles were indicated in filters from November 1962, associated with the highest gross beta activities, there was no general correlation between gross beta activity concentrations and the number of hotspots. The lack of correlation between the presence of particles and Pu and U concentrations is corroborated by the fact that particle indications are absent or at best ambiguous in filters from the spring months. The concentration of radionuclides is normally higher in the spring due to the arrival of the spring peak deposition. Since the absence of particles in debris from nuclear detonations is unlikely, it must be assumed that particles are either too small to be detected by digital autoradiography, or embedded too deeply in the air filter material. Considerable efforts were made to localize Pu or U containing particles by ESEM–XRMA and synchrotron; however, concentrations proved to be too low for detection by these methods.

3.3. Activity concentrations of Pu and ^{236}U in filters

The activity concentration of Pu, ^{236}U, ^{234}U and respective atom ratios and gross beta activities for all stations are presented in Table 2 and Supplementary materials Table S1. The activity concentrations of $^{239+240}$Pu and ^{236}U (μBq m^{-3} and nBq m^{-3}) have been derived from the mass concentrations in order to facilitate comparison with other publications.

3.3.1. Plutonium activity concentrations

The $^{239+240}$Pu activities varied widely (1.3–782 μBq m^{-3}) reflecting input of Pu from individual tests as well as stratospheric/tropospheric exchange which reaches its maximum in spring (Bennett, 2002). The activity concentrations for $^{239+240}$Pu were found to increase from 1957 to 1958 (Table 2). However, the filters from 1957 (October) and 1958 (June) are from different seasons. The 1958 filters were from a season associated with stratospheric/tropospheric exchange processes in which debris from the lower stratosphere is transferred to the troposphere. This increases the tropospheric inventory of radioactive debris independent of atmospheric testing. Testing in 1957 and 1958 took place at all former Soviet Union test sites, Christmas Island (UK) and US Pacific and continental sites. Large tests (>500 kt) took place at Christmas Island, Novaya Zemlya and Semipalatinsk. Since the air sampling in 1957 was performed in a period associated with little stratospheric/tropospheric exchange, Pu concentrations in these filters are likely to be primarily affected by tropospheric fallout. The sampling in 1958 on the other hand would have received Pu from both tropospheric and stratospheric fallout.

The lowest activity concentrations were observed in filters from 1957 and 1961. Two orders of magnitude higher activity concentrations in early November 1962 were likely associated with tropospheric fallout from detonations in Semipalatinsk (cf. Section 3.6.1). Gross beta activities in filters increased relatively rapidly (14 days) after the resumption of testing at Semipalatinsk and Novaya Zemlya in September 1961. In contrast, Pu concentrations increased slowly, and a substantial and stable increase did not take place until January 1962 after the large former Soviet Union test series in September through November 1961. Pu activity concentrations in air continued to increase steadily towards the summer of 1963. The Pu concentrations were generally within the same range as previously reported for air during the same period (Harley, 1980; Osborne, 1963; Salminen and Paatero, 2009).

3.3.2. Uranium-236 activity concentrations

Concentrations of ^{236}U were found to vary in the range 0.17 to 23 nBq m^{-3} (Table 2 and Supplementary materials, Table S1). The highest concentrations were found in November 1962 and June 1963. Minimum concentrations of ^{236}U were observed in the autumn of 1957 and 1961, periods associated with little stratospheric fallout.

3.4. Pu atom ratios

The ^{240}Pu/^{239}Pu atom ratios ranged widely from a minimum of 0.0517 (Ålesund 11 November 1962) to 0.237 (Bergen 03 June 1963). The ^{240}Pu/^{239}Pu atom ratios were generally lower in autumn and winter samples (September through January) than in spring and summer

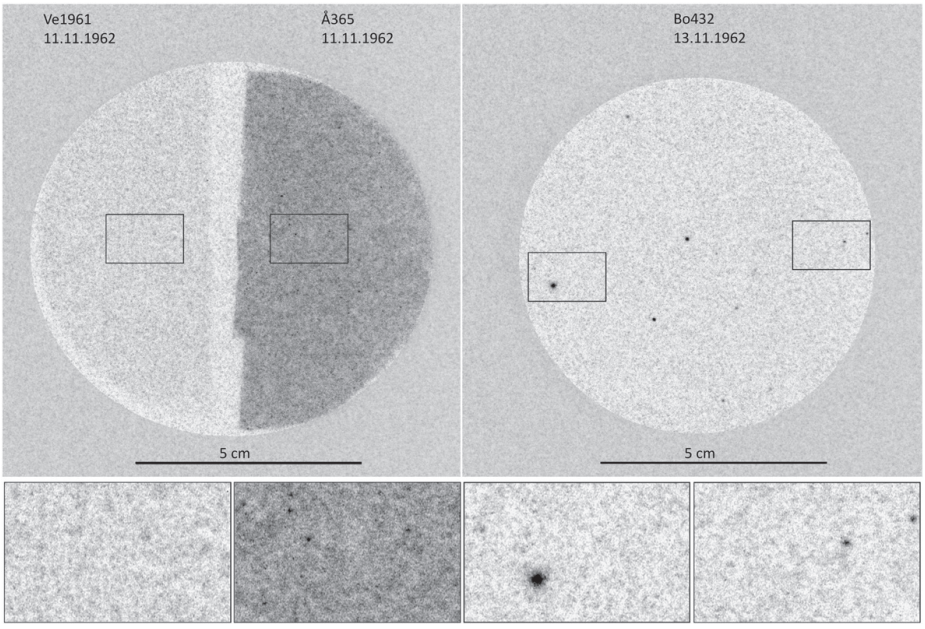

Fig. 3. Digital autoradiographs of selected filters from November 1962. Left hand side figure depicts the autoradiograph of two filter halves from Værnes and Ålesund on 11.11.1962, while the right hand side figure depicts a filter from Bodø on 13.11.1962. The filter areas inscribed in rectangles are shown below the figure at a higher magnification.

Table 2
Mean, median, minimum and maximum values of $^{239,240}Pu$, ^{236}U activity concentrations and $^{240}Pu/^{239}Pu$, $^{236}U/^{234}U$, and $^{236}U/^{239}Pu$ atom ratios for air filter samples, presented by year and for the entire period of 1957–1963.

Year		$^{240}Pu/^{239}Pu$	$^{236}U/^{239}Pu$	$^{239+240}Pu$ μBq m^{-3}	^{236}U nBq m^{-3}	$^{236}U/^{234}U$
1957–1963	Min	0.0517 ± 0.0009	0.0188 ± 0.0009	1.3 ± 0.1	0.17 ± 0.06	0.06 ± 0.01
	Max	0.237 ± 0.005	0.7 ± 0.2	782 ± 7	23 ± 4	2.0 ± 0.8
	Median	0.137	0.22	20.8	2.8	0.31
	Mean	0.13	0.24	83.9	5.5	0.54
		(n = 55)	(n = 13)	(n = 52)	(n = 16)	(n = 14)
1957	Min	0.09 ± 0.02		2.2 ± 0.1		
	Max	0.15 ± 0.02		7.4 ± 0.2		
	Median	0.12		3.3		
	Mean	0.12	0.7 ± 0.2	4.0	1.7 ± 0.4	0.12 ± 0.03
		(n = 5)	(n = 1)	(n = 4)	(n = 1)	(n = 1)
1958	Min	0.162 ± 0.007		22.1 ± 0.5		
	Max	0.170 ± 0.007		28.4 ± 0.6		
	Median	0.17		24.9		
	Mean	0.17	0.15 ± 0.03	25.1	2.2 ± 0.4	2.1 ± 0.8
		(n = 3)	(n = 1)	(n = 3)	(n = 1)	(n = 1)
1961	Min	0.067 ± 0.006	0.12 ± 0.02	1.3 ± 0.1	0.17 ± 0.06	0.06 ± 0.01
	Max	0.15 ± 0.02	0.6 ± 0.1	16.3 ± 0.5	2.1 ± 0.4	0.5 ± 0.2
	Median	0.09	0.40	2.9	0.60	0.29
	Mean	0.1	0.40	5.2	0.90	0.29
		(n = 11)	(n = 3)	(n = 11)	(n = 6)	(n = 4)
1962 excl. November episode	Min	0.110 ± 0.007		2.25 ± 0.09		
	Max	0.21 ± 0.01		36.0 ± 0.5		
	Median	0.14		21.4		
	Mean	0.14	0.24 ± 0.05	20.4	5 ± 1	0.20 ± 0.04
		(n = 16)	(n = 1)	(n = 15)	(n = 1)	(n = 1)
1962 November episode	Min	0.052 ± 0.001	0.0188 ± 0.0009	11.7 ± 0.2	4.6 ± 0.2	0.20 ± 0.01
	Max	0.077 ± 0.004	0.046 ± 0.002	782 ± 7	20.1 ± 0.6	0.34 ± 0.02
	Median	0.06	0.027	267	9.6	0.30
	Mean	0.06	0.030	323	11.1	0.29
		(n = 9)	(n = 4)	(n = 11)	(n = 4)	(n = 4)
1963	Min	0.190 ± 0.006	0.22 ± 0.04	18.2 ± 0.4	3.5 ± 0.7	0.3 ± 0.06
	Max	0.237 ± 0.005	0.28 ± 0.05	157 ± 2	23 ± 4	1.5 ± 0.3
	Median	0.22	0.27	26.7	3.5	1.1
	Mean	0.22	0.26	44.7	10.1	0.96
		(n = 9)	(n = 3)	(n = 8)	(n = 3)	(n = 3)

samples (March through July); this applies in particular to periods with atmospheric nuclear testing. Although the time series are by no way complete, we believe that this reflects influence of tropospherically transported debris from the northern hemisphere test sites. Previously reported $^{240}Pu/^{239}Pu$ atom ratios associated with low-yield detonations at Novaya Zemlya, Semipalatinsk and Nevada test sites are low (0.03–0.085) (Hicks and Barr, 1984; Smith et al., 1995, 2000; Yamamoto et al., 2004).

We believe that atom ratios obtained in our October 1957 samples (0.09–0.15) originate from two large detonations above Novaya Zemlya on 24.09 and 06.10.1957. We base this on the following argumentation. Debris collected in an air filter in the stratosphere in October 1958 originated from comparable detonations above Novaya Zemlya on 30 September 1958 (900 and 1200 kt) (Sisefsky (1961), and references therein). Thus, we infer that the $^{240}Pu/^{239}Pu$ atom ratio (0.101) obtained for the same filter by (Warneke, 2002), is representative of debris from detonations of approximately 1 Mt. Accordingly, the $^{240}Pu/^{239}Pu$ atom ratios obtained for our October 1957 samples (0.09–0.15) should originate from detonations of similar size. The Pu atom ratios of debris from two somewhat larger detonations that took place above Novaya Zemlya on 24 September, and 6 October 1957 (1600 and 2900 kt respectively), are expected to be similar to or somewhat higher than the ones associated with the above mentioned detonations. All other northern hemisphere detonations during August–October 1957 had considerably lower yields (<520 kt) and $^{240}Pu/^{239}Pu$ atom ratios in debris from these detonations should be significantly lower.

The three samples from June 1958 were found to have $^{240}Pu/^{239}Pu$ atom ratios (0.162–0.170) which are in accordance with previously published values in samples from the same period (Warneke et al., 2002). It is unlikely that tropospheric debris from the detonations in February and March 1958 should still reside in the troposphere at appreciable concentrations in the beginning of June. The values obtained are therefore likely to be representative of contemporary global fallout.

After the resumption of atmospheric testing in September 1961, the measured $^{240}Pu/^{239}Pu$ atom ratios were rather low (0.067–0.15), indicating strong influence of tropospherically transported debris. The ratios are generally much lower than the 0.198 observed by Warneke et al. (2002). However, the samples used by Warneke et al. (2002) were from an herbage archive harvested in June 1961, well before the resumption of atmospheric testing, thus representing stratospheric fallout. All atmospheric testing in the second half of 1961 was performed by the former Soviet Union; 26 and 28 tests were carried out over Novaya Zemlya and Semipalatinsk, respectively. By this time all former Soviet Union thermonuclear tests were carried out above Novaya Zemlya, and 6 detonations larger than 2500 kt were detonated above at this site in 1961. These detonations are likely to have produced debris with high $^{240}Pu/^{239}Pu$ atom ratios; however, this is not reflected in our results. According to Peterson (1970) the debris cloud from detonations of this size and at this latitude would rise to be completely injected into the polar stratosphere. Accordingly the debris would not be available to the filters before it is brought down to tropospheric levels after a considerable stratospheric residence time (0.5–2 years). In periods with frequent atmospheric testing the debris composition in air would be dominated by tests which inject the majority of their debris into the troposphere.

The samples from January through March 1962 generally exhibit lower $^{240}Pu/^{239}Pu$ atom ratios (0.110–0.13) than contemporary samples, e.g. Warneke et al. (2002). In 1962 there was no former Soviet Union atmospheric nuclear testing until August. There were numerous

tests at the US Pacific test sites from March through July. However, tropospheric debris from these tests is likely to be retained at low latitudes due to atmospheric circulation patterns (UNSCEAR, 2000a). It is therefore likely that the debris captured by these filters originate from the former Soviet Union tests in 1961. The lower $^{240}Pu/^{239}Pu$ atom ratios observed indicate that this debris was originally injected into the lower polar stratosphere by relatively large detonations (400–3000 kt). Debris from very large detonations (<5000 kt) should produce substantially higher atom ratios, e.g. Diamond et al. (1960), Yamamoto et al. (1996). However, this debris would predominately be injected into the upper polar stratosphere. The residence time in the lower polar stratosphere (9–17 km a.s.l) is estimated to 5 months and in the upper polar stratosphere (17–50 km a.s.l.) the residence time is estimated to 2 years (Peterson, 1970). Thus debris injected into the lower polar stratosphere should be expected to be deposited before the debris injected into the upper polar stratosphere. The first deposition of debris injected into the lower polar stratosphere should be expected the first spring after the detonations (Peterson, 1970). The filters from March were chosen based on the peaks in gross beta activities indicating the arrival of the spring peak. Nevertheless, it cannot be ruled out that the maximum deposition of stratospheric debris occurs later in the summer. Salminen-Paatero et al. (2012) observed prolonged periods with high $^{240}Pu/^{239}Pu$ atom ratio debris in Finland in June through December 1963. Filters from November 1962 were also analysed, however, these results are discussed in Section 3.6.1.

Atmospheric nuclear testing by the former Soviet Union and the USA had effectively ceased by the end of December 1962 and no sources of direct tropospheric Pu were present. The $^{240}Pu/^{239}Pu$ atom ratios measured for the 1963-samples, after the cessation of nuclear testing (0.190–0.237) are in accordance with the published values for the same period (Leifner and Chan, 1997; Olivier et al., 2004; Salminen-Paatero et al., 2012; Warneke et al., 2002).

3.4.1. Heavier plutonium isotopes: $^{241}Pu/^{239}Pu$, $^{242}Pu/^{239}Pu$ and $^{244}Pu/^{239}Pu$ atom ratios

Atom ratios of $^{241}Pu/^{239}Pu$, $^{242}Pu/^{239}Pu$ and $^{244}Pu/^{239}Pu$ relative to $^{240}Pu/^{239}Pu$ obtained in this work are presented in Tables 2 and 4, Supplementary materials Table S1 and Fig. 4. The filters from November 1962 were chosen from an episode of particularly high gross beta activities in the air filters. Pooled air filter samples (10 filters from Bergen October 1957, Røros March 1962 and June 1963) were chosen from a period of high gross beta activities in October 1957, and the spring peaks of 1961 and 1962.

The pooled air filter samples from April 1962 had significantly lower atom ratios (0.145 ± 0.003, 0.00038 ± 0.00008 and 0.0013 ± 0.0001) than those published by Kelley et al. (1999) for global fallout (0.180 ± 0.014, 0.0011 ± 0.0002 and 0.0037 ± 0.0003) with respect to all three $^{240}Pu/^{239}Pu$, $^{241}Pu/^{239}Pu$ and $^{242}Pu/^{239}Pu$ atom ratios, respectively. Twenty-five detonations took place above Novaya Zemlya in 1961, 11 of these detonations had a yield exceeding 500 kt. Debris from these detonations could potentially enhance the Pu atom ratios in air in 1962; however, this is not reflected in the $^{240}Pu/^{239}Pu$ $^{241}Pu/^{239}Pu$ or $^{242}Pu/^{239}Pu$ atom ratios in the pooled filters from 1962. A possible explanation for this could be suppression of the signal by tropospheric sources with lower atom ratios as discussed in Section 3.4. The Tsar Bomba detonated above Novaya Zemlya 31 October 1961 (~50 Mt) would have had very high neutron fluxes, potentially producing massive amounts of heavier Pu isotopes. However, it has been indicated that the device was downscaled from its original 100 Mt to ~50 Mt by replacing the ^{238}U tamper with lead (Lapp, 1970). This would reduce the production of higher Pu-isotopes significantly.

The pooled filter sample from June 1963 is indistinguishable from global fallout with respect to the $^{242}Pu/^{239}Pu$ atom ratio, albeit slightly higher with respect to the $^{240}Pu/^{239}Pu$ ratio. This is reasonable since there was no atmospheric testing between December 1962 and the sampling in June 1963. Thus Northern hemisphere tropospheric Pu by this time should be dominated by stratospheric fallout from the large Soviet testing series in 1961 and 62. The $^{244}Pu/^{239}Pu$ atom ratios measured in this work (1.7 ± 0.5) $\times 10^{-4}$ agrees well with the value (1.21×10^{-4}) reported by Winkler (2007) (cf. Fig. 4 and Table 1). To the knowledge of the authors the present results are the first $^{244}Pu/^{239}Pu$ results published in air filters.

3.5. Uranium atom ratios

3.5.1. $^{236}U/^{238}U$ atom ratios

$^{236}U/^{238}U$ atom ratios (0.0000034–0.00011) were calculated from the measured $^{236}U/^{234}U$ atom ratio assuming a $^{234}U/^{238}U$ natural ratio of 0.000055. As for the Pu atom ratios, the highest values were found in June 1963, in accordance with peak stratospheric deposition following the large atmospheric tests in 1961 and 1962. All values were substantially higher than values stated for global fallout by Sakaguchi

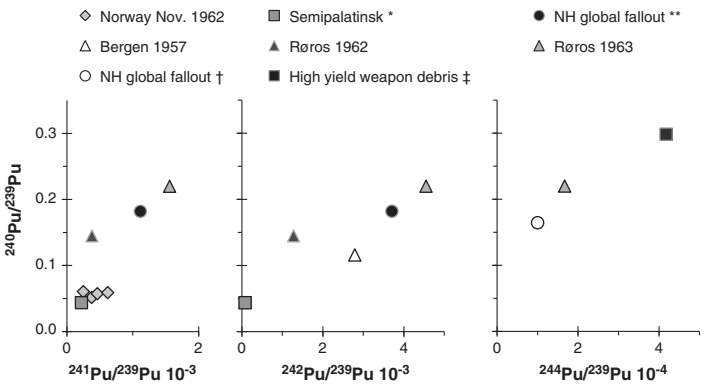

Fig. 4. Atom ratios of Pu ($^{241}Pu/^{239}Pu$, $^{242}Pu/^{239}Pu$ and $^{244}Pu/^{239}Pu$) (vertical axes) plotted against $^{240}Pu/^{239}Pu$ (horizontal axis). Reference date 01 January 2012. The November 1962 samples were individually analysed, while the autumn and spring samples from Bergen and Røros in 1957, 1962 and 1963 respectively were based on pooled samples from each period and site. Literature data from *Beasley et al. (1998) based on measurements of soils at ground zero in Semipalatinsk; **Kelley et al. (1999) soil samples collected worldwide; †Winkler (2007) sediment profile from Lake Erie; ‡Lachner et al. (2010), mixed high yield weapon debris from the Bikini atoll.

Table 3
Northern hemisphere atmospheric nuclear testing by site and time period.

Test site	Period	Sum yield (Mt)	Mean yield (kt)	Number of tests
Nevada test site	1945–1958	1	10	100
(USA)	1962	0.15	11	14
Pacific proving grounds	1946–1958	108	1721	63
(USA)	1961–1962	35	1154	30
Novaya Zemlya	1957–1958	21	766	27
(Former Soviet Union)	1961–1962	235	386	61
Semipalatinsk	1949–1958	6	127	49
(Former Soviet Union)	1961–1962	0.64	10	67

et al. (2009), and more in accordance with the results from soils contaminated by local fallout as reported by Ketterer et al. (2003).

3.5.2. $^{236}U/^{239}Pu$ atom ratios

Literature data on $^{236}U/^{239}Pu$ are scarce. Ratios measured in the present work ranged from 0.0188 to 0.7 with a mean value of 0.24 (Table 2 and Supplementary materials Table 1); this is within the range of ratios for global fallout (Ketterer et al., 2003; Sakaguchi et al., 2009; Srncik et al., 2011). The highest $^{236}U/^{239}Pu$ ratios were found in October 1957 and December 1961, which are also the periods with lowest concentration of both ^{236}U and ^{239}Pu in air. The lower ratios were associated with the episode of tropospheric deposition in November 1962 noted above for which $^{240}Pu/^{239}Pu$ ratios were similarly low.

3.6. Source identification

The high and accurate time resolution of the air filters permits identification of debris from test series, and in some cases individual tests. As mentioned above, there were three dominant test sites in the Northern hemisphere in the time period 1956–1962 (Table 3). The dominant Northern hemisphere test site in this time period by far was Novaya Zemlya, followed by Semipalatinsk and Nevada test site. It has been indicated that fallout from low-yield tests at the Nevada test site in 1952 has reached England (Warneke et al., 2002), and that this might also affect other Northern hemisphere sites. However, the close relationship between atmospheric testing at the two Soviet testing sites and the gross beta activities in air in Norway (cf. Fig. 2) indicates that testing at Novaya Zemlya and Semipalatinsk was the major contributor to the radioactivity collected in these air filters.

3.6.1. Transport of tropospheric fallout from Semipalatinsk to Norway

In November 1962 gross beta activities at all air filter stations in Norway increased abruptly up to a factor of 200 of the average recorded for the entire year 1962. The highest activity was reached in Ålesund on 11 November 1962 with 15 Bq m^{-3} (Table 4, cf. also Fig. 2). Increased activities were first observed at all stations in southern Norway; however, the peak activities arrived first at the mid-East (Værnes) and Northern (Bodø) stations. Peak concentrations occurred with a time lag of up to three days between the different stations. Pu concentrations and atom ratios were determined in 11 filters from this episode. The $^{240}Pu/^{239}Pu$ atom ratios (0.0517–0.077), $^{241}Pu/^{239}Pu$ (0.00025–0.00062) and $^{236}U/^{239}Pu$ (0.0188–0.046) deviated from published global fallout values (cf. Fig. 4, Table 4), but were generally in agreement with values published for soil (Beasley et al., 1998) and a radioactive particle (Lind, 2006) from Ground Zero in Semipalatinsk.

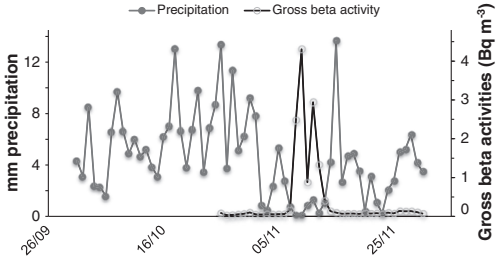

Fig. 5. Mean gross beta activity concentrations (open circles black line) and mean precipitation (filled circles grey line) at all stations in October/November 1962. Precipitation data from www.eklima.no.

Assuming a $^{240}Pu/^{239}Pu$ atom ratio of 0.0438 to be representative of bomb debris from Semipalatinsk (Beasley et al., 1998), and an atom ratio of 0.162 to be representative for global fallout in 1962 (Warneke et al., 2002), the following mixing equation can be set up to estimate the fraction of Pu derived from Semipalatinsk.

$$X = \left(R_{Sample} - R_{Global}\right) / \left(R_{Semipalatinsk} - R_{Global}\right) * 100$$

where X is the relative (%) contribution from Semipalatinsk, R_{Sample} is the atom ratio of the sample, $R_{Semipalatinsk}$ is the atom ratio measured at ground zero in Semipalatinsk (0.0438) and R_{Global} is the contemporary global fallout (0.162). The results and estimated Semipalatinsk contribution in the samples are given in Table 4.

This high gross beta activity incident has previously been suggested by other authors to be associated with an atmospheric detonation at Novaya Zemlya on 30 October–01 November 1962 (Hvinden et al., 1964; Peirson and Cambray, 1965). It appears that these authors did

Table 4
Results from measurements of samples from 9 November 1962–13 November 1962. Reference date 01 January 2012. † $^{236}U/^{239}Pu$ atom ratios calculated from the measured $^{236}U/^{234}U$ and the $^{234}U/^{238}U$ atom ratio of natural uranium (0.000055). Literature values brought in for comparison, a — Kelley et al. (1999); b — Ketterer et al. (2007); c — Beasley et al. (1998).

Station	Date 1962	Gross beta mBq m^{-3}	$^{239+240}Pu$ μBq m^{-3}	% Contribution Semipalatinsk	$^{240}Pu/^{239}Pu$	$^{241}Pu/^{239}Pu \times 10^{-4}$	$^{236}U/^{238}U\dagger \times 10^{-6}$	$^{236}U/^{239}Pu$
Sola	9.11	3142	169 ± 2	86	0.060 ± 0.001			
Gardermoen	9.11	9092	575 ± 5	85	0.0614 ± 0.0007		17 ± 1	0.0188 ± 0.0009
Røros	9.11	11526	487 ± 4	89	0.0574 ± 0.0006	4.6 ± 0.7	15.9 ± 0.9	0.0246 ± 0.0009
Bodø	9.11	8132	301 ± 3	91	0.054 ± 0.001			
Tromsø	10.11	2050	116 ± 2	84	0.063 ± 0.003			
Bergen	11.11	6327	267 ± 2	87	0.059 ± 0.001	6.2 ± 0.9		
Ålesund	11.11	15467	782 ± 7	93	0.0517 ± 0.0009	3.8 ± 0.5	27.4 ± 0.8	0.0297 ± 0.0009
Værnes	11.11	2362	121 ± 1	85	0.062 ± 0.002		41 ± 2	0.046 ± 0.002
Ålesund	12.11	8781	631 ± 5	86	0.0605 ± 0.0008	2.5 ± 0.5		
Vadsø	12.11	464	11.7 ± 0.2	72	0.077 ± 0.004			
Ålesund	13.11	1762	87 ± 1	83	0.064 ± 0.003			
Global fallout	–	–	–	–	0.182 ± 0.005[a]	11.2 ± 0.85[a]	–	0.05–0.5[b]
Semipalatinsk ground Zero	–	–	–	–	0.0438 ± 0.0001[c]	2.21 ± 0.035[c]		0.024 ± 0.0001[c]

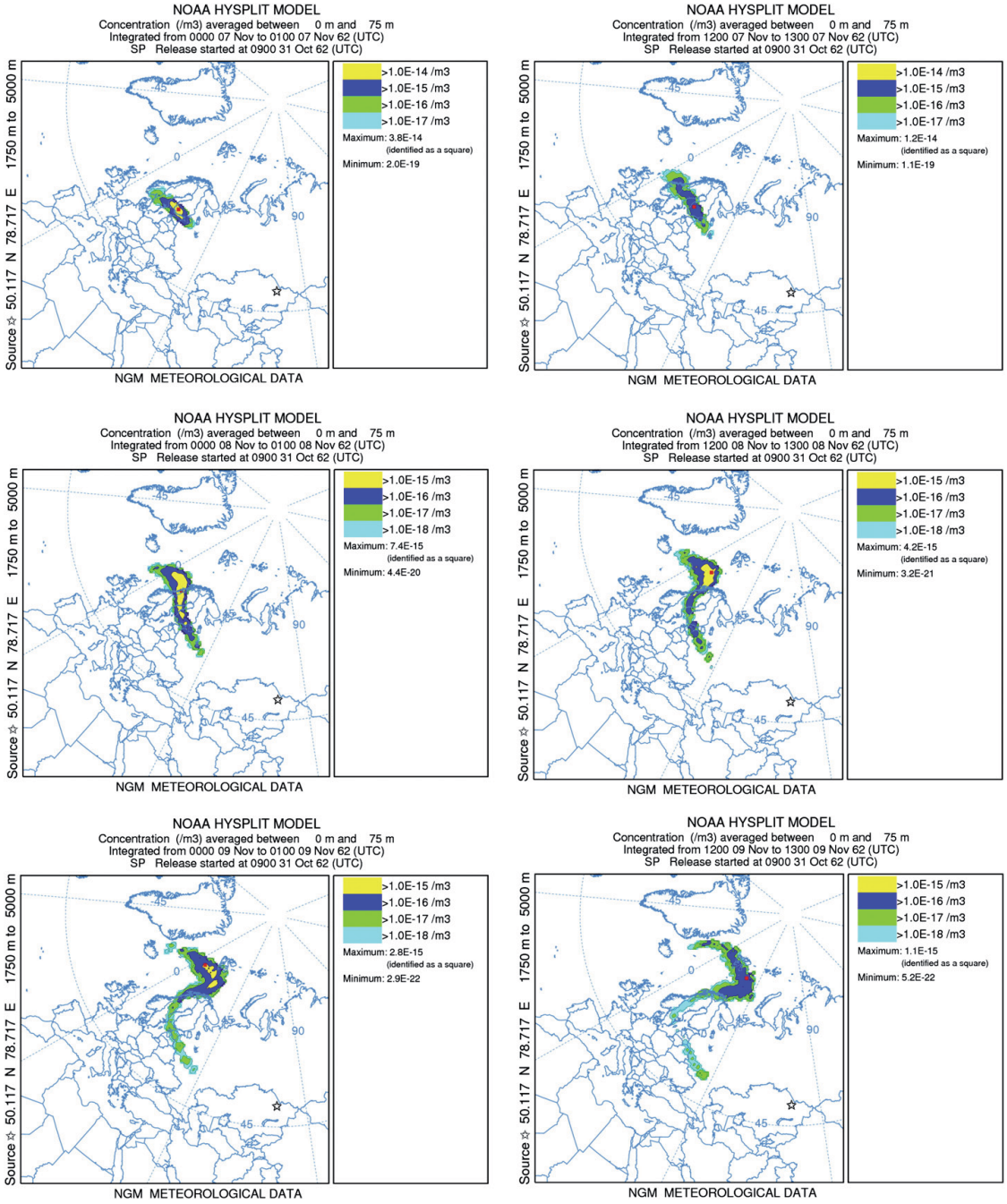

Fig. 6. Summary of HYSPLIT simulations of the release of radionuclides from a detonation of yield 10 kt which took place over Semipalatinsk testing site 31 October 1962. Simulated release heights were between 1750 and 5000 m, and post detonation concentrations between 0 and 75 m above ground were simulated. The plume position and air concentrations of debris from 7 November 1962 with 12 h increments is shown in the figure. The release location (Semipalatinsk) is indicated by a star in the lower right hand side of each map.

not possess a complete detonation record, and were unaware of testing activities in Semipalatinsk at the time. Winds over Kazakhstan in the period 30 October–5 November 1962 were easterly or north-easterly. A high pressure area (1035 hPa) North of Kazakhstan, forced debris towards the Black and Baltic Seas where a variable low pressure (995–1015 hPa) forced southerly and later east-south-easterly winds across Scandinavia (D. R. Kristoffersen, Personal communication, cf. Supplementary materials S2).

In Fig. 5 mean gross beta activities are plotted together with mean precipitation (mm water equivalent) at all air sampling stations. A similar plot can be made with temperatures, which starts to decrease after 6 November 1962 (not shown). The high gross beta activities of this specific incident seem to be associated with dry and cold air from continental Eastern Europe.

There were five northern hemisphere detonations in the time interval suggested by Hvinden et al. (1964) that could have generated the debris, two over Novaya Zemlya and three over Semipalatinsk. Debris from the high altitude detonation above the Kapustin Yar (Former Soviet Union) and Johnston Island (US) is unlikely to be present in surface air at this time. The detonations at Novaya Zemlya were fusion devices or boosted fission devices of relatively low-yield (240–280 kt). While we have not found any good correlation between fusion yield and $^{240}Pu/^{239}Pu$ atom ratios at low yields, it is reasonable to assume that both thermonuclear and/or boosted fission devices would produce higher atom ratios than those observed in the filters. The detonations over Semipalatinsk on the other hand were smaller, (1.2, 3 and 10 kt) and are more likely to produce the near weapon grade $^{240}Pu/^{239}Pu$, $^{241}Pu/^{239}Pu$ and $^{236}U/^{239}Pu$ atom ratios observed in the filters. The detonation height of the Novaya Zemlya detonations is unclear, UNSCEAR (2000a) and Björklund and Goliath (2009) list these as air burst, while Grønhaug (2001) questions whether the detonation height of one of the detonations could be low. The tests at Semipalatinsk on the other hand are listed as surface (30 October 1962) and air detonations (31 and 01 November 1962) respectively (Björklund and Goliath, 2009; Grønhaug, 2001; UNSCEAR, 2000a).

3.6.2. HYSPLIT simulation

Air concentration patterns calculated in HYSPLIT indicated that debris from detonations in the period 29 October 1962–2 November 1962 over Semipalatinsk were moving towards the West affecting ground level air in Western Europe and Norway. Fig. 6 shows a simulation of concentrations from a release over Semipalatinsk on 31 October 1962 (10 kt bomb, height of burst 700 m and plume rise up to 8 km, Peterson, 1970, and references therein). Debris from detonations at the Semipalatinsk testing site (50.1167 °N, 78.71667 °E, 1750–5000 m a.g.l.) in the period 30 October 1962–1 November 1962 could well explain the increasing activity concentrations seen in ground level air at all air filter stations in Norway. The simulated arrival of debris in eastern Norway on 7 November 1962 fits well with the first appearance of elevated gross beta activities at stations Gardermoen, Kjeller, Røros and Værnes. It is also in fine agreement with the calculations made by Hvinden et al. (1964). This indicates a transit time of debris from the Semipalatinsk test site to Norway of about 7–10 days under suitable weather conditions.

Debris from a simulated release above Semipalatinsk the 31 October 1962 first appears in the 0–75 m layer in Belorussia 5 November 62, thereafter moving towards Lithuania, Poland Latvia and Estonia. Sweden and southern Finland are reached on 6 November 62, and the plume reaches Eastern Norway in the evening of the same day. By this time the plume has stretched to a band covering western Russia south of Lake Ladoga, Southern Finland, Northern Estonia, Central Sweden and South Norway with the strongest concentrations appearing over Finland/Estonia. The plume then moves Northwards with the areas of highest concentration moving eastwards crossing Sweden and Norway. The plume moves northwards to reach Svalbard and the Fram Strait by 8 November 1962. A simulated release from 5000 to 8000 m above ground level from Semipalatinsk on 31 October 1962 gives a plume reaching England as described by Peirson and Cambray (1965). Simulations were also performed for detonations performed at Novaya Zemlya on 30 October 1962 and 01 November 1962 (not shown) demonstrating that direct transport of debris from these tests to Norway was not plausible.

The highest concentrations over Norway were measured in an area spanned by Røros and Gardermoen in East and Ålesund in West (cf. Fig. 1). Gross beta activities and $^{239+240}Pu$ activity concentrations were well correlated ($R^2 = 0.92$, $P = 0.000075$) during the incident, suggesting that these signals originate from the same source.

4. Conclusions

A series of ground level air filters from the period 1957–1963 have been examined. Activity concentrations $^{239+240}Pu$ and ^{236}U as well as atom ratios ($^{240}Pu/^{239}Pu$, $^{241}Pu/^{239}Pu$, $^{242}Pu/^{239}Pu$, $^{244}Pu/^{239}Pu$ and $^{236}U/^{239}Pu$) were determined. Results show substantial variations in both $^{240}Pu/^{239}Pu$ atom ratios (0.0517–0.237) and $^{239+240}Pu$ activity concentrations (1.3–782 μBq m^{-3}). The $^{240}Pu/^{239}Pu$ atom ratios during and after periods of intensive testing were substantially lower than contemporary global fallout, indicating significant tropospheric fallout, most likely from USSR testing sites in Semipalatinsk or Novaya Zemlya. An episode with elevated ^{236}U (4.6–20.1 nBq m^{-3}) and $^{239+240}Pu$ (11.7–782 μBq m^{-3}) activity concentrations, and atom ratios characteristic of the Semipalatinsk test site ($^{236}U/^{239}Pu = 0.0188–0.046$, and $^{240}Pu/^{239}Pu = 0.0517–0.077$) were observed in November 1962. A HYSPLIT simulation using real time meteorological data of this episode shows direct tropospheric deposition of debris from a detonation at Semipalatinsk to have arrived from East with the highest impact in Mid-East–Mid West Norway. The fine time resolution of the air filters permitted day by day fluctuations in both atom ratio and concentrations of anthropogenic U and Pu to be seen.

Supplementary data to this article can be found online at http://dx.doi.org/10.1016/j.envint.2013.05.017.

Acknowledgements

The authors gratefully acknowledge the support provided by the Research Council of Norway (Project no. 421048). We are thankful to the Norwegian Defence Research Establishment (FFI) for giving us access to their collection of air filters and letting us (destructively) analyse some of them. We are grateful to Dag Roger Kristoffersen at the Norwegian Meteorological Institute for sharing his insight in the meteorological conditions of central Asia. We are indebted to Signe Dahl for the kind assistance with the layout.

References

Beasley TM, Kelley JM, Orlandini KA, Bond LA, Aarkrog A, Trapeznikov AP, et al. Isotopic Pu, U, and Np signatures in soils from Semipalatinsk-21, Kazakh Republic and the Southern Urals, Russia. J Environ Radioact 1998;39:215–30.
Bennett BG. Worldwide dispersion and deposition of radionuclides produced in atmospheric tests. Health Phys 2002;82:644–55.
Björklund L, Goliath M. Kärnladdningars skadeverkningar. Totalförsvarets forskningsinstitut (Swedish Defence Research Agency); 2009.
Bodansky D. Nuclear energy: principles, practices, and prospects. Springer; 2004.
Bukharin O. Securing Russia's HEU stocks. Sci Glob Secur 1998;7:311–31.
Choppin GR, Liljenzin JO, Rydberg J. Radiochemistry and nuclear chemistry. Butterworth-Heinemann; 2002.
Clacher AP. Development and application of analytical methods for environmental radioactivity; 1995 [PhD thesis. Manchester].
Diamond H, Fields PR, Stevens CS, Studier MH, Fried SM, Inghram MG, et al. Heavy isotope abundances in Mike thermonuclear device. Phys Rev 1960;119:2000.
Draxler RR, Hess GD. Description of the HYSPLIT 4 modeling system. Silver Spring, Maryland: Air Resources Laboratory; 1997.
Draxler RR, Hess GD. An overview of the HYSPLIT_4 modelling system for trajectories, dispersion, and deposition. Aust Meteorol Mag 1998;47:295–308.
Eriksson M, Lindahl P, Roos P, Dahlgaard H, Holm E. U, Pu, and Am nuclear signatures of the Thule hydrogen bomb debris. Environ Sci Technol 2008;42:4717–22.

Fifield LK. Accelerator mass spectrometry of the actinides. Quat Geochronol 2008;3:276–90.
Forsberg CW, Hopper CM, Richter JL, Vantine HC. Definitions of weapons-usable Uranium-233. Oak Ridge, Tennessee: Oak Ridge National Laboratory; 1998.
Grønhaug K. Atmosfæriske prøvesprengninger i Sovietunionen — en oversikt. Norwegian Defence Research Establishment (FFI); 2001.
Hansen C. The swords of Armageddon, U.S. nuclear weapons development since 1945. In: Hansen C, editor. The swords of Armageddon. Chukelea publications; 1995.
Harley JH. Plutonium in the environment — a review. J Radiat Res 1980;21:83–104.
Hicks H, Barr D. Nevada test site fallout atom ratios: Pu-240/Pu-239 and Pu-241/Pu-239. Lawrence Livermore National Laboratory; 1984.
Hvinden T. Radioaktivt nedfall i Norge i 1957. Kjeller: Norwegian Defence Research Establishment (FFI); 1958.
Hvinden T, Lillegraven A, Lillesae O. Passage of radioactive cloud over Norway November 1962. Nature 1964;202:950. [-&].
Kelley JM, Bond LA, Beasley TM. Global distribution of Pu isotopes and Np-237. Sci Total Environ 1999;238:483–500.
Ketterer ME, Groves AD, Strick BJ. U-236 inventories, U-236/U-238, and U-236/Pu-239: the stratospheric fallout signature. Geochim Cosmochim Acta 2007;71:480.
Ketterer ME, Hafer KM, Link CL, Royden CS, Hartsock W. Anthropogenic U-236 at Rocky Flats, Ashtabula river harbor, and Mersey estuary: three case studies by sector inductively coupled plasma mass spectrometry. J Environ Radioact 2003;67:191–206.
Khalturin V, Rautian TG, Richards PG, Leith WS. A review of nuclear testing by the Soviet Union at Novaya Zemlya, 1955–1990. Sci Glob Secur 2005;13:1–42.
Kinser A. Simulating wet deposition of radiocesium from the Chernobyl accident; 2001 [PhD-thesis. Ohio].
Lachner J, Christl M, Bisinger T, Michel R, Synal HA. Isotopic signature of plutonium at Bikini atoll. Appl Radiat Isot 2010;68:979–83.
Lapp RE. Nuclear weapons — past and present. Sci Public Affairs Bull Atomic Scientists 1970;26:103–6.
Leifner R, Chan N. Stratospheric radionuclide (RANDAB) and trace gas (TRACDAB) databases. available from: http://cdiac.esd.ornl.gov/by_new/bysubjec.html#atmospheric, 1997.
Lind OC. Characterisation of radioactive particles in the environment using advanced techniques; 2006 [PhD-thesis. Ås].
Lockhart LB, Patterson RL, Anderson WL. Characteristics of air filter media used for monitoring airborne radioactivity. Washington DC: U.S. Naval Research Laboratory; 1964.
Moroz BE, Beck HL, Bouville A, Simon SL. Predictions of dispersion and deposition of fallout from nuclear testing using the NOAA-HYSPLIT meteorological model. Health Phys 2010;99:252–69.
Njølstad O. Atomic intelligence in Norway during the Cold War. J Strateg Stud 2006;29:653–73.
Olivier S, Bajo S, Fifield LK, Gaggeler HW, Papina T, Santschi PH, et al. Plutonium from global fallout recorded in an ice core from the Belukha glacier, Siberian Altai. Environ Sci Technol 2004;38:6507–12.
Osborne RV. Plutonium-239 and other nuclides in ground-level air and human lungs during spring 1962. Nature, 199; 1963143 [-&].
Oughton DH, Fifield LK, Day JP, Cresswell RC, Skipperud L, Di Tada ML, et al. Plutonium from Mayak: measurement of isotope ratios and activities using accelerator mass spectrometry. Environ Sci Technol 2000;34:1938–45.
Peirson DH, Cambray RS. Fission product fall-out from nuclear explosions of 1961 and 1962. Nature 1965;205:433. [-&].
Peterson KR. An empirical model for estimating world-wide deposition from atmospheric nuclear detonations. Health Phys 1970;18:357. [-&].
Rokop D, Efurd D, Benjamin T, Cappis J, Chamberlin J, Poths H, Roensch F. Isotopic signatures, an important tool in today's world. Los Alamos: Chemical Science and Technology Division, Los Alamos National Laboratory; 1995.
Sakaguchi A, Kawai K, Steier P, Quinto F, Mino K, Tomita J, et al. First results on U-236 levels in global fallout. Sci Total Environ 2009;407:4238–42.
Salminen-Paatero S, Nygren U, Paatero J. 240Pu/239Pu mass ratio in environmental samples in Finland. J Environ Radioact 2012;113:163–70.
Salminen S, Paatero J. Concentrations of Pu-238, Pu239 + 240 and Pu-241 in the surface air in Finnish Lapland in 1963. Boreal Environ Res 2009;14:827–36.
Saltbones J, Bartnicki J, Foss A. Handling of fallout processes from nuclear explosions in severe Nuclear Accident Program — SNAP. Oslo: The Norwegian Meteorological institute; 2003.
Sisefsky J. Debris from tests of nuclear weapons — activities roughly proportional to volume are found in particles examined by autoradiography and microscopy. Science 1961;133:735. [-&].
Sisefsky J. Investigation of nuclear weapon debris with X-ray microanalyser. Nature 1964;203:708. [-&].
Sisefsky J. Studies of debris particles from the fourth and fifth Chinese nuclear tests. Stockholm: Totalförsvarets forskningsinstitut (Swedish Defence Research Agency); 1967.
Small SH. Wet and dry deposition of fallout materials at Kjeller. Kjeller: Norwegian Defence Research Establishment (FFI); 1959.
Smith JN, Ellis KM, Naes K, Dahle S, Matishov D. Sedimentation and mixing rates of radionuclides in Barents Sea sediments off Novaya Zemlya. Deep-Sea Res II Top Stud Oceanogr 1995;42:1471–93.
Smith JN, Ellis KM, Polyak L, Ivanov G, Forman SL, Moran SB. (PU)-P-239,240 transport into the Arctic Ocean from underwater nuclear tests in Chernaya Bay, Novaya Zemlya. Cont Shelf Res 2000;20:255–79.
Srncik M, Steier P, Wallner A. Depth profile of 236U/238U in soil samples in La Palma, Canary Islands. J Environ Radioact 2011;102:614–9.
Sæbø A, Høibråten S, Engøy T. Måling av radioaktive stoffer i nedfall over Norge 1982–1997. Kjeller: Norwegian Defence Research Establishment (FFI); 1998.
UNSCEAR. Annex C, sources and effects of ionizing radiation. Vienna: United Nations Scientific Committee on the Effects of Atomic Radiation; 2000a.
UNSCEAR. Annex J, Exposures and effects of the Chernobyl accident. Vienna: United Nations Scientific Committee on the Effects of Atomic Radiation; 2000b.
Warneke T. High-precision isotope ratio measurements of uranium and plutonium in the environment; 2002 [PhD-thesis. Southampton].
Warneke T, Croudace IW, Warwick PE, Taylor RN. A new ground-level fallout record of uranium and plutonium isotopes for northern temperate latitudes. Earth Planet Sci Lett 2002;203:1047–57.
Wilcken K. Accelerator mass spectrometry of natural U-236 and Pu-239 with emphasis on nucleogenic isotope production; 2006 [PhD-thesis. Canberra].
Winkler S. Accelerator mass spectrometry of heavy radionuclides with special focus on Hf-182; 2007 [PhD-thesis. Canberra].
Yamamoto M, Hoshi M, Takada J, Sakaguchi A, Apsalikov KN, Gusev BI. Distributions of Pu isotopes and Cs-137 in soil from Semipalatinsk Nuclear Test Site detonations throughout southern districts. J Radioanal Nucl Chem 2004;261:19–36.
Yamamoto M, Ishiguro T, Tazaki K, Komura K, Ueno K. Np-237 in Hemp-palm leaves of Bontenchiku for fishing gear used by the fifth Fukuryu-Maru: 40 years after "Bravo". Health Phys 1996;70:744–8.